MONASH University

Innate immunity of mice to Hendra virus infection

Emma Louise Croser
BSc BVMS MVS MANZCVSc(Path)

A thesis submitted for the degree of *Doctor of Philosophy* at
Monash University in 2017

Faculty of Medicine, Nursing and Health Sciences

Hudson Institute of Medical Research
Centre for Innate Immunity and Infectious Diseases

CSIRO Animal, Food and Health Sciences, Australian Animal Health Laboratory

COPYRIGHT NOTICE

Contents

ABSTRACT

Henipaviruses (Nipah, Hendra and Cedar virus) are members of the Paramyxovirus family and are naturally harboured by bats. Humans and a variety of domestic animals are highly susceptible to Nipah virus (NiV) and Hendra virus (HeV) infection, and often succumb following a severe systemic disease that predominantly affects the respiratory tract, blood vessels, and central nervous system (CNS). In comparison, Cedar virus appears to be non-pathogenic, possibly because Cedar virus lacks the ability to transcribe viral proteins that are possessed by Hendra and Nipah virus and known to antagonise the host antiviral innate immune response.

Although HeV infection can cause disease in the CNS of laboratory mice, a generalised systemic illness does not develop. Rather, transient virus replication occurs in the respiratory tract with minimal detectable adaptive immune response. To elucidate the mechanisms responsible for the resistance of mice to generalised systemic infection and disease, this project examines the innate immune response of mice to henipaviruses using *in vivo* and *in vitro* models.

Firstly this study characterised HeV infection in immunologically intact (wild-type) mice following different exposure doses. The features of infection in mice were independent of virus exposure dose, and differ from those seen in other natural and experimental spill-over species.

The study then explored the characteristics of Henipavirus infection in mice genetically modified to lack specific key components of the Interferon (IFN) system, namely mice with a null mutations in subunits of the Type I interferon receptor (*Ifnar*) and mice with a null mutation for the transcription factor Signal transducer and activator of transcription 1 (Stat1) protein. This was done in order to assess the importance in mice of the IFN response to HeV, and whether the circumvention by henipaviruses of a wide range of anti-IFN strategies plays a role in the control of HeV replication in the mouse. While inactivation of the interferon signalling pathways facilitated systemic HeV replication as determined by viral load and diversity of infected tissues, important elements of HeV infection recorded in

other animal species, such as generalised illness, systemic vasculitis and severe tissue necrosis, were not observed in these null mutation mice. We therefore conclude that lack of signs of systemic illness and generalised pathology in HeV infected mice is not attributable solely to failure of viral evasion of the main IFN signalling pathways.

The impact was then assessed of viral strain on disease development in mice. For both wild-type and genetically modified mice, diseases induced by different HeV isolates (HeV/Australia/Horse/1994/Hendra and HeV/Australia/Horse/2008/Redlands) are indistinguishable.

The project then investigated HeV infection in *in vitro* cell systems. Despite the mouse possessing fully functional Henipavirus cellular receptors, researchers have previously reported slower Henipavirus infection dynamics in a small selection of rodent cell lines in comparison to cell lines from other species. To elucidate possible mechanisms behind the differences in *in vitro* infection dynamics, the project investigated the effect of Interferon Induced transmembrane (IFITM) proteins on HeV replication in human and mouse cell lines. No biologically significant effect of IFITM proteins on HeV infection was documented.

DECLARATION

This thesis contains no material which has been accepted for the award of any other degree or diploma at any university or equivalent institution and, to the best of my knowledge and belief, this thesis contains no material previously published or written by another person, except where due reference is made in the text of the thesis.

Signature: 

Print Name: Emma L Croser

Date: 08/08/2017

PUBLICATIONS DURING ENROLMENT

Croser, Emma L., & Marsh, Glenn A. (2013). The changing face of the henipaviruses. *Veterinary Microbiology, 167*(1–2), 151-158. doi: 10.1016/j.vetmic.2013.08.002

ACKNOWLEDGEMENTS

I would like to express sincere thanks to my supervisors, Dr Deborah Middleton, Dr Glenn Marsh and Professor Paul Hertzog. Dr Middleton (Deb) has an unparalleled sense of clarity for the scientific message, of which I remain in awe. She extensively proof read my thesis and in the process gave me a reschooling in grammar. Dr Glenn Marsh has the patience of a saint. He taught me all the laboratory techniques that a veterinary pathologist had never previously learnt or had completely forgotten, like pipetting, was there for and answered my numerous day to day questions and checked all my dilution calculations. Professor Hertzog gave me sage advice when I visited the Hudson Institute of Medical Research and through his group I encountered world leading immunology research. Dr Michelle Tate and Jodee Gould instructed me in several laboratory techniques for which I am highly appreciative.

The “Bat Pack” was a wonderful research group to be included in, thanks to all involved. In particular, Dr Ina Smith provided additional “gold standard PCR” help and advice throughout my thesis. Reuben, Shawn and Vicki fielded many of my questions. Thanks particularly for Reuben’s BSL4 and PCR assistance, Shawn’s GP2-293 cell culturing and Vicki’s Luminex tutorials. Leanne, your laboratory organisational assistance was missed when you left. To my fellow Bat Pack students/post docs, Jo, Bron, Kat and Sarah thanks for your company, it was fun.

The animal studies in this thesis would not have been possible without the assistance of the animal science team at AAHL. Susanne, I admire your care and compassion for all things furry. A big thank you to all who helped me with BSL4 animal monitoring, especially on weekends. Leah and Sarah your enthusiasm is infectious.

Clichéd as it is I do want to thank my parents, Elizabeth and Thomas Milne, for instilling in me the importance of education and a love of reading, enquiry and science.

To my husband, Russell Croser, unending gratitude for supporting me through everything despite your misgivings for 1) the massive drop in salary and 2) my chosen research topic. I survived, uninfected.

I would also like to thank the staff of the Veterinary Diagnostic Laboratory at Charles Sturt University, especially Professor Shane Radial and Dr Andrew Peters for their support which enabled me to spend time finishing writing the thesis. Their morning tea conversations, although insane, helped keep me sane through the writing process.

LIST OF UNITS

°C	Degrees Celsius
µg	Microgram
µl	Microlitre
µm	Micrometres
kg	Kilograms
mg	Milligrams
ml	Millilitres
hrs.	Hours

LIST OF ABBREVIATIONS

AAHL	Australian Animal Health Laboratory
Ag	Antigen
AGM	African green monkey
AQIS	Australian Quarantine and Inspection Service
ARDS	Acute respiratory distress syndrome
BBB	Blood brain barrier
Bind	Binding antibody response
Blk	Blocking antibody response
bp	Base pairs
BSA	Bovine serum albumin
BSL4	Biosafety (biosecurity) level 4
CDC	Centres for Disease Control
CedPV	Cedar virus
CI	Confidence interval
CNS	Central nervous system
CPE	Cytopathic effect
CSF	Cerebrospinal fluid
CSIRO	Commonwealth Scientific & Industrial Research Organisation
C_T	Cycle threshold
DMEM	Dulbecco's minimal essential medium
DNA	Deoxyribonucleic acid
EBOV	Ebola virus
EDTA	Ethylenediaminetetraacetic acid
ELISA	Enzyme-linked immunosorbent assay
EMEM	modified Eagle's minimal essential medium
Euth	Euthanasia
FB	Forebrain sample
FCS	Bovine foetal calf serum
H&E	Haematoxylin and eosin
HeV	Hendra virus
IAV	Influenza A virus
ID	Identification
ID_{50}	Median infectious dose
IFN	Interferon
IFNα	Interferon alpha
IFNβ	Interferon beta
IFNϒ	Interferon gamma
IFNλ	Interferon lambda
IFNAR1	Interferon alpha receptor subunit 1
IFNAR2	Interferon alpha receptor subunit 2

IFITM	Interferon induced transmembrane protein
IgG	Immunoglobulin G (gamma)
IgM	Immunoglobulin M (mu)
IHC	Immunohistochemistry
IL	Interleukin
IN	Intranasal
IP	Intraperitoneal
ISGF3	IFN stimulated gene factor 3
ISRE	IFN-stimulated regulatory elements
IT	Intratracheal
IV	Intravenous
LD_{50}	50% lethal dose
Les	Lesion
LNs	Lymph nodes
mAb	Monoclonal antibody
MDA-5	Melanoma Differentiation-Associated protein 5
MFI	Median fluorescent intensity
MOI	Multiplicity of infection
mRNA	Messenger RNA
n	Sample number
NCRIS	National Collaborative Research Infrastructure Strategy funded laboratory
NHP	Nonhuman primate
NIAID	National Institute of Allergy and Infectious Diseases
NIH	National Institute of Health
NiV	Nipah virus
NiV-B	NiV - Bangladesh isolate
NiV-M	NiV - Malaysia isolate
NSW	New South Wales
NW	Nasal wash
p	Probability value
PBS/ PBSA	Phosphate buffered saline
PBS-T	PBS with addition of Tween
PCR	Polymerase chain reaction
p.e.	Post exposure
PFU	Plaque-forming units
QLD	Queensland
qPCR	Quantitative PCR
REML	Residual (/restricted) maximum likelihood
RIG-1	Retinoic acid-inducible gene 1 protein
RNA	Ribonucleic acid
rpm	Revolutions per minute
rRNA	Ribosomal RNA
RSV	Respiratory Syncytial virus

RT-PCR	Reverse transcriptase PCR
SARS	Severe acute respiratory syndrome
SC	Subcutaneous
SD	Standard deviation
SeV	Sendai virus
SOC	Super optimal broth with catabolite repression
spp.	Species
STAT	Signal transducers and activators of transcription
SSPE	Subacute sclerosing panencephalitis
$TCID_{50}$	50% tissue culture infectious dose
TLR	Toll-like receptor
TNFα	Tumour necrosis factor alpha
USA	United States of America
VI	Virus isolation
VNT	Virus neutralising titre
WT	Wild type
w/v	Weight to volume

LIST OF FIGURES

LIST OF TABLES

CHAPTER 1: LITERATURE REVIEW

1.1 Introduction

Hendra virus (HeV) and Nipah virus (NiV) are unique among the paramyxoviruses in that they cause severe infection in a broad range of species and fatal disease in both humans and animals (Chua *et al.*, 2000; Geisbert *et al.*, 2010; Guillaume *et al.*, 2006; Li *et al.*, 2010; Marsh *et al.*, 2011; Westbury *et al.*, 1995; Williamson, 1999; Williamson *et al.*, 1998; Williamson *et al.*, 2000; Williamson *et al.*, 2001; Williamson & Torres-Velez, 2010). Because of the potential for HeV and NiV to cause severe disease in humans, together with the lack of a vaccine or therapies proven to be effective against disease in humans, these viruses are classified as biosafety level 4 (BSL4) agents. Their pathogenicity, presence in a wildlife population, and the ease with which they can be propagated, have led the henipaviruses to be classified as Select Agents of Concern for Biodefense by the USA Centers for Disease Control and Prevention and also the National Institute of Allergy and Infectious Diseases. The natural spill over host for HeV in Australia is the horse; with more than 80 horses known to have been infected (Queensland Government, 2013), and with most infections resulting in fatal disease. All cases of human HeV have occurred following epidemiologically significant exposure to infected horses. Horses are also susceptible to NiV infection, with equine cases observed during the NiV outbreak in Malaysia showing similar pathological features to HeV infections (Hooper *et al.*, 2001; Hooper & Williamson, 2000). There are several experimental animal models utilised for the study of Henipavirus disease and for the development of human vaccines and therapeutics. The ferret (Pallister *et al.*, 2009; Pallister *et al.*, 2011), hamster (Guillaume *et al.*, 2006; Guillaume *et al.*, 2009) and African green monkey (Bossart *et al.*, 2011; Rockx *et al.*, 2010) are the species studied in most detail.

A recombinant subunit vaccine has been released to assist in the prevention of HeV infection in horses and to reduce human exposure risks (Middleton *et al.*, 2014). An array of antiviral therapeutics is being explored, and a human monoclonal antibody against HeV G glycoprotein shows promise for early post exposure therapy.

1.2 History

HeV was first isolated in 1994 from an outbreak of fatal respiratory disease in racehorses and also in their trainer in Brisbane, Australia (Murray, 1996; Selvey *et al.*, 1995)(Table 1.1).

Table 1.1: Summary of HeV disease events in Australia. * Current to 8th August 2017

Year	No of disease events	Horse cases	Human cases	Human deaths
1994	2	22	3	2
1999	1	1	-	-
2004	2	2	1	-
2006	2	2	-	-
2007	2	2	-	-
2008	2	8	2	1
2009	2	6	1	1
2010	1	1	-	-
2011	18	23 (+1 dog)	-	-
2012	8	10	-	-
2013	7	7 (+1 dog)	-	-
2014	4	4	-	-
2015	3	3	-	-
2016	1	1	-	-
2017*	3	3	-	-

Retrospective investigations confirmed the virus was the cause of death of horses earlier in 1994 in Mackay, Queensland, and also a person in 1995 from relapsing encephalitis (Allworth *et al.*, 1995; O'Sullivan & Allworth, 1997; Rogers *et al.*, 1996). Since then there have been sporadic cases of the disease confirmed in horses in Queensland and northern New South Wales, with low morbidity but high case fatality rates features of HeV infection in both horses and humans (Field *et al.*, 2010).

Prior to 2011 there were a total of 14 known 'spill-over' events from the natural reservoir in flying-foxes, infecting 45 horses and 7 humans. All the human patients had close contact with an infected horse, and 4 of the human infections were fatal (Field *et al.*, 2010; Field *et al.*, 2000; Hanna, 2006; Marsh *et al.*, 2010; Playford *et al.*, 2010; PromedMail, 2009; Selvey *et al.*, 1995; Sullivan *et al.*, 1997). In 2011 there was an unprecedented rise in the number of HeV outbreaks, with 18 equine outbreaks recorded between June and October (Table 1.1).

Investigations into the role of climatic and environmental factors in facilitating the increase in Henipavirus spill over events remain inconclusive (McFarlane *et al.*, 2011; Plowright *et al.*, 2011).

NiV is also considered in this literature review as HeV and NiV are genetically very closely related and result in similar disease in infected patients. NiV was first identified as the cause of an outbreak of encephalitis among pig farmers and abattoir workers in Malaysia and Singapore in 1998-1999 (Chua *et al.*, 2000; Chua *et al.*, 1999; Paton *et al.*, 1999). The culling of over 1 million pigs controlled the disease outbreak but not before greater than 350 human cases including 109 fatalities occurred (Wong & Tan, 2012). In 2001 NiV emerged in Bangladesh as localised outbreaks, epidemiologically associated with ingestion of contaminated raw date palm sap. These outbreaks continue to occur almost annually, including in neighbouring Bengal and India (Luby & Gurley, 2012) and have resulted in over 200 human NiV cases with a case fatality rate of >70%, as reviwed by Clayton *et al.* (2013). Recently, a NiV outbreak was confirmed in the Philippines, wherein fatal human infections were linked to neurological disease and sudden death in the village horses (Ching *et al.*, 2015).

1.3 New viral discovery and globalisation

Although disease associated with henipaviruses has only been recognised in Australia, Malaysia, Singapore, Philippines, India and Bangladesh, evidence of the presence of Henipaviruses or Henipa-like viruses in bats has been detected across Central and South America, Africa, Asia, and Oceania (Figure 1.1). This includes fruit bats from the *Pteropus* genus as well as several other genera, in addition to insectivorous and microbats (Clayton *et al.*, 2013).

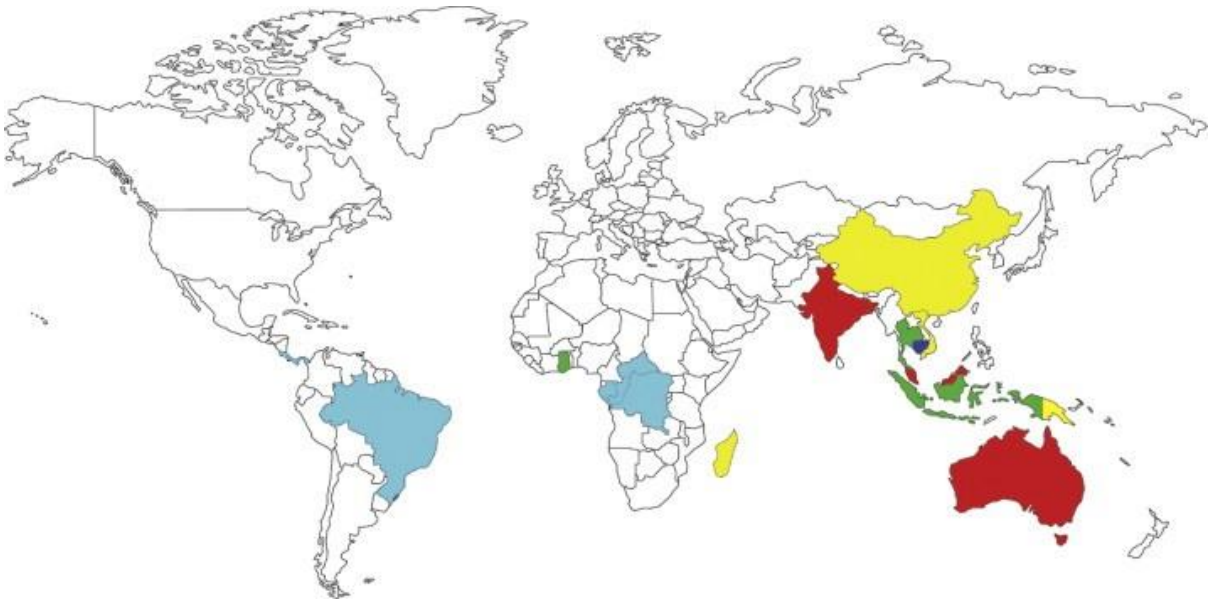

Figure 1.1 The global distribution of Henipa and Henipa-like viruses.
Red: countries where Henipavirus outbreaks have occurred. Dark blue: countries where Henipavirus has been isolated. Light blue: countries where RNA from a Henipavirus or Henipa-like virus has been discovered. Yellow: countries with serological evidence of Henipavirus exposure. Green: countries where there is both serological evidence of exposure and Henipavirus RNA has been discovered, from Croser and Marsh (2013).

The novel virus, Cedar virus (CedPV), was recently isolated from Australian fruit bats during HeV surveillance activities. Genome characterisation of this virus identified a close link to HeV and NiV suggesting it should be classified as a third member of Henipavirus genus. CedPV antibodies cross react with, but do not neutralise, HeV or NiV, but full genome analysis of CedPV shows it is more closely related to HeV and NiV than to the Henipa-like virus fragments detected in Africa (Marsh *et al.*, 2012).

1.4 Natural reservoir host and epidemiology of infection

Bats of the genus *Pteropus* (fruit bats, also called flying foxes) were identified as the reservoir host of henipaviruses (Chua *et al.*, 2002; Halpin *et al.*, 2000; Marsh *et al.*, 2012) with disease in other animals and humans representing 'spill over' infection. Experimental infection in individual bats is subclinical and characterised by a brief viraemia, very low viral load in tissues and very brief periods of low titre viral shedding (Halpin *et al.*, 2011; Williamson *et al.*, 1998; Williamson *et al.*, 2000). Infection has also been reported to recrudesce and transmit to naive bats (Sohayati *et al.*, 2011; Wang *et al.*, 2013). Maternal

antibody is passively transferred and present up to 14 months of age (Sohayati *et al.*, 2011). The recent characterisation of the immune transcriptome of the Australian flying fox, *Pteropus alecto* (Papenfuss *et al.*, 2012; Zhang *et al.*, 2013a) identified genes involved in antiviral immunity in the bat. As discussed below in "Henipavirus interactions with the innate immune system" (page 33), bats were demonstrated to have an unique interferon system that may be linked to the ability of bats to coexist with viruses in a way that minimises adverse impact on the host (Zhou *et al.*, 2016).

The mode of virus transmission between flying foxes, and 'spill over' from flying foxes to other animals, is not yet fully understood but most likely involves exposure to the urine or saliva of an infected bat (Chua *et al.*, 2002; Halpin *et al.*, 2000; Luby & Gurley, 2012). All cases of HeV infection in humans have arisen from close contact with infected horses (Field *et al.*, 2010; Murray *et al.*, 1999). All human patients had exposure, either during necropsy of infected horses, or from close contact with respiratory secretions and/or blood from infected horses. In all cases of human infection, HeV had not been considered as a differential diagnosis for the horse at the time of human exposure. In one case, human HeV infection is thought to have occurred through contact with an as yet asymptomatic infected horse in late incubation period (Field *et al.*, 2010; Playford *et al.*, 2010). Serosurveys of wildlife carers who handle injured and sick flying foxes have shown no evidence of HeV spreading directly from bat to humans (Nowak, 1995).

During the NiV outbreak in Malaysia and Singapore, infection originally occurred in people in close contact with infected pigs (Chua, 2003). Rare occurrences of infection were reported in people not in direct contact with pigs, such as presumed fomite transmission in one person who repaired pig cages and a suspected dog to human transmission in one person whose dogs became ill (Parashar *et al.*, 2000). There was little evidence for human to human spread. Only 3 out of 338 health care workers exposed to infected patients during the outbreak were positive for IgG antibodies (Mounts *et al.*, 2001) but they did not have a IgM response and were negative for neutralising antibodies; this was interpreted as a false positive IgG response. Further work up of a nurse with no exposure to sick animals and no pre-existing medical conditions, who worked in an intensive care unit where patients with acute NiV encephalitis were treated, revealed multiple brain lesions on MRI scan; these were characteristic for NiV encephalitis and were taken to support the possibility of a low

risk for nosocomial transmissibility of NiV (Tan & Tan, 2001). There was also a case of late-onset encephalitis in a family member of an infected person (Abdullah *et al.*, 2012). Direct bat to human infection occurs in the NiV outbreaks in Bangladesh and India, with a major source of infection being consumption of raw date palm sap which is contaminated with bat saliva and/or urine (Luby & Gurley, 2012). A particular feature of NiV in Bangladesh is the subsequent occurrence of human to human transmission. This may occur partly because of cultural practices of closely caring for ill family members, combined with poor levels of infection control such as no routine washing of hands (Luby & Gurley, 2012), but also may also reflect biological differences in viral strains. A larger proportion of respiratory disease is seen in human patients in Bangladesh, compared with the Malaysian outbreak (Hossain *et al.*, 2008). More recently in the Philippines horse to human transmission occurred, where humans were infected with NiV after slaughtering and consuming meat from horses that either died suddenly or were suffering from neurological disease (Ching *et al.*, 2015). Cats and a dog also succumbed after consuming the meat. Human to human transmission also was seen, both in people caring for ill family members and also in nursing staff caring for patients transported to the regional health care facility (Ching *et al.*, 2015). Although gloves and face masks were worn by health care workers, transmission may still have occurred from respiratory droplet transmission as the patients had productive coughs and eye protection was not used.

In Australia, some seasonality to HeV spill over events is observed, with an overlap of late stage pregnancy and birthing period in flying foxes and/or the dry season (McFarlane *et al.*, 2011). However, excretion of HeV in bat urine can be detected in colonies year round (Field *et al.*, 2011), suggesting other factors in addition to the presence of the virus are important contributors to spill over events. Investigations into climatic and environmental factors in facilitating spill over events prior to 2011 were inconclusive (McFarlane *et al.*, 2011; Plowright *et al.*, 2011), but some evidence exists of positive associations between pregnancy and HeV status of fruit bats, ecological stress and HeV status, incident location and proximity to flying fox roosts, and periods of lower rainfall (Field *et al.*, 2012). The outbreaks of NiV in Bangladesh occur seasonally between December and April. Rather than being directly associated with reservoir host factors, this coincides with the date palm sap harvesting season (Luby & Gurley, 2012). NiV seroprevalence has also been shown to be

higher in bats that were pregnant, or with a dependent pup and lactating (Rahman *et al.*, 2013), indicating metabolic stressors may contribute to higher infection rates. There are two hypotheses for temporal and spatial pulses of virus shedding in bat populations, namely episodic shedding from persistently infected bats or transient epidemics that occur as virus is transmitted among bat populations as reviewed by Plowright *et al.* (2014).

In 2011, the occurrence of 18 HeV incidents over a 3 month period was a notable departure from previous years' sporadic spill over events. The location of the incidents expanded the known southern and westerly range of disease occurrence by over 300 and 200 km respectively (Field *et al.*, 2012). Multiple host and environmental factors are proposed to account for this: flying fox viral excretion levels were substantially higher and shedding more prolonged than in the previous 3 years (Field *et al.*, 2012; Field *et al.*, 2011), and it is hypothesised that additional environmental factors such as decreased food resource availability and climatic conditions, prolonged survival of the virus in the environment, pasture state, and horse behaviour all contributed (Field *et al.*, 2012). A more moderate increase in incidents continued in the following year, with an additional 12 outbreaks between January 2012 and July 2013 (Queensland Government, 2013). The increased incidence of outbreaks in horses has not been associated with further cases of human infection. This is probably due to increased awareness in horse owners and veterinarians, fostering earlier consideration of HeV as a differential diagnosis and therefore increased implementation of risk minimising protocols (Field *et al.*, 2012), possibly assisted in later months by increasing numbers of vaccinated horses in known risk areas.

The genetic relatedness of HeV recovered from horses and flying foxes during spill over events supports the suggestion that different outbreaks result from independent spill over events from the fruit bat population, consistent with the presence of 'quasi-species' within the bat population (Marsh *et al.*, 2010; Smith *et al.*, 2011), rather than being associated with a particular HeV strain.

As seen with HeV, there are small strain differences in NiV isolated from bats in different parts of Asia (reviewed by (Rota & Lo, 2012). This also appears to be the case with NiV outbreaks in Bangladesh (Harcourt *et al.*, 2005; Lo *et al.*, 2012). By comparison, the genomic sequence of the viral isolates from humans and pigs in the Malaysian NiV virus outbreak

were almost identical (AbuBakar *et al.*, 2004; Chua *et al.*, 2000) suggesting there was one spill over event from bats to pigs with subsequent pig to pig transmission resulting in a sustained porcine epidemic (Luby & Gurley, 2012). The NiV Philippines is more closely related to Malaysian than Bangladesh strains, and alignment and phylogenetic relationships are illustrated in Figure 1.2 (from Ching *et al.*, 2015).

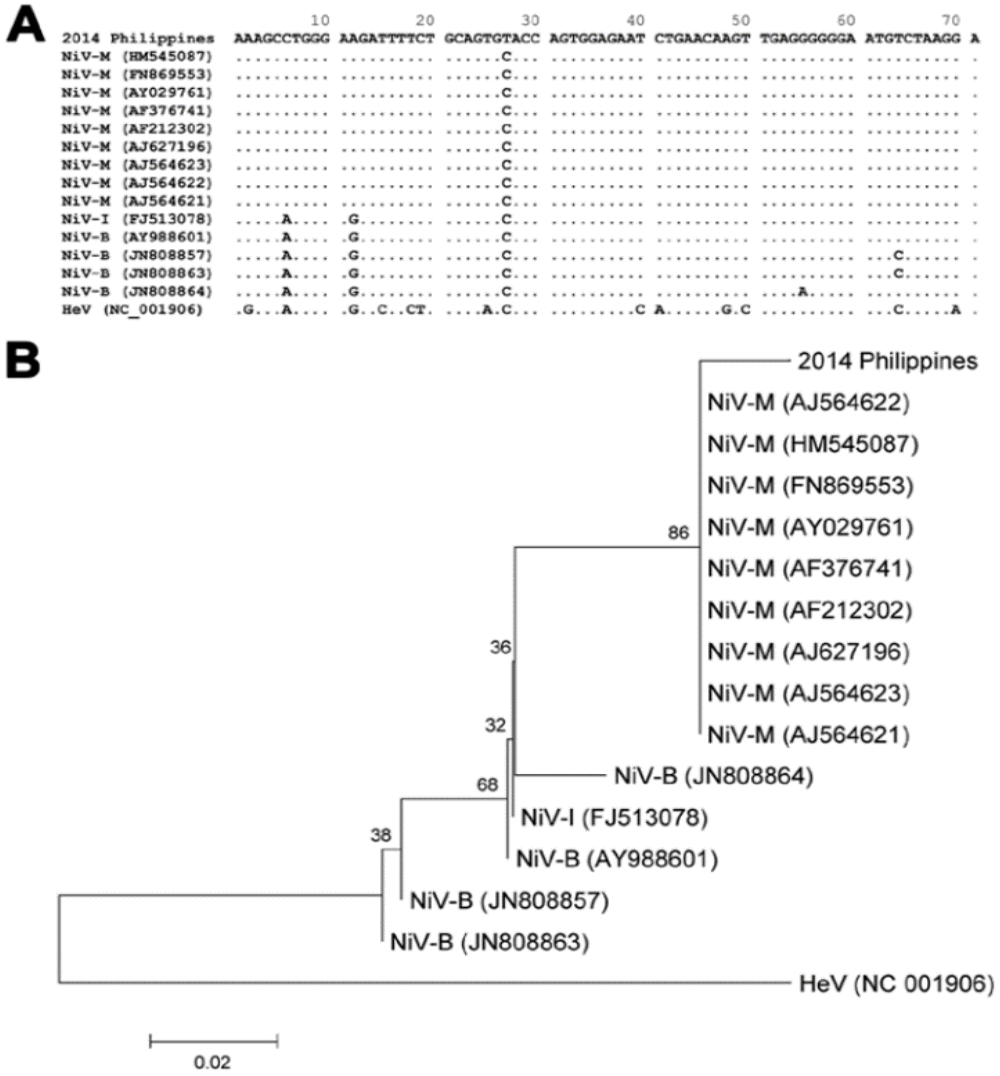

Figure 1.2: Alignment (A) and phylogenetic relationship (B) of partial phosphoprotein gene sequences of henipaviruses. The phylogenetic tree is drawn to scale; branch lengths in the same units as those of the evolutionary distances are used to infer the phylogenetic tree. The scale bar represents 0.02 substitutions per site (from Ching *et al.*, 2015).

Ecological drivers of pathogen spill over are undoubtedly complex and cross disciplinary approaches are required for increased understanding. Different epidemiological modelling

systems are being applied in order to better understand and predict disease emergence (Hayman *et al.*, 2013; Plowright *et al.*, 2011). The concept of the confluence of 'enabling conditions' required to successfully initiate a spill over event is described by Plowright *et al.* (2014). There needs to be an overlap in infected bats that are shedding the virus, virus must survive in the environment with horse management and behavioural factors allowing host exposure, and finally immunity and route of exposure determining host susceptibility.

1.5 Henipavirus infection in spill over hosts

1.5.1 HeV infection in horses

Both naturally acquired and experimental infections of horses are characterized by an acute febrile illness associated with respiratory and/or neurological signs (Hooper *et al.*, 1997b; Murray *et al.*, 1995). The incubation period in infected horses falls between 5 and 16 days (Marsh *et al.*, 2011; Murray *et al.*, 1995). Clinical signs include pyrexia, depression, loss of appetite and intermittent recumbency. The course of illness for fatally infected horses lasts approximately 48 hours from first signs to death (Field *et al.*, 2010). However, not all infections are fatal, with approximately 25% of horses surviving acute infection associated with the development of virus neutralising antibodies (Murray *et al.*, 1995; Queensland Biosecurity, 2011; Williamson *et al.*, 1998).

Respiratory signs may start with a mild serous nasal discharge (Marsh *et al.*, 2011) and rapidly progress to severe respiratory distress including tachypnoea, dyspnoea, and a terminal copious frothy nasal discharge (Rogers *et al.*, 1996; Selvey *et al.*, 1995). In addition, tachycardia, and marked oedema of the lips, face, head and neck have been noted in several affected horses (Field *et al.*, 2000; Rogers *et al.*, 1996).

Until 2008, the clinical syndrome associated with HeV infection in horses was predominately associated with a rapidly progressive febrile illness culminating in fulminating respiratory disease (Selvey *et al.*, 1995). Some of the early cases did exhibit neurological signs but these were reportedly mild, consisting of muscle twitching and restlessness (Rogers *et al.*, 1996; Williamson *et al.*, 1998). In contrast, the 2008 outbreak in the Brisbane suburb of Redlands affected 5 horses and presented primarily as neurological disease (Field *et al.*, 2010). Signs included ataxia, depression, disorientation, extreme hypersensitivity when approached,

head tilt, facial nerve paralysis, circling, head pressing, stranguria and recumbent periods. This difference in the clinical presentation of HeV infection in horses may have delayed its recognition.

The different clinical presentation in the Redlands outbreak was not attributable to the genetic makeup of the HeV isolates. Isolates obtained from infected horses from 1994 through to 2010 were compared and exhibited little (<1%) genetic variation (Marsh *et al.*, 2010) and horses experimentally infected with the Redlands 2008 strain (Hendra virus/Australia/horse/2008/Redlands, GenBank accession no. HM044317) exhibited clinical signs comparable to those seen in the initial outbreak with the "classical" 1994 strain (Hendra virus/Australia/horse/1994/Hendra, GenBank accession no. AF017149)(Marsh *et al.*, 2011). Accordingly, the differences in clinical presentation of horses in the Redlands outbreak were postulated to have resulted from a difference in exposure dose, or route of infection, or to merely reflect the spectrum of possible clinical manifestations of HeV disease (Field *et al.*, 2010).

Experimental studies in horses have used intravenous and intranasal/aerosolised exposure to virus at doses $>10^6$ $TCID_{50}$ (Hooper *et al.*, 1997b; Marsh *et al.*, 2011; Williamson *et al.*, 1998). In experimental studies in horses HeV was detected in respiratory secretions, saliva, urine and faeces (Hooper *et al.*, 1997b; Marsh *et al.*, 2011; Williamson *et al.*, 1998) and it was also demonstrated that by the time a horse is showing clinical signs, HeV virus had disseminated throughout the body and is present in body fluids (Marsh *et al.*, 2011). A HeV infected horse can shed HeV genetic material, and therefore potentially excrete HeV through nasal/nasopharyngeal secretions, from two days after virus exposure up to and including the time that it shows clinical signs. Therefore there is the risk of onward transmission to other susceptible species prior to the horse developing clinically detectable disease. Transmission risk increases with infection progression, and is highest during the terminal stages of disease (Marsh *et al.*, 2011). Horses are likely to be maximally infectious at necropsy, and infectious virus may persist on surfaces contaminated by body fluids at necropsy for a variable period (up to several days) depending on environmental conditions (Marsh *et al.*, 2011; Queensland Biosecurity, 2011).

Lesions in the horse are similar to those seen in humans succumbing to the acute disease, in that they are multi-systemic (lungs, lymph nodes, kidneys, spleen, bladder and meninges) and feature vasculitis and parenchymal necrosis. In horses, the lungs are most severely affected with severe pulmonary congestion and oedema, haemorrhage, thrombosis of smaller vessels, frequent endothelial syncytia and alveolar necrosis. Virus has been isolated from internal organs, urine and saliva (Hooper *et al.*, 1997b; Marsh *et al.*, 2011; Williamson *et al.*, 1998).

In the Malaysian outbreak of NiV, seroconversion was detected in horses (Mohd Nor *et al.*, 2000) and there is one brief description of non-suppurative meningitis with multifocal rarefaction of the brain parenchyma from a horse during the Malaysian outbreak (Hooper *et al.*, 2001). In the Philippines outbreak, affected horses reportedly exhibited neurological disease and sudden deaths but all were subsequently consumed and so no material was available for histopathology (Ching *et al.*, 2015). There have been no experimental studies using NiV in horses.

The occupational health and safety of staff, and the welfare challenge of caring for horses at BSL4, limit the number of Henipavirus studies that can be performed in horses. At BSL4, it is not feasible to maintain horses that have survived the acute infection for the purpose of studying the potential for viral recrudescence.

1.5.2 NiV infection in pigs

Both natural and experimental NiV infection in pigs are commonly asymptomatic or lead to mild clinical signs (Middleton *et al.*, 2002; Parashar *et al.*, 2000; Weingartl *et al.*, 2005; Weingartl *et al.*, 2006) although disease signs can be severe in some individuals (Mohd Nor *et al.*, 2000; Weingartl *et al.*, 2005). A febrile respiratory illness with epistaxis, dyspnoea and coughing is predominately seen in younger pigs. Neurological signs including agitation, muscle fasiculations, ataxia, paresis, and seizures, predominately occur in older pigs (Mohd Nor *et al.*, 2000).

Oronasal exposure to virus was followed by replication in the oropharynx with sequential spread to the upper respiratory tract epithelium and submandibular lymph nodes, and then the lower respiratory tract and additional lymphoid tissues (Weingartl *et al.*, 2005). Viral

antigen was also described within the olfactory nerve by day 3 post infection. The trigeminal, hypoglossal and the glossopharygeal nerves also were reported to stain positively for viral antigen by day 6. The presence of viral antigen in the granular cells of the olfactory bulb suggests the virus entered the brain via olfactory pathways, presenting an alternative route for CNS infection to haematogenous spread. Viral antigen was present throughout the body in small blood vessels (endothelium and smooth muscle of the vessel wall) and lymphatic vessels, lymphoid tissue of the tonsils, lymph nodes, the respiratory epithelium (nasal, tonsillar crypt, tracheal, bronchial and alveolar), renal tubular epithelium and interstitium. In the brain it was found in meninges (including in endothelial cells and the tunica muscularis of vessels), astrocytes and ependyma (Hooper *et al.*, 2001; Middleton *et al.*, 2002; Weingartl *et al.*, 2005; Weingartl *et al.*, 2006). In those pigs exhibiting neurological signs of NiV infection viral antigen was also present in neurones and glial cells in the peripheral cortex and olfactory bulb from day 5 post infection (Weingartl *et al.*, 2005). Overall, lesions in pigs were similar to those reported for both NiV and HeV infection in humans and HeV infection in horses, namely systemic vasculitis, alveolitis, meningitis and endothelial syncytial formation (Hooper *et al.*, 2001; Middleton *et al.*, 2002).

NiV was re-isolated from a range of organs as well as tonsil, nasal, and throat swabs but was only rarely recovered from urine (Middleton *et al.*, 2002; Weingartl *et al.*, 2005). Further investigation revealed viral antigen, RNA and recoverable virus to be present within porcine peripheral blood mononuclear cells (Stachowiak & Weingartl, 2012). By comparison, the peripheral blood mononuclear cells from humans and hamsters only mechanically carry NiV, no viral replication occurs within the cells (Mathieu *et al.*, 2011).

Challenge routes used in these experimental NiV infections of pigs included subcutaneous, oral, intranasal and ocular, with doses of either 10^7 PFU (Weingartl *et al.*, 2005; Weingartl *et al.*, 2006) or 50, 000 $TCID_{50}$ (Middleton *et al.*, 2002); all routes and doses resulted in infection.

1.5.3 HeV infection in pigs

A serological survey of Queensland piggeries revealed no evidence of Hendra or NiV infection occurring naturally in pigs in Australia (Black *et al.*, 2001), however antibodies to Henipavirus have been detected in domestic pigs in Ghana (Hayman *et al.*, 2011).

There is only one report of experimental HeV infection in pigs (Li *et al.*, 2010). Respiratory signs developed at day 5 and neurological signs developed at day 7 post infection, with clinical signs more severe than those reported with NiV infection. Pathological findings were limited to the respiratory tract and associated lymph nodes. Lesions were mild to severe and included, variously, petechial haemorrhages over the lung, bronchial and submandibular lymph nodes; pulmonary oedema; foci of inflammation associated with respiratory epithelial degeneration and syncytial cell formation; vasculitis adjacent to affected airways; and areas of pulmonary consolidation with severe interstitial pneumonia. Viral antigen was present within respiratory epithelial cells of the nasal turbinates; endothelial cells, lymphocytes, macrophages and dendritic cells of submandibular lymph nodes; as well as bronchial and bronchiolar epithelium. Virus was isolated from nasal, oral and rectal swabs, but not urine. The absence of viral RNA from RT-PCR in multiple organs not directly linked to the respiratory system and its draining lymph nodes (blood, spleen, brain, liver, heart, and uterus) supported a lack of systemic spread of infection.

1.5.4 HeV and NiV infection in humans, a secondary spill over host

Whilst there have only been 7 cases of human HeV infection, there have been over 500 cases of human NiV infection. The outcomes of HeV and NiV infection in humans appear to be similar. Infection is characterized by an acute influenza-like illness which may progress to pneumonia (Selvey *et al.*, 1995) or encephalitis with a high mortality rate (Chua *et al.*, 1999; Goh *et al.*, 2000; Hanna, 2006; Playford *et al.*, 2010; Wong *et al.*, 2009; Wong *et al.*, 2002a). Following an initial recovery, some patients suffer relapsing, or late-onset encephalitis months to years after the initial infection (Allworth *et al.*, 1995; O'Sullivan & Allworth, 1997; Tan *et al.*, 2002).

The incubation period ranges from a few days up to 14 days (Goh *et al.*, 2000; Hanna, 2006; Playford *et al.*, 2010; Selvey *et al.*, 1995). Mild symptoms include fever, headache, myalgia

and drowsiness. Central nervous system disease results in neurological signs include headache, confusion, dizziness, abnormal reflexes, and seizures progressing to an altered level of consciousness and coma (Wong & Tan, 2012). In the NiV Malaysia outbreak, all patients with normal level of consciousness recovered fully over the course of 2 weeks, whereas only 15% of patients with a reduced level of consciousness recovered. Of this latter group, approximately three-quarters recovered fully but one quarter had residual neurological deficits (Chua, 2003; Goh *et al.*, 2000). Some patients presented with a cough or pneumonia and on some occasions this progressed to acute respiratory distress syndrome (Goh *et al.*, 2000; Selvey *et al.*, 1995). A larger proportion of respiratory disease is seen in human patients in Bangladesh, compared with the Malaysian outbreak (Hossain *et al.*, 2008). Vomiting and diarrhoea were also occasionally reported in patients with NiV infection.

There are only 3 confirmed cases of people surviving HeV infection; in one patient viral RNA was detected in clinical samples during a one-month period during the acute phase with no evidence of shedding after this time (Taylor *et al.*, 2012).

Anti-Henipavirus antibodies develop in cerebrospinal fluid (CSF) and serum: IgM appears by 2 weeks post infection and is present for several months in recovered patients, while IgG seroconversion occurs from 3 weeks post infection and may be present for years (Hanna, 2006; O'Sullivan & Allworth, 1997; Selvey *et al.*, 1995; Tan & Tan, 2001; Wong & Tan, 2012).

The characteristic pathological feature of HeV and NiV infection is disseminated vasculitis with endothelial syncytia (Wong *et al.*, 2002a). The initial stage of virus replication is believed to occur in the nasopharynx, progressing to viraemia with dissemination to major organ systems. Viral antigen is present within the endothelium including in syncytia and the smooth muscle of the vessel wall (Wong *et al.*, 2002a), and damage to the vascular wall results in thrombosis and perivascular haemorrhage. Thrombosis of vessels leads to decreased perfusion within the dependent tissues resulting in ischaemic necrosis, oedema and inflammation throughout multiple organs with the greatest consequence in the brain (Wong & Ong, 2011). Viral inclusions, antigen and RNA are also present within parenchymal cells adjacent to lesions, for example in neuroglial cells, renal tubular epithelium, and pneumocytes in the alveoli of the lung (Wong *et al.*, 2009; Wong & Tan, 2012). In addition to

endothelial cell and parenchymal organ damage, including neuronal necrosis, there is extensive lymphoid necrosis.

Relapsing encephalitis is a feature of both HeV and NiV infection in people, and its pathogenesis appears distinct from the acute encephalitic infection. The lesions of encephalitis in the acute phase, as expected from haematogenous dissemination, are small, discrete, multiple and widely distributed (Wong *et al.*, 2009; Wong & Tan, 2012), consistent with systemic vasculopathy and ischaemic injury. In cases of relapsing encephalitis, lesions are confined to the central nervous system and there is no evidence of vascular pathology (Tan *et al.*, 2002; Wong, 2010). Affected areas are more extensive and comprise necrosis, oedema and mononuclear inflammation. There is prominent perivascular cuffing and gliosis in adjacent areas accompanying severe and widespread meningitis. Viral inclusions, antigen and RNA are present, mainly in neurones, ependyma and possibly glial cells and inflammatory cells, but infectious virus is not re-isolated from relapsing cases. It is surmised that relapsing encephalitis results from viral recrudescence from foci of virus persisting in the CNS from the initial acute infection, and parallels have been drawn to Measles virus encephalitis (subacute sclerosing panencephalitis, SSPE) (Tan *et al.*, 2002; Wong, 2010).

1.5.5 NiV and HeV infection in dogs, another probable secondary spill over host

Serological studies (Field *et al.*, 2001; Mills *et al.*, 2009) confirmed observations (Parashar *et al.*, 2000) that dogs were commonly infected with NiV during the Malaysian outbreak. This most likely occurred through direct contact with infected pigs or by eating uncooked pork products. The was no evidence to indicate dog-dog spread (Mills *et al.*, 2009). Necropsy data from two affected dogs, one of which had been found dead and the other exhibiting clinical signs similar to canine distemper (caused by a paramyxovirus of the genus *Morbillivirus*), revealed pulmonary oedema and interstitial pneumonia, non-suppurative meningitis with ischaemic rarefaction in the brain, and glomerulonephritis.

In July 2011, the first field case was reported of HeV antibody in a dog during the investigation of an equine HeV incident (PromedMail, 2011), and a second dog was diagnosed with HeV infection in July 2013 under similar circumstances (Kirkland *et al.*, 2015; PromedMail, 2013). No distinct clinical signs were reported in either dog. Histopathological

examination of the second animal revealed vasculitis with fibrinoid necrosis within the kidney, brain, lymph nodes, spleen, liver intestine and lung and non-suppurative inflammatory infiltrates throughout affected tissues. There was also moderate nonsuppurative meningitis and cerebral vasculitis with surrounding malacia. Immunohistochemical staining was positive for viral antigen in necrotic glomeruli and in the tunica media of a renal arteriole.

As described in the sections above, different infection phenotypes develop in naturally occurring spill over hosts. Severe systemic illness associated with destructive multisystemic lesions is seen in humans with NiV and HeV, and in horses with HeV. In contrast, while lesions associated with systemic viral infection occur in both porcine NiV infection and canine HeV infection, infected animals typically show subclinical to mild disease. This suggests that the susceptibility to severe systemic disease following henipavirus infection may be affected by, and reflect differences in, post-entry innate immune responses.

1.6 Henipavirus infection in laboratory animals

1.6.1 Severe systemic infection phenotype

The ferret, African green monkey (AGM), hamster and cat are species in which Henipavirus infection reliably results in severe multisystemic disease; these are considered to be human models of Henipavirus infection (Guillaume *et al.*, 2009; Wong *et al.*, 2003).

1.6.1.1 Experimental NiV and HeV infection in ferrets

Henipavirus infection in ferrets closely mirrors the characteristics of human infection and the species has been of value in pathogenesis studies and the evaluation of vaccines and therapeutics (Bossart *et al.*, 2009; Clayton *et al.*, 2012; Pallister *et al.*, 2009; Pallister *et al.*, 2011). They are uniformly susceptible to HeV and NiV infection and reliably develop disease following plausible natural routes of exposure. Clinical signs include depression, lack of grooming, cough (reported in NiV but not HeV infection), serous nasal discharge, dyspnoea, hind limb paresis and generalised tremors. Fever is present from day 6 post infection, and ferrets usually succumb to disease between days 7-10.

There were no differences in distribution or severity of lesions in ferrets following exposure to different infective doses of HeV virus (Pallister *et al.*, 2011). Gross pathological findings included cutaneous petechiation to ecchymoses, subcutaneous oedema of the head and neck, pulmonary petechiation, and haemorrhagic lymph nodes, including of the gastrointestinal tract and mesentery. Histopathological lesions were of systemic vasculitis with foci of necrosis, glomerulitis, splenitis (the latter two are likely to result from the vascular pathology), necrotising lymphadenitis (either resulting from vasculitis or direct infection of lymphoid cells) and severe bronchoalveolitis (from infection of respiratory epithelial cells and/or contribution of alveolar capillary degeneration). Endothelial and occasionally epithelial syncytical cells were often found. Positive immunostaining for viral antigen was present in endothelial cells in multiple organs, neurones and bronchoalveolar epithelium.

Virus was reisolated from a variety of organs, including brain, as well as nasal, oral, and rectal swabs, and urine, and occasionally from blood. Levels of viral genome were higher in oral secretions of ferrets infected with NiV-B than NiV-M, which may account in part for differences seen in transmissibility between humans of these two strains (Clayton *et al.*, 2012).

1.6.1.2 Experimental NiV and HeV infection in African green monkeys

The AGM is highly susceptible to lethal infection using an exposure dose of 10^4 PFU NiV or 10^5 $TCID_{50}$ HeV (Geisbert *et al.*, 2010; Rockx *et al.*, 2010). In both studies, animals developed a severe acute respiratory distress syndrome within 7 days post inoculation. There was severe systemic vasculitis with haemorrhage and oedema in almost every organ system examined, including the meninges. Viral antigen distribution matched the wide range of tissues described in the ferret.

However, by comparison to ferrets, the viral challenge dose was found to influence the disease course in non-human primates (Geisbert *et al.*, 2012). Monkeys exposed to lower doses of NiV ($<10^5$ PFU) survived longer and exhibited more neurological disease, whereas monkeys infected with higher doses ($>10^5$ PFU) succumbed earlier and primarily from respiratory disease. These experiments used an intra-tracheal route of exposure: this is

unlikely to exactly mimic a route of natural infection and does not so easily allow for investigation of alternative routes of CNS invasion, namely the olfactory or peripheral cranial nerve routes as proposed for pigs (Weingartl *et al.*, 2005), guinea pigs (Williamson *et al.*, 2001), hamsters (Munster *et al.*, 2012) and mice (Dups *et al.*, 2012).

The nonhuman primate (NHP) AGM model has proven suitable for assessing effectiveness of therapeutic agents (Bossart *et al.*, 2011; Rockx *et al.*, 2010), and the long history of pharmacokinetic comparisons between NHP and humans can provide meaningful indications of likely drug performance in humans. However, there are substantial ethical and welfare challenges associated with the use of NHP.

1.6.1.3 Experimental NiV and HeV infection in Syrian golden hamsters

Upon infection with either NiV or HeV hamsters exhibit both signs of respiratory (dyspnoea, serosanginous nasal discharge) and neurological (paralysis and tremors deteriorating to prostration, seizures) disease. Similar to the African green monkey, clinical signs and disease progression correlated with the infective dose, and were generally similar irrespective of route of infection (Guillaume *et al.*, 2009; Rockx *et al.*, 2011). Hamsters inoculated with 10^5 $TCID_{50}$ succumbed within 5 days with acute respiratory distress, whereas those inoculated with 10^2 $TCID_{50}$ developed milder respiratory disease which progressed to neurological disease and death by day 12 (Rockx *et al.*, 2011). At the lower dose rate, animals infected IN with HeV succumbed significantly earlier (day 7.5) than those infected IN with NiV (day 12).

Interestingly in the case of HeV infection, but not NiV infection, age also appeared to influence susceptibility in hamsters: 11 week old hamsters had a longer disease course than 7 week old hamsters and required a 10 fold higher dose of HeV to achieve 100% mortality (Guillaume *et al.*, 2004; Guillaume *et al.*, 2006; Guillaume *et al.*, 2009).

Time course studies showed similar progression for both viruses (Guillaume *et al.*, 2009; Rockx *et al.*, 2011) and supplemented information provided by studies in the pig (Weingartl *et al.*, 2005). On day 1-2, a necrosuppurative rhinitis was present as were small scattered foci of bronchial and peribronchial inflammation associated with small amounts of NiV viral antigen. Over days 3-5 in the lung the inflammatory aggregates became larger with

increasing extensive interstitial involvement, becoming widespread necrotising broncho-interstitial pneumonia and haemorrhage with large amounts of viral antigen throughout the lung (100% by day 5) and evident in pulmonary blood vessels. Necrotic bronchial epithelial cells with syncytial formation appeared. By day 5, antigen was also present in non-respiratory organs. In the brain it was manifest as large plaque like areas involving neurones and neuropil of the cerebellum and cerebral cortex, with smaller amounts in the meningeal vessels, parenchymal blood vessels and ependyma. In the spleen, antigen was identified in lymphocytes and blood vessels, while in the kidney it was present in glomerular tufts and tubular epithelial cells. Antigen was also found in hepatic blood vessels and sinusoids, and in cardiac endothelium and endocardium.

The presence of endothelial antigen preceded the development of fibrinoid necrosis of vessel walls and, as this progressed, syncytial cells were seen in increasing frequency leading to the formation of small necrotic plaques in the brain and spleen. Lesions in the brain were multifocal and randomly distributed, simultaneously affecting the cerebrum, cerebellum, hippocampus and the olfactory cortex, suggestive of haematogenous spread. There was a moderate to severe non suppurative meningitis +/- necrotising vasculitis, and areas of neuropil rarefaction and haemorrhage with neuronal necrosis and gliosis.

Virus was isolated from the brain by day 9 in NiV infected hamsters, in comparison to day 5 in HeV infected hamsters. In NiV infected hamsters lung lesions were seen to be resolving by days 10-12. No lymphoid replication of either virus was noted in the hamster, but this is likely a function of the extremely small size of peripheral lymph nodes precluding accurate sampling in the hamster by comparison with the pig (Weingartl *et al.*, 2005).

The hamster infection model has also been successfully utilized in studies evaluating antiviral therapies (Freiberg *et al.*, 2010; Guillaume *et al.*, 2006), and recently in transmission studies (de Wit *et al.*, 2011) and for comparison of NiV-B and NiV-M infections (DeBuysscher *et al.*, 2013). Interestingly in this study NiV-M-infected Syrian hamsters had more rapid virus replication, more severe pathology and increased death when compared to NiV-B-infected animals, a feature not noted in the ferret model (Clayton *et al.*, 2012).

The hamster model was the first model in which certain elements of the host response to infection were assessed in detail (Rockx *et al.*, 2011). IP-10 expression was up-regulated in both the lung and brain and this correlated both with virus replication and inflammatory cell influx in these tissues. IL-4, IL-6, TNFα and IFNϒ were also upregulated in the lung, but to a lesser degree and actually down regulated in early infection in the brain.

The hamster model was also used for further investigation of Henipavirus encephalitic disease and neuroinvasion (Munster *et al.*, 2012). The study showed that NiV initially predominantly targeted the olfactory epithelium in the nasal turbinates and crossed the cribriform plate via olfactory neurones, with subsequent dissemination through the olfactory tract in the ventral cerebral cortex via anterograde axonal transport. NiV entry into the CNS coincided with the occurrence of respiratory disease, suggesting that the initial entry of NiV into the CNS occurs simultaneously with, rather than as a result of, systemic virus replication.

1.6.1.4 Experimental HeV and NiV infection in Cats

Cats proved highly susceptible to HeV infection in the initial pilot study (Westbury *et al.*, 1995), with a short clinical course of 5-9 days culminating in severe respiratory disease and lesions mimicking those seen in horses (Hooper *et al.*, 1997b; Westbury *et al.*, 1996; Westbury *et al.*, 1995). They succumbed to non-parenteral (oral and nasal) and parenteral routes of exposure with a similar disease course (Hooper *et al.*, 1997b; Westbury *et al.*, 1996; Westbury *et al.*, 1995), although it was noted that intranasal and oral exposure resulted in more severe pulmonary lesions (Hooper *et al.*, 1997b). Doses used were 10^3 $TCID_{50}$ and 5000 $TCID_{50}$ (Hooper *et al.*, 1997b; Westbury *et al.*, 1996; Westbury *et al.*, 1995). Virus was reisolated from the respiratory tract, various internal organs including the brain and gastrointestinal tract (raising the possibility of faecal shedding), and urine (Hooper *et al.*, 1997b; Westbury *et al.*, 1996). Cat to cat in-contact transmission has been demonstrated (Hooper *et al.*, 1997b; Westbury *et al.*, 1996; Williamson *et al.*, 1998), although not all in-contact cats became infected, suggesting low transmissibility (Westbury *et al.*, 1996).

Experimental NiV infection in cats was similar to HeV infection, however NiV antigen was present extensively throughout all levels of the respiratory epithelium (including the

trachea) associated with ulceration and inflammation (Middleton *et al.*, 2002). Moderately severe non-suppurative meningitis was also present in addition to meningeal vasculitis (Middleton *et al.*, 2002). Findings in a pregnant cat infected with NiV mirrored those of pregnant HeV infected guinea pigs, confirming vertical transmission in this species (Mungall *et al.*, 2007). One field case of NiV infection is reported in the cat (Hooper *et al.*, 2001). In contrast to the experimental infections, the lung was less severely affected compared to the brain, kidney and liver.

1.6.2 Intermediate infection phenotype

Experimental infection of Guinea pigs with HeV or NiV and experimental NiV infection in squirrel monkeys may result in multisystemic disease but subclinical infection is common.

1.6.2.1 Experimental HeV and NiV infection in guinea pigs

Guinea pigs were one of only two small laboratory mammals that were found to be susceptible to disease in early pathogenicity studies involving HeV (the other being the cat) (Westbury *et al.*, 1995). When inoculated subcutaneously with 5 000 $TCID_{50}$ HeV they succumbed between day 7 and 15 post infection, with respiratory distress and pneumonia of similar appearance to that seen in the initial studies in horses. Systemic vascular degeneration with endothelial syncytial cell formation and thrombosis developed in many organs of some animals, similar to that reported in humans, ferrets and cats animals (Hooper *et al.*, 1997b; Williamson *et al.*, 2000; Williamson *et al.*, 2001). It was noted that the affected vessels were larger, reported as between 20 and 80 µm in diameter, than the microvascular predominance seen in other animals (Hooper *et al.*, 1997b) and this was proposed as an explanation for the lack of pulmonary oedema observed (Hooper *et al.*, 2001).

In a subsequent study, 50, 000 $TCID_{50}$ HeV administered subcutaneously produced clinical signs of head tilt, ataxia, torticollis and depression from day 7 to 15 post infection that was attributable to the presence of meningoencephalitis (Williamson *et al.*, 2001). Other challenge routes inconsistently resulted in infection, with IN infection inducing systemic vascular disease in some animals while intradermal (footpad) inoculation failed to establish infection (Hooper *et al.*, 1997b; Williamson *et al.*, 2001). A small mammal model of HeV

encephalitis was of interest and relevance when it was discovered that a human HeV fatality had occurred due to relapsing encephalitis (Allworth *et al.*, 1995) , but work was not pursued further in this species, perhaps because of the inconsistencies in disease induction.

Pregnant guinea pigs were also investigated because several of the early equine cases were pregnant mares (Murray *et al.*, 1995; Rogers *et al.*, 1996) and there was an apparent seasonality to outbreaks coinciding with the flying fox breeding cycle. In pregnant guinea pigs, placental lesions were present as part of systemic vascular degeneration. While several vessels in foetuses showed positive immunolabelling and virus was able to be isolated from foetal tissues, this was not associated with the presence of lesions (Williamson *et al.*, 2000). Antibodies were present in some animals that survived exposure (Hooper *et al.*, 1997b; Williamson *et al.*, 2000; Williamson *et al.*, 2001).

Guinea pigs have been experimentally infected with NiV, by the IP and IN routes, at doses ranging from 5 to 50, 000 $TCID_{50}$ and $>10^6$ PFU, with only some animals exhibiting transient mild clinical signs including fever, weight loss, ruffled fur and mild ataxia (Middleton *et al.*, 2007; Wong *et al.*, 2003). Lesions in affected subjects were, as in other species, systemic vasculitis with endothelial syncytia, and virus was isolated from various tissues and blood (Middleton *et al.*, 2007).

1.6.2.2 Experimental NiV infection in Squirrel monkeys

Squirrel monkeys were not consistently susceptible to disease except via intravenous inoculation, and the infection characteristics did not closely mimic findings in human infection (Marianneau *et al.*, 2010).

1.6.3 Mild systemic infection phenotype

1.6.3.1 Experimental HeV infection in wild type mice

Initial studies concluded that the mouse was resistant to Henipavirus infection and for many years it was discounted as a model for Henipavirus research (Westbury *et al.*, 1995; Wong *et al.*, 2003). However, more recent investigations in wild type mice (Dups *et al.*, 2012) have demonstrated that both young adult (10 week old) and aged (12 month old) C57Bl/6 and Balb-C mice challenged IN with 50 000 $TCID_{50}$ HeV are susceptible to viral encephalitis.

Subclinical neurological infection was also documented in Balb-C mice. A significant difference in response to infection was seen between aged and juvenile mice, where aged mice appear to have a greater propensity to develop clinical disease compared with juvenile animals.

Affected mice presented with peracute neurological disease characterised by depression, ataxia, hypersensitivity and tremors. Antigen was present in olfactory epithelium where viral infection also caused necrosis, erosion, and ulceration. In the brain HeV antigen appeared to be confined to neurones. The pattern and time course of detection of viral antigen and lesions proceeded through the olfactory bulb to the deeper structures in the olfactory pathway (such as the olfactory cortex including the olfactory tubercles, piriform lobe and amygdala), then onto the hippocampus, thalamus and hypothalamus. This supported a transneuronal mode of spread of virus within the murine brain, possibly mediated via synaptic connections. In addition, mild transient upper and lower respiratory tract infection was observed but this was associated with minimal pathological lesions, no evidence for systemic viral spread, and was followed by resolution with minimal evidence of an adaptive immune response in terms of virus neutralising antibody. The distribution of viral antigen in the mouse brain was different to the random, multifocal distribution of Henipavirus infection in humans, ferrets and AGM secondary to haematogenous dissemination from viraemia as described in the sections above.

The wide range of murine immunological and biochemical reagents, their small size, ready availability, and ease of handling make the mouse ideal for use in this research field under BSL-4 conditions.

1.6.3.2 Experimental NiV infection in wild type mice

Dups *et al.* (2014) subsequently investigated IN NiV infection in young adult and aged C57BL6 and BalbC wild type mice, and demonstrated that mice exposed to 50 000 $TCID_{50}$ of NiV-B or NiV M developed a subclinical self-limiting lower respiratory tract infection with no evidence of encephalitis or systemic infection.

Henipavirus infection phenotypes seen different animal models are compared in Table 1.2.

Table 1.2: Summary of Henipavirus infection phenotypes in different animal models

Animal model	Infection phenotype	Details
African Green Monkey	Severe multisystemic disease	Highly susceptible Challenge dose influenced disease course Severe acute respiratory distress syndrome and neurological disease. Severe multisystemic vasculitis. Pathogenesis and therapeutic studies
Ferret	Severe multisystemic disease	Uniformly susceptible independent of challenge dose Multisystemic vasculitis, necrotising lymphadentitis, bronchoalveolitis. Pathogenesis (including comparison of NiV-B to NiV-M), transmission, vaccine and therapeutic studies
Hamster	Severe multisystemic disease	Highly susceptible Challenge dose influenced disease course Multisystemic vasculitis. Respiratory and neurological disease Slight differences between NiV and HeV infection with respect to time to death and age affecting susceptibility Pathogenesis (including comparison of NiV-B to NiV-M and neuroinvasion models), transmission and therapeutic studies
Cat	Severe multisystemic disease	Highly susceptible Severe respiratory disease, multisystemic vasculitis Pathogenesis and transmission studies
Guinea pigs	Intermediate	Route dependent susceptibility, inconsistent infection Infection may result in multisytemic vasculitis, respiratory or neurological disease, subclinical infection common
Squirrel monkey	Intermediate	Susceptible by IV route only Multisystemic infection but mild histological lesions Respiratory and neurological disease
Immunocompetent mice	Mild	Route dependent infection Transient mild respiratory infection HeV but not NiV infection resulted in olfactory bulb encephalitis. Age related differences in susceptibility
Immune deficient mice		
- C57Bl6 Ifnar1-/-	Intermediate	Virus and route dependent. Much higher LD50 than hamster Susceptible to NiV infection and often fatal neurological disease. HeV systemic replication with subclinical disease
- A129/Sv Infar1-/-	Intermediate	Real time bioluminescent imaging of chimeric viruses Virus and route dependent. Subclinical and systemic infection with neurological disease
- NSG	Mild	Human lung xenograft model. Systemic infection with subclinical disease. Viral replication was much higher in human tissue graft than in mouse tissue

1.7 Henipavirus in other mice models

1.7.1 Experimental Henipavirus infection in *Ifnar1-/-* mice

While conducting the studies involved in this thesis, another research group reported fatal Henipavirus infection of *Ifnar1-/-* mice on a C57BL6 background (Dhondt *et al.*, 2013). These mice have a null mutation in the gene for a subunit of the type I interferon receptor (*Ifnar1-/-*). In these mice the type 1 IFN signalling response to the recognition of viral antigen within cells, subsequent induction of interferon stimulated genes (ISG) and the ensuing mediation of antiviral immunity is severely attenuated, making these mice highly susceptible to viral infection (Hwang *et al.*, 1995). The findings of Dhondt *et al.* (2013) pertaining to HeV infection in *Ifnar1-/-* mice are discussed in depth in Chapters 4, 5 and 6 of this thesis.

1.7.2 NiV infection in *Ifnar1-/-* mice

Dhondt *et al.* (2013) found that all *Ifnar1-/-* mice succumbed to IP challenge with NiV, and 3 out of 5 mice challenged IN with NiV also succumbed. The effect of age on NiV susceptibility was not investigated but a LD_{50} of 8 x 10^3 PFU was established using IP doses from 100 to 10^6 PFU of NiV in 9-10 week old *Ifnar1-/-* mice,. This was much higher than for the hamster model (Rockx *et al.*, 2011). Fatalities all occurred between day 6 and 10 post infection.

Clinical signs in affected *Ifnar1-/-* mice were mainly neurological and similar to those reported in wild type mice (Dups *et al.*, 2012). First signs were agitation and edginess and lack of grooming, progressing to positive grimace scoring which is an indication of pain in mice (Langford *et al.*, 2010; Leach *et al.*, 2012), lordosis, aggression, and finally locomotor disability, head tilt and paralysis. A 15-20% loss in body weight occurring 1-2 days prior to death was reported as a good predictive indicator of onset of terminal disease, which differed from findings previously reported in wild type mice (Dups *et al.*, 2012). Histological lesions in the lung were described as intense inflammation, oedema, focal necrotising alveolitis and vasculitis. Microscopic lesions in the brain were described as parenchymal and meningeal non-suppurative inflammation, widespread vasculitis associated with haemorrhage and perivascular cuffing. Eosinophilic inclusions in neurones in affected areas were interpreted by Dhondt *et al.* (2013) as indicating hypoxic-ischaemic neuronal injury, but these changes have been reported by other researchers in other species as

characteristic paramyxovirus inclusions. Immunohistochemical staining for viral antigen was positive in ependymal cells and neurones. There was also severe acute hepatitis with vasculitis and syncytial cell formation described. In the kidney, lesions were less severe and described as inflammation associated with vasculitis.

Dhondt *et al.* (2013) also reported, albeit briefly, findings after NiV exposure of wild type C57Bl/6 mice similar to Dups *et al.* (2014). While wild type mice did not succumb to IP NiV challenge, small amounts of NiV N protein were present on PCR within the lung and spleen of 2/6 mice in the highest challenge dose group (10^6 PFU) which was taken to support subclinical infection had occurred. Mild inflammation of the brain was also reported, but no viral antigen was present on immunohistochemical staining. No data was presented for IN challenge of wild type mice.

1.7.3 Other mice models

Towards the latter stages of this thesis two other papers were published addressing further aspects of murine Henipavirus infection. Specifically, one paper utilised *Ifnar1-/-* mice on a background of A129/Sv to perform real time bioluminescent imaging to assess viral replication and spread for determinants of virulence in chimeric henipaviruses (Yun *et al.*, 2015). The other paper examined a human lung xenograft model of NiV infection using NSG (or NOD/SCID/ɣcnull) mice to study the *in-vivo* pathogenesis of NiV infection in human lung (Valbuena *et al.*, 2014). Each of these papers will be considered in the discussion relating to the experimental findings.

Ephrin gene expression and distribution has been evaluated in healthy adult mice via mRNA concentration in microarray (Favre *et al.*, 2003) and mice genetically engineered with a LacZ-labelled Ephrin gene (Gale *et al.*, 2001). These studies have shown ephrin B2 to be highly expressed by endothelial cells in a large number of organs, by smooth muscle of arterial vessels and the endothelium, and by pericytes of the arteriolar side of capillary beds. In the brain, numerous neurones also express ephrin B2. In the lung it is expressed at higher levels in the endothelial cells than in other lung cell populations (Favre *et al.*, 2003). When mouse ephrin B2 is expressed in previously non-permissive cell lines they are highly functional and have a high affinity for binding with the Henipavirus attachment glycoprotein (Bossart *et al.*,

2008). However, there are some rat and mice cell lines shown to express ephrin B2, both through the presence of encoding RNA and receptor labelling on the cell surface, which are not permissive to Henipavirus infection (Yoneda *et al.*, 2006).

These combined findings suggest the relative resistance of wild type mice to systemic Henipavirus infection may be in part attributable to a post entry event. Uncovering the mechanism of Henipavirus restriction in murine models may inform future development of post-exposure therapeutics applicable for human use.

1.8 Henipavirus molecular virology

Paramyxoviruses are large, enveloped, negative sense, single stranded, non-segmented RNA viruses of the order Mononegavirales, family Paramyxoviridae and are characterised by the presence of a fusion (F) protein which causes viral-cell membrane fusion at a neutral pH. This family shares a close relationship to Orthomyxoviridae and Rhabdoviridae because of the similarity of their envelope glycoproteins and non-segmented genomes respectively (Fields *et al.*, 2007)

The family Paramyxoviridae is morphologically distinguished by the size and shape of the viral nucleocapsid. Within the family Paramyxoviridae there are five genera, *Respirovirus, Rubulavirus, Avulavirus, Morbillivirus* and *Henipavirus* in addition to a number of distinct viruses which are not currently classified into genera (Figure 1.3). Genera are based on the biological criteria of antigenic cross-reactivity between viruses, the presence (*Respirovirus* and *Rubulavirus*) or absence (*Morbillivirus* and *Henipavirus*) of neuraminidase activity, the differing coding potentials of the P genes and the presence of an additional gene (the SH gene) in some rubulaviruses, J virus, and Beilong virus (Fields *et al.*, 2007)

Hendra, Nipah and Cedar viruses comprise the genus Henipavirus (Chua *et al.*, 2000; Marsh *et al.*, 2012; Rota *et al.*, 1999; Wang *et al.*, 2001) , although there have recently been several novel Henipa-like viruses discovered that will likely add to the genus (Drexler *et al.*, 2009; Sasaki *et al.*, 2012). Cedar virus and the Henipa-like viruses are discussed further under the heading “New viral discoveries and globalisation”.

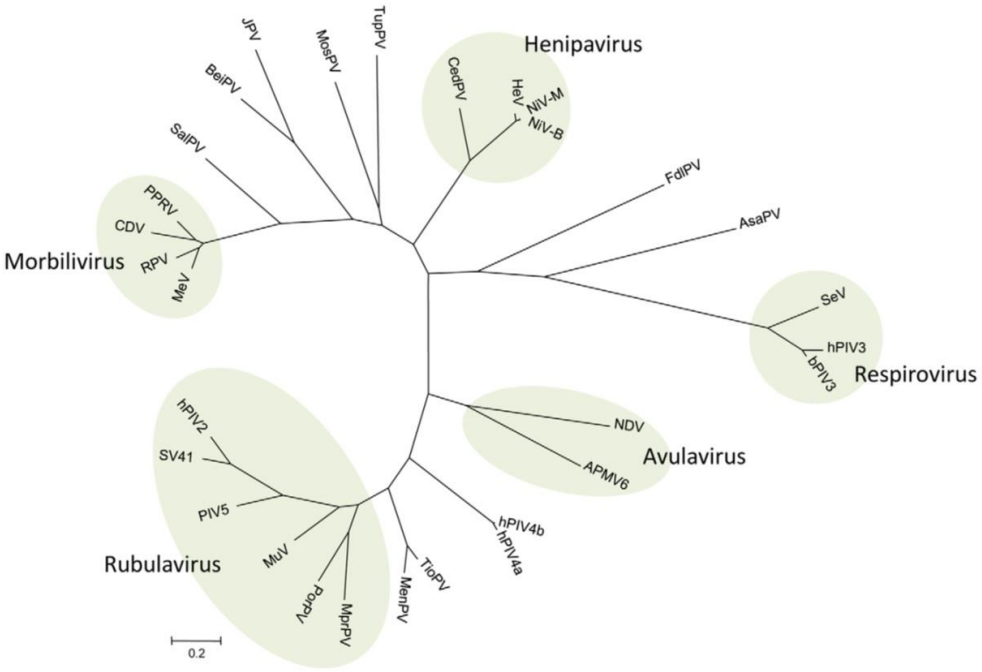

Figure 1.3 Phylogenetic tree based on the N protein sequences of selected paramyxoviruses (Marsh *et al.*, 2012) Note: incorrect spelling of Morbillivirus taken directly from published figure. More recently discovered NiV-I for isolates from India, and NiV-P for an isolate from the Philippines, have since been added to the Henipavirus phylogenetic tree (Ching *et al.*, 2015) these are illustrated in Figure 1.2.

1.8.1 The viral genome

Complete genomes of all fully sequenced paramyxoviruses are available from www.ncbi.nlm.nih.gov

The Paramyxoviridae genome ranges from 15000 to slightly over 19000 nucleotides (Fields *et al.*, 2007). The Henipaviruses, with Cedar virus at 18162 nucleotides, Hendra virus at 18234 nucleotides, and Nipah virus at 18246 nucleotides, are significantly larger than most other paramyxoviruses (Harcourt *et al.*, 2000a; Marsh *et al.*, 2012; Wang *et al.*, 2000) with the exception of the rodent paramyxoviruses J virus, Beilong virus and Tailam virus (Jack *et al.*, 2005; Li *et al.*, 2006; Woo *et al.*, 2011).

The genome consists of a 3’ leader sequence of approximately 50 nucleotides; 6 genes, comprising the nucleocapsid (N), phosphoprotein (P), matrix (M), fusion glycoprotein (F), attachment glycoprotein (G), large (L) polymerase; and a 5’ trailer sequence of 50 – 161 nucleotides. The 3’ leader and 5’ trailer sequences are genus specific and serve as promoters for transcription and replication (Fields *et al.*, 2007).

The larger Henipavirus genome is due to a longer open reading frame encoding the P gene and unique, long, untranslated regions at the 3' end flanking each gene except the L gene (Harcourt *et al.*, 2001; Harcourt *et al.*, 2000a; Wang *et al.*, 2000; Yu *et al.*, 1998).

1.8.2 Viral structure

Paramyxoviridae are generally spherical and range from 150-500 nm in diameter, but pleomorphic and filamentous forms may be observed. They have a lipid bilayer envelope derived from the host cell membrane. Attachment (HN or G) and fusion (F) glycoproteins project from the envelope surface. Matrix protein forms a layer underlying the envelope but, while closely associated with the lipid bilayer, M proteins are not intrinsic membrane proteins. The small integral membrane protein, SH, is found only in some rubulaviruses. The nucleocapsid is helical, and comprised of a core of N protein and genomic RNA to which P and L proteins are attached. Protein V is an internal component of the virion in rubulaviruses, but in other members of the Paramyxovirus family is only found in virus-infected cells.

1.8.3 Viral receptors

Henipaviruses and morbilliviruses are the only two paramyxoviruses that use host cell proteins as receptors. The Henipavirus attachment glycoprotein G binds with the ephrin-B2 ligand and/or the ephrin-B3 ligand for infection (Bonaparte *et al.*, 2005; Bossart *et al.*, 2008; Negrete *et al.*, 2005).

Ephrin-B2 and B3 are trans-membrane proteins of the tyrosine kinase family involved in bi-directional cellular signaling. They are comprised of an extracellular ligand-binding domain, a transmembrane domain and a cytoplasmic kinase domain (Zhou, 1998).

Analysis of ephrin B2 and B3 DNA and protein sequences from human, horse, pig, cat, dog, mouse and two species of flying fox (*Pteropus alecto and Pteropus vampyrus*) showed they are highly conserved across species, ranging from 91-98% homology at the amino acid level, with mice demonstrating the lowest level of conservation (Bossart *et al.*, 2008). There were minor alterations in protein sequences in both the bat and mouse but these caused no significant functional differences. HeV and NiV use both ephrin B2 and B3 receptors with

similar affinity (Bossart *et al.*, 2008). This suggests that the host receptor molecules do not play a major role in any differences in the characteristics of infection that may be seen between species.

Ephrin B2 is expressed in a wide variety of tissues both during embryogenesis and in mature animals. However expression is highest during embryogenesis where it functions in modulating cell migration and morphogenesis, especially with respect to neuronal dendritic processes and angiogenesis (Augustin & Reiss, 2003; Palmer & Klein, 2003; Poliakov *et al.*, 2004; Zhou, 1998). In adults, ephrin B2 expression is highest within the brain, arterial endothelial cells, the smooth muscle cells of the arterial walls, at sites of angiogenesis, lung, placenta and prostate (Gale *et al.*, 2001; Liebl *et al.*, 2003). Ephrin B3 is mostly restricted to the central nervous system, with some expression in the prostate and heart (Pernet *et al.*).

Cell expression of ephrin B2 and B3 correlates with Henipavirus tissue tropism and disease pathology. The cells most severely affected and exhibiting the highest high levels of viral antigen are neurons, endothelial cells, the smooth muscle of the tunica media of arterial walls, vessels of the white pulp in the spleen (which are arterial), the sinusoidal lining of lymph nodes, and placental tissues (Hooper *et al.*, 2001; Lee, 2007; Makinen *et al.*, 2005; Williamson *et al.*, 1998; Wong *et al.*, 2002a).

On the other hand, P815 mouse mast cells and 208f rat embryonic fibroblasts are cell lines that express ephrin B2 on their cell surfaces but are non-permissive to Henipavirus infection (Yoneda *et al.*, 2006). Additionally, the efficiency of virus replication in the L2 rat lung epithelium and 4/4RM4 rat epithelium cell lines is lower compared to human cells (HeLa and 293T) and hamster (CHO) cells expressing human ephrin B2, as evidenced by delayed development of CPE and a marked reduction in the size and number of syncytia, (Yoneda *et al.*, 2006). This suggests factors other than host cell receptors affect the efficiency of Henipavirus infection and replication.

The level of ephrin B2 mRNA expression does not necessarily correlate with the level of ephrin B2 protein on the cell surface. In the mouse, ephrin B2 protein distribution in the brain has been assessed via immunohistochemical staining (Migani *et al.*, 2009) and correlates reasonably well with ephrin B2 expression as assessed by mRNA via *in situ*

hybridisation (Liebl *et al.*, 2003). In nervous tissue, ephrin B2 is localised to neuronal cell bodies with subcellular localisation to the somatic membrane. Interestingly, although mRNA expression is high within the olfactory bulb, the neurones within the mitral cell, granule cell, and glomerular layers of the olfactory bulb stain only weakly for ephrin B2 on their surface. And the latter are the areas in which we see a large amount of HeV antigen in mice with HeV encephalitis established via intranasal exposure and infection of olfactory sensory neurones (Dups *et al.*, 2012). Ephrin B2 immunoreactivity is more intense within neuron cell bodies of the olfactory tubercle, and greater yet in neurones within the pyriform cortex lying further along the olfactory tract. Differences between mRNA expression and the presence of stained protein on the cell surface are also present within the layers of the hippocampus (Liebl *et al.*, 2003; Migani *et al.*, 2007).

The high level of conservation of the ephrin B2 and B3 receptors and their similar level of function across a wide range of species, coupled with similar receptor usage by both HeV and NiV, account for the broad range of species infected by henipaviruses which is unparalleled by other paramyxoviruses.

1.8.4 Viral replication

Viral replication takes place in the cytoplasm. Viral RNA synthesis requires the nucleocapsid (N), P and large (L) proteins (Halpin *et al.*, 2004) and assembly requires translocation of the matrix (M) protein to the nucleus (Wang *et al.*, 2010).

The large protein (L protein) is the catalytic subunit of the viral polymerase. The P protein is a non-enzymatic essential component of the viral RNA-dependant RNA polymerase complex (Harcourt *et al.*, 2000b; Wang *et al.*, 1998). Viruses in the *Paramyxovirinae* subfamily have the ability to encode multiple proteins from the P gene. The coding capacity of the P gene is extended by the presence of overlapping open reading frames (ORF), allowing the addition/s of one, two or three guanine (G) residues at a characteristic editing site to produce P, V and W proteins respectively. The presence of an alternative translation codon produces the C protein (Harcourt *et al.*, 2000b; Wang *et al.*, 1998; Wang *et al.*, 2000). The frequency at which the P protein is edited is much higher in henipaviruses than in other paramyxoviruses. The frequency of editing also varies with time, with little editing early in

infection but increased frequency over time with the insertion of up to 11 residues later in infection (Kulkarni *et al.*, 2009; Lo *et al.*, 2009).

1.8.5 Viral attachment, membrane fusion and viral entry:

Paramyxoviruses are enveloped viruses and viral entry requires fusion of the viral envelope with the cell membrane (Smith *et al.*, 2009). Membrane fusion is also essential for cell to cell fusion (syncytium formation) contributing to cell to cell viral transmission: syncytia are a hallmark of infected tissues in Henipavirus infections (Escaffre *et al.*, 2013a; Hooper *et al.*, 2001; Hooper *et al.*, 1997b; Wong & Ong, 2011). Similar to other paramyxoviruses, membrane fusion involves a coordinated interaction of the attachment (G) glycoprotein and fusion (F) glycoprotein.

In comparison to other members of the subfamily *Paramyxovirinae* which utilise haemagglutinin-neuraminidase (HN) attachment glycoproteins, the Henipavirus G glycoprotein lacks haemagglutinating activity and does not bind to sialic acid residues or retain neurominidase activity (Fields *et al.*, 2007). Instead, the pneumonoviruses (RSV) and henipaviruses express a distinct attachment protein (G) (Lamb *et al.*, 2006) that recognises cell surface receptors, namely ephrin B2 or B3 for henipaviruses. Current NiV and HeV models of infection propose that binding of G to ephrin B2 or B3 triggers activation of the fusion cascade but, although many specific contributions have been discovered, the intricacies of this process have not yet been fully elucidated (Aguilar & Iorio, 2012).

The Paramyxovirus fusion (F) protein is a class I fusion protein. This class of fusion protein is shared with many other viruses including Ebola virus (GP2 protein), HIV-1 (gp41 protein), Moloney murine leukaemia virus (p15E protein) and Influenza virus (haemagglutin protein) (Baker *et al.*, 1999; Carr & Kim, 1993; Fass *et al.*, 1996; Malashkevich *et al.*, 1999). These F proteins are synthesised as inactive precursors that require protease cleavage to become biologically active. The majority of paramyxoviruses utilise furin for F protein cleavage, a ubiquitous calcium dependent host cell serine protease active during transport through the trans-Golgi secretory pathway (Smith *et al.*, 2009). A small number of F proteins are cleaved by a tissue specific protease after they reach the cell surface, for example SeV F protein. In comparison and unique to henipaviruses, the Henipavirus precursor F protein is cleaved by

Cathepsin-L in acidic lysosomes/endosomes (Meulendyke *et al.*, 2005; Michalski *et al.*, 2000; Pager & Dutch, 2005) in a process that requires endocytic recycling (Popa *et al.*, 2012). However, the route and mechanisms of the endocytic pathway and the signals involved are still largely unknown.

1.9 Henipavirus interactions with the innate immune system:

The type I interferons are a family of cytokines that are critical to the innate immune response to viral infection, as has been extensively reviewed (Gerlier & Lyles, 2011; Gibbert *et al.*, 2012; Katze *et al.*, 2002; Piehler *et al.*, 2012; Randall & Goodbourn, 2008; Teijaro, 2016). In humans and mice, the type I IFN are comprised of 13 subtypes of IFNα and 14 subtypes of IFNβ as well as IFNε, IFNκ, IFNτ and IFNω have been identified to date. They elicit a wide variety of responses which have been recently compared and contrasted (Ng *et al.*, 2016), including antiviral and antibacterial activities, and have a role in regulation of the development and activation of virtually every effector cell of the innate and adaptive immune response.

1.9.1 Interferon production

The interferon response is initiated in cells by the detection of the presence of viral genome by pathogen pattern recognition receptors. In the case of RNA viruses like henipaviruses, these include Toll-like receptors (TLR) 3, 4, 7 and 8 as endoplasmic sensors and retinoic acid-inducible gene 1 protein (RIG-1) and Melanoma Differentiation-Associated protein 5 (MDA-5) as cytoplasmic sensors. Binding of viral RNA with TLR3 leads to downstream signalling through the TLR adaptor molecule 1 (TRIF) whereas all other TLR use MyD88. Binding with either RIG-1 or MDA-5 mediates an interaction with the mitochondrial-bound protein IPS-1. Activation via both recognition receptor types results in the triggering of a signalling cascade in which the transcription factors IRF3 and/or NFκB are phosphorylated, permitting their translocation from the cytoplasm into the nucleus where they induce the synthesis of IFNα, IFNβ and IFNλ.

1.9.2 Interferon signalling

Once IFNs are produced they are secreted from the cell and bind to their receptor, a transmembrane protein, on adjacent cells. All subtypes of type I interferons characterized so far interact with, and signal through, a common receptor, namely the interferon type 1 receptor (IFNAR). IFNAR is composed of two subunits, IFNAR1 and IFNAR2. Binding of IFN to IFNAR leads to activation of the Janus protein tyrosine kinases, TYK2 and JAK1, which in turn initiates phosphorylation of the signal transducers and activators of transcription, STAT1 and STAT2. Phosphorylated STAT1 and STAT2 form a heterodimer and translocate to the nucleus and, together with IRF9, form the transcription factor ISGF3 (IFN stimulated gene factor 3). ISGF3 binds IFN-stimulated regulatory elements (ISREs) and activates the transcription of IFN-stimulated genes, resulting in the production of a multitude of proteins that are responsible for an antiviral state. For example, antiviral proteins produced include protein kinase R (PKR), oligoadenylate synthetase (OAS), myxovirus resistance protein (Mx), apolipoprotein B mRNA-editing enzyme catalytic polypeptide-like (APOBEC), or tripartite motifs (TRIM) which directly inhibit viral replication. IFN stimulated genes also enhance the proliferation and cytotoxicity of NK cells, up-regulate MHC expression of antigen presenting cells, enhance the interaction of dendritic cells with lymphocytes and antibody production by B cells, and augment the cytotoxicity of CD8+ T lymphocytes and macrophages, important features of the adaptive immune response.

The type III interferon, interferon lambda (IFNλ), is also induced in response to viral infection and has similar biological activities to the type 1 IFNs (Ank *et al.*, 2006; Pulverer *et al.*, 2010; Randall & Goodbourn, 2008; Sommereyns *et al.*, 2008). While the receptors for type I IFNs are expressed in most cell types, receptors for IFNλ are concentrated in organs with a high epithelial content such as intestines, skin, and lungs. While IFNλ uses a different transmembrane cell receptor composed of IL-10Rβ and IL-28Rα subunits for signalling rather than IFNAR, signal transduction proceeds down the same pathway of STAT phosphorylation. Both the interferon signalling and production pathways and their antagonism by henipaviruses are illustrated in Figure 1.4.

1.9.3 Henipavirus antagonism of the innate immune response

Similar to other paramyxoviruses, the P gene of HeV and NiV can be edited to encode several viral proteins, the P, V, W and C proteins, which all inhibit the host IFN antiviral response in one or more ways. The interactions of Paramyxovirus, and specifically Henipavirus, P gene products with the interferon response have been extensively investigated in many different cell types and their detailed molecular basis explored and reviewed (Basler, 2012; Chambers & Takimoto, 2009; Goodbourn & Randall, 2009; Ramachandran & Horvath, 2009; Shaw, 2009). The extent of inhibition of the interferon response is reported to vary between investigators and cell types.

Interferon production is inhibited by the Henipavirus V and W proteins (Figure 1.4). The V protein is cytoplasmic and binds to MDA-5, preventing downstream signalling. This binding has been confirmed to occur in a mouse derived cell line (L929) (Childs *et al.*, 2007), but the lack of systemic disease in wild type mice infected with Henipavirus suggest that MDA-5 inhibition is not on its own sufficient for full expression of potential viral pathogenicity in this animal species. The V protein also binds LGP2 in a similar fashion to MDA-5, and, while not involved in active signalling, LGP2 has a role in regulating IFN production through RIG-1 and MDA-5 interaction. The W protein is localised to the nucleus and interferes with the activated form of IRF3 in the nucleus. In the presence of W protein, activated IRF3 is less stable and this reduces activation of the IFNβ promoter. Interestingly if the V protein is artificially localised within the nucleus it too can perform this function.

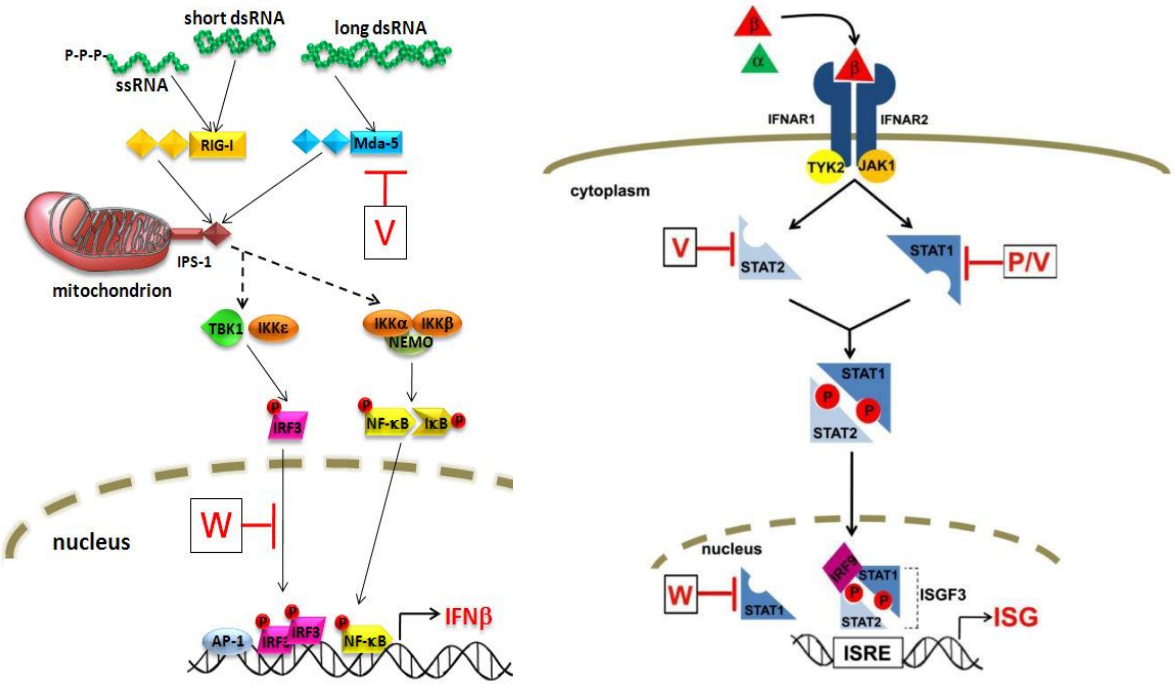

Figure 1.4: Interferon production (left) and interferon signalling (right) pathways and their inhibition by Henipavirus proteins, from Shaw (2009). Detection of viral RNAs by RIG-I and MDA-5 activates a signalling cascade though IPS-1 leading to the phosphorylation of IRF3 and NFκB. The activated transcription factors translocate to the nucleus and induce synthesis of IFN-β. The V protein prevents signalling by interacting with MDA-5, while the W protein interferes with the activated form of IRF3 in the nucleus. IFN-α/β binds to the interferon type 1 receptor (composed of IFNAR1 and IFNAR2 subunits). The receptor-ligand interaction activates the Janus protein tyrosine kinases, TYK2 and JAK1, which in turn activate the STAT1 and STAT2 transcription factors via tyrosine phosphorylation. The phosphorylated STATs form a heterodimer and translocate to the nucleus where together with IRF9, they form the ISGF3 (IFN stimulated gene factor 3) complex. This transcription factor complex binds to IFN-stimulated response elements (ISRE) and activates transcription of IFN-stimulated genes (ISG). The P and V proteins bind to STAT1 and the V protein also binds to STAT2 in the cytoplasm preventing activation in response to IFN. The W protein acts via the same mechanism but it sequesters STAT1 in the nucleus in an inactive form.

The ability of Henipavirus proteins P, V and W to prevent IFN signalling is dependent on STAT1 binding and inhibition of activation (Figure 1.4). The presence of P, V and W proteins inhibit the phosphorylation of STAT1 (Rodriguez *et al.*, 2003). In uninfected cells, non-activated STAT1 cycles between the cytoplasm and the nucleus. In infected cells, the P and V protein bind STAT1 in the cytoplasm and prevent its activation. Additionally, the V protein can also bind to STAT2. In the presence of V protein, STAT1 and STAT2 are sequestered into a high molecular weight multi-protein complex, but this is dependent on the presence of STAT1. The W protein binds to STAT1 and sequesters it in the nucleus, in its inactive form.

Of the three proteins, W protein has the strongest STAT1 inhibitory activity and the P protein the weakest activity (Shaw, 2009).

The presence of the P gene viral proteins V and C is important to the pathogenesis of Henipavirus-associated disease. W-deficient virus induced lethal disease in hamsters, but V-deficient and C-deficient viruses did not result in death of animals at any dose tested (Yoneda *et al.*, 2010) but the V and C proteins, in addition to their anti-interferon actions, also contribute to viral replication (Ciancanelli *et al.*, 2009; Yoneda *et al.*, 2010); attenuation of viral load may contribute to a decreased severity of disease. The major genetic difference between the apparently non-pathogenic Henipavirus, Cedar virus, and HeV or NiV lies within the P gene. Unlike HeV, NiV, and almost all known paramyxoviruses, the Cedar virus P gene lacks both RNA editing and also the coding capacity for the V protein. Preliminary studies indicated that Cedar virus infection of ferrets and guinea pigs was subclinical, and in human cells a more robust IFNβ response is able to be induced than with HeV (Marsh *et al.*, 2012). These observations support the role of the V protein in virulence. Bearing in mind its non-pathogenicity in ferret and guinea pig infection models, the discovery of CedPV provides an important tool for future research into the molecular basis of pathogenicity of henipaviruses.

In vivo studies have also demonstrated the importance of a functional interferon system in the pathogenesis of Henipavirus disease: hamsters were protected against lethal disease when the interferon system was stimulated with a synthetic RNA analogue (poly (I): poly ($C_{12}U$)) at the time of NiV infection. (Georges-Courbot *et al.*, 2006).

There is also interest in the response to Henipavirus infection in the natural host, pteropid bats. Both interferon production and signalling was blocked in different cell lines including primary cells from *Pteropus alecto* infected with HeV and NiV (Malaysia and Bangladesh strains) (Crameri *et al.*, 2009; Virtue *et al.*, 2011). This is startling given the lack of disease in experimentally infected bats (Middleton *et al.*, 2007), and lack of association with any naturally occurring disease in the reservoir species, and suggests other factors are mitigating the adverse impact of infection in this species. The recent characterisation of the immune transcriptome of the Australian flying fox, *Pteropus alecto* (Papenfuss *et al.*, 2012) identified

genes involved in antiviral immunity in the bat and should direct further investigations into understanding the control of viral replication in bats.

1.10 Vaccines and therapeutics

There are no licensed or proven effective antiviral therapies available to treat human Henipavirus infections (Mahalingam *et al.*, 2012). Ribavirin and chloroquine have not been effective in animal models (Freiberg *et al.*, 2010; Georges-Courbot *et al.*, 2006; Pallister *et al.*, 2009; Rockx *et al.*, 2010) although an open label trial of the use of ribavirin in encephalitic patients during the Malaysian NiV outbreak suggested the drug reduced mortality (Chua, 2003). However ribavirin has not been an effective treatment in human HeV cases (Mahalingam *et al.*, 2012; Playford *et al.*, 2010). The most promising post exposure therapy is passive immunotherapy with the human monoclonal antibody (mAb) 102.4, against the HeV glycoprotein (G) protein (Bossart *et al.*, 2011; Bossart *et al.*, 2009). This was unsuccessful when trialled in one human HeV infected patient, however, a major factor likely contributing to treatment failure was that the patient was already suffering from severe encephalitis at the time of administration (Mahalingam *et al.*, 2012). There is clearly a place for additional therapies to assist in the post-exposure management of Henipavirus infections in people, possibly as a combined therapy with mAb 102.4.

In November 2012 a commercial HeV sub-unit vaccine for horses was released (Middleton *et al.*, 2014). The vaccine induces neutralising antibody which protects horses from lethal HeV challenge, eliminates viral shedding and prevents viral replication in tissues. Not only does this protect the health of the horse, but more importantly breaks the chain of transmission from bats to humans, reducing the risk to people in contact with horses. Availability of this vaccine will hopefully assist in reversing the very real trend (Mendez *et al.*, 2012) of Australian veterinarians leaving equine practice.

1.11 Project aim

This project aims to elucidate the mechanisms responsible for the resistance of mice to generalised HeV systemic infection and disease.

Determining the factors that suppress systemic replication of HeV and HeV-associated disease in mice is of ongoing importance, as they may guide new therapeutic approaches for prevention and control of HeV infection in humans.

CHAPTER 2: MATERIALS AND METHODS

2.1 Biosafety level 4 laboratory practice

All BSL-4 work was performed within the laboratory and animal rooms of the National Collaborative Research Infrastructure Strategy (NCRIS) funded BSL-4 facility, within the CSIRO Australian Animal Health Laboratory, Geelong, Australia.

Within the BSL-4 Laboratory, staff wore a fully encapsulating Sperian biocontainment suit (Delta Protection, France). Suits received an external piped air supply through a flexible filtered hose connected by a one way valve. Positive air pressure within the suit was constantly maintained with respect to ambient room pressure. To exit the BSL-4 laboratory operators passed through a chemical decontamination shower to clean the suit surface, then a personal shower. The integrity of the biocontainment suits was regularly tested, routinely maintained, and gloves were changed regularly.

All work was undertaken following legislation and guidelines pertaining to Security Sensitive Biological Agents (SSBAs), the Australian Quarantine Investigation Service (AQIS), the Office of the Gene Technology Regulator (OGTR), The Australian Security and Investigation Organisation (ASIO) and the AAHL Security Advisory Group (ASAG).

2.2 Viruses

For most studies, the HeV isolate used was a clinical isolate of HeV, from a horse in an outbreak associated with human infection, HeV/Australia/Horse/2008/Redlands, GenBank accession no. HM044317 (Marsh *et al.*, 2011). This was passaged 3 times on Vero cells and has a titre of $10^{7.5}$ $TCID_{50}$ in Vero cells. In Chapter 6, an isolate from the original outbreak, HeV/Australia/Horse/1994/Hendra, GenBank accession no. AF017149 (Murray *et al.*, 1995) was used for comparison purposes. This was passaged 4 times on Vero cells and has a titre of $10^{7.1}$ $TCID_{50}$/ml in Vero cells.

The Ebola (EBOV) virus used in Chapter 7 was a Zaire ebolavirus, Mayinga strain (GenBank accession no. NC 002549), obtained from Heinz Feldmann (Laboratory of Virology, Rocky

Mountain Laboratories, NIAID, NIH USA) which had a titre of 8.9 x 10^7 $TCID_{50}$/ml in VeroE6 cells.

2.3 Deactivation of BSL-4 viruses

All infectious or potentially infectious material derived from animal and cell infection studies was handled within the NCRIS BSL-4 laboratory. To remove material for further processing, inactivation methods were employed in accordance with AAHL standard operating procedures for operation at BSL4 and AQIS regulations for handling of imported infectious materials.

Tissue samples collected for histopathology were immersed in 10% neutral buffered formalin at 1:10 ratio within the BSL4 room for at least 48 hours, and then processed for histopathology. Serum samples were inactivated by exposure to 50 kGy γ-irradiation prior to handling for serology assays. At the completion of cell infection studies supernatants were collected and the cells were fixed in 10% neutral buffered formalin. For inactivation of HeV, the cells remained in formalin solution for at least 30 minutes. To ensure EBOV inactivation, the cells remained within formalin solution for 48 hours. Samples for RNA extraction were collected into a guanidinium thiocyanate-based solution (MagMAX™, Ambion®, Life Technologies) for processing for RNA extraction.

2.4 Animal infection studies:

2.4.1 Animal ethics statement:

These studies were approved by the Commonwealth Scientific and Industrial Research Organisation (CSIRO), Australian Animal Health Laboratory (AAHL) Animal Ethics Committee (AEC), approval numbers; 1549, 1599, 1600, 1601. They were also approved as external experimental work, approval number MMCA/2013/29-FW, through the AEC of the Hudson Institute of Medical Research, Monash University. Experiments were conducted in compliance with the Australian National Health and Medical Research Council's (ANHMRC) Australian Code of Practice for the Care and Use of Animals for Scientific Purposes, 7th Edition 2004 and 8th Edition 2013.

2.4.2 Mice

Wild type (WT) mice (C57BL6JArc) were sourced from the Animal Resources Centre, Canning Vale, Western Australia, Australia.

Ifnar1-/- and *Ifnar2*-/- on a background of C57BL6 mice were sourced from the Centre for Innate Immunity and Infectious disease, Hudson Institute of Medical Research, Clayton, Victoria, Australia (Hardy *et al.*, 2001; Hwang *et al.*, 1995).

Stat1-/- mice on a background of C57BL6 were obtained from the School of Molecular Bioscience, The University of Sydney, New South Wales, Australia (Meraz *et al.*, 1996).

2.4.3 Husbandry and housing

Mice were housed in an Optimice® cage carousel system (Animal Care Systems, Colorado, USA). Biocontainment for individual cages is achieved using controlled low velocity one-pass airflow through HEPA filters on entry and exit from each cage. Paper pellet bedding (Breeder's Choice cat litter, Australia) was used to maintain an absorptive but low dust environment to prevent filter clogging. Mice were housed in single sex same-litter groups, with up to 5 mice per cage. They were provided with cardboard nesting boxes, with soft nesting material. Environmental enrichment included wooden chew blocks, carrot pieces and commercial mouse toys. Mice were fed a commercial chow. Food and fresh water were available *ad libitum*. In addition, a pinch of muesli was scattered around the cage daily to provide additional enrichment.

2.4.4 Prior to virus exposure

Under brief inhalational anaesthesia (Isofluorane USP, Baxter), 100 µl of whole blood was collected into serum separator tubes (Microtainer Gold; BD Biosciences) for serology. Where indicated, mice were also implanted with subcutaneous microchips for reading identification and body temperature (LifeChip with Bio-Thermo Technology, Destron Fearing). Mice were then transferred into the NCRIS BSL-4 laboratory and allowed 7 days to acclimatise prior to virus exposure. A secondary form of identification with coloured ink tail bands was also provided as a way to easily identify mice prior to confirmation by scanning.

2.4.5 Virus exposure

2.4.5.1 Viral dose preparation

Each viral inoculum was prepared directly prior to use in the laboratory adjacent to the animal rooms within the NCRIS BSL4 facility. Virus was diluted with sterile PBSA and split into two aliquots; this was done for each dose where required. One aliquot was kept refrigerated in the laboratory and one aliquot was relocated into the animal room and stored on ice for the duration of challenge. There was enough inoculum remaining after animal exposure to perform back titrations from both aliquots, to document the doses used in the mice.

2.4.5.2 Anaesthesia and recovery

All mice were anaesthetised via intraperitoneal injection of medetomidine (9 mg/kg, Domitor, Novartis) combined with ketamine (67.5 mg/kg, Ketamil, Illium). Adequacy of anaesthesia was assessed by loss of palpebral reflex and loss of withdrawal reflex. Once mice were anaesthetised a small amount of lubricating eye ointment (Lacri-lube, Allergan Australia) was instilled to prevent drying of the cornea. Mice were kept wrapped in polar fleece material on a heat mat to maintain body temperature and exposed to HeV by either intranasal drop or intraperitoneal injection. Atipamazole was then administered intramuscularly (4.5 mg/kg, Antisedan, Zoetis) to speed recovery by reversing the action of medetomidine. Once mice had retained their righting reflex and were moving more freely they were returned to their cage. Water soaked chow was placed at floor level in the cage to provide and encourage ease of access to water and nutrition in the recovery phase of anaesthesia.

2.4.5.3 Intranasal (IN) exposure

The virus was administered in a volume of 30 µl. This was drawn up in a 200 µl pipette, with a new 100 µl tip for each mouse. Anaesthetised mice were placed in dorsal recumbency and virus was administered by slow single drop application to alternating nares. As the mouse inhaled the drop was internalised. Once the preceding drop had disappeared, the next drop was placed on the contralateral nostril.

2.4.5.4 Intraperitoneal (IP) exposure

The virus was administered in a volume of 300 µl. This was drawn up in a 1 ml syringe with a 26 gauge needle attached. Anaesthetised mice were placed in dorsal recumbency and had the challenge dose administered via IP injection, with the needle directed through the skin and entering the peritoneal space adjacent to the right caudal nipple. Afterwards the mice remained in dorsal recumbency and injection site was wiped with a Virkon ™ S (Antec International Limited, U.K) soaked gauze swab. To prevent skin irritation the skin was wiped again with a saline soaked swab approximately 5 minutes later, once the mouse was becoming mobile from anaesthetic recovery. No injection site leakage of inoculum was observed.

2.4.6 Handling and monitoring of mice exposed to HeV at BSL4

Mice were monitored daily, and this was increased to twice daily if any mice exhibited clinical abnormality. An example of the monitoring sheet is provided below (Figure 2.1). Initial daily observation assessed undisturbed mice by means of examination through the see-through walls of the cage for normal behavioural traits, physical appearance and posture, activity levels, and demeanour. Mice were then assessed against similar criteria during stimulation: the cage lid was opened and mice were encouraged to move around. A Kevlar glove was donned for handling, weighing and microchip scanning of individual mice.

Grimace scale scoring (Leach *et al.*, 2012; Matsumiya *et al.*, 2012) was also assessed when looking directly at mice with the cage lid open. The grimace scale was used in an attempt to objectively measure pain in mice, in case early cases of encephalitis were associated with pain prior to onset of neurological signs. The grimace scale assesses the 5 facial expressions that can be used to objectively measure pain in mice (Leach *et al.*, 2012; Matsumiya *et al.*, 2012). These expressions are orbital tightening, nose bulge, cheek bulge, ear position and whisker change and are scored on a scale of 0-2 where 0 = not present, 1 = moderately visible and 2 = severe or clearly apparent.

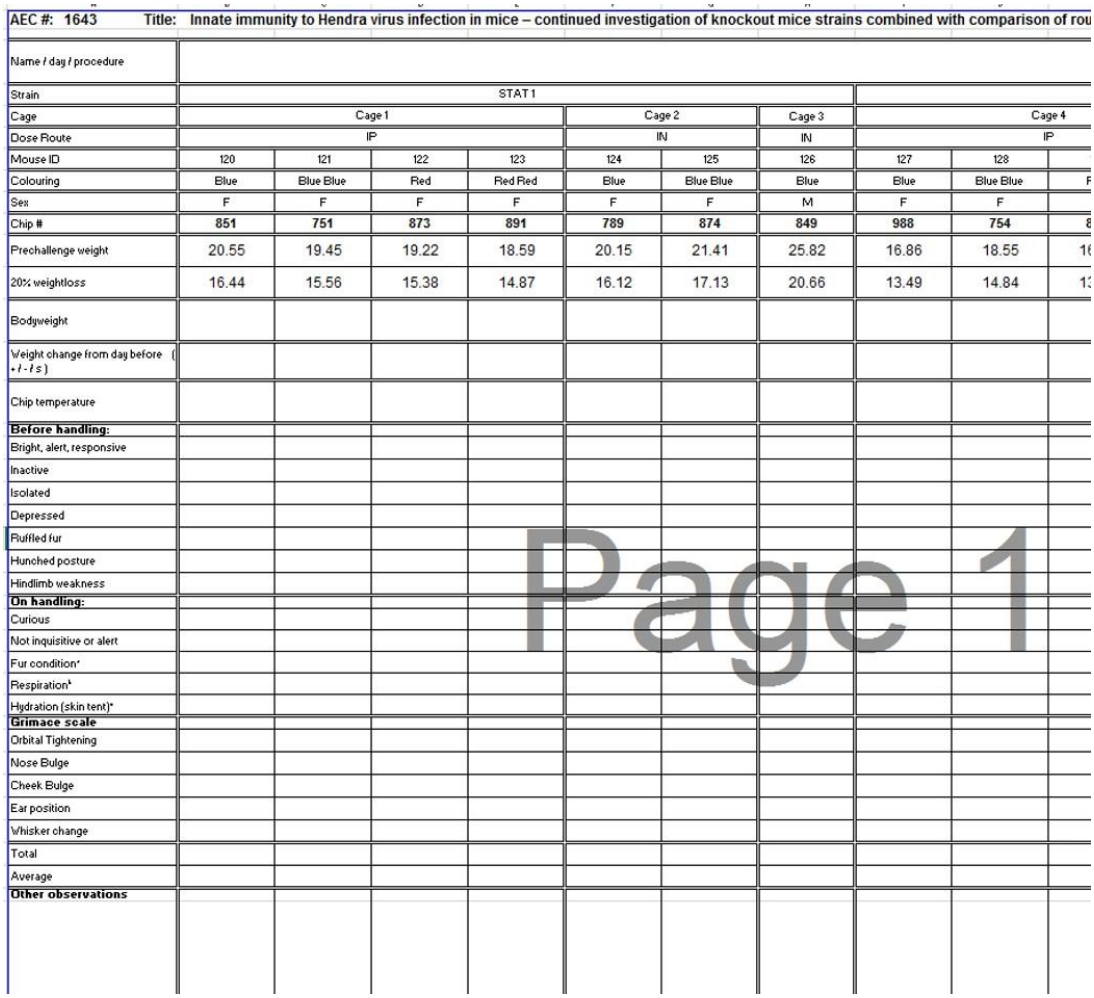

AEC #: 1643	Title:	Innate immunity to Hendra virus infection in mice – continued investigation of knockout mice strains combined with comparison of rou									
Name / day / procedure											
Strain		STAT1									
Cage		Cage 1				Cage 2		Cage 3	Cage 4		
Dose Route		IP				IN		IN	IP		
Mouse ID		120	121	122	123	124	125	126	127	128	
Colouring		Blue	Blue Blue	Red	Red Red	Blue	Blue Blue	Blue	Blue	Blue Blue	
Sex		F	F	F	F	F	F	M	F	F	
Chip #		**851**	**751**	**873**	**891**	**789**	**874**	**849**	**988**	**754**	
Prechallenge weight		20.55	19.45	19.22	18.59	20.15	21.41	25.82	16.86	18.55	1
20% weightloss		16.44	15.56	15.38	14.87	16.12	17.13	20.66	13.49	14.84	1
Bodyweight											
Weight change from day before (+ / - / s)											
Chip temperature											
Before handling:											
Bright, alert, responsive											
Inactive											
Isolated											
Depressed											
Ruffled fur											
Hunched posture											
Hindlimb weakness											
On handling:											
Curious											
Not inquisitive or alert											
Fur condition*											
Respiration*											
Hydration (skin tent)*											
Grimace scale											
Orbital Tightening											
Nose Bulge											
Cheek Bulge											
Ear position											
Whisker change											
Total											
Average											
Other observations											

Figure 2.1: Mouse monitoring sheet example

2.4.7 Euthanasia

Euthanasia occurred either at the end of the study or earlier if predetermined humane end-points were reached. Mice were anaesthetised via IP injection of medetomidine (12 mg/kg, Domitor, Novartis) combined with ketamine (90 mg/kg, Ketamil, Illium). Once adequately anaesthetised, mice were exsanguinated by cardiac puncture, the cervical spine was cut with scissors, and the thorax opened.

2.4.7.1 Predetermined humane end-points

Predetermined humane end-points were defined using data generated from previous HeV studies in mice (Dups *et al.*, 2012). For this study, clinical disease was graded as either mild, moderate, or severe (Table 2.1).

Table 2.1: Clinical disease grading for mice infected with HeV

Mild	• mild lethargy • decreased curiosity in surroundings • mild weight loss (2-5%) • performing normal mouse behaviours
Moderate	• lethargic • disinclined to examine surroundings • progressive weight loss 7-10% • performing some abnormal mouse behaviours e.g. excessive facial grooming, agitated when disturbed, vertical tail posture
Severe	• fluffed up fur • inactivity • progressive weight loss >20% • Neurological signs e.g. ataxia and tremors, seizures • Grimace scale: grade >1.

Animals displaying mild to moderate clinical signs were monitored twice daily. They were euthanased if clinical signs progressed from moderate towards severe, as these mice were considered unlikely to recover from infection. Distinct neurological signs were categorised as severe, because previous experience in wild type mice of several strains had shown them to be an early and reliable indicator of impending rapid and severe deterioration. In summary, mice were euthanased if neurological signs developed; or 3 consecutive days of weight loss occurred; or when weight loss reached 20% of initial weight; or when an average Grimace score above 1 was recorded.

The small number of BSL4 trained personnel involved in animal experimentation made it very difficult to conduct a truly blinded study. The rigorous end points aimed to reduce observational bias.

2.4.8 Sample collection

2.4.8.1 Whole blood and serum

Blood was collected into EDTA (Microtainer Purple; BD Biosciences) for qPCR and for virus isolation, where specified, and into serum separator tubes (Microtainer Gold; BD Biosciences) for serology. The EDTA tube was gently inverted to mix and prevent clotting before being stored in ice then subsequently frozen at -80 ^{0}C. The serum tube was stored

upright at room temperature for at least 30 minutes before being centrifuged at 3000 g for 15 minutes. The serum was removed into Sarstedt tubes for storage at -80 ^{0}C. Post infection serum samples were transported from the BSL4 facility and subjected to 50 kGy ϒ-irradiation to inactivate virus prior to processing.

2.4.8.2 Tissues for qPCR and virus isolation

A range of tissues, as specified in each experiment, was collected for qPCR and viral isolation into 750 µl of viral transport media containing 250 µl aluminium silicate beads (Biospec Products Inc.) All samples were stored at -80 ^{o}C until the end of each experiment then processed in one batch. Tissue samples were subsequently thawed then homogenised in an MP bead-beater at 4.0 m/sec for 30 seconds, then centrifuged at 17 000 rpm for 2 minutes before the supernatant was used for qPCR and virus isolation.

2.4.8.3 Tissues for histopathology

Tissue samples from major organs including the brain (as described below), lungs (including trachea or primary bronchus), thymus, heart, spleen, liver, kidneys, gonads, salivary gland, lymph nodes (submandibular, cervical chain, mesenteric, and inguinal, where identifiable), and small and large intestine were collected into 10% neutral phosphate buffered formalin (ACFB 'Confix Blue (10% NBF x5 concentrate); Australian Biostain) and fixed for a minimum of 48 hours in BSL4 at room temperature.

2.4.8.3.1 Brain sampling

The brain was removed paying particular attention to intact extraction of the olfactory bulbs. Gentle, blunt dissection rather than a scalpel blade was used in removing the olfactory bulb. This was done in order to minimise injury to the cribiform plate to reduce the risk of cross contamination from olfactory mucosa. The brain was then bisected longitudinally (Figure 2.2, thick line). One half was apportioned into formalin and, once fixed, sectioned transversely at approximately every 2 mm (not demonstrated in the image), and further processed for histopathology. From the other side of the brain, a transverse section was taken and placed into virus isolation media for qPCR and virus isolation. This included the olfactory bulb (Figure 2.2, Olf. Bulb) and approximately 3 mm of rostral

cerebral cortex (containing the olfactory tract), and hereon was designated as the "forebrain" sample throughout the thesis (Figure 2.2, FB).

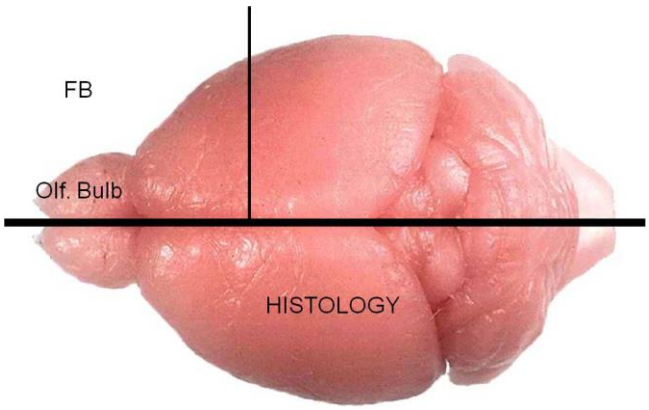

Figure 2.2: Dorsal view of a whole mouse brain demonstrating sectioning for samples.
Olf. Bulb, olfactory bulb; FB, forebrain

2.5 Sample analysis

2.5.1 Histopathology and immunohistopathology

Formalin fixed tissues were dehydrated in graded alcohols, paraffin embedded, sectioned (3-4 µm), stained with haematoxylin and eosin (H&E, Lillie-Mayer Haematoxylin; Australian Biostain Pty Ltd and Alcoholic Eosin/Phloxine 0.1%; Australian Biostain Pty Ltd), and examined by light microscopy. Positive charged adhesion microscope slides (Hurst Scientific Pty Ltd) and DAKO PT Link kits were used for immunohistochemistry. Paraffin sections were quenched with 10% hydrogen peroxide for 10 minutes, incubated at 97 °C for 30 minutes in high pH target retrieval solution (EnVision FLEX Target Retrieval Solution, High pH; DAKO), and quenched with a 3% solution of hydrogen peroxide. Sections were then incubated with a rabbit serum directed against recombinant-expressed purified anti-Nipah N protein (produced by the CSIRO Australian Animal Health Laboratory, Geelong, Australia (Hooper *et al.*, 2001; Murray *et al.*, 1995) at a concentration of 1:1600 for one hour followed by horseradish peroxidase-conjugated secondary antibody (Envision Flex HRP; DAKO) for 45 min. Sections were stained with aminoethylcarbazol substrate chromogen (DAKO Envision)

for 10 min and counterstained with Lillie-Mayer's haematoxylin (Lillie-Mayer Haematoxylin; Australian Biostain Pty Ltd). Tissue sections from an uninfected animal and from a confirmed infected animals from prior experimental studies were included as negative and positive immunohistopathology controls respectively. Cover slips were mounted using aqueous mounting media (Faramount Aqueous Mounting Medium Ready-to-use; DAKO), and the slides examined by light microscopy. For each study individual slides were examined without identification as to animal group.

2.5.2 RNA extraction

A 50 µL aliquot of the homogenised tissue supernatant was placed into 130 µL of guanidinium thiocyanate-based solution (lysis/binding solution MagMAX™, Ambion®, Life Technologies) for processing for RNA extraction. Extraction was performed using a robotic magnetic particle plate-based instrument (Kingfisher Flex™ purification system, Thermo Fisher Scientific Inc.) as per manufacturer's protocol for DNA/RNA. Briefly, 100 µL of sample in MagMAX was resuspended in magnetic bead solution in a microtitre deep well 96 plate and underwent binding, mixing, washing and elution purification phases using a KingFisher Viral NA kit. The final elution stage was into a well of a 96 well plate, this was stored at -80 ^{o}C.

2.5.3 Reverse transcriptase PCR

TaqMan RT-PCRs were performed as a one-step assay for the detection of the HeV-N gene and paired with a house keeping ribosomal RNA molecule 18S to normalise for original sample tissue quantity. Primers were obtained from Geneworks (Australia) from previously published sequences (Table 2.2) (Feldman *et al.*, 2009) and TaqMan MGB probes from Applied Biosystems.

Table 2.2: RT-PCR primers and probe sequences, HeV-N proteins (Feldman *et al.*, 2009)

N gene	NFWD*	GATATITTTGAMGAGGCGGCTAGTT
	NREV1*	CCCATCTCAGTTCTGGGCTATTAG
	NREV2*	TCCCATCTGAGCTCTGGACTATTAGT
	NPRHeV*	6FAM-CTACTTTGACTACTAAGATAAGA-MGB
18S	18S rRNA FwD	CGGCTACCACATCCAAGGAA
	18S rRNA Rev	GCTGGAATTACCGCGGCT
	18S rRNA VIC	VIC-TGCTGGCACCAGACTTGCCCTC-TAMRA

One-step real-time PCR assays were performed using Agpath-ID One-step RT-PCR kit (Applied Biosystems/Ambion) for TaqMan and Superscript III/PlatinumTaq and SYBR green One-step qRT-PCR kit (Invitrogen) for SYBR Green assays according to manufacturer's instructions.

All reactions were performed in duplicate on the same plate and each plate also contained positive tissue extracts from previous experiments performed at the institution, negative tissue and negative extraction (MagMAX and nfH_2O) controls. Each reaction was to a total volume of 25 µL with reagents listed in Table 2.3. Each individual reaction was within a well of a 96 well plate and was prepared in an amplicon free clean room. 2 µL of extracted sample was added in the working laboratory and the plate briefly sealed and centrifuged to ensure contents were properly mixed and in the bottom of the well.

Table 2.3: RT-PCR reagents

Reagent	Volume for 1 reaction
Nuclease free water ($_{nf}H_2O$)	5.4 µL
2X RT-PCR buffer	12.5 µL
25X RT-PCR enzyme mix	1.0 µL
Forward primer (18 µM) Final conc 900 nM	1.25 µL
Reverse primer (18 µM) Final conc 900 nM	1.25 µL
TacMan Probe (5.0 µM) FAM, Final conc 250 nM	1.25 µL
18S rRNA VIC labelled primer/probe mixture	0.38 µL
Total volume:	23 µL

Assays were performed using an ABI 7500 Fast Real-Time PCR System with version 2.0.6 detection software, with thresholds defined as 0.3 for HeV and 0.2 for 18S to enable comparisons across different plates. The following cycling conditions were used:

1 X 45 ^{o}C 10 mins

1 X 90 ^{o}C 10 mins

45 X 60 ^{o}C 45 sec

A positive result was defined as a cycle threshold (C_T) value of <39.6 when there was an appropriate amplification curve trace. The C_T value was based on standard curves previously established in this laboratory group, where this C_T value represented one copy of HeV-N gene RNA (Dups *et al.*, 2012). Results were normalised to 18S to reflect a standardised number of HeV-N gene copies for the amount of tissue in the sample.

The intercept and slope values used in the formulas for these calculations were derived from the previously established standard curves. The following formulas were used:

HeV- N gene copies = 10^((C_T – 39.15)/-3.27)

18S copies = 10^((C_T – 51.43)/-3.254)

2.5.4 Viral titration

2.5.4.1 Back titration of viral inoculum

Tenfold serial dilutions of cell culture supernatants were prepared in 96 well plates with DMEM media, from neat to a 10^7-fold dilution, to a total volume of 250 µl per well. 50 µl of diluent was then inoculated in quadruplicate onto 80% confluent cells in 100 µl of growth media.

HeV titrations were performed with Vero cells and checked at days 3 and 5 for viral cytopathic effect (CPE).

EBOV titrations were performed with Vero E6 cells and incubated for 7 days before fixing in formalin and performing immunofluorescence staining to assess antigen containing wells. The limiting dilutions at which CPE or viral antigen could be observed for HeV and EBOV

respectively were used to determine the $TCID_{50}$ per ml, using the Reed-Muench method for evaluation of 50% end points (Reed & Muench, 1938).

2.5.4.2 Virus isolation

For virus isolation, wells in a 24 well plate were seeded with 10^5 Vero cells in 500 µl of media and incubated overnight to obtain 90% confluence. 400 µl of media was removed and the wells inoculated with 100 µl of supernatant from the tissue sample homogenate, and rocked gently over 30 minutes before 400 µl of fresh media was added. The plates were incubated and observed over 5 days for the development of CPE. Each sample was tested in two wells of a 24 well plate and assessed as either positive or negative for CPE.

2.5.5 Serology

In 21 day studies, sera collected from mice both prior to virus exposure and at euthanasia were analysed for both antibody binding to HeV soluble G protein (HeV $_s$G) and receptor blocking antibodies using a Luminex microsphere assay as previously described (Bossart *et al.*, 2007; McNabb *et al.*, 2014). Briefly, magnetic beads pre-coupled to HeV $_s$G were sonicated for 60 seconds to adequately disperse before diluting 1 µL of beads per well to be tested in 2% skim in PBS-T in a flat bottomed 96 well plate, covered in foil to protect from light and rocked at room temperature for 30 minutes. A magnetic plate holder was used to settle the beads so the solution could be discarded before washing twice with PBS-T in an automated plate washer.

For the binding antibody assay 100 µL of serum sample diluted 1:100 in PBS-T was added to each well, for the receptor blocking assay 100 µL of serum sample diluted 1:50 in PBS-T was added to each well. The plate was covered and rocked at room temperature for another 30 minutes. The solution was discarded using the magnetic plate holder and the wells again washed twice with PBS-T. For the binding antibody assay 100 µL of biotinylated Protein A diluted 1:500 and Protein G diluted 1:250 in PBS-T was added to the wells, for the receptor blocking assay 100 µL of biotinylated Ephrin B2 diluted 1:1000 in PBST was added to the wells. The plate was covered in foil and shaken for 30 minutes at room temperature. The solution was discarded using the magnetic plate holder and the wells again washed twice

with PBS-T. 100 µL of Streptavidin PE was diluted 1:1000 in PBS-T and added to the wells, the plate covered in foil and shaken for 30 minutes at room temperature before being read.

Assays were performed on a Bio-Plex Protein Array System. The machine parameters were set for detection of 100 beads per well to give median fluorescent intensities from 100 replicates for each sample. Data acquisition and analysis was performed with Bio-Plex Manager Software (v 4.1) (Bio-RadLaboratories, Inc., CA, USA).

For the antibody binding assay a positive result was defined as samples with median fluorescence intensity (MFI) greater than the mean of all pre-challenge samples plus 3 x the standard deviation (Bossart *et al.*, 2007; McNabb *et al.*, 2014)

The receptor blocking assay is a surrogate test for a virus neutralization assay. HeV antibodies in serum block the binding of Ephrin B2 with HeV-sG protein. Results are displayed as % inhibition and are calculated from the equation: (1−M.F.I. serum/M.F.I. negative serum) × 100 (Bossart *et al.*, 2007). A negative blocking response in mice was considered to be <6.4%, based on the mean % blocking + 3SD obtained from sera analysed within this laboratory that had been collected from mice which had not been exposed to HeV.

2.6 Cell culture

All media was supplemented with 10% foetal calf serum (FCS, Hyclone), 10 mM HEPES buffer (Sigma) and 200 units/ml penicillin, 200 µg/ml streptomycin and 0.5 µg/ml amphotericin B (Antibiotic-Antimycotic, Gibco), unless otherwise specified. Cells were incubated at 37 ^{o}C in 5% CO_2.

L929, Mouse subcutaneous connective tissue (fibroblast) NCTC clone 929 derivative of strain L cells (L929, ATCC: CCL-1), A549 human lung carcinoma cell line (A549, ATCC: CCL-185) cells and African green monkey kidney epithelial cells (Vero, ATCC: CCL-81) were maintained in Dulbecco's minimal essential medium (DMEM, Gibco® Life Technologies).

GP2-293 retroviral packaging cell line cells (Clontech® Laboratories Cat. No. 631460) were maintained in Dulbecco's Modified Eagle's Medium (DMEM) with high glucose (4.5 g/L) , 4 mM L-glutamine (Gibco® Life Technologies) with the addition of 1 mM sodium pyruvate.

To passage, growth medium was discarded and the monolayer was gently washed three times with sterile PBSA before the addition of trypsin (0.5% in PBSA; trypsin-EDTA, Gibco) at a volume sufficient to cover the monolayer. Cells were trypsinised at 37 °C until complete detachment of the monolayer from the culture flask was observed by light microscopy. Cells were resuspended in growth media and added to new culture flasks at dilutions appropriate for the cell density required.

2.7 Other media, buffers and solutions

2.7.1 Phosphate buffered saline (PBSA)

Deionised water with w/v 0.2% KCl, 0.8% NaCl, 0.02% KH_2PO_4, 0.115% Na_2HPO_4

2.7.2 PBS-T

PBSA with the addition of 0.05% w/v Tween (VWR BDH Prolabo)

2.7.3 Tris acetate buffer (TAE)

40 mM Tris-acetate, pH 8.1 and 10 mM ethylenediaminetetraacetic acid (EDTA)

2.7.4 Viral transport media

PBSA with 1% Bovine serum albumin, 200 units/ml penicillin, 200 µg/ml streptomycin and 0.5 µg/ml amphotericin B (Antibiotic-Antimycotic, Gibco)

2.7.5 LB agar plates containing 100µg/mL ampicillin

200 ml LB media, 200 µL ampicillin aliquoted into petridishes, procedure performed adjacent to a Bunsen burner

2.8 Microscopy

An EVOS FL microscope (Life Technologies) was used in the BSL3 laboratory to view cells for monitoring growth, trypsinisation, assessing and photographing immunofluorescence. A Phase Contrast ELWD0.3 microscope (Nikon) was used for assessing cells for the presence of cytopathic effect (CPE) and syncytia in the BSL4 laboratory. Photomicrography was

conducted on an Olympus BX51 microscope with an Olympus DP71 digital camera using Olympus Corporation DP controller software V 3.1.1.267.

CHAPTER 3: THE IMPACT OF EXPOSURE DOSE ON HENDRA VIRUS INFECTION PHENOTYPE IN WILD TYPE MICE

3.1 Introduction and background

Naturally occurring Henipavirus virus infection in people (Escaffre *et al.*, 2013b; Hooper *et al.*, 2001; Vigant & Lee, 2011; Wong & Ong, 2011; Wong *et al.*, 2009; Wong & Tan, 2012) and horses (Hooper *et al.*, 1997a), and experimental infection of non-human primates (Bossart *et al.*, 2011; Geisbert *et al.*, 2010; Marianneau *et al.*, 2010; Rockx *et al.*, 2010), horses (Marsh *et al.*, 2011), cats (Hooper *et al.*, 1997b; Middleton *et al.*, 2002; Mungall *et al.*, 2006; Westbury *et al.*, 1996; Westbury *et al.*, 1995; Williamson *et al.*, 1998), ferrets (Bossart *et al.*, 2009; Pallister *et al.*, 2011), and Syrian golden hamsters (Guillaume *et al.*, 2006; Guillaume *et al.*, 2009; Rockx *et al.*, 2011; Wong *et al.*, 2003) is established within the respiratory epithelium leading to necrotising alveolitis, with pulmonary haemorrhage and oedema. Viral replication spreads from respiratory epithelium to the endothelium of small vessels in the lungs (Wong *et al.*, 2002b) causing vasculitis with mural necrosis and endothelial syncytia. Henipavirus may then enter the blood stream and disseminate throughout the body leading to fulminating systemic infection: the CNS, kidney and many other major organs are affected (Hooper *et al.*, 2001; Rockx, 2014; Williamson & Torres-Velez, 2010; Wong *et al.*, 2002a). Infection in the CNS is characterised by vasculitis, thrombosis and parenchymal necrosis and may be accompanied by an inflammatory response including neutrophils, macrophages, lymphocytes and microglial reaction. There is also glomerulitis and renal tubular necrosis, and extensive infection of lymphoid tissues with lymph node oedema and haemorrhage, lymphoid depletion, and acute necrotising inflammation within the spleen (Hooper *et al.*, 2001; Rockx, 2014; Williamson & Torres-Velez, 2010; Wong *et al.*, 2002a)

In the highly susceptible hamster, ferret and cat, (Hooper *et al.*, 1997b; Pallister *et al.*, 2011; Rockx *et al.*, 2011; Westbury *et al.*, 1996; Westbury *et al.*, 1995) severe systemic disease is reliably observed following exposure to 5 000 $TCID_{50}$ HeV via either parenteral or non-parenteral routes: hamsters and ferrets may succumb to doses as low as <1 and 50 $TCID_{50}$ respectively (Pallister *et al.*, 2011; Rockx *et al.*, 2011).

Some studies in these species have reported dose-dependent differences in incubation period, lesion distribution, and localising signs. For example, hamsters exposed to 10^5 $TCID_{50}$ HeV succumbed within 3 days p.e. to severe acute respiratory distress, while those exposed to the lower dose of 10^2 $TCID_{50}$ developed respiratory signs by day 5 p.e., followed by neurological signs, and succumbed by day 7 p.e. (Rockx *et al.*, 2011). Differences in dose and clinical signs between different animal models are summarised in Table 3.1.

Table 3.1: Comparison of infection phonotype, dose and clinical disease for animals models of HeV infection

Animal model	Infection phenotype	Dose and disease
African Green Monkey	Severe multisystemic disease	Experimental doses of 10^5 and above used Severe respiratory disease in untreated animals Ribivarin slowed disease progression and altered to more neurological disease
Ferret	Severe multisystemic disease	As little as < 1 $TCID_{50}$ is fatal Doses of 50 – 50 000 $TCID_{50}$ showed no differences in distribution or severity of lesions
Hamster	Severe multisystemic disease	As little as 5 $TCID_{50}$ is fatal 10^5 $TCID_{50}$ severe acute respiratory distress day 3 p.e 10^2 $TCID_{50}$ neurological signs and death by day 7 p.e.
Cat	Severe multisystemic disease	5 000 $TCID_{50}$ reliably indices severe respiratory disease
Guinea pigs	Intermediate	5 000 $TCID_{50}$ respiratory disease 50 000 $TCID_{50}$ neurological disease
Squirrel monkey	Intermediate	
Immunocompetent mice	Mild	5000 $TCID_{50}$ SC resulted in no disease 50 000 $TCID_{50}$ mild respiratory tract infection and olfactory tract associated encephalitis

p.e.: post exposure

African green monkeys are also highly permissive to HeV infection, although studies in this species have been confined to virus doses of 10^5 and above (Rockx *et al.*, 2010). Rockx *et al* reported slower clinical progression of HeV infection and an alteration in clinical phenotype in AGM treated with ribivarin. While animals given the antiviral drug all succumbed to infection, this was manifest primarily as a neurological disease. In contrast, untreated controls typically developed severe respiratory disease. Ribivarin may have a similar impact on the HeV infection phenotype in AGM to a reduction in viral exposure dose in hamsters, presumably via suppression of virus replication. In the case of guinea pigs, respiratory distress and pneumonia occurred following inoculation with HeV SC at the lower dose of 5 000 $TCID_{50}$ (Hooper *et al.*, 1997b; Westbury *et al.*, 1995), while encephalitis was the

predominant clinicopathological feature at the higher dose of 50 000 $TCID_{50}$ SC (Williamson *et al.*, 2001). By contrast, there were no differences observed in distribution or severity of lesions in ferrets following oronasal exposure to doses of HeV ranging from 50 – 50 000 $TCID_{50}$ (Pallister *et al.*, 2011). Currently, there is no obvious pathophysiological explanation for these suggested species differences in the relationship between infection phenotype and exposure dose.

Various clinical manifestations have also been noted with field HeV infection of the horse. Initially, field cases were reportedly characterised by rapidly progressive febrile illness associated with fulminating respiratory disease, although mild neurological signs were recorded in a small number of early cases (Rogers *et al.*, 1996; Williamson *et al.*, 1998). However, cases have also been reported in which the primary presentation was neurological disease (Field *et al.*, 2010) including ataxia, hypersensitivity, head tilt, facial nerve paralysis, circling, and head pressing. While it is possible that differences in clinical phenotype may reflect genomic variation between strains of HeV, analysis of HeV isolates from infected horses has shown strong sequence conservation over time (Marsh *et al.*, 2010). Differences may also be attributable - by an as yet undetermined means - to exposure dose, exposure route or features of the individual host animal.

In contrast to the impact of HeV on the species discussed above, an early study by Westbury *et al* (Westbury *et al.*, 1995) reported no infection after exposure of immunologically intact, juvenile, BALB/c mice to 5000 $TCID_{50}$ HeV SC. The mice remained clinically well over the 21 day study period and at euthanasia there was no evidence of infection as assessed by gross pathology, histological or immunohistochemical testing, virus isolation or serology by VNT. A similar conclusion was drawn by Wong *et al* (Wong *et al.*, 2003) following parenteral as well as IN exposure of Swiss brown mice to NiV.

In a more recent study using a plausible natural route of exposure (IN) and with access to a wider range of more sophisticated molecular and serological tests, aged BALB/c and C57BL6 mice exposed to an IN dose of 50 000 $TCID_{50}$ of HeV routinely developed asymptomatic and self-limiting infection of the upper and lower respiratory tracts (Dups *et al.*, 2012). Infection was associated with the development of a binding antibody response to HeV sG by Luminex assay, but antibody was not reliably detected by VNT. Virus was re-isolated from lung tissue

of mice between days 4 – 10 p.e.. Viral antigen was present in pulmonary tissue between days 6 – 14 p.e., and was visible as small dense foci of staining within cells of the alveolar walls, but was not accompanied by cellular necrosis or other evidence of inflammatory reaction. IN administration exposed the olfactory mucosa to virus, and cells within the olfactory mucosa were also permissive to infection: infection in this location resulted in focal necrotising inflammation. Viral antigen and lesions attributable to viral infection were not identified in other organs apart from brain, discussed below, although low levels of viral genome were recovered sporadically from the heart, blood, thymus, and cervical, cranial mediastinal and mesenteric lymph nodes. In terms of generalised systemic infection, it was concluded that virus replication in mice was confined to the upper and lower respiratory tracts without significant viremia. Moreover, where pulmonary infection occurred, it was not associated with necrotising lesions or severe inflammation.

In some mice, infection also developed in the CNS and was accompanied by clinical signs of neurological disease. In a time-course study, encephalitis associated with viral antigen was first detected within the olfactory bulb from days 6 to 8 p.e., followed by the sequential appearance of viral antigen in the pyriform lobe, olfactory tubercle and amygdala from days 9 to 20 p.e. Occasionally, antigen was seen in the hippocampus in mice euthanased from day 17 onwards. All of these sites are components of the olfactory cortex and are intimately associated with one another via synaptic connections. Accordingly, it was hypothesised that CNS infection in the wild-type mouse may occur after IN exposure by direct contact of virus with olfactory sensory neurones and subsequent trans-neuronal spread, rather than as a consequence of viremia (Dups *et al.*, 2012).

In the case of NiV, no clinical abnormalities have been described in wild-type mice exposed under various experimental conditions including different virus doses and exposure routes. These include 4 week old outbred Swiss mice exposed IN and IP and with, respectively, 6 x 10^5 and 10^7 PFU of NiV (Wong *et al.*, 2003), 4-12 week old C57BL6 mice given 10^4 - 10^6 PFU IP (Dhondt *et al.*, 2013), and 8 week old and 12 month old C57BL6 and BALB/c mice exposed to 50 000 $TCID^{50}$ IN (Dups *et al.*, 2014). Dhondt *et al* (2013) reported very low levels of viral genome within the lung and spleen of some C57BL6 mice at the 21 day experimental end point. Subclinical self-limiting lower respiratory tract infection was later confirmed in aged BALB/c mice given virus IN (Dups *et al.*, 2014), with-re-isolation of NiV from RNA positive

lung tissue of asymptomatic mice up to 10 days post exposure. As for HeV, there was no evidence for significant NiV viraemia or infection of other systemic organs. In contrast to HeV, there was no evidence for NiV infection of mouse brain (Dups *et al.*, 2014).

3.2 Aims and hypothesis of this chapter

3.2.1 Aims of this chapter

- To compare the phenotype of HeV infection in mice with reported findings from other species under comparable conditions of virus exposure
- To further characterise HeV infection in mice by exposing them to different doses of virus, to determine whether the infection phenotype varies with the amount of virus in the inoculum
- To inform the selection of a virus dose for application to future studies in mice

3.2.2 Hypothesis

In comparison to other laboratory species, mice are resistant to systemic disease following challenge with routinely used doses of HeV and the disease phenotype is independent of challenge dose.

3.3 Experimental design

Dose ranging experiments were performed as two observational studies, an acute study of 7 days duration and a chronic study of 21 days duration. Each study used 12 week old female wild-type C57BL6 mice. There were 5 different treatment groups in each study, with five mice per group. Mice were housed together in same dosage groups. The virus inoculum was a low passage isolate from the spleen of a horse (Hendra virus/Australia/Horse/2008/Redlands). Under general anaesthesia, mice were exposed IN to a dose of 5, 50, 5 000, 50 000 or 500 000 $TCID_{50}$ HeV in saline in a volume of 30 µl.

After exposure to HeV, mice were assessed at least daily for clinical signs of disease. Mice were euthanased at the end of each study (day 7 or day 21), or earlier if they had reached their predetermined humane endpoint for clinical disease. At post mortem, samples from major organs including a brain hemi-section were collected into 10% neutral buffered

formalin for routine histopathology and immunohistochemistry (IHC). Tissues samples from the lung, contralateral forebrain (FB), and spleen were also collected into viral transport medium for qualitative virus re-isolation as well as RNA extraction.

For virus isolation, wells in a 24 well plate were seeded with 10^5 Vero cells in 500 µl of medium and incubated overnight to obtain 90% confluence. 400 µl of medium was removed and the wells inoculated with 100 µl of sample, and rocked gently over 30 minutes before 400 µl of fresh medium was added and the plates incubated and observed over 5 days for the development of CPE. Each sample was tested in two wells of a 24 well plate and assessed as either positive or negative for CPE.

Multiplex TaqMan reverse-transcription (RT) PCR (qPCR) targeting the HeV-N gene as well as host cell 18S rRNA was performed on extracted RNA, with HeV- N gene values normalized to host cell 18S rRNA. Samples with a mean HeV-N gene C_T value ≤ 39.6 were defined as positive for HeV RNA (Dups *et al.*, 2012).

For mice in the 21-day study, sera were collected both prior to virus exposure and at euthanasia and analysed for antibody responses against HeV using a Luminex microsphere HeVsG binding assay and a receptor blocking assay as previously described (Bossart *et al.*, 2007; McNabb *et al.*, 2014).

3.4 Data analysis

The primary readout for these studies was the infection phenotype observed in individual mice following exposure to virus. A mouse was defined as infected with HeV if it met the following criteria:

- *In the 7 day study*, immunohistopathology was positive for viral antigen or virus was re-isolated from tissue/s
- *In the 21 day study*, immunohistopathology was positive for viral antigen, or infectious virus was re-isolated from tissues, or the serum was positive for binding and/or receptor blocking antibodies against HeV $_s$G protein
- *In both studies*, detection of viral genome in brain tissue was also considered sufficient to confirm virus replication in that organ, on the basis that unilateral replication within the olfactory pathway is feasible after IN exposure, virus cannot reliably be re-isolated from

mouse brain even when there is ample evidence of replication (Dups *et al.*, 2012), and partitioning of brain samples for testing occurred on the mid-line.

Detection of viral genome alone was not considered sufficient evidence to confirm replication within tissues other than brain, as it may have merely reflected residual genomic material from the inoculum or genomic fragments within lymph or phagocytes. Rather, the outcome of routine PCR testing was used to select samples for progression to testing by virus isolation.

Infected mice were then assigned a phenotype on the basis of whether they did not exhibit clinical signs during the period of observation (subclinical), they exhibited clinical signs of general malaise with disseminated virus replication in major organ systems (systemic), or they exhibited signs consistent with involvement of the CNS and evidence of virus replication in brain (neurological).

Limited statistical analysis was performed, comprising contingency analysis of infection outcomes in the two study groups, and in specific dosage groups across the two studies (Fisher's exact tests).

Estimation of the median infectious dose (ID_{50}) for each study was calculated according to the trimmed Spearman-Karber method (Hamilton *et al.*, 1977). This method was selected as it offers advantages over traditional probit and logit methods when applied to logarithmic dose intervals with small group sizes, and does not assume parametric data. However, the trimmed version of the Spearman-Karber estimator is not as sensitive to anomalous responses as the conventional version.

3.5 Results

3.5.1 7 day study

3.5.1.1 Clinical observations

The exposure of mice to HeV was generally well tolerated; it did not cause a sneeze reflex and only occasionally led to brief periods of apnoea and/or increased respiratory rate and effort. However, the procedure was more poorly tolerated in mice exposed to 500 000

TCID50, where the viral inoculum was between a 1:1 and a 1:2 dilution and was comparatively viscous. Drop application to the nares often resulted in a period of apnoea from 5-30 seconds that was followed by gasping and increased respiratory effort. The time taken to administer the inoculum was therefore much slower in this group, and so the anaesthetic time increased by approximately 20 minutes for mice receiving this dose.

All mice continued to gain weight during the study. Mice given 5, 50, 500, 5000 or 50 000 $TCID_{50}$ HeV remained clinically healthy up to the time of elective euthanasia on Day 7. Three of 5 mice given 500 000 $TCID_{50}$ HeV (mice #26, #28 and #30) reached their predetermined humane endpoint on Day 7 and were euthanased as scheduled on that day (Table 3.2). In the undisturbed state they were sitting still and isolated from the other mice in the cage, with a hunched posture and ruffled fur. They were hyper responsive to stimulation and became agitated, moving quickly with jerky movements, and also displayed excessive facial grooming and a stiff vertical tail posture. Each of these mice displayed acute neurological disease manifest as mild ataxia and tremors.

Table 3.2: 7-day dose ranging study

Dose $TCID_{50}$	Mouse ID	Infection status	Infection phenotype	Olfactory epithelium Ag *	Lung Ag/PCR	Forebrain (FB) Ag/PCR
5	1-5	All negative	NA	-	-/-	-/-
50	6-10	All negative	NA	-	-/-	-/-
500	11-15	All negative	NA	-	-/-	-/-
5 000	16-20	All negative	NA	-	-/-	-/-
50 000	21	Positive	Subclinical	-	+/-	-/-
	22	Positive	Subclinical	+	-/-	-/-
	23	Negative	NA	-	-/-	-/-
	24	Negative	NA	-	-/-	-/-
	25	Positive	Subclinical	+	+/-	-/-
500 000	26	Positive	Neurological	+	-/-	+/+ VI+
	27	Negative	NA	-	-/-	-/-
	28	Positive	Neurological	+	+/+	+/-
	29	Positive	Subclinical	+	-/-	-/-
	30	Positive	Neurological	+	-/+	+/- VI+

Ag: immunohistochemical staining for viral antigen in tissue
PCR: qPCR for viral genome in tissue
VI+: virus isolation was performed on all samples, positive samples are shown
"+" present
"-" not present
* PCR not performed on olfactory mucosa

3.5.1.2 Pathology and immunohistopathology

No significant gross lesions were identified on post-mortem examination in any mouse.

No lesions were detected in histological sections from mice in the groups given 5, 50, 500 or 5000 $TCID_{50}$ of HeV. In 2 of 5 mice in the 50 000 $TCID_{50}$ dose group and 4 of 5 mice in the 500 000 $TCID_{50}$ dose group there was focal to multifocal erosive rhinitis, with mild to marked neutrophilic infiltration and exocytosis with a mucocellular exudate overlying affected areas (Figure 3.1). Sloughed epithelial cells contained large glassy eosinophilic intra-nuclear inclusions that stained intensely for viral antigen (Figure 3.1 C &D). Viral antigen was also detected in individual olfactory epithelial cells without evidence of tissue injury or inflammatory reaction.

Pulmonary lesions, such as necrosis or infiltration by inflammatory cells, were not identified in any mouse of any dosage group. Occasional small foci of viral antigen were found in the alveolar wall of 2 of 5 mice given 50 000 $TCID_{50}$ and 1 of 5 mice given 500 000 $TCID_{50}$ (Figure 3.2). As the alveolar wall is a very delicate and complex structure containing alveolar type I and type II epithelial cells, capillary endothelium, and macrophages, together with fibrocytes responsible for a very fine supporting stroma, it was not possible to identify infected cell types with confidence by light microscopy. In the absence of pathological lesions further labelling with cell specific markers was not pursued.

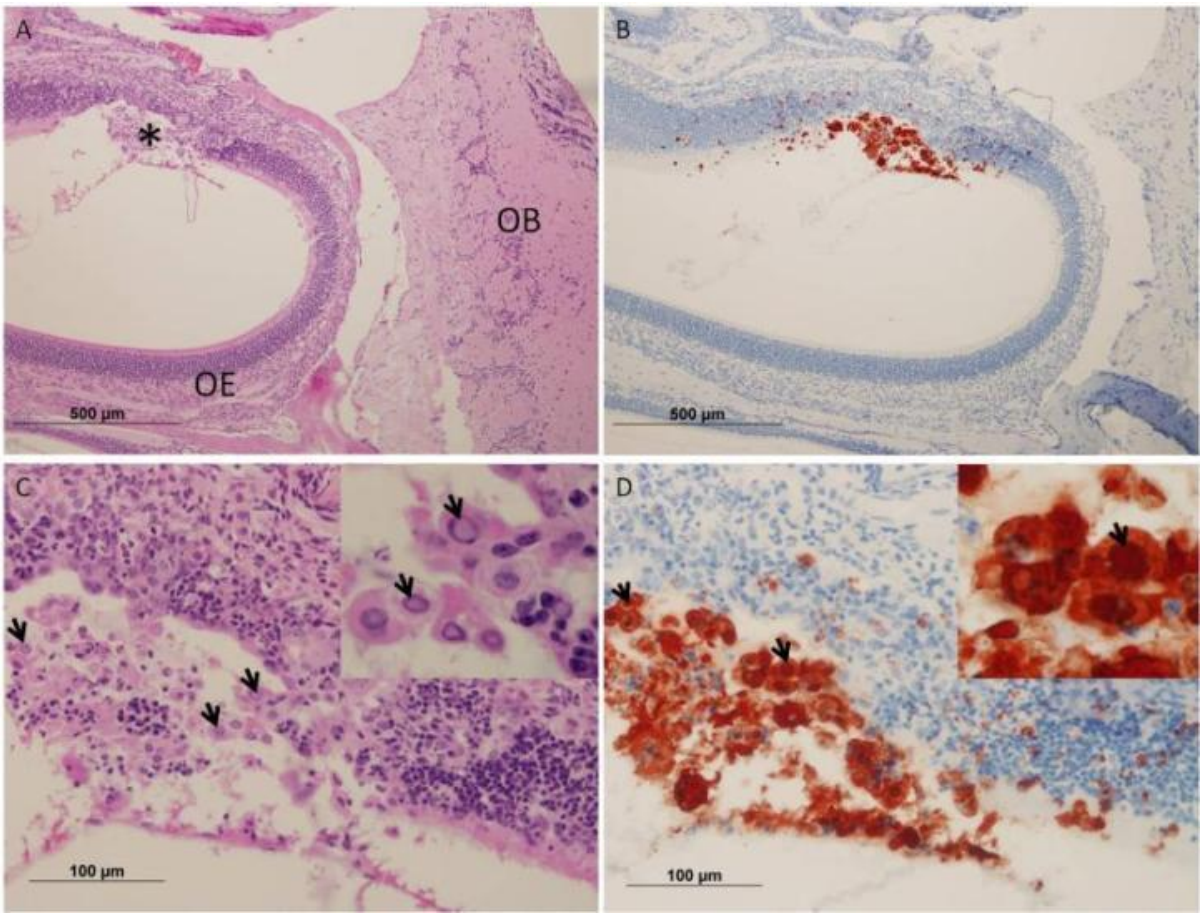

Figure 3.1: Focal rhinitis in the olfactory epithelium associated with HeV 7 days post infection, from mouse #29 from the 500 000 $TCID_{50}$ dose group. A) H&E section, area of erosion*, Olfactory epithelium OE, Olfactory bulb OB B) Immunohistochemical section, the affected area is staining positive by NiV anti-N antibody. C) H&E section, original magnification 40x, with inset 100x, large glassy eosinophilic intranuclear inclusions are seen in sloughed epithelial cells (arrows). D) Immunohistochemical section, original magnification 40x, with inset at 100x, large intranuclear inclusions stain strongly positive by NiV anti-N antibody

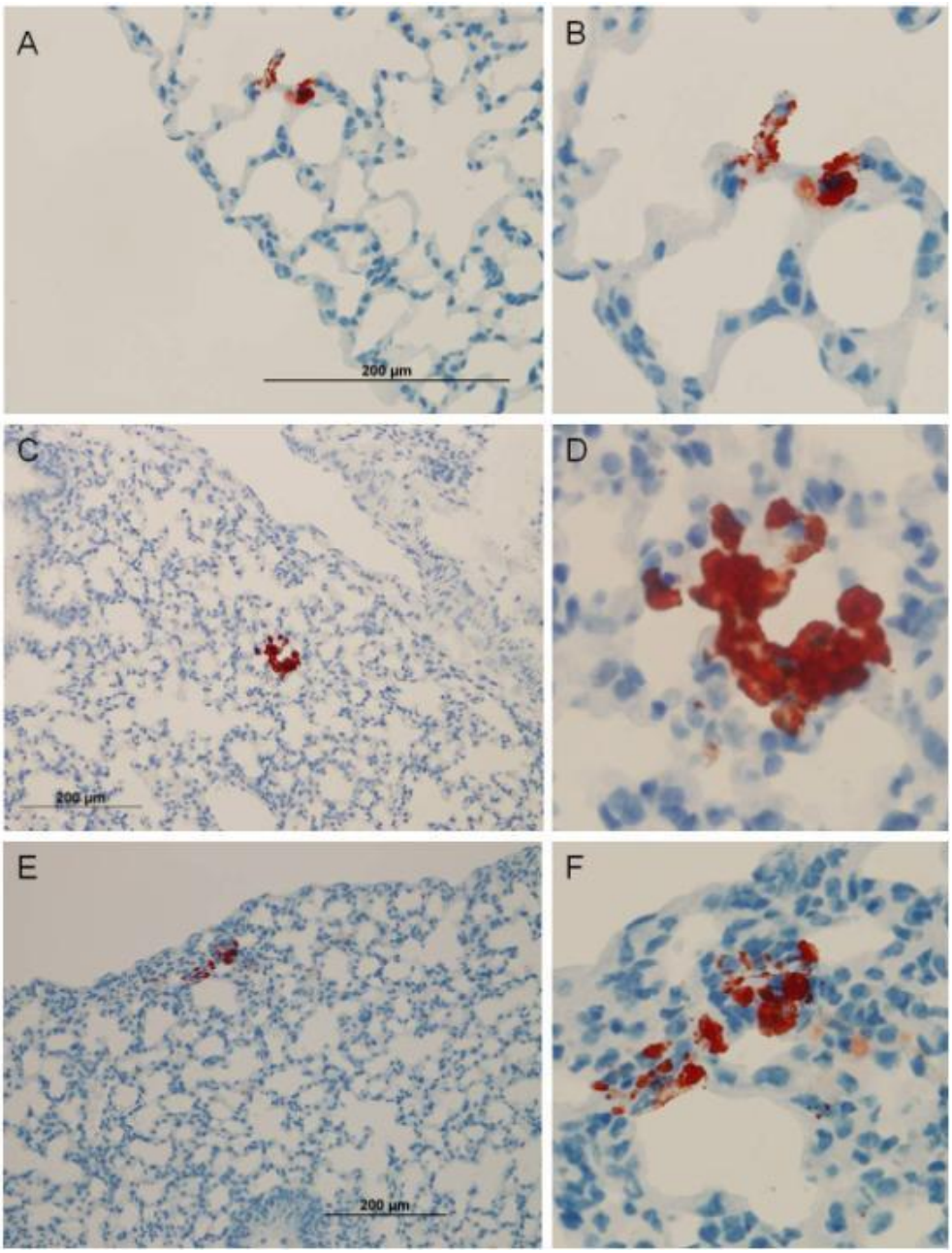

Figure 3.2: Small foci of viral antigen in the alveolar walls were not associated with inflammation or necrosis. **A:** IHC section showing small focal alveolar antigen staining in mouse #28 from the 500 000 $TCID_{50}$ dose group. **B:** closer view of A, original magnification 400x. **C:** lung from mouse #25 from the 50 000 $TCID_{50}$ dose group. **D:** higher magnification for more detail, original magnification 400x. **E:** lung from mouse #21 from the 50 000 $TCID_{50}$ dose group. **F:** higher magnification for more detail, original magnification 200x. This area is at the very periphery of the lobe and there is mild atelectasis: the apparent increase in cellularity is artefactual.

All three mice in the 500 000 $TCID_{50}$ dose group that exhibited neurological signs had evidence of viral replication within the forebrain, specifically the olfactory bulb, manifest as positive IHC staining for viral antigen within the olfactory bulb in nerve fibres in glomerular and medullary layers, as well as neurones and their processes (Figure 3.3 and Figure 3.4).

Viral replication was not confirmed by immunohistochemistry in any other mouse tissues (including spleen), consistent with failure of virus to disseminate via the haematogenous route. Similarly, there was no viral antigen identified in brain parenchymal blood vessels, meninges, or brain sites other than the olfactory bulb, consistent with CNS infection not having occurred via the haematogenous route.

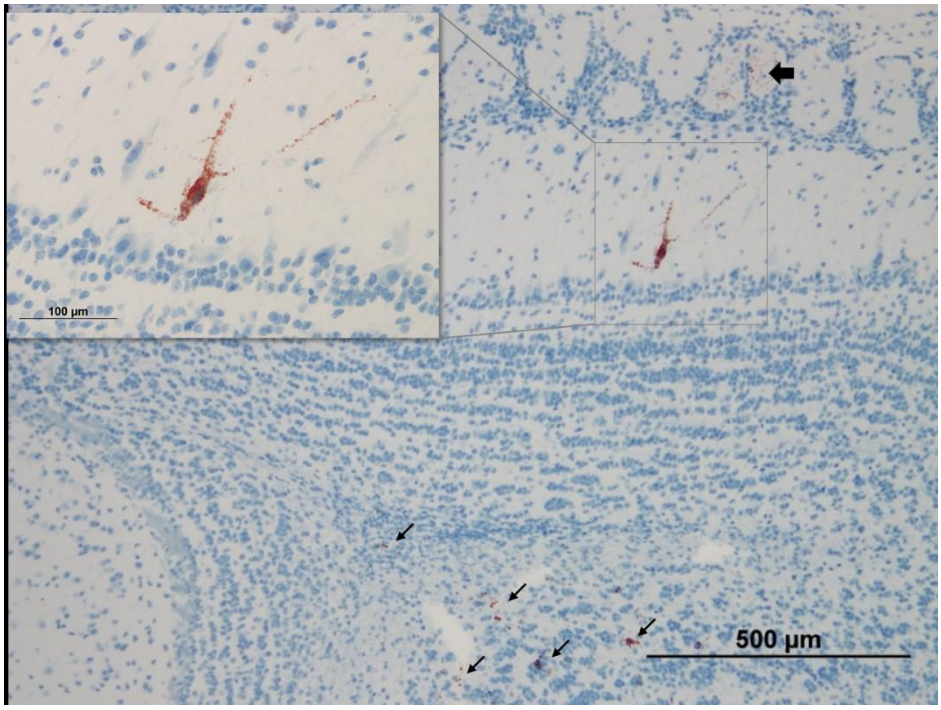

Figure 3.3: IHC stained section from the olfactory bulb of mouse #26, NiV anti-N antibody. There is staining within the glomerular layer (thick arrow) and medulla (thin arrows) as well as within neurones and their processes within the external plexiform layer (inset shows higher magnification of infected neuron). For IHC control olfactory bulb refer to Figure 3.4.

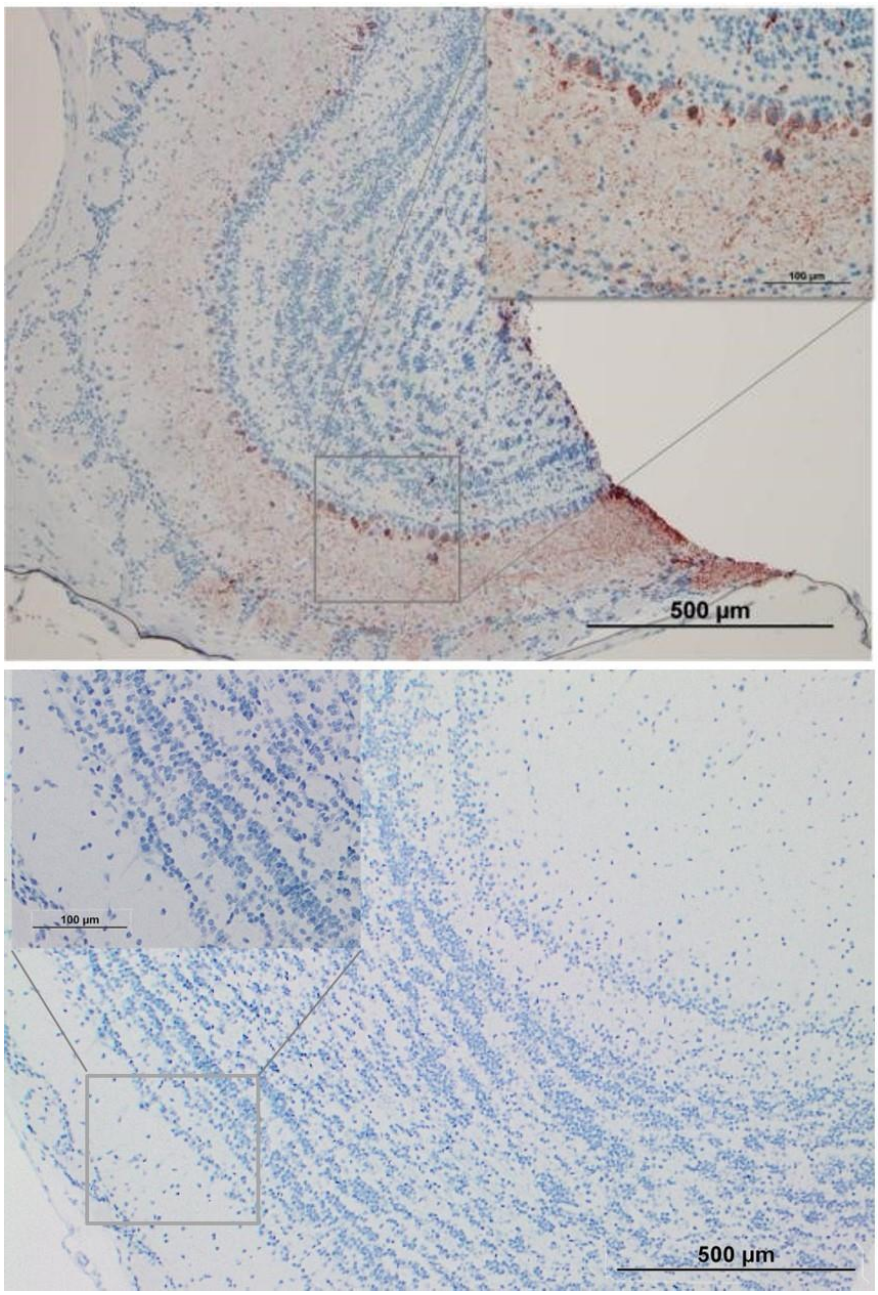

Figure 3.4: Top: IHC stained section from the olfactory bulb of mouse #28, 100x magnification, with insert original magnification of 400x. Antigen staining is distributed throughout all layers of the olfactory bulb but is most notable within the external plexiform and the mitral cell layers. Bottom: IHC control olfactory bulb from uninfected mouse.

3.5.1.3 Molecular virology and classical virology

HeV genome was not detected within the lung or brain of any mouse from the 5, 50, 500, 5000, or 50 000 $TCID_{50}$ dose groups (Table 3.2) including the lung of 2 animals receiving 50 000 $TCID_{50}$ in which antigen had been identified in IHC sections. In the 500 000 $TCID_{50}$ group, viral genome was recovered from the lung of 2 mice (mice #28 and #30). One of these mice

(mouse #28) also had viral antigen detected in the lung on IHC. Viral genome was detected in the brain of 1 of 3 mice (mouse #26) that were positive for viral antigen on IHC of the contralateral hemi-section of brain and showed neurological signs. There was no evidence of viral genome within the spleen of any mouse in the 7 day study.

PCR data for mice ultimately categorised as infected in the 500 000 $TCID_{50}$ dose group are summarised in Figure 3.5.

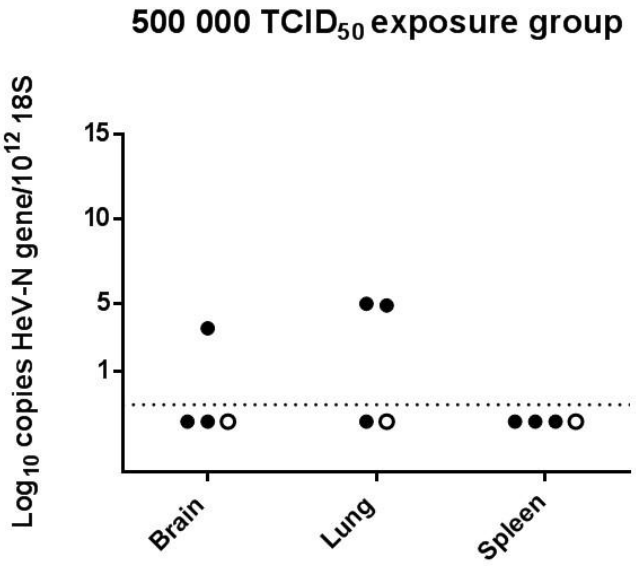

Figure 3.5: 7-day dose ranging study - qPCR data presented as Log_{10} copies of HeV-N gene normalised to 10^{12} copies of 18S in tissues of mice infected after IN exposure to 500 000 $TCID_{50}$ of HeV.
Solid circle represents a mouse with neurological phenotype
Open circle represents a mouse with subclinical phenotype

Virus was re-isolated from the brain of two mice in the 500 000 $TCID_{50}$ dosage group (mice # 26 and #30). Both of these mice exhibited neurological clinical signs and both were positive for antigen staining by IHC within the olfactory bulb. Virus was not isolated from the brain of the other mouse in the 500 000 $TCID_{50}$ dosage group which also had exhibited neurological signs and was positive for antigen staining on IHC within the olfactory bulb. Virus was not re-isolated from any lung samples.

3.5.2 21 day study

3.5.2.1 Clinical observations

The exposure of mice to HeV was generally well tolerated, with the exception of the 500 000 $TCID_{50}$ exposure group in which similar difficulty was encountered to that described above in the 7 day experiment.

All mice continued to gain weight during the study. Mice given 5, 50 or 500 $TCID_{50}$ of HeV remained clinically healthy up to the time of elective euthanasia on Day 21. One of 5 mice (mouse #53) given 50 000 $TCID_{50}$ was recorded as being inactive when undisturbed on Day 10 post-exposure, with mild hyper-responsiveness once stimulated, but the mouse was normal the following day and HeV infection was not confirmed in this animal. Another mouse (mouse #54) given 50 000 $TCID_{50}$ showed mild hyper-responsiveness to stimulation consisting of jumpy, jerky movements on Days 15, 16 and 19. The signs in this animal also resolved before progression to humane endpoints for euthanasia, but it was later confirmed to have been infected on the basis of serology.

One of 5 mice given 5 000 $TCID_{50}$ (mouse #47), 1 of 5 mice given 50 000 $TCID_{50}$ (mouse #55) and 5 of 5 mice given 500 000 $TCID_{50}$ reached their predetermined humane endpoint and were euthanased from Day 8 to Day 15 post-exposure (Table 3.3). Each of these mice displayed acute severe neurological disease manifest as a period of mild neurological signs lasting 6-12 hours before progression occurred to the defined pre-determined humane end points. In the early stages of clinical disease, the mice acted normally during undisturbed observation but, when disturbed by the observer, they were hyper responsive and moved with fast jerky movements. These signs progressed to isolation from the group while undisturbed, hunched posture with ruffled fur, and were associated with an altered grimace score – especially in relation to ear and whisker position (as described in Chapter 2). They also displayed mild ataxia and tremors, increased-excessive facial grooming or scratching at the face and neck region, and some had a stiff vertical tail posture. Their grip strength was poor and they displayed postural and proprioceptive deficits.

Table 3.3: 21-day dose ranging study

Dose $TCID_{50}$	Mouse ID	Infection status	Infection phenotype	Olfactory epithelium Ag *	Lung Ag/PCR	Forebrain Ag/PCR	Spleen Ag/PCR	Euthanasia Day	Serology Bind/Block
5	31-35	All negative	NA	-	-/-	-/-	-/-	21	-/-
50	36-40	All negative	NA	-	-/-	-/-	-/-	21	-/-
500	41	Negative	NA	-	-/-	-/-	-/-	21	-/-
	42	Negative	NA	-	-/-	-/-	-/+	21	-/-
	43	Positive	Subclinical	-	-/-	+/-	-/-	21	-/-
	44	Negative	NA	-	-/-	-/-	-/-	21	-/-
	45	Negative	NA	-	-/-	-/-	-/-	21	-/-
5 000	46	Negative	NA	-	-/-	-/-	-/+	21	-/-
	47	Positive	Neurological	-	-/-	+/+	-/-	11	-/-
	48	Negative	NA	-	-/-	-/-	-/-	21	-/-
	49	Negative	NA	-	-/-	-/-	-/-	21	-/-
	50	Negative	NA	-	-/-	-/-	-/-	21	-/-
50 000	51	Negative	NA	-	-/-	-/-	-/-	21	-/-
	52	Negative	NA	-	-/-	-/-	-/-	21	-/-
	53	Negative	NA	-	-/-	-/-	-/-	21	-/-
	54	Positive	Subclinical	-	-/-	-/-	-/+	21	+/-
	55	Positive	Neurological	+	-/-	+/+	-/-	8	-/-
500 000	56	Positive	Neurological	-	-/+	+/+	-/-	15	+/-
	57	Positive	Neurological	+	+/+	+/+ VI+	-/-	7	-/-
	58	Positive	Neurological	-	+/+	+/+ VI+	-/-	8	-/-
	59	Positive	Neurological	+	+/+ VI+	+/+	-/-	8	-/-
	60	Positive	Neurological	+	-/+	+/+ VI+	-/+	8	-/-

Table 3.2: 21-day dose ranging study

Grey highlighted mice showed no evidence of infection.

Ag: immunohistochemical staining for viral antigen in tissue

PCR: qPCR for viral genome in tissue

VI+: virus isolation was performed on all samples, positive samples are shown

Serology: “Bind” Luminex antibody binding assay, “Block” Luminex receptor blocking assay

“+” present

“-“ not present

* PCR not performed on olfactory mucosa

3.5.2.2 Pathology and immunohistopathology

No significant gross lesions were identified on post-mortem examination in any animal.

No lesions were detected in histological sections from mice in the groups given 5, 50 or 500 $TCID_{50}$ of HeV. Focal to multifocal rhinitis as described earlier was present in 1 of 5 mice from the 50 000$TCID_{50}$ group (Mouse #55) and 3 of 5 mice from the 500 000 $TCID_{50}$ group (mice #57, 59 and 60) (Table 3.3) euthanased at humane endpoint on post-exposure days 8, 7, 8 and 8 respectively. In each case, rhinitis was associated with the presence of viral antigen within the olfactory epithelium.

There was no evidence of tissue injury such as accumulation of inflammatory cells or necrosis in the lung of any mouse, but small foci of positive IHC staining for viral antigen were found in the alveolar wall of 3 of 5 mice given 500 000 $TCID_{50}$ (mice #57, 58 and 59). Each of these mice had reached a humane end point for neurological signs necessitating euthanasia on days 8 and 9 post infection, prior to the appearance of detectable antibody in serum. Antigen staining resembled that seen in the lung of mice in the 7 day study.

Viral antigen was detected by IHC in the olfactory bulb of all mice that were euthanased at humane endpoint (which was always on account of neurological signs), and was frequently seen highlighting the neuronal processes and cell bodies of neurons as well as more diffuse globular scattering. In one mouse (mouse #56) which was euthanased on Day 15, viral antigen was also detected in the pyriform lobe. This observation is consistent with viral propagation along the olfactory tract, as previously proposed (Dups *et al.*, 2012).

Where viral antigen was detected in brain this was usually associated with distinct neuropathology. The lesions consisted of mild to marked mononuclear (predominately lymphocytic, with some plasma cells and histiocytes) inflammatory cell infiltration of the meninges (constituting meningitis) of the rostral brain extending over the most rostral aspects of the frontal lobe of the cerebral cortex (Figure 3.6). Within the olfactory bulb, especially in the glomerular layer, the inflammatory infiltrate was also present within the parenchyma and accompanied by injury to neuronal cells (constituting encephalitis). Small condensed fragments of nuclear debris, representing cellular necrosis, were frequently

present within the glomerular and external plexiform layers of the olfactory bulb (Figure 3.6). There was also mild multifocal gliosis with perivascular cuffing in the cerebral cortex immediately adjacent to the olfactory bulb. In one mouse given the 500 $TCID_{50}$ dose (Mouse #43) which remained clinically normal throughout the study period, small amounts of viral antigen were seen throughout the glomerular layer, external plexiform layer, and medulla of the olfactory bulb in the absence of discernible meningoencephalitis.

Where detected, the amount of viral antigen - as judged by number of globules and extent of distribution throughout the olfactory bulb - was not appreciably different between 5 000, 50 000 and 500 000 $TCID_{50}$ dose groups (Figure 3.7, plates A, B and C respectively). However, more antigen staining was visible in these mice compared to mice in the 7-day study (Figure 3.7, plates D and E from mice in the 7-day study provided for comparison)

Viral replication was not confirmed by immunohistochemistry in any other mouse tissues (including spleen), consistent with absence of haematogenous dissemination. Similarly, there was no viral antigen identified in brain parenchymal blood vessels, meninges, or brain sites other than olfactory bulb and pyriform lobe as described above, consistent with CNS infection not having occurred via the haematogenous route.

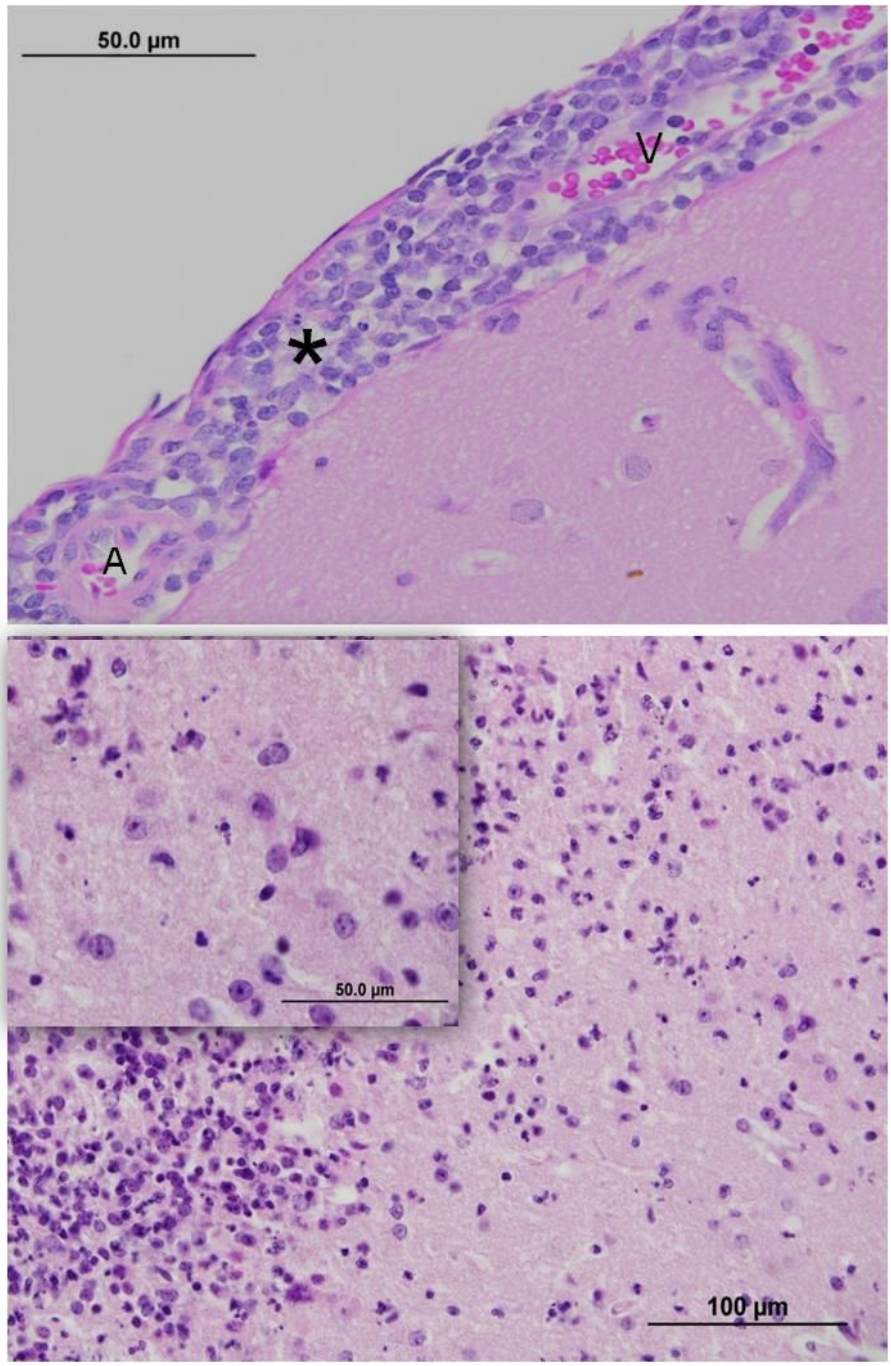

Figure 3.6: H&E stain sections. Top; the rostral cerebral cortex from mouse #56 from the 500 000 $TCID_{50}$ dose group which was euthanased 15 days p.e.. The meninges are expanded by numerous mononuclear inflammatory cells (*). A small artery (A) and a small vein (V) show no evidence of vasculitis. Bottom; olfactory bulb from mouse #58 which was euthanased on day 8. Small condensed fragments of nuclear debris, reflecting neuronal necrosis, were frequently present in the glomerular external plexiform layers of the olfactory bulb from infected mice.

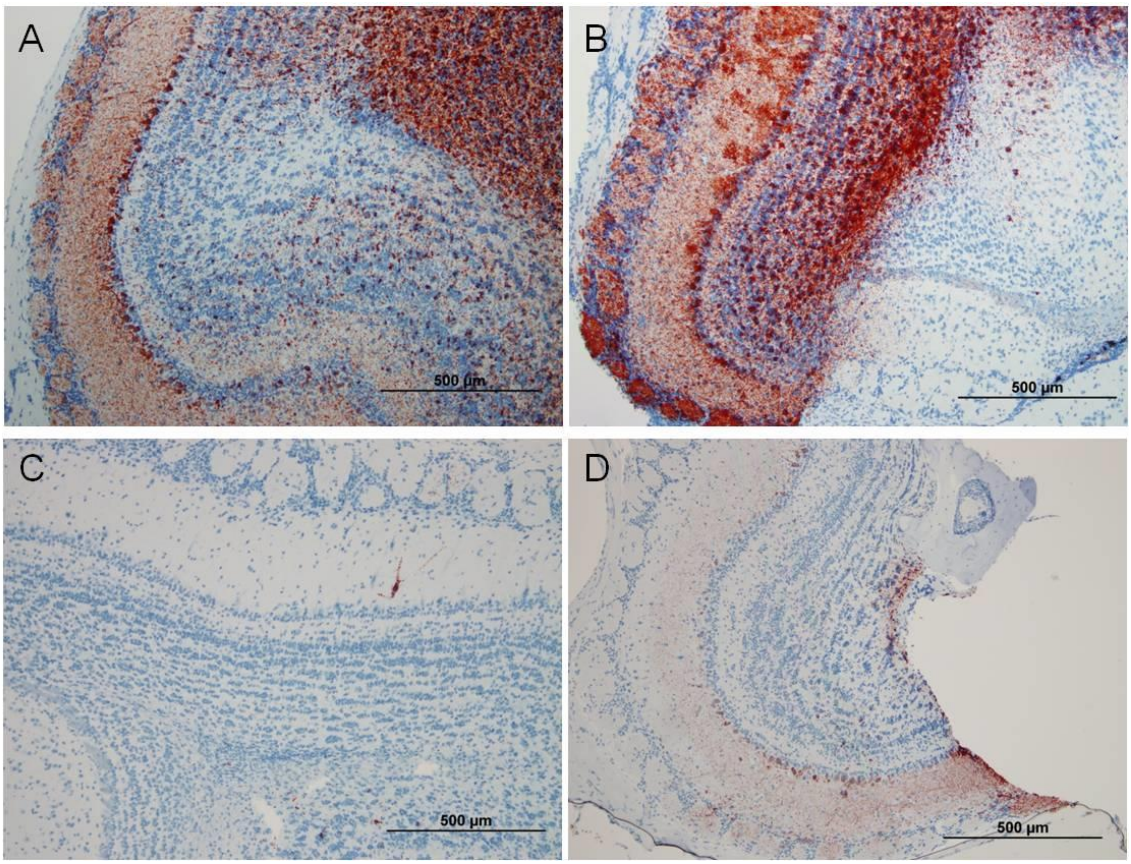

Figure 3.7: IHC stained sections of olfactory bulb from mice that exhibited neurological disease necessitating euthanasia, original magnification x 100. **A:** 21-day study, mouse #47 from the 5 000 $TCID_{50}$ dose group, euthanased on day 11. **B:** 21-day study, mouse #55 from the 50 000 $TCID_{50}$ dose group, euthanased on day 8. **C** and **D** are for comparison from mouse #26 and mouse #28 from the 500 000 TCID50 dose group in the 7-day study, euthanased on day 7.

3.5.2.3 Molecular virology and classical virology

HeV genome was not detected within the lung or brain of any mouse from the 5, 50, or 500 $TCID_{50}$ dose groups (Table 3.3), including the brain of mouse #43 from the 500 $TCID_{50}$ dose group in which the contralateral hemi-section was positive for viral antigen. Viral genome was detected in the brains of mice #47 and # 55 from the 5 000 and 50 000 $TCID_{50}$ dose groups, which were euthanased on account of neurological signs on post-exposure days 11 and 8 respectively. Viral genome was recovered from the lung and brain of all mice in the 500 000 $TCID_{50}$ group; each mouse was euthanased on account of neurological disease from day 8 to 15 p.e..

Viral genome was recovered from the spleen of 4 mice, one in each of the 500, 5 000, 50 000 and 500 000 $TCID_{50}$ groups (Table 3.3). In two of these, mouse #42 given 500 $TCID_{50}$ and mouse #46 given 5 000 $TCID_{50,}$ there was no corroborative evidence for HeV infection; accordingly, these mice were not considered to have met the case definition for infected mice.

PCR data for mice that were ultimately categorised as infected in the 21 day study are presented in (Figure 3.8). The level of viral genomic copies within the forebrain appeared similar irrespective of dose rate and euthanasia day. Interestingly, copy numbers recorded in brain samples were always higher than any recorded for lung.

Virus was re-isolated from the brain of 3 of 5 mice given 500 000 $TCID_{50}$, each of which had been euthanased on Day 7 or 8 post exposure on account of neurological disease. Virus was also re-isolated from the lung of one of these same animals.

Virus was not re-isolated from the spleen of any mouse.

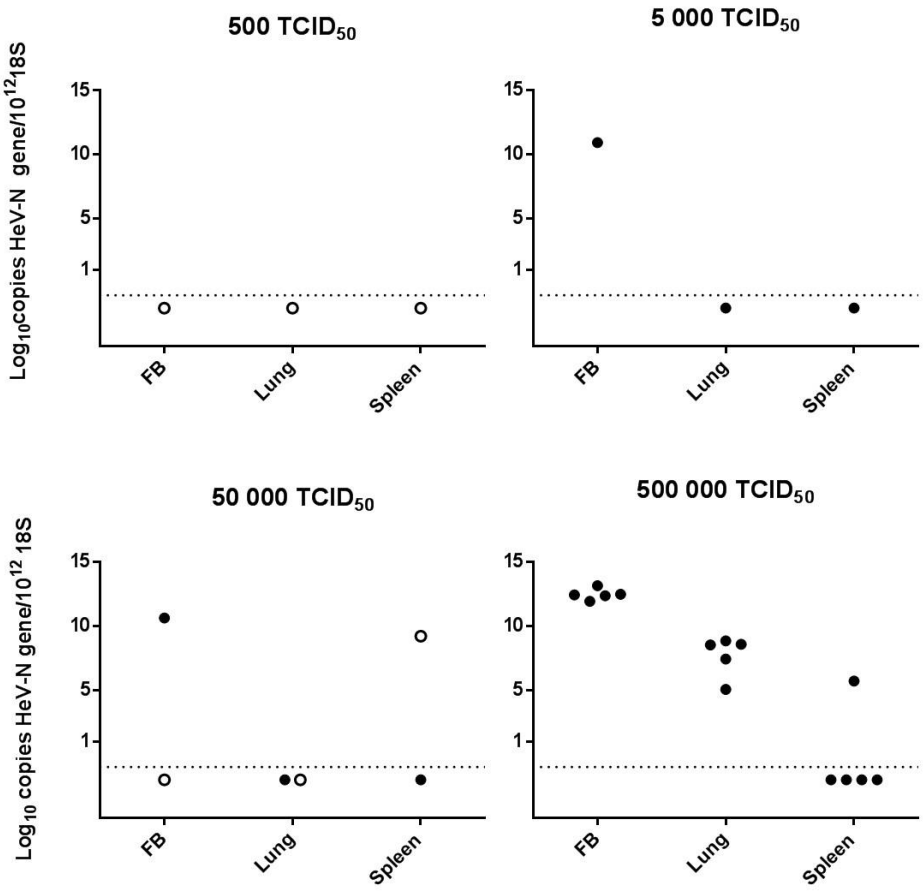

Figure 3.8: 21-day dose ranging study qPCR data from infected mice, presented as Log_{10} copies of HeV-N gene normalised to 10^{12} copies of 18S in forebrain (FB), lung and spleen of mice exposed IN to 500, 5 000, 50 000 and 500 000 $TCID_{50}$ of HeV.

Solid circle represents a neurological phenotype

Open circle represents a subclinical phenotype

3.5.2.4 Serology

All mice receiving 5, 50, 500 or 5 000 $TCID_{50}$ HeV remained negative for antibody by Luminex binding assay. This included mouse #43 (500 $TCID_{50}$ dose group) which had viral antigen in brain at Day 21, and mouse #47 (5 000 $TCID_{50}$ dose group) which had been euthanased on Day 11 on account of neurological signs. Two mice were positive for a binding antibody response to HeV $_s$G by Luminex binding assay. One of these mice (mouse #54, 50 000 $TCID_{50}$ dose group) remained clinically well until the end of the study period, and the other (mouse #56, 50 000 $TCID_{50}$ dose group) succumbed to neurological disease at Day 15. No mice developed an antibody response to HeV $_s$G by Luminex receptor blocking assay.

3.5.2.5 Assignment of infection status, infection phenotype, and median infectious dose (ID_{50}) calculations

The infection status of each mouse was determined according to the criteria established above (see 1.4 Data Analysis). An infection phenotype for each animal was then assigned following integration of the clinical and laboratory findings. Outcomes are presented in Table 3.2 and Table 3.3.

In the 7-day study, HeV infection was not confirmed in any mice exposed to doses of 5, 50, 500 or 5 000 $TCID_{50}$. A subclinical infection phenotype was recorded in both 50 000 $TCID_{50}$ and 500 000 $TCID_{50}$ dosage groups in mice with evidence of virus replication in lung and/or olfactory epithelium. An infection phenotype with disseminated organ involvement and systemic illness was not identified in any dosage group. An infection phenotype characterised by neurological signs was manifest in mice given 500 000 $TCID_{50}$.

In the 21-day study, HeV infection was not confirmed in any mice exposed to doses of 5 or 50 $TCID_{50}$. A subclinical infection phenotype was recorded in both 500 $TCID_{50}$ and 50 000 $TCID_{50}$ dosage groups in mice with evidence of virus replication in brain or through the development of antibody. An infection phenotype with disseminated organ involvement and systemic illness was not identified in any dosage group. An infection phenotype characterized by neurological signs was manifest in mice given 5 000, 50 000 and 500 000 $TCID_{50}$.

For the 7-day study, infection occurred in 0 of 5 mice in the 5, 50, 500 and 5000 $TCID_{50}$ dose groups, and in 3 of 5 and 4 of 5 mice in the 50 000 and 500 000 $TCID_{50}$ dose groups respectively. For the purpose of ID_{50} calculation, it was assumed that the next highest dose (5 000 000 $TCID_{50}$) in the series would have led to 100% infection. On this basis, the ID_{50} for the 7- day study was calculated to be $5 \times 10^{4.1}$ $TCID_{50}$ (62 946 $TCID_{50}$).

For the 21-day study, infection occurred in 0 of 5 mice in the 5 and 50 $TCID_{50}$ dose groups, 1 of 5 mice in the 500 $TCID_{50}$ dose group, 1 of 5 mice in the 5 000 $TCID_{50}$ dose group, 2 of 5

mice in the 50 000 $TCID_{50}$ dose group and 5 of 5 mice in the 500 000 $TCID_{50}$ dose group. The ID_{50} for the 21-day study was calculated to be 5 x $10^{3.7}$ $TCID_{50}$ (25 059 $TCID_{50}$).

There was no significant difference between the 7-day study and the 21-day study with respect to the overall likelihood of a mouse being identified as infected by HeV (Fisher's exact test, p = 0.77). Similarly, there was no significant difference between the two studies in the likelihood of recording a subclinical phenotype versus a neurological phenotype in infected mice (Fisher's exact test, p=0.30).

On the basis of the assessed similarities in the 7-day and 21-day studies in respect of infection rates and infection phenotypes, data from the two studies were pooled for an additional analysis to test the relationship between exposure dose and infection phenotype. There was a significantly higher likelihood of observing a neurological phenotype when the exposure dose approximated 10 x ID_{50} (500 000 $TCID_{50}$) compared to a dose of ~1 x ID_{50} (50 000 $TCID_{50}$) (Fisher's exact test, p=0.02) (Figure 3.9).

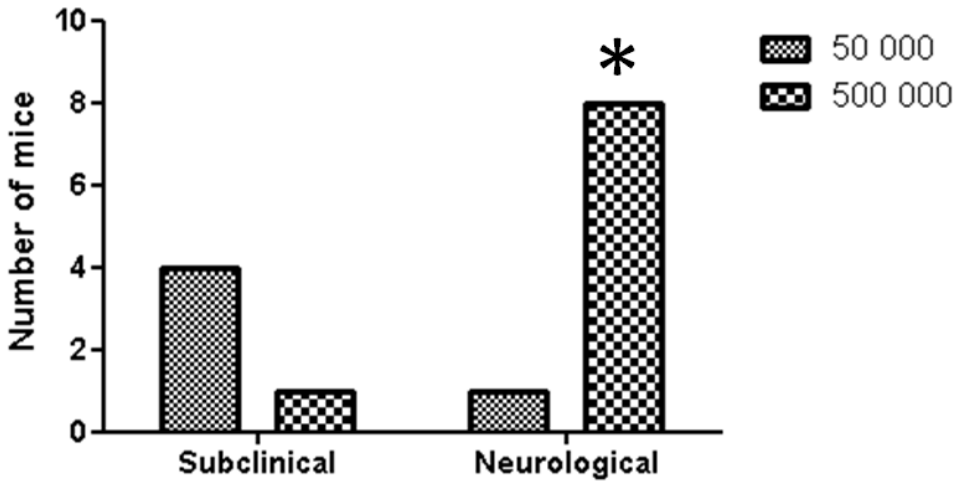

Figure 3.9: Infection phenotypes from 50 000 and 500 000 $TCID_{50}$ dosage groups (combined data from 7-day and 21-day studies). There was a significantly higher likelihood * (p=0.02) that mice given 500 000 $TCID_{50}$ will show a neurological infection phenotype rather than a subclinical infection phenotype.

3.6 Discussion

This chapter describes the infection phenotype induced in C57BL6 mice following IN exposure to HeV at different doses, ranging from 5 to 500 000 $TCID_{50}$ in a tenfold dilution series. Clinical signs were monitored for either 7 or 21 days, and tissue tropism, viral replication, and the extent and severity of lesions induced by infection at the time of euthanasia were assessed for each dose.

The studies generally proceeded without complication, however it was noted that mice given the highest dose of HeV (500 000 $TCID_{50}$) developed transient apnoea after drop application of inoculum to the nares, followed by a period of gasping and increased respiratory effort. This was attributed to the viscosity of the inoculum at low dilution, and could not have been avoided. However, as further drop application was not continued in each mouse until breathing had returned to normal, mice receiving this dose experienced longer times under anaesthesia compared to the other groups. There was no evidence that this introduced a variable beyond infectious dose. No alterations were seen in distribution or severity of either lower airway infection or olfactory bulb associated encephalitis resulting from an increase in respiratory effort in the 500 000 $TCID_{50}$ dose group compared to the 50 000 $TCID_{50}$ dose group.

Virus replication was confirmed in the olfactory mucosa of mice sampled either 7 or 8 days post-exposure from both 7 and 21-day studies. These findings generally align with the observations made by Dups *et al.* (2012) on the incidence and duration of positive IHC in the olfactory epithelium, where staining was usually found from day 6 to 10, but less reliably thereafter. Positive staining of the olfactory mucosa was also localised, meaning that even in acutely infected animals affected areas of tissue may not always have been present within the sections examined. In comparison to humans which have a relatively simple nasal architecture, mice have more complex anatomy with an intricate branching turbinate structure due to the importance of olfaction in the species. It is unknown whether the olfactory route is important in human Henipavirus infection. There was no histological change in the olfactory bulb of 9 human NiV patients but magnetic resonance imaging revealed involvement of the uncus of the temporal lobe in 30% of cases (Sarji *et al.*, 2000). As the uncus is covered by part of the olfactory cortex this was interpreted as providing

indirect evidence of virus entry through the nasal airways, along the olfactory bulb, and into the uncus (Borisevich *et al.*, 2017). Additionally, Borisevich *et al.* (2017) demonstrated that human olfactory neurons are highly susceptible to infection with henipaviruses making this a plausible pathway for neuroinvasion in humans.

The area of the nasal cavity affected by HeV in mice was the caudal part, corresponding to areas covered by olfactory epithelium. Olfactory epithelium lines approximately the caudal 50% of the nasal airway chambers in the mouse, compared to only 1% of the surface area in humans (van Riel *et al.*, 2015). The olfactory epithelium is a specialised sensory neuroepithelium containing olfactory sensory neurones, supporting sustentacular cells, and regenerative basal cells. Olfactory sensory neurones have a ciliated apical surface projecting through the epithelial surface, providing an extensive surface area for reception of odorants. An axon projects from the base of the cell and joins axons from other olfactory sensory neurones to form non-myelinated nerve fascicles. These olfactory nerve fascicles perforate the cribriform plate to form the nerve fibre layer of the olfactory bulb in the brain (Harkema *et al.*, 2006). The nasal epithelium is lined by mucus which is propelled at different speeds and directions depending on intranasal location. Interestingly, the mucus covering the olfactory epithelium moves very slowly: it has an estimated turnover time of several days, whereas mucus covering the respiratory epithelium moves rapidly and has an estimated turn over time of 10 minutes in the laboratory rat (Morgan *et al.*, 1984). The observation that HeV replication in mice was localised to the caudal nasal cavity could reflect a relative sensitivity of murine olfactory sensory neurones to HeV infection compared to other cells within the nasal mucosa, or perhaps an enhanced propensity for infection becoming established due to the prolonged virus contact time allowed by the slow mucociliary clearance rate from this area. In any event, virus localisation at that site provided the opportunity for anterograde spread into the CNS via the nasal cavity.

HeV was re-isolated from lung or forebrain samples of some mice. For lung, the single positive sample was obtained in the 21-day study on Day 8 post-exposure, consistent with the observations of Dups *et al.* (2012), who reported that live virus was reliably recovered from the lung of infected mice between days 4 and 9 post-exposure (Dups *et al.*, 2012). By contrast, the present work confirmed virus replication in lung by IHC in 3 mice in the 21 day study that were sampled prior to Day 10 as well as 3 mice in the 7-day study. In this

experiment a qualitative method assessed paired samples of 100 µl of specimen introduced over cells in 100 µl of media which, after 30 minutes, was diluted in an additional 400 µl of media. By comparison, for each sample Dups *et al.* performed paired serial 1:10 dilutions within 96 well plates.

Successful re-isolation of virus from the forebrain of mice given 500 000 $TCID_{50}$ HeV in both the 7-day and 21-day studies, each of which also showed neurological signs, was of interest. Dups *et al.* (2012) did not re-isolate HeV from brain samples of C57Bl6 and BalbC mice exhibiting neurological disease collected between 12 and 21 days after IN exposure to 50 000 $TCID_{50}$ HeV. These authors postulated that HeV replication in forebrain was restricted to neurons and that trans-neuronal spread occurred via cell contact dependent processes without budding of infectious virions. Further experimental work with neuronal culture in microfluidic chambers demonstrated that while HeV could not be re-isolated from neuronal culture alone, it could be re-isolated if infected axons came into close contact with "budding-competent" Vero cells (Dups, 2015). It is therefore feasible that the positive virus re-isolation results in the current work, from samples obtained slightly earlier in the infection course (days 7 and 8 post-exposure), may reflect transient involvement of "budding competent" cell populations within the CNS of infected mice. Such cells might include microglia, endoneural cells within olfactory nerves, or the arachnoid cuff of the meninges at the cribriform plate adjacent to the nasal mucosa. The majority of Dups *et al's* work was conducted with BALB/c mice, and there may also be differences in the biology of HeV infection of the brain that is attributable to mouse strain.

PCR testing of the lung sample was negative in two of three mice in the 7-day study where virus replication had been confirmed in that tissue on the basis of IHC. By IHC, the foci of virus infected cells throughout the lung parenchyma were both small and infrequent. In sampling the lung for testing, tissue pieces were collected from similar areas of both right and left lung lobes, and these were either formalin-fixed for histopathology or homogenised and the supernatant used for both PCR and virus isolation. The most plausible explanation in this instance for a positive IHC result in lung in the absence of detectable viral genome during acute infection is sampling artefact: by chance, the tissue collected for PCR/virus isolation did not contain a focus of viral infection. In the lung of one mouse in the 7-day study, and in the lung (two mice) and spleen (four mice) in the 21-day study, positive PCR

results were also obtained in the absence of successful virus isolation or demonstration of viral antigen in tissues. Although PCR is an analytically sensitive test, for reasons described earlier a positive PCR result alone was not considered sufficient - in this experimental challenge study - to confirm virus replication within lung or spleen

PCR testing of forebrain samples was also negative in 1 of 5 samples where virus had been re-isolated. This finding is difficult to interpret as both PCR and VI testing were carried out on the same primary samples, so the most plausible explanation is cross-contamination during the process of virus isolation although it is not clear how this might have occurred. Interestingly, the mouse was confirmed to have been infected by a positive IHC result on the contralateral forebrain sample.

Also, a negative PCR and VI result was obtained for the forebrain of one mouse in each of the 7-day and 21-day studies (mouse #28 and #43 respectively) where virus replication had been confirmed by IHC in the contralateral hemibrain specimen. In these instances, the most plausible explanation is unilateral initiation of viral replication within the olfactory sensory neurons and olfactory bulb. The finding of unilateral involvement of forebrain may also be time dependent, occurring prior to bilateral propagation of virus through the anterior commissure, as has been demonstrated with herpes virus infection in the olfactory bulb (Jennische *et al.*, 2015). As the mice with presumed unilateral involvement were sampled 7 and 21 days post-exposure, this also suggests the factors governing the rate of propagation of HeV within brain vary substantially between individuals. Mice that were positive by IHC as well as PCR and/or VI were concluded to have initiated viral replication on both sides of the nasal cavity. Confinement of lHC staining within the olfactory bulb and piriform lobe suggests that transneuronal propagation of viral infection has not yet reached the level of anterior commissure to allow lateral spread.

Previously Dups *et al* demonstrated that respiratory infection in mice is successfully controlled without evidence of a robust adaptive immune response in the form of virus-neutralising antibodies, although most mice had binding antibody responses to HeV sG by Luminex assay (Dups *et al.*, 2012). Limited serological data was generated in the current work, with 2 out of 4 infected mice that survived for over 10 days developing detectable antibodies against HeV. One of the 2 mice had a neurological infection phenotype

(euthanased on humane grounds on day 11); and the site of HeV replication in the other mice (electively euthanased on day 21) was not determined.

Although HeV replication was confirmed in lung and forebrain of mice in the 7-day study, and in mice euthanased at various time-points in the 21-day study, a systemic infection phenotype characterised by general clinical malaise, induction of pathology in other organ systems, and disseminated virus replication, was not observed in any study group. Rather, the outcome of mouse exposure to HeV was either subclinical infection or neurological disease. In the case of subclinical infection, virus replication was localised in upper and/or lower respiratory tract, or in brain. Although there was no significant difference between the two studies in the likelihood of recording a subclinical phenotype versus a neurological phenotype in infected mice, it is reasonable to suggest that tissue localisation of HeV within subclinically infected animals may change with time post-exposure. For example, subclinical infection due to virus replication in respiratory tract may be difficult to confirm after day 17 post-exposure (Dups *et al.*, 2012). In addition, it is possible that subclinical infection with HeV replication in the forebrain may have evolved into a clinical neurological disease with a longer period of observation.

The findings in lung are consistent with a previous report of self-limiting subclinical lower respiratory tract infection in mice exposed to 50 000 $TCID_{50}$ HeV IN, in which viral antigen was visible in lung from 6 days post-exposure, live virus was isolated up to day 10 post-exposure, and viral RNA was present from 2 to 14, and in some cases up to 21, days post-exposure (Dups *et al.*, 2012). Importantly, the current work also confirmed that viral replication in mouse lung was not associated with detectable inflammatory lesions such as bronchoalveolitis, pulmonary vasculitis, pulmonary haemorrhage or oedema.

These observations are a distinct contrast to findings in the horse (Hooper *et al.*, 1997a; Marsh *et al.*, 2011), cat (Hooper *et al.*, 1997b), ferret (Pallister *et al.*, 2011), non-human primate (Bossart *et al.*, 2011; Rockx *et al.*, 2010) and hamster (Guillaume *et al.*, 2009; Rockx *et al.*, 2011) in which virus replication routinely results in an infection phenotype characterised by severe generalised disease. This necessitates euthanasia of experimental animals within 5 to 10 days post-exposure, and the acute, fulminating systemic illness is attributable to wide-spread vasculitis affecting multiple major organ systems, particularly

the lung and central nervous system. Pulmonary involvement in these animals is characterized by severe necrotising bronchoalveolitis and an intense influx of inflammatory cells. Multi-systemic disease is manifest as parenchymal necrosis and intense inflammation in additional key organs and tissues including lymph nodes, spleen, liver and kidney.

An acute neurological disease attributable to HeV replication in brain was also replicated in both 7 and 21-day studies, with viral antigen in brain limited to the olfactory bulb and pyriform lobe and frequently located within neuronal cell bodies and processes. Although inflammatory reactions or evidence of tissue injury were not detected at day 7 post-exposure, lesions were visible in mice euthanased on day 8 post-exposure. As they developed, the lesions consisted of non-suppurative meningoencephalitis, neuronal degeneration, and glial reaction. Importantly, endothelial viral antigen or vasculitis – reflecting hematogenous spread of virus to the CNS - was not detected in any mouse. In addition, the timeframe over which neurological disease became apparent (day 7 to day 15) would not be expected to have obscured any systemic infection that may also have occurred. The observations in mouse CNS are similar to those previously reported for mice exposed IN to 50 000 TCID50 HeV by Dups *et al.* (2012), where viral antigen was detected in the olfactory tract from day 6 post-exposure.

The encephalitic pattern of HeV infection seen in mice, centred on the olfactory tract, differs from that seen in the brain of other species such as human (Escaffre *et al.*, 2013b; Wong & Ong, 2011), horse (Hooper *et al.*, 1997a; Marsh *et al.*, 2011; Selvey *et al.*, 1995), ferret (Pallister *et al.*, 2011), non-human primates (Bossart *et al.*, 2011; Rockx *et al.*, 2010), hamster (Guillaume *et al.*, 2009; Rockx *et al.*, 2011), cat and guinea pig (Hooper *et al.*, 1997b). In these species multifocal lesions are randomly distributed throughout the brain, simultaneously affecting the cerebrum, cerebellum, hippocampus and also olfactory cortex: they are characterised by vasculitis with surrounding areas of parenchymal necrosis consistent with haematogenous dissemination of virus. However, a similar olfactory tract encephalitis, in addition to the severe systemic disease mentioned above, has also been described in hamsters challenged IN with NiV (Munster *et al.*, 2012). Munster *et al.* (2012) concluded that NiV entry into the CNS by the olfactory route coincided with the occurrence of respiratory disease, suggesting that the initial entry of NiV into the CNS occurs in hamsters simultaneously with, rather than as a result of, systemic virus replication.

In the current study, HeV replication in the forebrain of mice was likely established via involvement of olfactory sensory neurons, and clinically significant infection was always attributable to virus replication in brain. Overall, the findings of these studies are consistent with a resistance of mice to generalised systemic infection under exposure conditions that would be expected to induce fulminating illness and widespread virus replication in other mammals as described above. This suggests that either no significant viraemia develops in HeV infected mice or that most peripheral tissues of mice are not permissive to HeV replication. Importantly, where HeV replication was confirmed in mouse lung, there was also no evidence for significant tissue injury.

For each study, the incidence of HeV infection in mice was dose dependent and permitted estimates of ID_{50} to be carried out. In spite of the small group sizes, the estimated ID_{50} was similar for both studies (differing by less than ½ log), with the lower value being recorded in the 21-day study. The observed variation in estimated ID_{50} between the two studies was attributable to the subclinical infection of one mouse in the 500 $TCID_{50}$ dose group and neurological disease in a mouse given 5 000 $TCID_{50}$ in the 21-day study, and absence of infection in one mouse given 500 000 $TCID_{50}$ in the 7-day study. Subclinical infection of the forebrain confirmed at day 21 in the first individual may be a consequence of a longer incubation period associated with receiving a lower virus dose, as reported with HeV infection in hamsters (Rockx *et al.*, 2011). However, the difference overall between the two studies in the number of mice infected at each dose was concluded to be a chance observation, especially as 2 of the 3 doses used were below the estimated ID_{50}.

In a previous time-course study in aged Balb/c mice, using an IN HeV challenge dose of 50 000 $TCID_{50}$, infection was uniformly established in 21 mice sampled from days 4 to 28 post-exposure (Dups *et al.*, 2012). These findings were consistent with a lower ID_{50} for that cohort than was observed here for young C57Bl mice and suggest that, where practicable, mouse age and strain should be standardized for a particular virus dose in any series of HeV exposure studies.

As previously stated and in contrast to observations from the current mouse study, hamsters (Rockx *et al.*, 2011), ferrets (Pallister *et al.*, 2011) cats and Guinea pigs (Hooper *et al.*, 1997b; Westbury *et al.*, 1996; Westbury *et al.*, 1995) reliably develop uniformly severe

systemic disease with disseminated virus replication following exposure to 5 000 $TCID_{50}$ HeV via either parenteral or non-parenteral routes: hamsters and ferrets in small group studies (n=5 and n=2 respectively) have also succumbed to doses as low as <1 and 50 $TCID_{50}$ respectively (Pallister *et al.*, 2011; Rockx *et al.*, 2011). Considered together, the dose responses of mice following HeV exposure in the current studies support an innate resistance of mice to HeV infection compared to other commonly studied mammals.

In the current work, subclinical infection was documented in more than one different dosage group in both the 7-day and 21-day study, ranging from a mouse given 500 $TCID_{50}$ in the 21-day study to a mouse given 500 000 $TCID_{50}$ in the 7-day study. Similarly, a neurological infection phenotype was also seen in a range of dosage groups: 5 000, 50 000 and 500 000 $TCID_{50}$ in the 21-day study, but only the 500 000 $TCID_{50}$ group in the 7-day study. Under the study conditions used here, it is clear that a particular HeV infection phenotype cannot be induced in individual animals by administering a particular dose of virus or by selecting either a 7 or 21 day study length. However, when the infection data of the two studies were combined for doses at or above the $ID_{50,}$ mice given 500 000 $TCID_{50}$ were more likely to develop a neurological as opposed to subclinical infection compared to those given 50 000 $TCID_{50}$.

The overall conclusion was that neurological disease, attributable to anterograde infection of the CNS, would be an expected complication of any future studies targeting the mechanisms of control of systemic replication of HeV in mice, and would be difficult to prevent under the study conditions described. However, it was also observed that the risk of inducing neurological disease may be increased following the administration of 500 000 $TCID_{50}$ HeV IN.

The hypothesis has been partially proven; in comparison to other laboratory species, mice appear resistant to systemic disease following challenge with routinely used doses of HeV. However, doses may impact infection phenotype. 500 000 $TCID_{50}$ dosing was more likely to cause neurological disease phenotype.

Selection of a virus dose rate for application to future studies on mechanisms of control of systemic HeV infection in mice is not straightforward. A balance needs to be found between

providing a high likelihood of infecting mice from the exposure dose, while minimising the chances of anaesthetic complications following virus administration and of inducing anterograde infection of the CNS. Accordingly, the recommendation for a dose rate for future studies in mice, where the focus will be on non-neurological infection is 50 000 $TCID_{50}$. It is considered prudent to avoid the 500 000 $TCID_{50}$ dose for two reasons. Firstly, that dose induced complications during administration and, secondly, the increased likelihood of neurological disease may lead to a requirement for euthanasia of animals earlier than is optimal for the experimental design. At a dose of 50 000 $TCID_{50}$ it is reasonable to expect some animals to have subclinical respiratory tract infection, especially in 7-day studies, or subclinical infection of brain, and also for some animals not to be infected by the exposure dose. However, use of this dose has previously permitted meaningful scientific outcomes in both C57Bl6 and BalbC mice in earlier work (Dups *et al.*, 2012). It is understood that animal studies at BSL4 involve severe restrictions on animal numbers and place limitations on statistical analysis (Mire *et al.*, 2014), and that the variability inherent within the mouse HeV infection model will pose an additional challenge to the interpretation of study findings. However, understanding how mice limit HeV replication and avoid serious injury to parenchymal organs may be the key to the development of novel infection management strategies for application in other species.

CHAPTER 4: MICE DEFICIENT IN INTERFERON SIGNALLING SHOW MORE WIDESPREAD HENDRA VIRUS REPLICATION WITHOUT DEVELOPING A SYSTEMIC INFECTION PHENOTYPE

4.1 Introduction and background

The findings of the previous chapter, supported by those of earlier studies (Dups *et al.*, 2012), confirm that wild type C57Bl6 mice are resistant to the development of a systemic HeV infection phenotype (comprising general clinical malaise, induction of pathology in diverse organ systems, and disseminated virus replication) under exposure conditions that would be expected to induce fulminating illness and widespread virus replication in other susceptible mammals. In infected WT mice, viral replication was limited to the upper and lower respiratory tracts and brain. Inflammatory lesions were only identified in the olfactory mucosa and in the brain, where they centred on the olfactory tract consistent with an anterograde infection route.

Many viruses have developed multifaceted anti-interferon strategies (as reviewed by Basler, 2012; Chambers & Takimoto, 2009; Goodbourn & Randall, 2009; Ramachandran & Horvath, 2009; and Shaw, 2009). For example, and similarly to other paramyxoviruses, the P gene of HeV and NiV can be edited to encode several viral proteins, the P, V, W and C proteins, which all inhibit the host IFN antiviral response in one or more ways (Basler, 2012). The ability of Henipavirus proteins P, V and W to prevent IFN signalling is dependent on STAT1 binding and inhibition of activation. The presence of P, V and W proteins inhibits the phosphorylation of STAT1. In uninfected cells, non-activated STAT1 cycles between the cytoplasm and the nucleus. In infected cells, the P and V protein bind STAT1 in the cytoplasm and prevent its activation. In addition, the V protein is cytoplasmic and binds to MDA-5, preventing downstream signalling. This binding has been confirmed to occur in an infected mouse derived cell line (L929) (Childs *et al.*, 2007), but the lack of systemic disease in wild type mice infected with HeV suggests that, should MDA-5 inhibition also be occurring *in vivo*, this is not on its own sufficient for full expression of potential viral pathogenicity in this animal species.

The HeV receptor in mice, murine ephrin B2, is highly functional and has a high affinity for binding with the Henipavirus attachment glycoprotein (Bossart *et al.*, 2008). It is therefore

possible that the observed resistance of wild type mice to systemic Henipavirus infection is, at least in part, attributable to post-entry events and reflects multifactorial ineffective antagonism of interferon by Henipavirus in mouse tissues.

There are three families of IFN; IFN type 1, comprising IFN α and IFN β, IFN type II comprising IFN ϒ, and IFN type III comprising IFN λ. Type I and III IFNs are co-expressed by virus infected cells and are the predominant contributors to the establishment of an antiviral state, as has been extensively reviewed (Ank *et al.*, 2006; Gerlier & Lyles, 2011; Gibbert *et al.*, 2012; Katze *et al.*, 2002; Piehler *et al.*, 2012; Pulverer *et al.*, 2010; Randall & Goodbourn, 2008; Sommereyns *et al.*, 2008). IFN Type II also elicits antiviral activity, although this is not its primary biological function, as reviewed by Donnelly and Kotenko (2010).

Each IFN family has its own specific cell surface receptor. Of relevance to this study is the IFN type I receptor which is a heterodimer composed of two sub-units termed Interferon-α receptor subunit 1 (IFNAR1, or IFN-αR1 as in shown in Figure 4.1) and Interferon-α receptor subunit 2 (IFNAR2), or the murine homologues *Ifnar1* and *Ifnar2* respectively. Binding of IFNs to their specific cell surface receptors activates signalling pathways as reviewed by Donnelly and Kotenko (2010), and a step common to the signalling pathways of all three IFN families is phosphorylation of STAT1 (or the murine homologue *Stat1*). There is some overlap in signal transduction pathways, but within the IFN type I and III signalling pathways phosphorylated STAT1 predominantly forms a complex with STAT2 and interferon regulatory factor 9 (IRF9), whereas within the IFN type II pathway phosphorylated STAT1 predominately forms a homodimer (as shown in Figure 4.1). The complex containing phosphorylated STAT1 translocates to the nucleus where it binds with either interferon stimulated response elements (ISRE) for IFN Type I and III responses or gamma activated sequences (GAS), for IFN type II responses. This initiates the transcription of interferon regulated genes whose products directly inhibit viral transcription and replication (Donnelly & Kotenko, 2010).

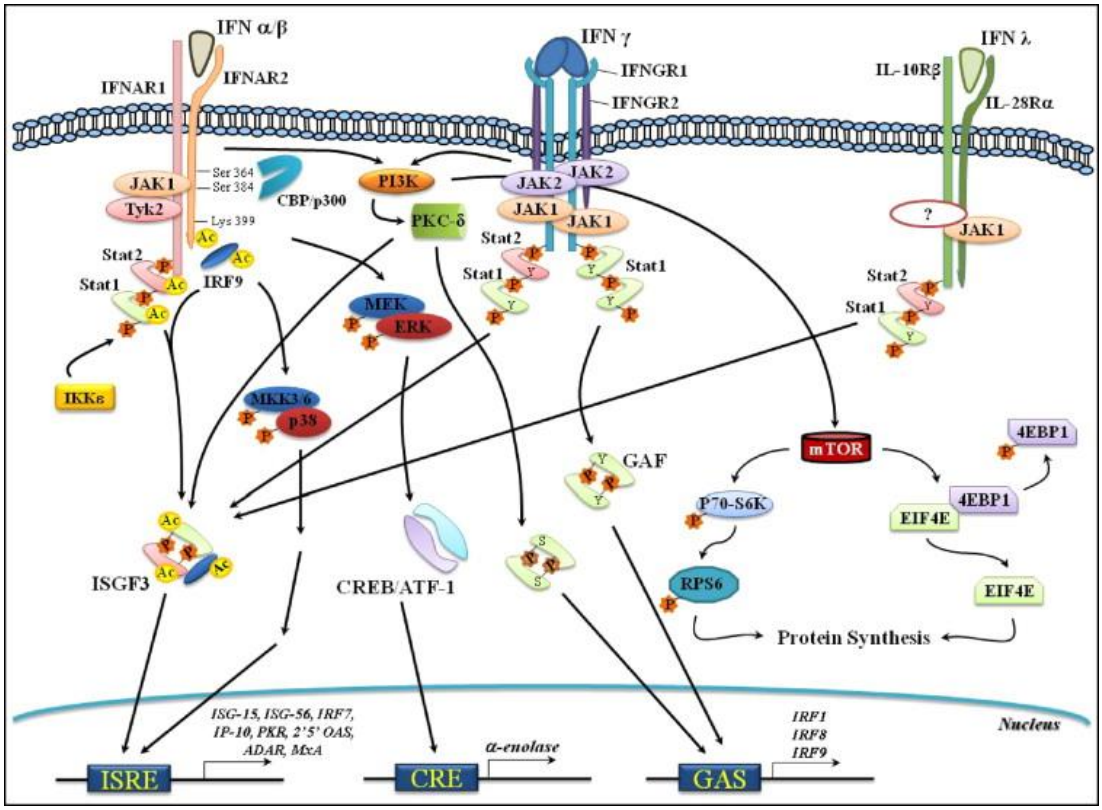

Figure 4.1: A model of the IFN receptor signalling pathway. From Bonjardim *et al.* (2009). The type I, type II, and type III IFNs bind to distinct receptor complexes on the cell membrane. Signal transduction activated by the binding of IFNs to their cognate receptors induces expression of many IFN-stimulated genes (ISGs). The proteins encoded by these genes in turn mediate the antiviral activity of the IFNs, particularly the type I and III IFNs.

An increasingly diverse array of genetically modified immune-deficient mice is being used to further the study of the pathogenesis of filoviruses (Bradfute *et al.*, 2012), Dengue virus (Zompi & Harris, 2012), Yellow Fever virus (Thibodeaux *et al.*, 2012), Junin virus (Kolokoltsova *et al.*, 2010), Epizootic Haemorrhagic Disease virus (Eschbaumer *et al.*, 2012), Blue Tongue virus (Caporale *et al.*, 2011), and Severe Acute Respiratory Syndrome Corona virus (Mahlakõiv *et al.*, 2012). The mouse strains that have proved of most value in these studies are mice lacking functional Interferon-α sub-unit 1 receptors (*Ifnar1*) and are denoted as *Ifnar1-/-* mice. In *Ifnar1-/-* mice, the type 1 interferons (Interferon α and Interferon β) produced in response to recognition of viral antigen within cells are unable to signal the induction of interferon stimulated genes and the ensuing mediation of antiviral immunity. As a result, these mice are highly susceptible to viral infection (Hwang *et al.*, 1995). Mice lacking other components of the interferon production or signalling pathways

can also be used to further explore the up- or down- stream intricacies of viral antagonism of the interferon pathway (Baños-Lara *et al.*, 2013; Bradfute *et al.*, 2012; Mahlakõiv *et al.*, 2012; Pasieka *et al.*, 2011).

The HeV mouse infection model as described in Chapter 3 provides a tool for the study of mechanisms of suppression of HeV replication. Accordingly, this chapter describes HeV infection in C57Bl6 mice genetically modified to lack specific key components of the IFN signalling system, in order to explore components of the innate immune system that may protect this species from HeV associated systemic disease.

On the basis of outcomes from the published studies on virus pathogenicity cited above, mice deficient in Interferon type 1 cell surface receptor components (*Ifnar*1-/-) were selected for use in the current HeV work. Similarly, we had access to a small number of mice with a null mutation for *Ifnar2* (or Ifn-αR2 as denoted in Figure 4.1), denoted as *Ifnar2-/-* mice: these were included for purposes of comparison, because it has been shown that IFN β can signal through IFNAR1 in an IFNAR2 independent manner, and the difference is of pathological relevance (de Weerd *et al.*, 2013).

Lastly, we incorporated *Stat1-/-* mice because STAT1 is common to the signalling pathways of all three IFN families and such mice are exquisitely sensitive to viral infection (Durbin *et al.*, 2002; Hofer *et al.*, 2012; Karst *et al.*, 2003; Pasieka *et al.*, 2008; Raymond *et al.*, 2011; Zornetzer *et al.*, 2010). *Stat1-/-* mice are unresponsive to IFN types I and II (Hofer *et al.*, 2012; Meraz *et al.*, 1996; Raymond *et al.*, 2011). However, there are STAT1 independent signalling pathways which can be activated by both IFN type I and IFN type II, although the biological significance of these alternative pathways remains unclear (Muller *et al.*, 1994)

4.2 Aim and hypothesis of this chapter

4.2.1 Aim

To evaluate the contribution of IFN signalling in mice to their resistance to systemic disease induced by HeV infection, by assessing the degree of general clinical malaise, severity of pathology in diverse organ systems, and distribution and level of virus replication in mice deficient in IFN signalling - *Ifnar1-/-, Ifnar2-/-* and *Stat1-/-* - following IN exposure to virus.

4.2.2 Hypothesis

IFN signalling deficient mice will be susceptible to systemic disease induced by HeV infection

4.3 Experimental design

Experiments were performed as three separate studies. Firstly, a pilot study was carried out using *Ifnar1-/-* mice for preliminary characterization of HeV infection in an Ifnar knockout mouse model, primarily to assess whether animal monitoring requirements or humane intervention points would require modification from those used in earlier work. Two additional studies were then conducted on the basis of mouse availability, one using *Ifnar1-/-* mice and *Ifnar2-/-* mice (Study 1) and the other *Stat1-/-* mice (Study 2).

Each study was observational and of 21 days duration, and incorporated wild type mouse controls. Mice were of mixed sex, and were housed in groups of up to 5 mice with same sex litter-mates.

Pilot study – Seven *Ifnar1-/-* mice on a C57Bl6 background (Hwang *et al.*, 1995) and 6 C57Bl6 WT mice were used in this study. *Ifnar1-/-* mice were 8 weeks old, while the control mice (closest available age-match) were 11 weeks old.

Study 1 - Three *Ifnar1-/-* and 4 *Ifnar2-/-* (Fenner *et al.*, 2006) mice on a C57Bl6 background and 5 C57Bl6 WT mice were used in this study. *Ifnar1-/-* mice were 11 to 13 weeks old, while the *Ifnar2-/-* and control mice were 12 weeks old.

Study 2 - Three *Stat1-/-* mice on a C57Bl6 background (Wang *et al.*, 2002) and 3 C57Bl6 WT mice were used in this study. *Stat1-/-* mice were 12.5 to 16 weeks old, while the control mice (closest available age-match) were 12 weeks old.

All mice were implanted with a subcutaneous temperature and identification chip and allowed to acclimatise for 7 days prior to virus exposure. The virus inoculum was a low passage isolate from the spleen of a horse (Hendra virus/Australia/Horse/2008/Redlands). Under general anaesthesia, mice were exposed IN to a dose of 50 000 $TCID_{50}$ HeV in saline in a volume of 30 µl.

After exposure to HeV, mice were assessed at least daily for clinical signs of disease as per the monitoring sheet shown Chapter 2. Mice were euthanased at the end of the study period (day 21), or earlier if they had reached their predetermined humane endpoint for clinical disease as defined in Chapter 2. At post mortem, tissue samples were collected into 10% neutral buffered formalin for routine histopathology and IHC. Samples included brain hemi-section, lung, spleen, liver, kidney, bladder, reproductive tract (ovaries and uterus in female mice and testes and accessory sex glands in male mice), stomach, duodenum, jejunum, ileum, caecum and colon, pancreas, lymph nodes (parotid, cervical chain, mesenteric), adrenal glands, myocardium, thymus, trachea, oesophagus, skeletal muscle, diaphragm and femoral bone marrow.

Tissues samples from the lung, contralateral forebrain (FB), spleen, liver, and kidney were also collected into viral transport media for qualitative virus re-isolation as well as RNA extraction. Blood was collected into EDTA for qualitative virus re-isolation as well as RNA extraction. 1 ml of sterile saline was gently flushed retrograde through the nasal passages from a catheter placed into the nasopharynx and collected as it dripped from the nares. This nasal wash fluid was used for qualitative virus re-isolation as well as RNA extraction.

For virus isolation each sample was tested in two wells of a 24 well plate and assessed as either positive or negative for CPE. Multiplex TaqMan reverse-transcription (RT) PCR (qPCR) targeting the HeV-N gene as well as host cell 18S rRNA was performed on extracted RNA, with HeV- N gene values normalized to host cell 18S rRNA. Samples with a mean HeV-N gene C_T value ≤ 39.6 were defined as positive for HeV RNA (Dups *et al.*, 2012).

Sera were collected both prior to virus exposure and at euthanasia and analysed for antibody responses against HeV using a Luminex microsphere HeVsG binding assay and a receptor blocking assay (Bossart *et al.*, 2007; McNabb *et al.*, 2014).

4.3.1 Assignment of infection status and infection phenotype

The primary readout for these studies was the infection phenotype that was observed in individual mice following exposure to virus. Mouse infection status was determined and then an infection phenotype was assigned according to the criteria used in Chapter 3. In summary, a mouse was defined as infected with HeV if immunohistopathology of tissue/s

was positive for viral antigen, or infectious virus was re-isolated from tissue/s, or the serum was positive for binding antibodies against HeV $_{s}$G protein. In the case of brain, detection of viral genome in brain tissue was considered sufficient to confirm virus replication in that organ. Categories for infection phenotype comprised subclinical (no clinical signs observed during the study), systemic (exhibition of signs of general malaise with disseminated virus replication and significant pathology in major organ systems), and neurological (exhibition of signs consistent with involvement of the CNS and evidence of virus replication in brain).

4.4 Data Analysis

Mice were recorded as febrile if their temperature was > 39.3 ^{o}C (in-house reference for C57Bl6 mice).

Statistical analysis was carried out using GraphPad Prism 7.02. Survival curves were conducted using log-rank tests (Mantel-Cox). Bodyweight and temperature data up to the time of first mouse euthanasia were analysed in two-way mixed ANOVAs, with time as a within-subject variable and treatment group as a between-subject variable. Where indicated, infection rate, infection phenotype, and likelihood of virus replication in individual organs were subjected to contingency analysis (Fisher's exact test). Comparison of rates of virus replication in organs used data from mice euthanased between day 6 and day 17 post-exposure (p.e.), prior to the time of expected virus clearance (Dups *et al.*, 2012). The exception was in the assessment of data from brain samples, where there is documented evidence of persistent replication of HeV: for this tissue, data from all mice were incorporated into any contingency analysis, irrespective of euthanasia day.

Viral genetic loads in the different tissues were log-transformed and compared by ordinary two-way ANOVAs, with tissue type and treatment group as the independent variables. Data from all mice were used for these analyses, irrespective of euthanasia day.

4.5 Results

4.5.1 Pilot study

4.5.1.1 Clinical observations

The IN exposure of mice to 50 000 TCID50 HeV was generally well tolerated by both WT and *Ifnar1-/-* mice; it did not cause a sneeze reflex and rarely led to brief periods of apnoea and/or increased respiratory rate and effort.

Five of 6 WT mice and 7 of 7 *Ifnar1-/-* mice met the criteria for HeV infection, and the WT mouse with no evidence of infection was excluded from further analysis. All remaining WT mice reached a predetermined humane endpoint for neurological disease and were euthanased on days 8, 9 or 10 (Table 4.1). Six of 7 *Ifnar1-/-* mice reached a predetermined humane endpoint for neurological disease and were euthanased on days 7, 8, 9 or 10 (Table 4.1). The clinical signs were indistinguishable from those seen in WT mice, including demonstration of ataxia and tremors. One *Ifnar1-/-* mouse remained clinically healthy up to the time of elective euthanasia on day 21 (Table 4.1). There was no significant difference between the two treatment groups in either the likelihood of establishing HeV infection or in their infection survival curves.

Table 4.1 Pilot study, summary of data used to assess infection status

Mouse Type	Mouse ID	Euth. Day	Infection phenotype	Olfactory mucosa Ag/PCR*VI*	Lung Ag/PCR VI	Forebrain Ag/PCR VI	Spleen Ag/PCR VI	Liver Ag/PCR VI	Kidney Ag/PCR	Blood PCR VI	Serology Bind/Blk
WT	61	8	Neurological	+/+	+/-	+/+ +VI	-/-	-/-	-/-	-	-/-
	62	8	Neurological	+/+ +VI	-/+	+/+ +VI	-/-	-/-	-/-	-	-/-
	63	9	Neurological	+/+ +VI	-/+ +VI	+/+	-/-	-/-	-/-	-	-/-
	64	10	Neurological	+/+ +VI	-/-	+/+ +VI	-/-	-/-	-/-	-	-/-
	65	10	Neurological	+/-	+/-	+/+ +VI	-/-	-/-	-/-	-	-/-
Ifnar1-/-	66	7	Neurological	+/+ +VI	+/-	+/+ +VI	+/+ +VI	+/+	-/-	-	-/-
	67	7	Neurological	+/+ +VI	+/-	+/+ +VI	+/+ +VI	+/+	-/-	-	-/-
	68	21	Subclinical	-/-	-/-	-/+	-/-	-/-	-/-	-	-/-
	69	10	Neurological	+/-	+/+	+/+ +VI	+/+	-/+	-/-	-	-/-
	70	8	Neurological	+/+ +VI	+/+ +VI	+/ + +VI	+/+	+/+	-/-	-	-/-
	71	9	Neurological	+/-	+/+	+/+ +VI	+/+	+/+	-/-	+	-/-
	72	10	Neurological	+/-	+/+	+/-	+/-	-/-	-/-	-	-/-

Ag: immunohistochemical staining for viral antigen in tissue

PCR: qPCR for viral genome in tissue

VI+: virus isolation, performed only all samples, only positive samples are indicated above

* PCR and VI performed on retrograde nasal washings

“+” present

“-“ not present

Euth. Day: day of euthanasia

Bind: Luminex binding assay

Blk: Luminex receptor blocking assay

Bodyweight data is presented in Figure 4.2. All mice gained weight at least up to day 5 p.e.. All mice euthanased for neurological disease, apart from 1 WT mouse, started to lose weight from 72 to 24 hrs prior to euthanasia. There was a significant interaction between time and test group ($p = 0.0149$) on bodyweight: in WT mice mean bodyweight was higher on day 7 p.e. compared to day 0, and in *Ifnar1-/-* mice mean bodyweight was lower on day 7 p.e. compared to day 4 p.e.. However, there was no significant difference between the test groups at any time from day 0 to day 7 p.e..

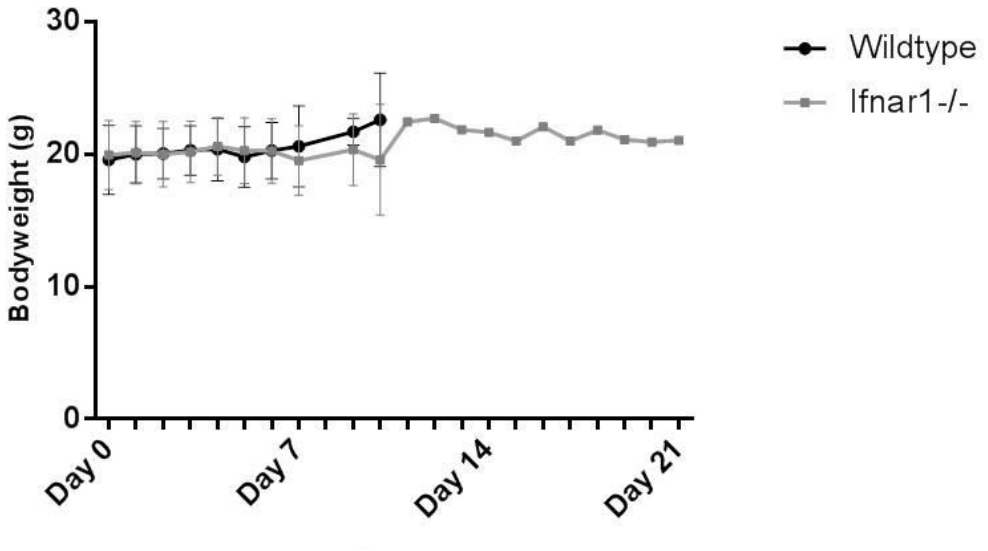

Figure 4.2: Pilot study, combined mouse weights (with mean and SD) over days post infection.

Temperature data is presented in Figure 4.3. No mouse in either test group developed a fever (T> 39.3 C^{o}) during the study. There was a significant interaction between time and test group (p = 0.0026) on temperature: mean temperature was lower on day 4 p.e. compared to days 1, 2, 3, 5 and 6 p.e. in WT mice and compared to day 2 and day 7 p.e. in *Ifnar1-/-* mice. Mean temperature was also slightly lower in *Ifnar1-/-* mice on day 6 vs. day 7 p.e.. Slightly but significantly higher mean temperature (difference 0.92 C^{o}) was recorded in *Ifnar1-/-* mice on day 7 p.e., but this was not considered to be clinically significant.

Environmental factors that may have impacted on temperature records derived from subcutaneous chips, including ambient room temperature and rates of air turnover, were stable over the study period. Therefore, the timing of mouse scanning in relation to disturbance of mice to conduct health checks and husbandry is most likely to have contributed to the temperature differences observed, most notably on day 4 p.e..

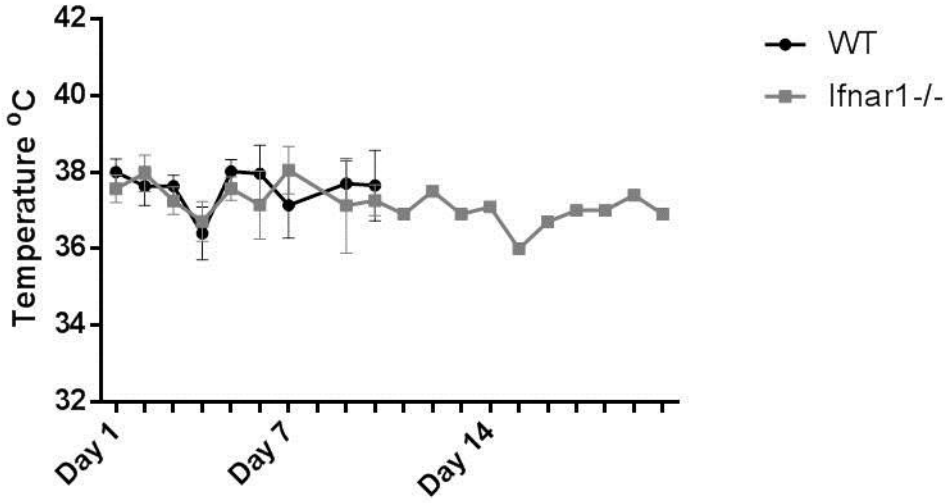

Figure 4.3: Pilot study, combined mouse temperatures (^{o}C with mean and SD) over days post infection.

4.5.1.2 Pathology and immunohistopathology

Immunohistopathological findings in WT mice were similar to those already described in Chapter 3 and are presented in Table 4.2.

Briefly, there was mild to moderate multifocal rhinitis associated with positive staining for viral antigen within the olfactory epithelium of all WT mice in this study. Occasional small foci of positive IHC staining for viral antigen were present within the lung, without other evidence for tissue injury such as infiltration of inflammatory cells or necrosis.

Positive IHC staining for viral antigen occurred in the olfactory pathway of the brain in all WT mice, consistent with anterograde viral propagation via the nasal cavity. There was mild encephalitis in the olfactory bulb characterised by a mild mononuclear inflammatory infiltrate and injury to neuronal cells. There was also mild multifocal gliosis with perivascular cuffing in the cerebral cortex immediately adjacent to the olfactory bulb and an associated mild to moderate non-suppurative meningitis.

HeV antigen was also identified in a cervical chain lymph node in one mouse, possibly as an extension of infection from the nasal cavity via afferent lymphatics. Viral antigen or lesions were not identified in other tissues including: renal parenchyma, bladder, reproductive tract (ovaries and uterus in female mice and testes and accessory sex glands in male mice), stomach, duodenum, jejunum, ileum, caecum and colon, pancreas, parotid and mesenteric lymph nodes, adrenal glands, myocardium, thymus, trachea, oesophagus, skeletal muscle, diaphragm and femoral bone marrow.

Table 4.2: Pilot study, summary of pathology findings

	ID # Thesis	Meninges Ag/les	Forebrain Ag/les	Ependyma Ag/les	Endothelium Ag/les	Olfactory mucosa Ag/les	Olfactory lymphoid tissue Ag/les	Olfactory nerve perineurium Ag/les	Olfactory regional LNs Ag/les	Lung Ag/les	Spleen Ag/les	Liver Ag/les
WT	61	-/+	+/+	-/-	-/-	+/+	-/-	-/-	-/-	+/-	-/-	-/-
	62	-/-	+/+	-/-	-/-	+/+	-/-	-/-	-/-	-/-	-/-	-/-
	63	-/-	+/+	-/-	-/-	+/+	-/-	-/-	-/-	-/-	-/-	-/-
	64	-/+	+/+	-/-	-/-	+/+	-/-	-/-	+/-	-/-	-/-	-/-
	65	-/+	+/+	-/-	-/-	+/+	-/-	-/-	-/-	+/-	-/-	-/-
Ifnar1	66	+/+	+/+	-/-	+/-	+/+	-/-	-/-	-/-	+/-	+/-	+/-
	67	+/+	+/+	-/-	+/-	+/+	+/-	+/+	-/-	+/-	+/-	+/-
	68	-/-	-/-	-/-	-/-	-/-	-/-	-/-	-/-	-/-	-/-	-/-
	69	-/+	+/+	-/-	-/-	+/+	-/-	-/-	-/-	+/-	+/-	-/-
	70	+/+	+/+	+/-	+/-	+/+	+/-	+/+	+/-	+/-	+/-	+/-
	71	-/+	+/+	-/-	-/-	+/+	-/-	-/-	-/-	+/-	+/-	+/-
	72	-/+	+/+	-/-	-/-	+/+	-/-	-/-	-/-	+/-	+/-	-/-

Ag: antigen

Les: inflammatory and/or necrotising lesion

LNs: lymph nodes

Six out of 7 *Ifnar1-/-* mice had lesions in the olfactory epithelium similar to WT mice. There were multifocal areas of moderately severe necrosis, and erosion and ulceration of the olfactory epithelium associated with a mixed but predominately neutrophilic inflammatory infiltrate. There was copious antigen staining the olfactory mucosa and in the mucus overlying infected areas.

Small foci of positive IHC staining for viral antigen were present throughout the lung of *Ifnar1-/-* mice and resembled those described in WT mice. Similarly to the lung of WT mice, there was no other evidence of tissue injury in the lung of any *Ifnar1-/-* mouse. The morphology of individual IHC positive foci within the lung was similar to WT mice and, while detailed morphometrics was not carried out, the number of foci appeared to be increased in *Ifnar1-/-* mice. For example, rather than the <1 per 100x field or 1-2 within a lobe section observed in WT mice, there were 1-3 per 100x field or 5+ per section of lung lobe in *Ifnar1-/-* mice.

IHC viral antigen staining was detected in the olfactory bulb of all *Ifnar1-/-* mice, apart from the mouse which had remained clinically healthy throughout the study period (Table 4.2). Viral antigen extended to the piriform lobe and amygdala in 4 of the 6 affected mice. Using routine morphological assessment, the amount of viral antigen did not differ between *Ifnar1-/-* and WT mice. A distinct neuropathology was usually associated with the finding of viral antigen in the brain of *Ifnar1-/-*mice. Within the olfactory bulb, this comprised a mild to moderately severe inflammatory infiltrate that contained neutrophils as well as mononuclear cells, occasionally accompanied by small areas of haemorrhage. Similar to WT mice, *Ifnar1-/-* mice also had non-suppurative meningitis extending over the most rostral aspects of the frontal lobe of the cerebral cortex. However, unlike WT mice, HeV antigen was found within the meningeal inflammatory infiltrates of 3 *Ifnar1-/-* mice (Mice #66, #67 and #70, Figure 4.4, images A, B and C). In one of these mice, antigen was also identified within ependymal cells of the 3rd ventricle (Figure 4.4, image D).

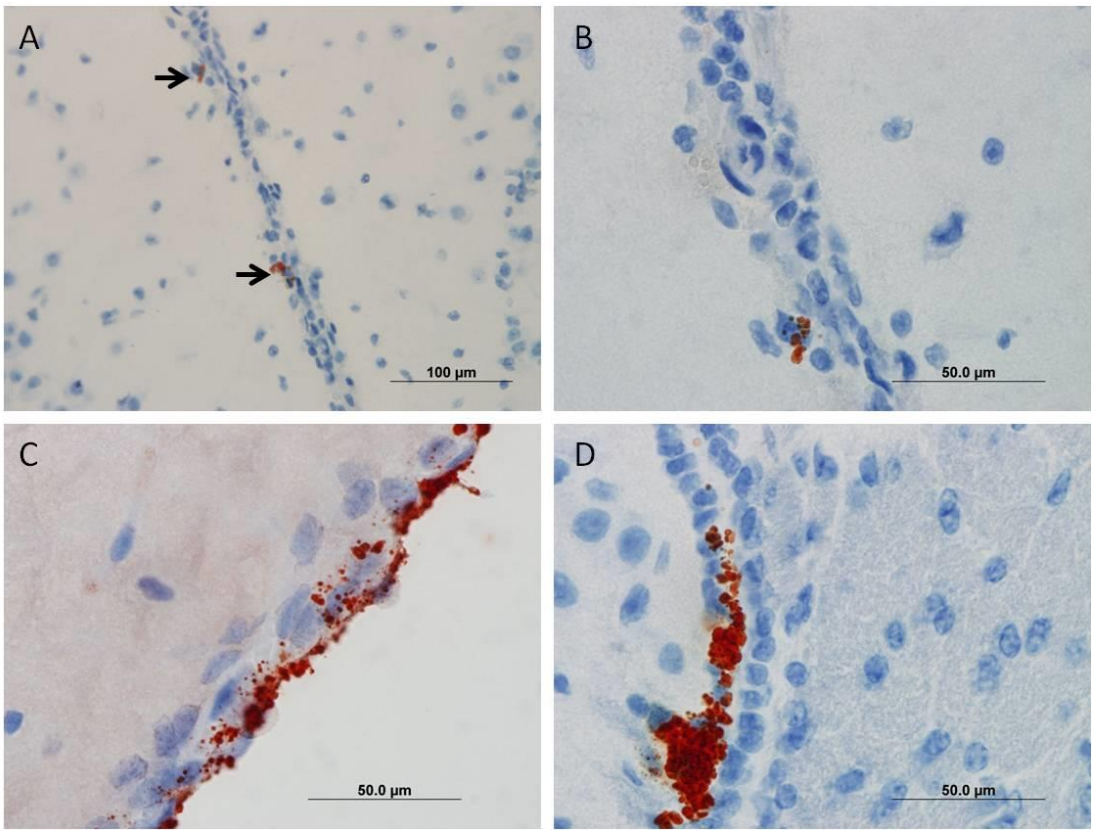

Figure 4.4: IHC stained sections. A and higher magnification B, antigen within the meninges associated with inflammatory cells; C, antigen within the meninges; D, antigen within ependymal cells.

In two *Ifnar1-/-* mice (Mice #66 and 70) there was a severe mixed inflammatory cell infiltrate and antigen staining in the perineurium of olfactory nerve fibres traversing the caudal nasal submucosa before it crossed through the cribiform plate. Viral antigen was also present within the endothelium of thin walled vessels within the nasal submucosa in three *Ifnar1-/-* mice (Figure 4.5). These vessels were most likely lymphatics, as they were immediately adjacent to but distinct from parallel thin walled vessels containing erythrocytes (veins). The presence of viral antigen in endothelium was not associated with degeneration of the vascular wall or with its infiltration by inflammatory cells: thus, vasculitis or lymphangitis was not evident.

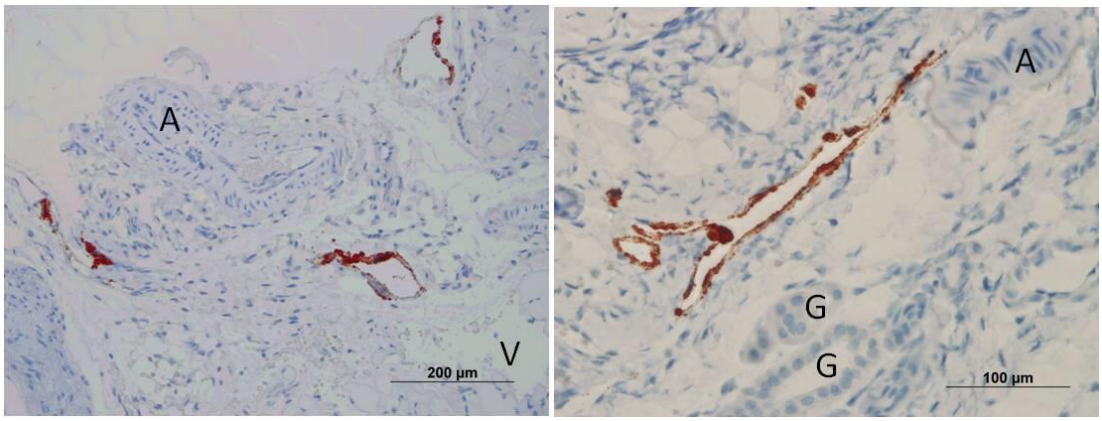

Figure 4.5: IHC stained sections showing viral antigen within the endothelium of vessels. A, artery; V, vein containing erythrocytes; G, submucosal glands

In addition, and also in contrast to WT mice, HeV antigen was identified within submucosal lymphoid tissue within the nasal cavity of two *Ifnar1-/-* mice (Mice #67 and #70, Figure 4.6 image A) and, most likely as an extension of infection from the nasal cavity, within the parotid lymph node and cervical chain lymph nodes in Mouse #70 (Figure 4.6 image B). However, lymphocytolysis, necrosis, inflammation, and haemorrhage were not observed in affected tissues.

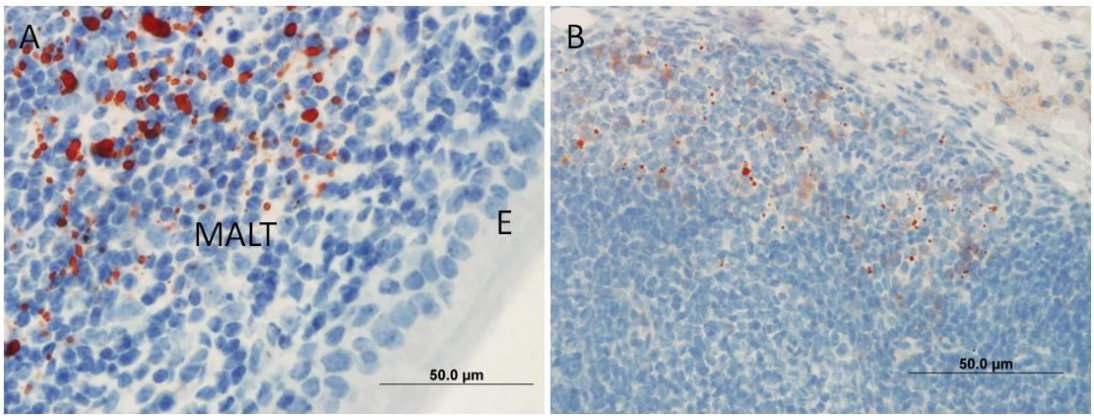

Figure 4.6: IHC stained sections. A, viral antigen within mucosal associated lymphoid tissue in the nasal submucosa (MALT); B viral antigen within a cervical lymph node.

Similarly, multiple small to moderately sized foci of HeV antigen were identified in the spleen of the 6 *Ifnar1-/-* mice euthanased for acute neurological disease (Figure 4.7). The presence of viral antigen in the spleen was not associated with lymphocytolysis, necrosis, inflammation or haemorrhage.

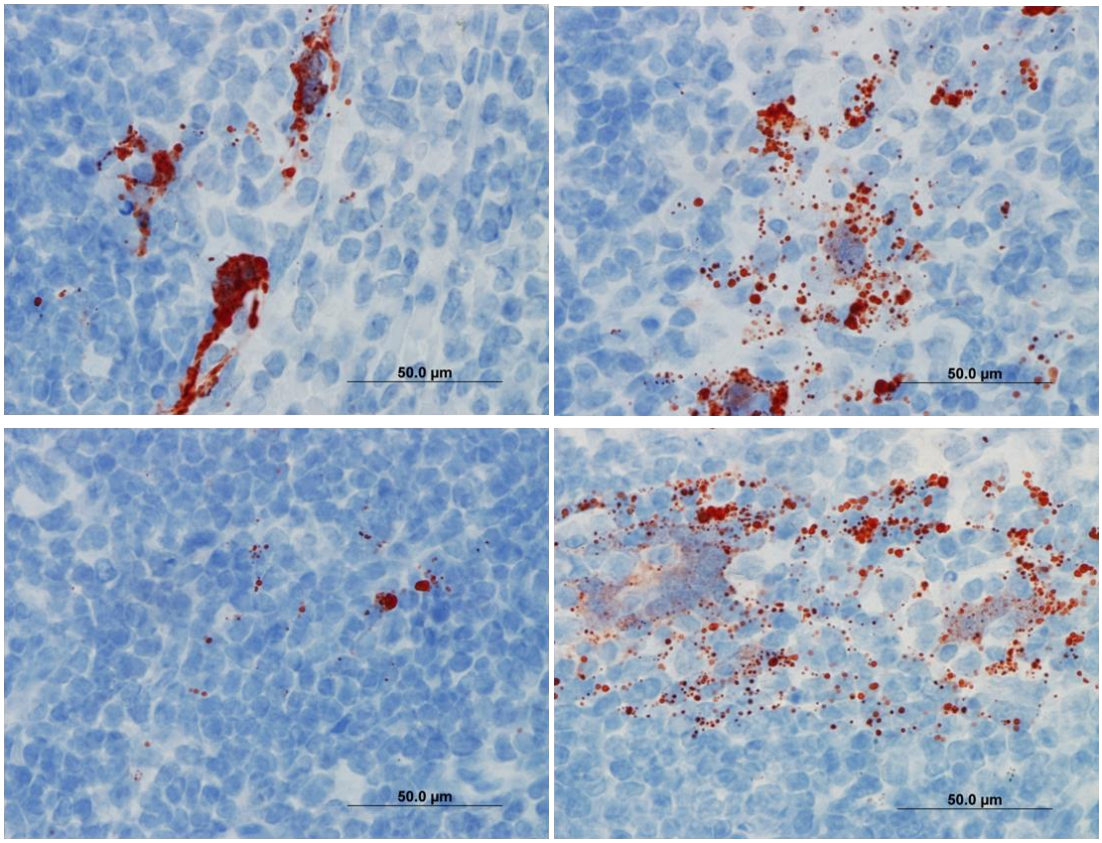

Figure 4.7: IHC sections of spleen from different mice demonstrating focal aggregates of viral antigen without lymphocytolysis, necrosis, inflammation or haemorrhage.

Viral antigen was also detected in the liver parenchyma of two *Ifnar1-/-* mice where it was associated with sinusoidal lining cells (Figure 4.8).

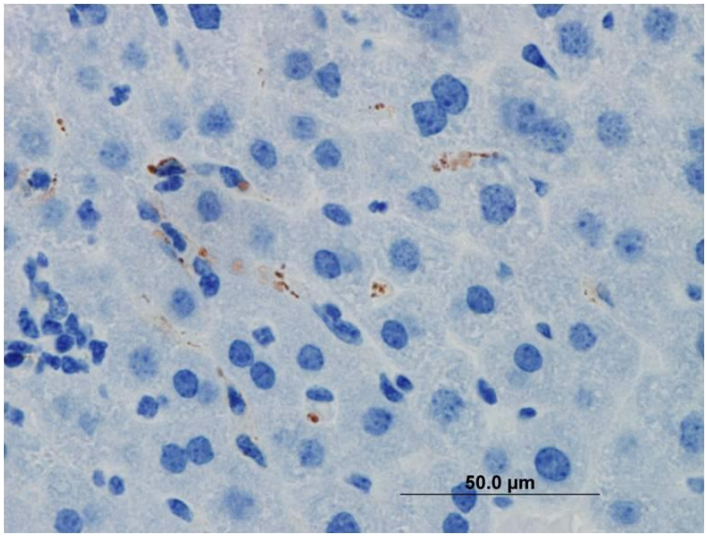

Figure 4.8: IHC stained section of liver showing viral antigen associated with sinusoidal structures

HeV antigen or associated lesions were not detected within any other tissues including: renal parenchyma, bladder, reproductive tract (ovaries and uterus in female mice and testes and accessory sex glands in male mice), stomach, duodenum, jejunum, ileum, caecum and colon, pancreas, mesenteric lymph nodes, adrenal glands, myocardium, thymus, trachea, oesophagus, skeletal muscle, diaphragm and femoral bone marrow.

4.5.1.3 Molecular virology and classical virology

Viral genome was detected in at least one tissue of all mice shown to have been infected after exposure to HeV (Data presented in Table 4.1 and Figure 4.9).

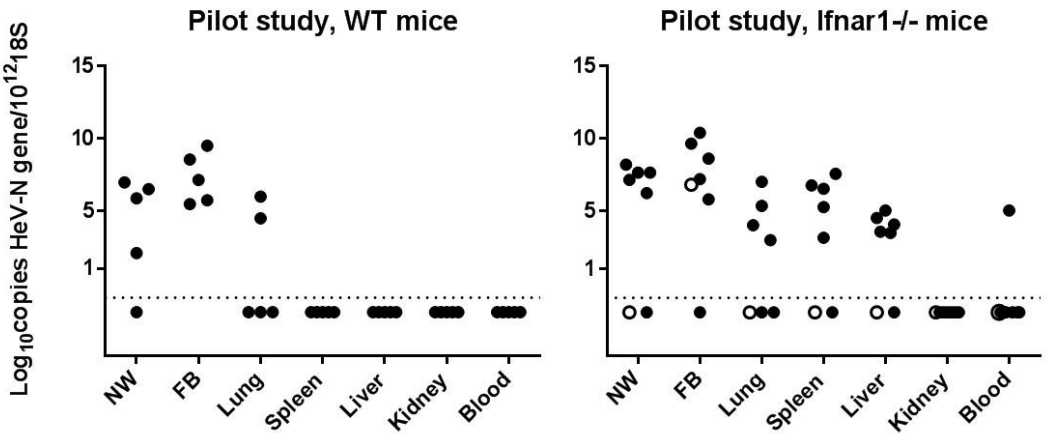

Figure 4.9: Pilot study qPCR data. Log_{10} HeV-N gene copies normalised to 18S in different organs

NW: Nasal flush

FB: Forebrain

Open circle: remained clinically healthy

Solid circle: showed neurological signs

Dotted line: level of assay detection

HeV genome was present in the nasal wash of 4 out of 5 WT mice and 5 out of 7 *Ifnar1-/-* mice, each of which had been euthanased on account of neurological signs. Virus was re-isolated from the nasal wash of 3 of 5 WT mice and 3 of 7 *Ifnar1-/-* mice (Table 4.1).

HeV genome was present in the forebrain samples of 5 out of 5 WT mice and 6 out of 7 *Ifnar1-/-* mice, including the *Ifnar1-/-* mouse which remained clinically healthy throughout the study (Figure 4.9). Virus was also re-isolated from the contralateral forebrain of 4 out of 5 WT mice and 5 out of 7 *Ifnar1-/-*mice (Table 4.1), each of which had been euthanased on account of neurological signs.

HeV genome was detected in the lung of 2 out of 5 WT mice and 4 out of 7 *Ifnar1-/-* mice (Figure 4.9). Virus was re-isolated from the lung of one WT and one *Ifnar1-/-* mouse (Table 4.1).

HeV genome was not identified in the spleen of WT mice, but was found in 5 out of 7 *Ifnar1-/-* mice (Figure 4.9). Virus was also re-isolated from the spleen of two *Ifnar1-/-* mice, providing additional indirect evidence for the occurrence of viraemia in *Ifnar1-/-* mice (Table 4.1).

In the liver, HeV genome was not found in WT mice, but testing was positive in 5 out of 7 *Ifnar1-/-* mice (Figure 4.9). Virus was not re-isolated from the liver of any mice (Table 4.1).

All kidney samples tested negative for HeV genome; viral genetic material was identified in the blood sample of a single *Ifnar1-/-* mouse (Figure 4.9).

There was no significant interaction between tissue type and treatment group for viral genetic load. There were significant effects of treatment group on viral genetic load within the tissues tested ($p = 0.010$), with higher mean viral genetic loads in the spleen of *Ifnar1-/-* mice compared to WT mice ($p = 0.0089$). There was also a significant effect of tissue type on viral genetic load ($p < 0.0001$) with higher levels in forebrain compared to all other tissues ($p < 0.0001$) for both test groups. The exception was for the spleen in *Ifnar1-/-* mice, where mean levels of viral genome were not significantly different from those in brain. In addition, within *Ifnar1-/-* mice, there was significantly more HeV genome in the spleen compared to kidney ($p = 0.0070$) or blood ($p = 0.0409$).

4.5.1.4 Serology

All mice were negative for antibody by Luminex binding assay and receptor blocking assay (Table 4.3). These findings were attributed to all but one mouse having been euthanased between day 7 and day 10 p.e., which may have been an insufficient time period in which to develop a detectable antibody response. The *Ifnar1-/-* mouse that survived to day 21 p.e. was negative for antibody but only had evidence of infection within the forebrain. This may reflect poor stimulation of an adaptive immune response because the infection in this case was confined within the brain. The presence of a blood brain barrier and the immune

privileged status of the CNS are thought to contribute to the late stage development of antibodies in Rabies virus infection (Johnson *et al.*, 2010).

Table 4.3: Serology from Pilot study

	Assay			Antibody binding	Receptor blocking
Mouse Type	Mouse #	ID delete	Euth. Day	MFI Post Challenge	% Inhibition
WT	61	2	8	69	0
	62	4	8	57	0
	63	9	9	44	0
	64	10	10	48	0
	65	11	10	50	0
Ifnar1-/-	66	17	7	26	1
	67	18	7	37	1
	68	19	21	57	0
	69	20	10	48	1
	70	21	8	36	1
	71	22	9	60	0
	72	23	10	48	0
Positive controls	Horse			**29409**	71%
	Mouse			**4900**	ND
	Rabbit NiV			ND	72%

ND: Not done

Euth.: Euthanasia

Luminex binding assay: for this experiment the mean of all pre-challenge sera was 52 MFI, 1SD = 18.5, and therefore a positive result was defined as >108 MFI.

Luminex receptor blocking assay: the % inhibition of positive control sera was >75 %. The % inhibition in sera from all mice subjects was < 6.4%.

Positive results are shown in bold.

4.5.1.5 Assignment of infection phenotype

As for Chapter 3, an infection phenotype was assigned to each mouse after integration of clinical observations, the sites in which virus replication had been confirmed, and the presence of associated pathological lesions.

For infected WT mice, 5 out of 5 mice demonstrated acute neurological disease. Each had virus replication confirmed in brain accompanied by mild to moderately severe meningoencephalitis. Each mouse also had virus replication confirmed in olfactory mucosa that was associated with rhinitis: in 1 out of 5 mice infection extended to a regional lymph node without evidence for lymphadenitis. Virus replication was also confirmed in the lung of 3 out of 5 WT mice, but an associated pneumonia was not identified. Virus replication was not confirmed in any other tissues including liver, spleen, kidney, or blood of WT mice. Mild weight loss usually preceded the onset of neurological signs, but this was not accompanied by fever. The loss of weight was therefore attributed to the developing neuropathology, which was likely to have led to reduced intake of food and water.

On the basis of these findings, each WT mouse was assigned a neurological infection phenotype (Table 4.1).

For infected *Ifnar1-/-* mice, 6 out of 7 demonstrated acute neurological disease over a similar timeframe to WT mice. Each of these 6 mice had virus replication confirmed in brain, accompanied by mild to moderately severe meningoencephalitis. Although there was no significant difference between the treatment groups in the likelihood of virus replication in brain, qualitative differences were recorded: unlike WT mice, neutrophils were present in the inflammatory infiltrate of *Ifnar1-/-* mice and viral antigen was identified in meningitic lesions and ependymal cells of some mice. Each of these 6 mice also had virus replication confirmed in olfactory mucosa that was associated with rhinitis: in 1 out of 6 mice infection extended to a regional lymph node without evidence for lymphadenitis. Virus replication was also confirmed in the lung of 6 out of 7 *Ifnar1-/-* mice, but an associated pneumonia was not identified. There was no significant difference between the treatment groups in the likelihood of virus replication in lung.

In contrast to WT mice, virus replication was confirmed in the spleen (5 out of 7) and also the liver (4 out of 7) of *Ifnar1-/-* mice. For spleen, the likelihood of confirming virus replication was significantly higher in *Ifnar1-/-* mice compared to WT mice ($p = 0.0022$). For liver, there was a trend towards an increased likelihood of confirming virus replication in *Ifnar1-/-* mice compared to WT mice ($p = 0.0606$). Replication of HeV (as determined by IHC) was also identified in the mucosal-associated lymphoid tissue, parotid and cervical

chain lymph nodes, and the nasal submucosal vascular endothelium of some *Ifnar1-/-* mice. However, apart from meningoencephalitis, the presence of viral antigen in these areas was not associated with significant pathology in the form of an inflammatory response or necrotizing lesions.

Ifnar1-/- mice showed mild weight loss from up to 72 hours prior the onset of neurological signs but, as in WT mice, this was not accompanied by a febrile response in any mouse. Similar to WT mice, this loss of weight was attributed to the developing neuropathology. One *Ifnar1-/-* mouse remained clinically healthy throughout the period of observation.

Considering the findings overall, 6 out of 7 *Ifnar1-/-* mice were assigned a neurological infection phenotype and 1 out of 7 a subclinical infection phenotype (Table 4.1).

There was no significant difference between WT and *Ifnar1-/-* mice in the incidence of infection phenotypes that were assigned following exposure to HeV, or between infection survival curves. In addition, and on that basis, no modifications were made to the monitoring or intervention strategies used in subsequent studies using immune-deficient mice.

4.5.2 Study 1

4.5.2.1 Clinical observations

As in the Pilot study, the IN exposure of mice to 50 000 TCID50 HeV was well tolerated by WT, *Ifnar1-/-* and *Ifnar2-/-* mice.

All mice in the study met the criteria for HeV infection. Three out of 5 WT mice reached their predetermined humane endpoint for neurological disease and were euthanased on days 10 or 16 p.e. (Table 4.4). Two of 5 WT mice remained clinically healthy up to the time of elective euthanasia on day 21.

All 3 *Ifnar1-*/- mice reached their predetermined humane endpoint for neurological disease and were euthanased on days 11 and 12 p.e. (Table 4.4). Three of 4 *Ifnar2-*/- mice reached their predetermined humane endpoint for neurological disease and were euthanased on days 7, 9 or 10 p.e. (Table 4.4). The remaining *Ifnar2-*/- mouse remained clinically healthy up

to the time of elective euthanasia on day 21. There were no significant differences between the survival curves for the three treatment groups.

Table 4.4: Study 1, summary of data used to assess infection status

Mouse type	Mouse ID	Euth. day	Infection phenotype	Olfactory mucosa Ag/PCR*/VI*	Lung Ag/PCR/VI	Forebrain Ag/PCR/VI	Spleen Ag/PCR/VI	Liver Ag/PCR/VI	Kidney Ag/PCR/VI	Blood PCR/VI	Serology Bind/Blk
WT	73	21	Subclinical	-/-	-/-	-/+	-/-	-/-	-/-	-/-	+/-
	74	21	Subclinical	-/-	-/-	-/+	-/-	-/-	-/-	-/-	-/-
	75	16	Neurological	-/-	+/-	+/+	-/-	-/+	-/-	-/-	+/-
	76	16	Neurological	-/-	+/-	+/+	-/-	-/-	-/-	-/-	-/-
	77	10	Neurological	+/-	+/+	-/+	-/-	-/-	-/-	-/-	-/-
Ifnar1-/-	78	11	Neurological	+/+	+/-	+/+	+/+	+/+	-/-	-/-	+/-
	79	11	Neurological	+/-	+/+	+/+ +VI	-/-	-/-	-/-	-/-	+/-
	80	10	Neurological	+/+ +VI	+/+	+/+ +VI	+/+	+/-	-/-	-/-	+/-
Ifnar2-/-	81	10	Neurological	+/+	+/+ +VI	+/+ +VI	+/+	-/-	-/-	-/-	+/-
	82	9	Neurological	+/+ +VI	+/+	+/+ +VI	+/+	-/-	-/-	-/-	+/-
	83	21	Subclinical	+/- +VI	+/+	+/+ +VI	+/+ +VI	+/+	-/-	-/-	+/-
	84	7	Neurological	+/- +VI	+/+	+/+	+/+	-/+	-/+	+	-/-

Ag: immunohistochemical staining for viral antigen in tissue

PCR: qPCR for viral genome in tissue

VI+: virus isolation was performed on all samples, only positive results are indicated

* For olfactory mucosa PCR and VI was performed on retrograde nasal washings

"+" present

"-" not present

Euth. Day: day of euthanasia

Bind: Luminex binding assay

Blk: Luminex receptor blocking assay

Bodyweight data is presented in Figure 4.10. One of 3 WT mice, 3 of 3 *Ifnar1*-/- mice, and 3 of 4 *Ifnar2*-/- mice euthanased for neurological disease had started to lose weight from 72 to 24 hrs prior to euthanasia. There was no significant interaction between time and test group on bodyweight. Overall, there were significant effects of both time (<0.0001) and test group (p = 0.0418) on bodyweight from day 0 to day 7 p.e.. These were attributable to all mouse groups gaining weight between day 0 to day 7, with a plateau by day 2 or day 3 p.e., and to *Ifnar2*-/- mice being significantly lighter than *Ifnar1*-/- mice overall.

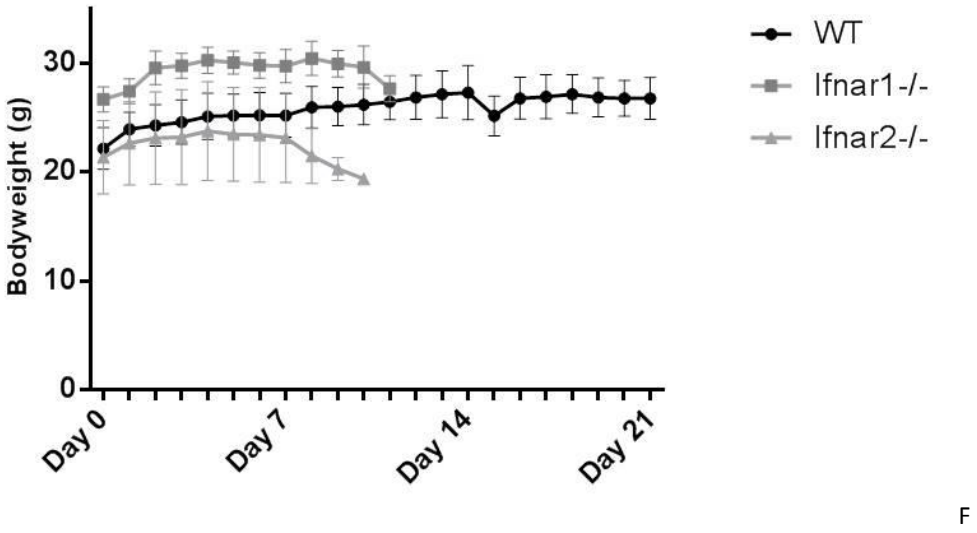

F

Figure 4.10: Study 1, combined mouse weights (grams with mean and SD) over days post infection.

Temperature data is presented in Figure 4.11. One WT mouse that was electively euthanased on day 21 p.e. had a temperature above the normal range on day 10 p.e. (39.4 ^{o}C) and on day 16 p.e. (40.0 ^{o}C), as did one *Ifnar1-/-* mouse on day 0 p.e. (39.7 ^{o}C): no mouse in any test group developed a sustained febrile response post-exposure to HeV. There was no significant interaction between time and test group. Overall, there were no significant effects of test group on temperature from day 0 to day 7 p.e.. There was a significant effect of time on temperature (0.0041), with lower temperatures on day 3 p.e. compared to days 1, 5 and 7 p.e..

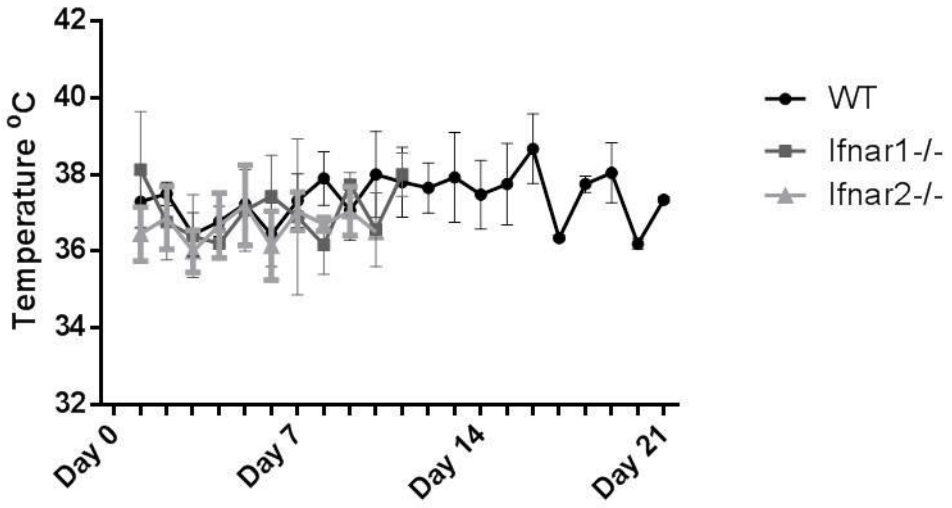

Figure 4.11: Study 1, combined mouse temperature (^{o}C with mean and SD) over days post infection.

As in the Pilot Study, ambient room temperature and rates of air turnover were stable over the study period. The timing of mouse scanning in relation to disturbance of mice for conducting health checks and husbandry is most likely to have contributed to the temperature differences observed with time, notably on day 3 p.e..

Ifnar1-/- mice are capable of a febrile response (Canakoglu *et al.*, 2015) but may develop hypothermia rather than a pyrogenic response with viral infection; this can also be seen in WT mice (Kolokoltsova *et al.*, 2014; Traynor *et al.*, 2007) (Kolokoltsova *et al.*, 2010). However, the observed falls in temperature were not consistent in either WT or interferon

signalling deficient mice across all studies, and so they are unlikely to be related to HeV infection. This reinforces the conclusions of the effect of timing of the scanning procedure.

4.5.2.2 Pathology and immunohistopathology

WT mice: Histopathological findings in WT mice euthanased on account of neurological signs were similar to those described in the Pilot study and are presented in Table 4.5.

Briefly, there was rhinitis associated with viral antigen deposits in one mouse euthanased on day 10 p.e.. Occasional small foci of positive IHC staining for viral antigen were present within the lung of the 3 clinically affected mice, without other evidence for pneumonia (Table 1.5). Each of the 3 WT mice that developed neurological signs had meningitis, and 2 of 3 had rostral encephalitis with HeV antigen detected by immunohistochemistry. Histological lesions or viral antigen were not detected in remaining tissues of these mice, or in any sample from the 2 mice that remained clinically healthy to day 21 p.e..

Table 4.5: Study 1, summary of pathology findings

Mouse type	Mouse ID	Meninges Ag/les	FB Ag/les	Ependyma Ag/les	Endothelium Ag/les	Olfactory epithelium Ag/les	Olfactory lymphoid tissue Ag/les	Olfactory nerve perineurium Ag/les	Olfactory regional LNs Ag/les	Lung Ag/les	Spleen Ag/les	Liver Ag/les
WT	73	-/-	-/-	-/-	-/-	-/-	-/-	-/-	-/-	-/-	-/-	-/-
	74	-/-	-/-	-/-	-/-	-/-	-/-	-/-	-/-	-/-	-/-	-/-
	75	-/+	+/+	-/-	-/-	-/-	-/-	-/-	-/-	+/-	-/-	-/-
	76	-/+	+/+	-/-	-/-	-/-	-/-	-/-	-/-	+/-	-/-	-/-
	77	-/+	-/-	-/-	-/-	+/+	-/-	-/-	-/-	+/-	-/-	-/-
Ifnar1-/-	78	+/+	+/+	-/-	-/-	+/+	-/-	-/-	-/-	+/-	+/-	+/-
	79	-/+	+/+	-/-	-/-	+/+	-/-	-/-	-/-	+/-	-/-	-/-
	80	-/+	+/+	-/-	-/-	+/+	-/-	-/-	-/-	+/-	+/-	+/-
Ifnar2-/-	81	-/+	+/+	-/-	+/-	+/+	-/-	-/-	+/-	+/-	+/-	-/-
	82	-/+	+/+	+/-	-/-	+/+	-/-	-/-	-/-	+/-	+/-	-/-
	83	+/+	+/+	-/-	+/-	+/+	+/-	+/-	-/-	+/-	+/-	+/-
	84	+/+	+/+	-/-	+/-	+/+	-/-	-/-	-/-	+/-	+/-	-/-

FB: Forebrain

Ag: antigen

Les: inflammatory and/or necrotising lesion

LNs: lymph nodes

Ifnar1-/- mice: *Ifnar1-/-* mice in Study 1 exhibited generally similar histopathological changes to those described for *Ifnar1-/-* mice in the Pilot study. These included mild to moderate, erosive to ulcerative, rhinitis with large amounts of antigen staining in inflamed areas in all 3 mice (Table 4.5). However, unlike the Pilot study, viral antigen was not detected in the endothelium of nasal submucosal blood vessels, submucosal lymphoid tissue, or in the perineurium of the olfactory nerve. As in *Ifnar1-/-* mice in the Pilot study, there were also numerous small foci of viral antigen in lung without evidence of pneumonia.

IHC viral antigen staining was detected in the olfactory bulb of all *Ifnar1-/-* mice in Study 1 (Table 4.5) and extended along the olfactory tract to the piriform lobe and amygdala in 2 of 3 mice. Similar to the Pilot study, viral antigen was present within the meningeal inflammatory infiltrate of one *Ifnar1-/-* mouse (Table 4.5). Where viral antigen was detected in brain this was associated with distinct neuropathology which mirrored the changes described in *Ifnar1-/-* mice in the pilot study, and comprised meningoencephalitis with a mixed inflammatory cell infiltrate that included neutrophils.

As in the Pilot study, 2 of 3 *Ifnar1-/-* mice in Study 1 had HeV antigen staining in the spleen which was not associated with lymphocytolysis, necrosis, inflammation or haemorrhage (Table 4.5).

HeV antigen was also detected in the liver of 2 of 3 *Ifnar1-/-* mice in Study 1 (Table 4.5), sometimes but not necessarily associated with small foci of hepatic necrosis. Similar foci of hepatic injury were also identified in the absence of viral antigen. These lesions are consistent with idiopathic focal hepatic necrosis and are considered to be an incidental finding, especially in inbred mice (Sundberg *et al.*, 1997).

Viral antigen or histological lesions were not detected within remaining tissue samples of *Ifnar1-/-* mice.

Ifnar2-/- mice: *Ifnar2-/-* mice exhibited similar histopathological changes to those described in *Ifnar1-/-* mice within Study 1 and the Pilot study.

Rhinitis associated with HeV antigen deposition was present in all four *Ifnar2-/-* mice, and was most severe in Mouse #83 which had remained clinically healthy and had been

euthanased at the experimental end point of 21 days p.e. Antigen was also identified within nasal submucosal lymphoid tissue and endothelium of either veins or lymphatic vessels in this animal. The presence of viral antigen in the nasal submucosal endothelium was not associated with degeneration of the vascular wall or its infiltration by inflammatory cells. HeV antigen staining was also identified within cervical lymph node in another *Ifnar2-/-* mouse (Mouse #81): this was not associated with lymphocytolysis, necrosis, inflammation or haemorrhage. A further *Ifnar2-/-* mouse (Mouse #84) also had a mixed inflammatory infiltrate in the perineurium between olfactory nerve fibres traversing the caudal nasal submucosa before it crossed the cribiform plate, similar to that described in *Ifnar1-/-* mice in the Pilot study.

Numerous small foci of viral antigen were seen in the lung of 3 of 4 *Ifnar2-/-* mice, comparable to those observed in *Ifnar1-/-* mice. Inflammatory, haemorrhagic or necrotic lesions were not detected in the lungs of these mice.

IHC viral antigen staining was detected in the olfactory bulb of all 4 *Ifnar2-/-* mice, including the mouse which remained clinically healthy throughout the 21 days of study period (Mouse #83). Viral antigen was also present in the piriform lobe and amygdala in 2 of these mice (Mice #81, and 82). Similar to *Ifnar1-/-* mice, HeV infection within the olfactory tract was associated with a suppurative meningoencephalitis including small areas of haemorrhage. HeV antigen was seen in the inflamed meninges of 2 of 4 *Ifnar2-/-* mice (Mice #83 and #84), including the meningeal vascular endothelium of one mouse (Figure 4.12). The presence of viral antigen within the meningeal vascular endothelium was not associated with vascular wall degeneration or vasculitis. One of 4 *Ifnar2-/-* mice (Mouse #82) also had a focus of HeV antigen within ependymal cells.

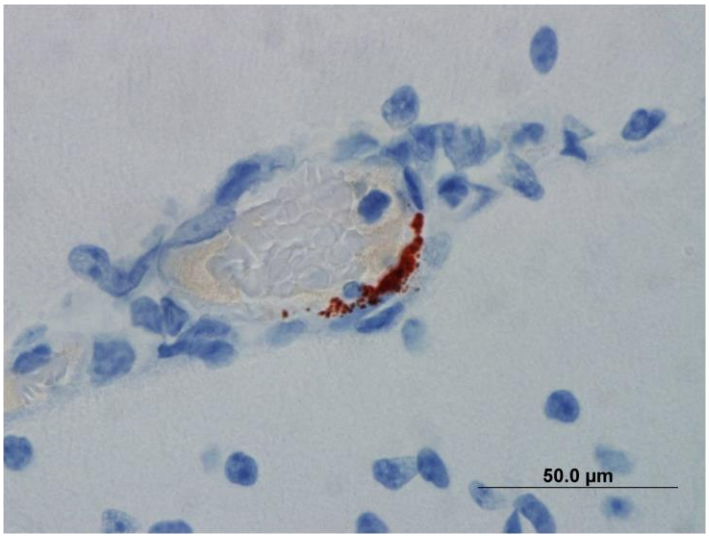

Figure 4.12: IHC stained section of brain showing meningeal blood vessel with viral antigen within the endothelium

Similar to *Ifnar1-/-* mice, 4 of 4 *Ifnar2-/-* mice had multifocal aggregates of HeV antigen within the spleen. The liver of 1 of 4 *Ifnar2-/-* mice (Mouse #83) was positive for viral antigen; antigen deposits were sometimes associated with small inflammatory foci as previously described.

HeV antigen was not detected within the other tissues examined from *Ifnar2-/-* mice.

4.5.2.3 Molecular virology and classical virology

Viral genome was detected in at least one tissue of all mice shown to have been infected after exposure to HeV (Data presented in (Figure 4.13).

Figure 4.13: Study 1 qPCR data. Log_{10} HeV-N gene copies normalised to 18S in different organs

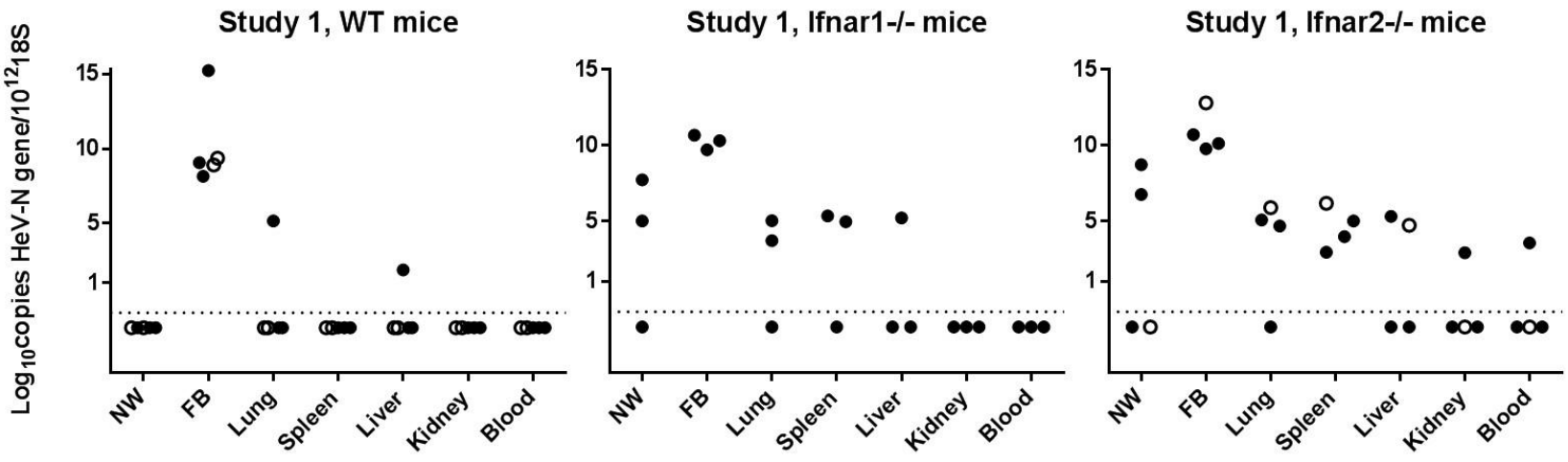

FB: Forebrain

NW: Nasal wash

Open circle: remained clinically healthy

Solid circle: showed neurological signs

Dotted line: level of assay detection

HeV genome was present in the forebrain samples of all mice, including the two WT mice and one *Ifnar2-/-* mice which remained clinically healthy throughout the study (Table 4.4 and Figure 4.13). Virus was also re-isolated from the contralateral forebrain of 2 out of 5 WT mice, 2 out of 3 *Ifnar1-/-*mice, and 3 out of 4 *Ifnar2-/-*mice (Table 4.4). Each of these mice had been euthanased on account of neurological signs, apart from one *Ifnar2-/-*mouse that had remained healthy throughout the study.

HeV genome was present in the nasal washings of 2 out of 3 *Ifnar1-/-* mice and 2 out of 4 *Ifnar2-/-* mice, each of which had been euthanased on account of neurological signs. Virus was re-isolated from the nasal washings of one of these *Ifnar1-/-* mouse and one *Ifnar2-/-* mouse (Table 4.4 and Figure 4.13).

HeV genome was detected in the lung of 1 out of 5 WT mice, 2 out of 3 *Ifnar1-/-* mice, and 3 out of 4 *Ifnar2-/-*mice. Virus was re-isolated from the lung of one *Ifnar2-/-* mouse (Table 4.4 and (Figure 4.13).

HeV genome was not identified in the spleen of WT mice, but was found in 2 out of 3 *Ifnar1-/-* mice and 4 out of 4 *Ifnar2-/-* mice (Table 4.4 and Figure 4.13). Virus was also re-isolated from the spleen of one *Ifnar2-/-* mouse, providing additional indirect evidence for the occurrence of viraemia in *Ifnar2-/-* mice (Table 4.4)
In the liver, a low level of HeV genome was found in 1 out of 5 WT mouse, in addition to 1 out of 3 *Ifnar1-/-* mice and 2 out of 4 *Ifnar2-/-* mice (Table 4.4 and Figure 4.13). Virus was not re-isolated from the liver of any mice.

Viral genome was also detected in the kidney and blood of 1 out of 4 *Ifnar2-/-* mice (Table 4.4 and Figure 4.13).

There was no significant interaction between tissue type and test group for viral genetic load. There were significant effects of test group on viral genetic load within the tissues tested ($p = 0.0010$), with higher overall mean viral genetic loads in the *Ifnar2-/-* mice group compared to WT mice ($p = 0.0007$). Within tissues, there were significantly higher mean viral genetic loads in the spleen of both *Ifnar1-/-* mice ($p = 0.0343$) and *Ifnar2-/-* mice ($p = 0.0015$) compared to WT mice. There was also a significant effect overall of tissue type on

viral genetic load ($p < 0.0001$), with higher levels in forebrain compared to all other tissues ($p < 0.0001$), and higher levels in lung compared to kidney ($p = 0.0483$).

4.5.2.4 Serology

Two out of 5 WT mice tested positive for a binding antibody response. The WT mouse which survived to day 21 p.e. was negative for antibody but only had evidence of infection within the forebrain. This may reflect poor stimulation of an adaptive immune response because the infection in this case was confined within the brain, as occurs with Rabies virus infection (Johnson *et al.*, 2010). Similarly, WT mice were euthanased on days 10 and 16 p.e. were also seronegative although HeV antigen was present in lung as well as in the forebrain. However, it is not clear why antibody was not detected in these mice, especially as Dups *et al.* (Dups *et al.*, 2012) found binding antibody in all mice that developed clinical disease. Three out of 3 *Ifnar1-/-* and 3 out of 4 *Ifnar2-/-* mice tested positive for a binding antibody response (Table 4.6). The *Ifnar2-/-* mouse that was negative was euthanased on day 7 p.e., and there may have been insufficient time for the adaptive immune response to generate antibody.

Table 4.6: Serology results for Study 1; IN HeV exposure of WT, *Ifnar1-/-* and *Ifnar2-/-* mice

	Assay			Antibody binding	Receptor blocking
Mouse type	Mouse #	ID delete	Euth day	MFI Post Challenge	% Inhibition
WT	73	89	21	**16676**	0
	74	90	21	163	0
	75	91	16	**24942**	2
	76	92	16	336	1
	77	93	10	201	1
Ifnar1-/-	78	75	11	**25150**	0
	79	76	11	**1379**	0
	80	78	10	**24317**	0
Ifnar2-/-	81	79	10	**16003**	0
	82	80	9	**1025**	0
	83	86	21	**11107**	0
	84	87	7	196	2
Positive controls	Horse			**28279**	**79**
	Mouse			**3980**	NA
	Rabbit			**29257**	**75**

ND: Not done

Euth.: Euthanasia

Luminex binding assay: for this experiment the mean of all pre-challenge sera was 428 MFI, 1SD = 185, and therefore a positive result was defined as >983 MFI.

Luminex receptor blocking assay: the % inhibition of positive control sera was >75 %. The % inhibition in sera from all mice subjects was < 6.4%. Positive results are shown in red.

Interestingly one *Ifnar2-/-* mouse (Mouse #83) remained clinically healthy to the experimental end point on day 21 p.e. and had a binding antibody response. This mouse had lesions of acute rhinitis and viral replication was present in the olfactory bulb, nasal wash and spleen. Cross contamination during post mortem examination is unlikely in this case as no other mouse euthanased on day 21 p.e. in Study 1 had viral antigen present in tissues. Post mortem techniques were followed to minimise cross contamination, including changing the absorbable towelettes and disposable scalpels between mice, thoroughly rinsing instruments (scalpel, scissors and forceps) and changing the region of the towelette used between sampling different organs. At completion the entire surface was disinfected with Virkon®. This individual may have been infected from a clinically affected cage mate in the

terminal stages of disease, possibly through nasal droplets rather than from the primary inoculum.

4.5.2.5 Assignment of infection phenotype

WT mice: For infected WT mice, 3 out of 5 demonstrated acute neurological disease that was accompanied by mild to moderately severe non-suppurative meningoencephalitis. One of these 3 mice also had virus replication confirmed in olfactory mucosa that was associated with rhinitis. Virus replication was also confirmed in the lung each of these 3 mice, but an associated pneumonia was not identified. Virus replication was not confirmed in any other tissues including liver, spleen, kidney, or in the blood of WT mice. No WT mice developed a sustained febrile response following exposure to HeV, including prior to the onset of neurological signs. In one mouse, mild weight loss preceded the onset of neurological signs and was attributed to the developing neuropathology. Two of 5 WT mice infected by HeV remained clinically healthy during the study period.

On the basis of these findings, 3 WT mice were assigned a neurological infection phenotype and 2 mice were assigned a subclinical phenotype (Table 4.4).

Ifnar1-/- mice: Three of 3 infected *Ifnar1-/-* mice demonstrated acute neurological disease over a similar timeframe to WT mice. Each of these mice had virus replication confirmed in brain that was accompanied by mild to moderately severe meningoencephalitis with a mixed inflammatory cell infiltrate that included neutrophils. They also had virus replication confirmed in olfactory mucosa that was associated with rhinitis: in 1 mouse infection extended to a regional lymph node without evidence for lymphadenitis. Virus replication was also confirmed in the lung of 3 out of 3 *Ifnar1-/-* mice, but an associated pneumonia was not identified. No *Ifnar1-/-* mice developed a febrile response following exposure to HeV, including prior to the onset of neurological signs.

In contrast to WT mice, virus replication was confirmed in the spleen (2 out of 3) and also the liver (2 out of 3) of *Ifnar1-/-* mice. Replication of HeV (as determined by IHC) was also identified in the meninges of one mouse. However, apart from the rhinitis and meningoencephalitis, the presence of viral antigen in these tissues was not associated with significant pathology in the form of an inflammatory response or necrotising lesions.

On the basis of these findings, 3 out of 3 infected *Ifnar1-/-* mice were assigned a neurological infection phenotype (Table 4.4).

Ifnar2-/- mice: Three of 4 infected *Ifnar2-/-* mice demonstrated acute neurological disease over a similar timeframe to WT mice. Each of these mice had virus replication confirmed in brain, accompanied by mild to moderately severe meningoencephalitis with a mixed inflammatory cell infiltrate that included neutrophils. They also had virus replication confirmed in olfactory mucosa that was associated with rhinitis Virus replication was also confirmed in the lung of each mouse, but an associated pneumonia was not identified. No *Ifnar2-/-* mice developed a febrile response following exposure to HeV, including prior to the onset of neurological signs.

In contrast to WT mice, virus replication was confirmed in the spleen of the 3 *Ifnar2-/-* mice that showed neurological disease. Replication of HeV (as determined by IHC) was also identified in the meninges (2 out of 3 mice) and vascular endothelium (2 out of 3 mice). However, with the exception of rhinitis and meningoencephalitis, the presence of viral antigen in these tissues was not associated with significant pathology in the form of an inflammatory response or necrotising lesions.

The remaining mouse remained clinically well throughout the study period. It, too, had virus replication confirmed in the brain, accompanied by mild to moderately severe meningoencephalitis with a mixed inflammatory cell infiltrate that included neutrophils. It also had rhinitis associated with virus replication within the nasal mucosa. Virus replication was also confirmed in the lung of this mouse, as well as in spleen, liver and (as determined by IHC) meninges and vascular endothelium. Apart from meningoencephalitis and rhinitis, the finding of viral antigen in this mouse was not associated with significant pathology in the form of an inflammatory response or necrotising lesions. Interestingly, virus was re-isolated from the brain and spleen of this mouse on day 21 p.e. and in the presence of antibodies to HeV as assessed by Luminex binding assay.

On the basis of these findings, 3 out of 4 infected *Ifnar2-/-* mice were assigned a neurological infection phenotype and one mouse was assigned a subclinical phenotype (Table 4.4).

Summary comments: There were no significant differences between WT, *Ifnar1-/-*and *Ifnar2-/-* mice in infection survival curves. As the data set did not meet the criteria for valid Chi^2 calculations, two data rows (*Ifnar1-/-* and *Ifnar2-/-*) were combined in a biologically plausible way for contingency analysis of infection phenotypes. On that basis, there was no significant difference between phenotypes assigned to WT mice or immune-deficient mice. Similarly, there was no significant difference between test groups in the likelihood of virus replication in brain, and all mice examined between day 6 and day 16 p.e. showed virus replication in lung. However, immune-deficient mice were significantly more likely to replicate virus in spleen compared to WT mice ($p = 0.0476$).

4.5.3 Study 2

4.5.3.1 Clinical observations

As in the Pilot study and Study 1, the IN exposure of mice to 50 000 TCID50 HeV was well tolerated by both WT and *Stat1-/-* mice.

All mice met the criteria for HeV infection. Two out of 3 WT mice reached their predetermined humane endpoint for neurological disease and were euthanased on day 9 and 13 p.e. (Table 4.7). One WT mouse remained clinically healthy up to the time of elective euthanasia on day 21. All 3 *Stat1-/-* mice reached their predetermined humane endpoint for neurological disease and were euthanased on day 10 or 14 (Table 4.7). The clinical signs were indistinguishable from those seen in WT mice, including demonstration of ataxia and tremors. There was no significant difference between the survival curves of the two test groups.

Table 4.7: Study 2, summary of data used to assess infection status

Mouse type	Mouse ID	Euth. day	Infection phenotype	Olfactory mucosa Ag/PCR*/VI*	Lung Ag/PCR/VI	Forebrain Ag/PCR/VI	Spleen Ag/PCR/VI	Liver Ag/PCR	Kidney Ag/PCR/VI	Blood PCR/VI	Serology Bind/Blk
WT	85	21	Subclinical	-/-	-/-	+/+	-/-	-/-	-/-	+/-	+/-
	86	13	Neurological	-/-	+/-	+/+	-/-	-/-	-/+	-/-	-/-
	87	9	Neurological	+/-	-/+	+/+ +VI	-/-	-/-	-/-	-/-	-/-
Stat1-/-	88	10	Neurological	+/+ +VI	+/+	+/+ +VI	+/+ +VI	-/-	-/-	-/-	-/-
	89	14	Neurological	+/+	+/+	+/+ +VI	+/+	-/-	-/+	+/+	+/-
	90	10	Neurological	+/+ +VI	+/+ +VI	+/+ +VI	+/+ +VI	-/-	-/-	-/-	+/-

Ag: immunohistochemical staining for viral antigen in tissue

PCR: qPCR for viral genome in tissue

VI+: virus isolation performed on all samples, only positive results indicated above

* For olfactory mucosa PCR and VI was performed on retrograde nasal washings

"+" present

"-" not present

Euth. Day: day of euthanasia

Bind: Luminex binding assay

Blk: Luminex receptor blocking assay

Bodyweight data is presented in Figure 4.14. All mice euthanased for neurological disease, apart from one *Stat1-/-* mouse, started to lose weight from 72 to 24 hrs. prior to euthanasia. There was no significant interaction between time and test group on bodyweight. There was a significant effect of time on bodyweight (<0.0001), with increased weight over baseline on day 4, 5, 6, 8 and 9 p.e.. There was no significant effect of treatment group on bodyweight up to day 9 post-exposure to HeV.

Figure 4.14: Study 2, combined mouse weights (grams with mean and SD) over days post infection.

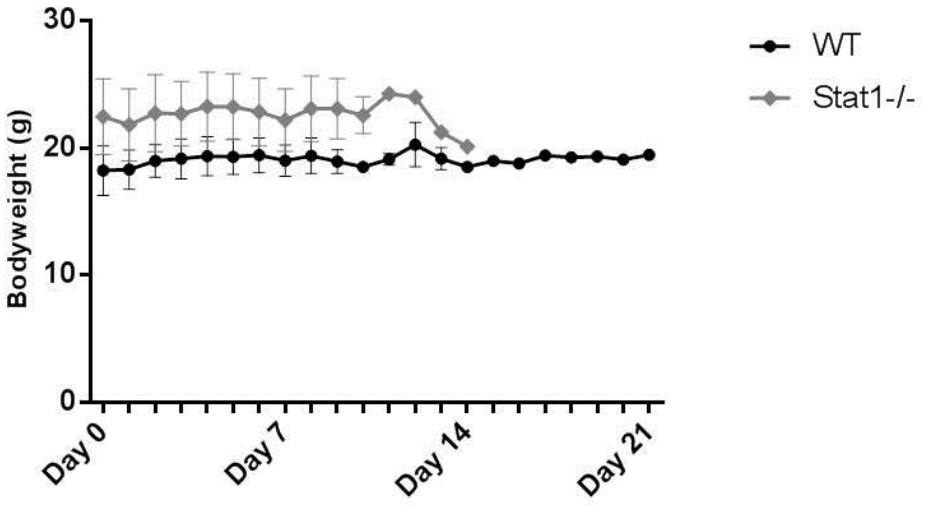

Temperature data is presented in Figure 4.15. No mouse developed a febrile response post-exposure to HeV. There was no significant interaction between time and test group on temperature. There was no significant effect of time on temperature up to day 9 post-exposure to HeV. There was a significant effect of test group on temperature ($p = 0.0468$): a higher mean temperature (of 1.2 ^{o}C) was recorded for *Stat1-/-* mice on day 6 p.e. alone ($p = 0.0458$). This was at least 4 days prior to euthanasia of any *Stat1-/-* mouse and the finding was not considered to be of clinical significance.

Figure 4.15: Study 2, combined mouse temperature (^{o}C with mean and SD) over days post infection.

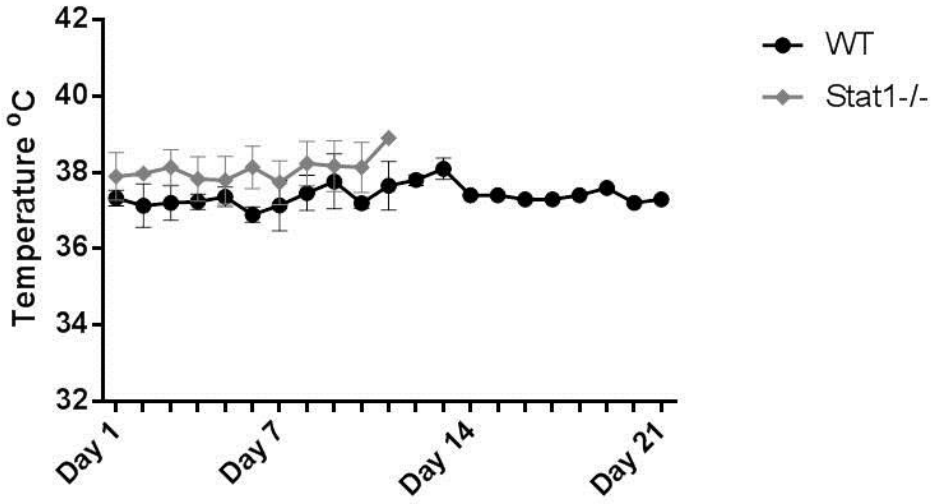

4.5.3.2 Pathology and immunohistopathology

WT mice: The histopathological findings in the two WT mice that were euthanased due to neurological disease were similar to those observed in WT mice previously assigned a neurological phenotype and are presented in Table 4.8.

Table 4.8: Study 2, summary of pathology findings

Mouse type	Mouse ID	Meninges Ag/les	Forebrain Ag/les	Ependyma Ag/les	Endothelium Ag/les	Olfactory mucosa Ag/les	Olfactory lymphoid tissue Ag/les	Olfactory nerve perineurium Ag/les	Olfactory regional LNs Ag/les	Lung Ag/les	Spleen Ag/les	Liver Ag/les
WT	85	-/+	+/+	-/-	-/-	-/-	-/-	-/-	-/-	-/-	-/-	-/-
	86	-/+	+/+	-/-	-/-	-/-	-/-	-/-	-/-	+/-	-/-	-/-
	87	-/+	+/+	-/-	-/-	+/+	-/-	-/-	-/-	-/-	-/-	-/-
Stat1-/-	88	+/+	+/+	-/-	-/-	+/+	-/-	-/-	-/-	+/-	+/-	-/-
	89	+/+	+/+	-/-	-/-	+/+	-/-	-/-	-/-	+/-	+/-	-/-
	90	+/+	+/+	-/-	-/-	+/+	-/-	-/-	-/-	+/-	+/-	-/-

Ag: antigen

Les: inflammatory and/or necrotising lesion

LNs: lymph nodes

One of these 2 WT mice had mild to moderate rhinitis associated with positive staining for viral antigen within the olfactory epithelium. Occasional small aggregates of HeV antigen were also seen within the lung of one of the mice, without other evidence for tissue injury such as infiltration of inflammatory cells or necrosis. Viral antigen in brain was localised to the rostral olfactory tract, and there was associated non-suppurative meningoencephalitis. Viral antigen or lesions were not identified in other tissues (Table 4.8).

In the remaining WT mouse that had remained clinically healthy, there was mild olfactory bulb meningoencephalitis associated with positive viral antigen staining within the olfactory bulb. Viral antigen or lesions were not identified in other tissues of this animal (Table 4.8).

Stat 1 mice: All 3 *Stat1-/-* mice had severe rhinitis associated with viral antigen within the mucosa similar to WT mice. Similar to some *Ifnar1-/-* mice, 2 out of 3 *Stat1-/-* mice also showed mixed inflammatory cell infiltrates in the perineurium between olfactory nerve fibres traversing the caudal nasal submucosa before they crossed through the cribriform plate, although viral antigen was not detected. There were numerous small foci of viral antigen in the lung and, as for the lung of WT, *Ifnar1-/-* and *Ifnar2-/-* mice, there was no evidence of tissue injury associated with antigen deposition.

All 3 *Stat1-/-* mice had HeV antigen in olfactory bulb neuropil; staining extended into the piriform lobe and amygdala, and to the hippocampus in one mouse. There were marked and predominately neutrophilic infiltrates into the olfactory bulb together with areas of haemorrhage scattered throughout the neuropil. There was marked meningitis with a mixed inflammatory cell infiltrate (including neutrophils) as well as perivascular cuffing in the affected areas. Similar to *Ifnar1-/-* and *Ifnar2-/-* mice, viral antigen was scattered throughout the meningeal inflammatory infiltrate (Table 4.8).

All 3 *Stat1-/-* were positive for HeV antigen in the spleen, and this was not associated with lymphocytolysis or necrosis. In addition, there were large multifocal to coalescing foci of neutrophilic infiltration admixed with haemorrhage scattered randomly throughout the spleen. Small foci of mixed inflammatory cells were also observed in the liver. In both liver and spleen, the neutrophilic infiltrates were not associated with HeV antigen deposition.

Accordingly, the infiltrates were interpreted as incidental findings for this mouse strain (Durbin *et al.*, 1996).

Viral antigen or lesions were not identified in any other tissues from *Stat1-/-*mice.

4.5.3.3 Molecular virology and classical virology

Viral genome was detected in at least one tissue of all mice shown to have been infected after exposure to HeV (Data presented in Figure 4.16).

Figure 4.16: Study 2, qPCR data. Log_{10} HeV-N gene copies normalised to 18S in different organs

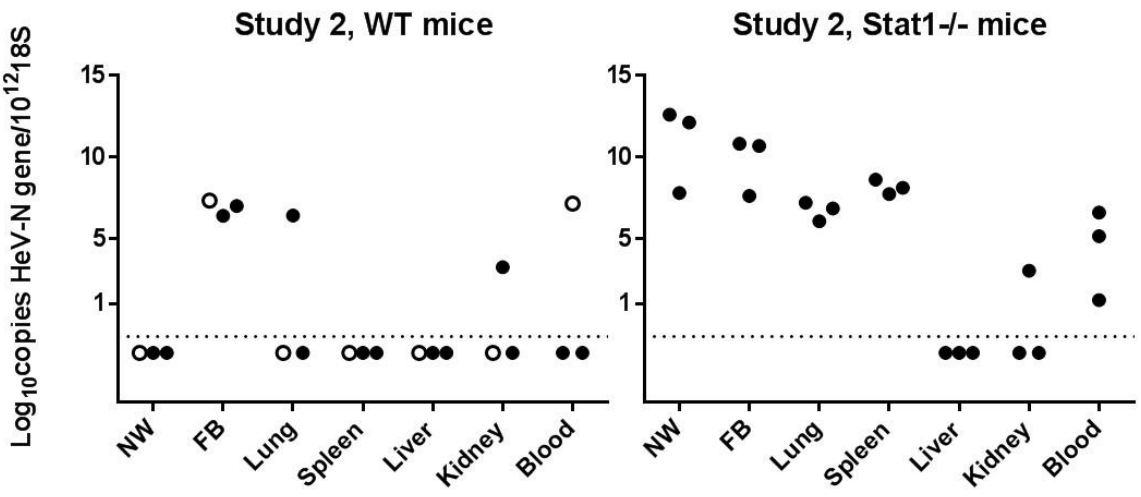

FB: Forebrain

NF: Nasal wash

Open circle: remained clinically healthy

Solid circle: showed neurological signs

Dotted line: level of assay detection

In Study 2, viral genome was detected in the forebrain of all mice (Table 4.8 and Figure 4.16), including one WT mouse that remained clinically healthy until day 21 p.e.. Virus was also re-isolated from the forebrain of one WT mouse and 3 out of 3 *Stat1-/-* mice (Table 4.7), each of which had been euthanased on account of neurological signs.

HeV genome was present in the saline flush from the nostrils of all 3 *Stat1-/-* mice (Figure 4.16). Virus was re-isolated from 2 out of 3 of these mice (Table 4.7).

HeV genome was detected in the lung of 1 out of 3 WT mice and 3 out of 3 *Stat1-/-* mice. Virus was re-isolated from the lung of one *Stat1-/-* mouse (Table 4.7).

HeV genome was not identified in the spleen of WT mice, but was found in 3 out of 3 *Stat1-/-* mice (Table 4.7 and Figure 4.16). Virus was also re-isolated from the spleen of two *Stat1-/-* mice, providing additional indirect evidence for the occurrence of viraemia in *Stat1-/-* mice (Table 4.7).

HeV genome was not identified within the liver of any mouse, but it was found in kidney of one each of WT and *Stat1-/-* mice (Table 4.7 and Figure 4.16). Additionally there was viral genome detected in the blood of one WT and two *Stat1-/-* mice. Virus was re-isolated from the blood of one of these *Stat1-/-* mice, confirming the potential for HeV viraemia in this murine genotype.

There was no significant interaction between test group and tissue type on HeV genetic load. There was a significant effect of test group on viral genetic load ($p = 0.0007$), with higher mean viral genetic loads in the spleen of *Stat1-/-* mice compared to WT mice ($p = 0.0017$). There was also a significant effect overall of tissue type on viral genetic load ($p = 0.0006$), with higher mean levels in forebrain compared to spleen ($p = 0.0348$), kidney ($p = 0.0002$) and blood ($p = 0.0077$). Within *Stat1-/-* mice, mean HeV genome levels were also lower in kidney compared to lung ($p = 0.0479$) and spleen ($p = 0.0091$).

Due to the small sample sizes in this study, contingency analysis to compare HeV tissue replication rates between WT and *Stat1-/-* mice was not carried out.

4.5.3.4 Serology

One out of 3 WT and 2 out of 3 *Stat1-/-* mice had a positive binding antibody responses (Table 4.9).

Table 4.9: Serology in IN exposed WT and *Stat1-/-* mice

	Assay			Antibody binding	Receptor blocking
Mouse type	Mouse #	ID delete	Euth. Day	MFI Post Challenge	% Inhibition
WT	85	131	21	**6797**	1
	86	132	13	51.5	0
	87	133	9	52.5	1
Stat1-/-	88	124	10	53	0
	89	125	14	**4375**	6
	90	126	10	**133**	4
Positive controls	Horse			**28955**	**82**
	Mouse			**4905**	NA
	Rabbit NiV			ND	**75**

ND: Not done

Euth.: Euthanasia

Luminex binding assay: for this experiment the mean of all pre-challenge sera was 58 MFI, 1SD = 11, and therefore a positive result was defined as >90 MFI. For the Luminex receptor blocking assay the % inhibition of positive control sera was >74%. The % inhibition in sera from all mice subjects was < 6.4% Positive results are shown in bold

4.5.3.5 Assignment of infection phenotype

An infection phenotype was assigned to each mouse as described above. For infected WT mice, 2 out of 3 demonstrated acute neurological disease. Both mice had virus replication confirmed in brain that was accompanied by mild to moderately severe non-suppurative meningoencephalitis. Virus replication was also confirmed in the nasal mucosa and lung of 1 out of 3 WT mice, but an associated pneumonia was not identified. Virus replication was not confirmed in any other tissues outside of the respiratory tract and olfactory tract, including liver, spleen, kidney, or blood of WT mice. Mild weight loss preceded the onset of neurological signs, but this was not accompanied by fever. The loss of weight was therefore attributed to the developing neuropathology.

The remaining infected WT mouse remained clinically healthy throughout the study period. It had asymptomatic encephalitis attributable to HeV, and antibodies to HeV by Luminex binding assay.

Considering the findings overall, 2 out of 3 WT mice were assigned a neurological infection phenotype and 1 out of 3 a subclinical infection phenotype (Table 4.7).

Three of 3 *Stat1-/-* mice developed an acute neurological disease over a similar timeframe to WT mice. Each of these mice had virus replication confirmed in brain, accompanied by mild to moderately severe meningoencephalitis. However, as found with *Ifnar1-/-* and *Ifnar2-/-* mice, there were qualitative differences to the pathology recorded for WT mice. In particular, neutrophils were present in the inflammatory infiltrate of *Stat1-/-* mice and viral antigen was identified within meningitic lesions. Virus replication was confirmed in olfactory mucosa of 3 out of 3 *Stat1-/-* mice and was associated with rhinitis. Virus replication was also confirmed in the lung of 3 out of 3 *Stat1-/-* mice, but an associated pneumonia was not identified.

Virus replication was also confirmed in the spleen of 3 out of 3 *Stat1-/-* mice: re-isolation of HeV from the blood of one mouse confirmed that viraemia may be a feature of HeV infection in this mouse genotype. However, apart from rhinitis and meningoencephalitis, the presence of HeV antigen in tissues was not associated with significant pathology in the form of an inflammatory response or necrotizing lesions.

Two *Stat1-/-* mice showed mild weight loss from up to 72 hours prior the onset of neurological signs but, as in WT mice, this was not accompanied by a febrile response in any mouse. Similar to WT mice, the loss of weight was attributed to the developing neuropathology.

Considering the findings overall, 3 out of 3 *Stat1-/-* mice were assigned a neurological infection phenotype (Table 4.7). There was no significant difference between WT and *Stat1-/-* mice in the incidence of infection phenotypes that were assigned following exposure to HeV, or to the infection survival curves.

4.6 Discussion

The aim of this study was to evaluate the contribution of IFN signalling to the resistance of mice to systemic HeV disease, by assessing the impact of HeV exposure on *Ifnar1-/-, Ifnar2-/-* and *Stat1-/-*mice compared to WT mice. Following IN exposure to HeV, clinical

observations including bodyweight and temperature were recorded for up to 21 days, tissue distribution and levels of virus replication were assessed, the severity of pathology in diverse organ systems was evaluated, and an infection phenotype was assigned to each mouse. Group survival curves were also compared.

Other studies comparing the impacts of viral infection in immunocompetent and *Ifnar1-/-* (Bradfute *et al.*, 2012; Eschbaumer *et al.*, 2012; Hwang *et al.*, 1995; Orozco *et al.*, 2012; van den Broek *et al.*, 1995; Wernike *et al.*, 2012) or *Stat1-/-* mice (Bente *et al.*, 2010; Bowick *et al.*, 2012; Bradfute *et al.*, 2012; Durbin *et al.*, 1996; Gil *et al.*, 2001; Meraz *et al.*, 1996; Raymond *et al.*, 2011) have shown interferon-signalling deficient mice are more likely to develop infection and disease with increased mortality. As a corollary, they also have more severe clinical signs, more severe pathology in a wider range of organs, more widespread viral distribution, and higher tissue viral loads. While none of these papers specifically consider henipaviruses, similar findings have been reported for diverse virus families including Bunyaviridae, Reoviridae, Flaviviridae, Arenaviridae, Picornaviridae, Togaviridae, Rhabdoviridae, Poxviridae, Filovirdae, and Herpesviridae. This underscores the generality of the contribution of interferon signalling to antiviral immunity, and the plausibility of the hypothesis that systemic disease may be more likely to be observed in immunodeficient mice exposed to HeV.

It was also postulated that *Ifnar2-/-* mice might develop a different disease phenotype to *Ifnar1-/-* mice, as IFN-β can ligate to and signal through IFNAR1 in an IFNAR2 independent manner. This IFNAR1/IFN-β interaction modulates a distinct set of genes compared to signalling from the conventional IFNAR1-IFNAR2 complex (de Weerd *et al.*, 2013). These authors showed that sepsis induced by lipopolysaccharide is ameliorated in *Ifnar1-/-* but not in *Ifnar2-/-* mice, however it was not known whether differences are observed in the impact of viral infection.

Unlike *Ifnar1-/-* and *Ifnar2-/-* mice where deficiencies are confined to Type I IFN signalling, STAT1 mice are deficient in Type I, Type II and Type III IFN responses. *Stat1-/-* mice are highly sensitive to infection by microbial pathogens and viruses and it could be postulated that they would show a more severe infection phenotype than either *Ifnar1-/-* or *Ifnar2-/-* mice. In fact it has been shown that *Ifnar1-/-* mice are more resistant to infection with wild

type isolates of filoviruses than *Stat1-/-* mice, with *Stat1-/-* mice routinely succumbing to the majority of Filovirus isolates (Bray, 2001; Raymond *et al.*, 2011). However, IFNϒ can still regulate the expression of a large number of genes in the absence of STAT1 (Gil *et al.*, 2001; Ramana *et al.*, 2001; Wang *et al.*, 2002): in one report, *Stat1-/-* mice displayed a susceptibility to viral infection that was similar to *Ifnar1-/-* mice but less than mice lacking a combination of both *Ifnar* and IFNϒ receptors (IfnαβϒR-/- mice) (Gil *et al.*, 2001).

Animal studies at BSL4 generally involve relatively small group sizes and place restrictions on meaningful statistical analysis of data (Mire *et al.*, 2014). The limitations imposed by small data sets were also recognised in our study. Accordingly, multiple variables were assessed and the data integrated to increase accuracy and precision of evaluation of infection characteristics in individual mice. Using this approach, we identified several key pathogenetic findings that were statistically significant, were observed across all studies, and were biologically plausible.

In the current work, *Ifnar1-/-* and *Ifnar2-/-* mice were more likely to have replicated HeV in the spleen and to a higher level compared to WT mice, and the few splenic isolates were all from *Ifnar1-/-* and *Ifnar2-/-* mice. These findings are consistent with an increased role of viraemia in HeV infection of *Ifnar1-/-* and *Ifnar2-/-* mice compared to WT mice: viraemia may also account for the HeV replication observed within liver, ependymal cells, and vascular endothelium seen only in *Ifnar1-/-* and *Ifnar2-/-* mice. However, the low incidence of recovery of viral genome from the blood of *Ifnar1-/-* and *Ifnar2-/-* mice euthanased at humane endpoint suggests that any viraemic phase is transient and, overall, that replication of HeV in vascular endothelium is not a major feature of the infection in these mice. The viraemia in interferon signalling deficient mice may have been driven by higher levels of viral replication in the lung as IHC findings suggested they had increased numbers of antigenic foci in the lungs. However, this was not supported by estimates of viral genetic load, which were similar between *Ifnar1-/-* and *Ifnar2-/-* mice and WT mice. More accurate comparison of levels of HeV replication in lung would be possible by carrying out an elective euthanasia study, with more highly controlled sampling times post-exposure between the different test groups.

Viral replication within the meninges was also only recorded in *Ifnar1-/-* and *Ifnar2-/-* mice. This, too, may be attributable to viraemia. But the possibility cannot be ruled out of ascending infection via the olfactory nerve perineurium (where viral antigen was also detected in a few *Ifnar1-/-* and *Ifnar2-/-* mice) and extension into the arachnoid where this protrudes through the cribiform plate. The neutrophils observed in the inflammatory infiltrates within the CNS of *Ifnar1-/-* (and also *Ifnar2-/-*) mice may be intrinsic to their response to virus infection and tissue injury. *Ifnar1-/-* mice have more myeloid lineage cells within the peripheral blood and bone marrow than do WT mice because their bone marrow is spared from the antiproliferative effects of Type 1 IFNs (Hwang *et al.*, 1995). In addition, the percentage of cells with Mac-1 and Gr-1 positive expression is increased, and Mac-1 regulates leukocyte adhesion and migration to mediate the inflammatory response (Muller, 2013). In this instance it is not necessary to postulate secondary bacterial involvement, although early recruitment and augmentation of neutrophil response has been demonstrated in *Ifnar1-/-* mice with septic peritonitis (Weighardt *et al.*, 2006).

In spite of evidence for more widespread HeV replication in *Ifnar1-/-* and *Ifnar2-/-*mice compared to WT mice, there were no significant pathological lesions in the tissues involved. As a plausible biological consequence, there was no difference detected in the constitutional impact of HeV infection in *Ifnar1-/-* and *Ifnar2-/-*mice compared to WT mice. Interestingly, no mouse in any test group developed a sustained febrile response during the study periods, although it is known that *Ifnar1-/-* mice (Canakoglu *et al.*, 2015) and *Stat1-/-* mice (Bente *et al.*, 2010) can mount a rise in temperature in response to viral infection. There was also no significant difference between *Ifnar1-/-* and *Ifnar2-/-* mice compared to WT mice in any other measure of infection severity and, as for WT mice, all clinically affected *Ifnar1-/-* and *Ifnar2-/-*mice showed signs attributable to anterograde infection of the CNS.

With respect to the study using small groups of *Stat1-/-* mice and WT mice, insufficient animals required euthanasia at humane endpoint to permit between-group comparison of the likelihood of virus replication in spleen. However, and similar to *Ifnar1-/-* and *Ifnar2-/-* mice, *Stat1-/-* mice had significantly higher levels of HeV genome in spleen compared to WT mice: virus was reisolated from the spleen of only *Stat1-/-* mice. As for *Ifnar1-/-* and *Ifnar2-/-* mice, these observations are consistent with an increased role for viraemia in HeV

infection of *Stat1-/-* mice. Similarly, HeV replication observed within the meninges of only *Stat1-/-* mice may be accounted for by viraemia. But, as discussed above, meningeal infection may also have been a consequence of ascending infection via the perineurium of the olfactory nerve, and its pathogenesis within this specific study cannot be confirmed. Like *Ifnar1-/-* and *Ifnar2-/-* mice, the inconsistent recovery of viral genome or live virus from the blood of *Stat1-/-* mice euthanased at humane endpoint suggests that the viraemic phase is transient in mice of this genotype. The finding of HeV genome in the blood of one WT mouse also supports viraemia being an occasional feature of HeV infection in immunologically intact mice: interestingly, there was no evidence for virus replication at distant sites in this animal.

As for *Ifnar1-/-* and *Ifnar2-/-* mice, the neutrophils observed in the inflammatory infiltrates within the CNS of *Stat1 -/-* mice may be intrinsic to their response to virus infection and tissue injury. Although *Stat1-/-* mice have normal production and differentiation of myeloid cells (Durbin *et al.*, 1996), they show exaggerated and prolonged neutrophilic infiltration in models of arthritis (de Hooge *et al.*, 2004) and exacerbation of the inflammatory response with high numbers of neutrophils in brain parenchyma in INF-α associated encephalopathy (Wang *et al.*, 2002).

HeV replication in the spleens of *Stat1-/-* mice was not associated with detectable tissue injury or associated inflammatory response. This aligns with no significant differences to WT mice having been observed over the course of the study in respect of body temperature, body weight, survival curves and the range of infection phenotypes seen within study groups.

Mice deficient in IFN-signalling showed more widespread replication of HeV compared to WT mice. However, the clinical syndromes induced were similar to those observed in WT mice, and were limited to either anterograde encephalitis or subclinical infection. In contrast, ferrets exposed to <5000 $TCID_{50}$ HeV IN consistently developed acute, fulminating systemic infection characterised by fever and clinical depression (Pallister *et al.*, 2011) and horses given 2 x 10^6 $TCID_{50}$ HeV IN /PO also showed fever, depression, agitation and dyspnoea prior to euthanasia at humane endpoint (Marsh *et al.*, 2011). In an earlier study, cats exposed to $10^{3.6}$ $TCID_{50}$ HeV by oral, IN and SC routes developed depression, fever and

increased respiratory rate with rapid progression to humane endpoint or death within 1 day (Westbury *et al.*, 1996). Similarly, AGM exposed IT to 4 x 10^5 $TCID_{50}$ HeV also exhibited a rapidly progressive clinical illness characterised by fever, depression and respiratory signs, with a clinical course lasting approximately 3 days (Rockx *et al.*, 2010).

Compared to WT mice, mice deficient in IFN-signalling showed HeV replication in a limited number of additional sites, primarily the spleen and liver and occasionally in the perineurium of the olfactory nerve, meninges, and focal areas of vascular endothelium. By contrast, HeV replication in ferrets is extensive including multiple vascular sites, intra-abdominal lymph nodes, renal glomeruli, lymph endothelium, testicular tissue, cardiac myocytes, and pancreatic and intestinal epithelial cells (Pallister *et al.*, 2011). A similar range of tissues to those reported for ferrets supports HeV replication in the horse, with the addition of ovary, uterus and adrenal gland (Marsh *et al.*, 2011); in the cat, with the addition of uroepithelium (Hooper *et al.*, 1997b); and in the AGM, with the addition of bone marrow (Rockx *et al.*, 2010).

Measurement of tissue levels of HeV genome in the current studies were conducted under similar test conditions and in the same laboratory to the ferret study by Pallister *et al.* (2011) and the horse study by Marsh *et al.* (2011). Reconfiguration of data for control animals in those experiments, including calculation of 18sRNA gene copy number, allowed direct comparison of HeV genomic loads in selected tissues of ferrets, horses and mice deficient in interferon signalling (Appendix 1). Mean genomic loads were comparable in the spleen and liver of interferon signalling deficient mice to those found in ferrets and horses.

However, unlike ferrets and horses, viral replication in interferon signalling-deficient mice is not accompanied by inflammatory or necrotising lesions (apart from in upper respiratory tract and forebrain). For example, Pallister *et al.* (2011) described wide-spread vasculitis, necrotising lymphadenitis, glomerulitis, splenitis and bronchoalveolitis in ferrets, while horses showed systemic vasculitis affecting the meninges, brain, nasal mucosa, trachea, lung, multiple different lymph nodes, spleen, liver, kidney, heart, ovary, uterus and intestine, as well as severe pulmonary oedema and alveolitis, glomerulitis, necrotising lymphadenitis and myocarditis (Marsh *et al.*, 2011). Similarly to ferrets and horses, cats showed severe pneumonia with serofibrinous and necrotising alveolitis, with widespread

vasculitis, and necrotic and haemorrhagic lymph nodes with numerous pyknotic and karyolytic lymphocytes (Hooper *et al.*, 1997b). And, lastly, AGM also showed pulmonary oedema and alveolitis with fibrin deposition within alveolar spaces (Rockx *et al.*, 2010). In each of these species epithelial and /or endothelial syncytial cells were also observed in affected tissues.

Overall, the hypothesis that IFN signalling deficient mice will be susceptible to systemic disease induced by HeV infection was disproven. The study findings for the present chapter suggest that, although mice deficient in interferon signalling were slightly more permissive to HeV infection, the resistance of WT mice to widespread HeV replication and fulminating systemic disease could not be attributed solely to the efficacy of mouse interferon signalling pathways against HeV-mediated anti-interferon mechanisms.

However, anterograde encephalitis regularly occurred in both WT and interferon signalling deficient mice requiring their euthanasia on humane grounds from day 7 p.e. It is possible that at least in some animals this may have limited the opportunity for full expression of the impact of systemic HeV replication. In addition, anterograde encephalitis also complicated the assessment of the role of viraemia in the pathogenesis of CNS infection in interferon signalling deficient mice, notably determination of the source of the antigen within meningeal lesions.

While these studies were being carried out, Dhondt *et al.* (2013) reported lethal Henipavirus infection in 50% of 11 week old *Ifnar1-/-* mice on a C57BL6 background exposed by the IP route. Affected mice exhibited neurological signs and, in addition to non-suppurative meningoencephalitis, also were reported to have focal necrotising alveolitis and vasculitis. By contrast, also to findings in the current work, *Ifnar1-/-* mice exposed to 10^6 PFU IN showed no clinical signs. However viral genome was found in brain tissue, although levels were lower in mice exposed IN compared to IP. Immunohistopathology was not described for mice given virus IN, and the role of anterograde infection of the CNS in these mice was not discussed.

The findings of Dhondt *et al.* (2013) suggest that *Ifnar1-/-* mice exposed IP may be more permissive to HeV disease than mice exposed to virus by the IN route. In addition, Dups *et*

al. (2012) did not observe infection – and specifically anterograde encephalitis - in WT C57Bl6 mice after parenteral (SC) exposure to HeV. To further test the conclusions from the current work, and with the aim of reducing complications associated with anterograde infection of the CNS, it will be necessary to investigate the outcomes of IP exposure of interferon signalling-deficient mice to HeV under equivalent study conditions to those used in the present chapter.

CHAPTER 5: WILD TYPE MICE SHOW AN INCREASED ROLE FOR VIRAEMIA, AND MICE DEFICIENT IN INTERFERON SIGNALING DO NOT DEVELOP A SYSTEMIC INFECTION PHENOTYPE, AFTER INTRAPERITONEAL EXPOSURE TO HENDRA VIRUS.

5.1 Introduction and background

Following IN exposure to HeV, mice deficient in IFN signalling (*Ifnar1-/-*, *Ifnar2-/-* and *Stat1-/-* mice) demonstrated more widespread viral replication compared to WT mice – notably in spleen and liver, but also olfactory nerve perineurium, meninges and vascular endothelium. However, as for WT mice, affected mice showed only a neurological syndrome or subclinical infection: inflammatory lesions detectable under the light microscope were confined to the nasal cavity and the brain, and meningoencephalitis was attributable to anterograde infection via olfactory sensory neurones. Unlike other animal species susceptible to systemic HeV infection, neither vasculitis, with vascular wall degeneration and inflammatory cell infiltration, nor necrotising lesions within infected viscera were identified in immune-deficient mice. Anterograde neurological infection occurred frequently in IFN-signalling deficient mice and complicated the assessment of whether or not CNS infection might also have been acquired by the haematogenous route in these mice. In addition, neurological disease led to their euthanasia from day 7 post-exposure on humane grounds, and so there may not have been sufficient time in all mice to assess the full impact of the more widespread replication of HeV.

In species that are more permissive to Henipavirus infection compared to mice, the effects of different routes of exposure on either susceptibility to infection or infection characteristics have varied from animal to animal. For example, cats succumbed to non-parenteral (oral and nasal) and parenteral (subcutaneous) routes of exposure with a similar disease course (Hooper *et al.*, 1997b; Westbury *et al.*, 1996; Westbury *et al.*, 1995), although it was noted that intranasal and oral exposure resulted in more severe pulmonary lesions (Hooper *et al.*, 1997b). In guinea pigs, administration of HeV subcutaneously led to neurological signs from day 7 to 15 p.e., and was attributed to meningoencephalitis (Williamson *et al.*, 2001), while intranasal exposure induced systemic vascular disease in some animals. On the other hand, intradermal (footpad) inoculation failed to establish

infection (Hooper *et al.*, 1997b; Williamson *et al.*, 2001). In hamsters, severe respiratory disease, with dose-dependent progression to neurological signs, was observed following exposure to HeV via either parenteral or non-parenteral routes (Guillaume *et al.*, 2009; Rockx *et al.*, 2011).

In mice, Dups *et al.* (2012) were unable to confirm infection – and specifically anterograde encephalitis - in WT C57Bl6 mice after SC exposure to HeV. However, during the course of the studies in Chapter 4, Dhondt *et al.* (2013) reported lethal neurological disease in 50% of 11 week old *Ifnar1-/-* mice on a C57BL6 background following HeV exposure by the IP route. The anatomic distribution of brain lesions in these mice – specifically in the context of anterograde encephalitis - was not described. However, vasculitis was reportedly present suggesting a role for viraemia in the pathogenesis of the encephalitis. Unfortunately, the outcome of IP exposure of WT mice to HeV was not described, although they were reportedly resistant to infection by NiV. Interestingly, and in marked contrast to the findings in Chapter 4, Dhondt *et al.* (2013) found *Ifnar1-/-* mice were resistant to HeV-associated disease after IN exposure, suggesting there was a biologically significant difference in their test system to the one used in the current work.

Having observed that i) WT C57Bl6 mice are resistant to infection by HeV after parenteral (SC) exposure, including to the development of meningoencephalitis (Dups *et al.*, 2012), and ii) *Ifnar1-/-* mice are susceptible to infection (with a neurological syndrome and uncharacterised meningoencephalitis) by HeV after parenteral (IP) exposure (Dhondt *et al.*, 2013) we generated the following hypothesis: IP exposure of WT C57Bl6 and of *Ifnar1-/-*, *Ifnar2-/-* and *Stat1-/-* mice to HeV would facilitate consolidation of our earlier observations on HeV infection characteristics in IFN-signalling deficient mice, by eliminating the confounding effects of anterograde infection of the CNS. Accordingly, a further study was initiated employing the equivalent test system used in Chapter 4.

5.2 Aim and hypothesis of this experiment

5.2.1 Aim

To re-evaluate the contribution of IFN signalling in mice to their resistance to systemic disease induced by HeV infection, by assessing the degree of general clinical malaise, severity of pathology in diverse organ systems, and distribution and level of virus replication in mice deficient in IFN signalling - *Ifnar1-/-, Ifnar2-/-* and *Stat1-/-* - following IP exposure to virus.

5.2.2 Hypothesis

IP exposure will eliminate the confounding effects of anterograde infection of the CNS and facilitate the development of systemic HeV disease in *Ifnar1-/-*, *Ifnar2-/-* and *Stat1-/-* mice. WT mice are expected to be resistant to infection with HeV via the IP route.

5.3 Experimental design

Experiments were performed as two separate studies based on mouse availability, one using *Ifnar1-/-* and *Ifnar2-/-* mice (Study 1) and the other using *Stat1-/-* mice (Study 2). Each study was observational and of 21 days duration, and incorporated wild type mouse controls. Mice were of mixed gender, and were housed in groups of up to 5 mice with same sex litter-mates.

Study 1 - Five *Ifnar1-/-* and 5 *Ifnar2-/-* mice on a C57Bl6 background and 5 C57Bl6 WT mice were used in this study. Two *Ifnar1-/-* mice were 12.5 weeks old, 2 were 15.5 weeks old and 1 was 10 weeks old. The *Ifnar2-/-* and control mice (closest available age-match) were 12.5 weeks old.

Study 2 - Four *Stat1-/-* mice on a C57Bl6 background and 4 C57Bl6 WT mice were used in this study. *Stat1-/-* mice were 12.5 weeks old, while the control mice (closest available age-match) were 12 weeks old.

All mice were implanted with a subcutaneous temperature and identification chip (LifeChip with Bio-Thermo Technology, Destron Fearing) and allowed to acclimatise for 7 days prior to virus exposure. The virus inoculum was a low passage isolate from the spleen of a horse

(Hendra virus/Australia/Horse/2008/Redlands). Under general anaesthesia, mice were exposed IP to a dose of 50 000 $TCID_{50}$ HeV in saline to a volume of 300 µl. The injection site was disinfected after inoculation and monitored during recovery from anaesthesia. No leakage of inoculum was observed from the injection site.

After exposure to HeV, mice were assessed at least daily for clinical signs of disease as per the monitoring sheet shown in Chapter 2. Mice were euthanased at the end of the study period (day 21), or earlier if they had reached their predetermined humane endpoint for clinical disease as defined in Chapter 2. At post mortem samples from major organs including brain hemi-section were collected into 10% neutral buffered formalin for routine histopathology and IHC. Samples included brain hemi-section, lung, spleen, liver, kidney, bladder, reproductive tract (ovaries and uterus in female mice and testes and accessory sex glands in male mice), stomach, duodenum, jejunum, ileum, caecum and colon, pancreas, lymph nodes (parotid, cervical chain, mesenteric), adrenal glands, myocardium, thymus, trachea, oesophagus, skeletal muscle, diaphragm and femoral bone marrow.

Tissue samples from the lung, contralateral forebrain (FB), spleen, liver and kidney were also collected into viral transport media for qualitative virus re-isolation as well as RNA extraction. Blood was collected into EDTA for qualitative virus re-isolation as well as RNA extraction. 1 ml of sterile saline was gently flushed retrograde through the nasal passages from a catheter placed into the nasopharynx and collected as it dripped from the nares. This nasal wash fluid was used for qualitative virus re-isolation as well as RNA extraction.

For virus isolation each sample was tested in two wells of a 24 well plate and assessed as either positive or negative for CPE. Multiplex TaqMan reverse-transcription (RT) PCR (qPCR) targeting the HeV-N gene as well as host cell 18S rRNA was performed on extracted RNA, with HeV- N gene values normalized to host cell 18S rRNA. Samples with a mean HeV-N gene C_T value ≤ 39.6 were defined as positive for HeV RNA (Dups *et al.*, 2012).

Sera were collected both prior to virus exposure and at euthanasia and analysed for antibody responses against HeV using a Luminex microsphere HeVsG binding assay and a receptor blocking assay (Bossart *et al.*, 2007; McNabb *et al.*, 2014).

5.3.1 Assignment of infection status and infection phenotype

The primary readout for these studies was the infection phenotype that was observed in individual mice following exposure to virus. Mouse infection status was determined and then an infection phenotype was assigned according to the criteria used in Chapter 3. In summary, a mouse was defined as infected with HeV if immunohistopathology of tissue/s was positive for viral antigen, or infectious virus was re-isolated from tissues, or the serum was positive for binding antibodies against HeV $_{s}$G protein. In the case of brain, detection of viral genome in brain tissue was considered sufficient to confirm virus replication in that organ. Categories for infection phenotype comprised subclinical (no clinical signs observed during the study), systemic (exhibition of signs of general malaise with disseminated virus replication and significant pathology in major organ systems), and neurological (exhibition of signs consistent with involvement of the CNS and evidence of virus replication in brain).

5.4 Data analysis

Mice were recorded as febrile if their temperature was > 39.3 ^{o}C (in-house reference for C57Bl6 mice).

Statistical analysis was carried out using GraphPad Prism 7.02. Survival curves were conducted using log-rank tests (Mantel-Cox). Bodyweight and temperature data up to the time of first mouse euthanasia were analysed in two-way mixed ANOVAs, with time as a within-subject variable and treatment group as a between-subject variable.

Where indicated, infection rate, infection phenotype, and likelihood of virus replication in individual organs were subjected to contingency analysis (Fisher's exact test). Comparison of rates of virus replication in organs used data from mice euthanased between day 6 and day 17 p.e., prior to the time of expected virus clearance (Dups *et al.*, 2012). The exception was in the assessment of data from brain samples, where there is documented evidence of persistent replication of HeV: for this tissue, data from all mice were incorporated into any contingency analysis, irrespective of euthanasia day.

Viral genetic loads in the different tissues were log-transformed and compared by ordinary two-way ANOVAs, with tissue type and treatment group as the independent variables. Data from all mice were used for these analyses, irrespective of euthanasia day.

5.5 Results

5.5.1 Study 1

5.5.1.1 Clinical observations

The IP exposure of mice to 50 000 TCID50 HeV was well tolerated by all WT, *Ifnar1-/-* and *Ifnar2-/-* mice. The injection site was monitored during anaesthetic recovery and no leakage of inoculum was observed.

All mice with the exception of one WT mouse met the criteria for HeV infection. The WT mouse with no evidence of infection was excluded from further analysis. The remaining 4 WT mice remained clinically healthy up to the time of elective euthanasia on day 21 p.e. (Table 5.1).

Two out of 5 *Ifnar1-/-* mice (Table 5.1) reached their predetermined humane endpoint for neurological disease, similar to that recorded for IN exposed mice, and were euthanased on day 7 p.e. The remaining 3 *Ifnar1-/-* mice remained clinically healthy up to the time of elective euthanasia on day 21.

Three out of 5 *Ifnar2-/-* mice (Table 5.1) reached their predetermined humane endpoint for neurological disease, similar to that recorded for IN exposed mice, and were euthanased on days 7 or 8 p.e. The remaining 2 *Ifnar2-/-* mice remained clinically healthy up to the time of elective euthanasia on day 21.

There were no significant differences between the survival curves for the three treatment groups.

Table 5.1: Study 1, summary of data used to determine infection status

Mouse Type	Mouse ID	Euth. Day	Infection phenotype	Olfactory mucosa Ag/PCR*/VI*	Lung Ag/PCR/ VI	Forebrain Ag/PCR/VI	Spleen Ag/PCR/VI	Liver Ag/PCR/VI	Kidney Ag/PCR/VI	Blood PCR/VI	Serology Bind/Block
WT	91	21	Subclinical	-/-	-/-	-/-	+/+	-/+	-/-	-	+/-
	92	21	Subclinical	-/-	-/-	-/-	+/+	-/+	-/-	+/-	+/-
	93	21	Subclinical	-/-	-/-	-/-	-/-	-/-	-/-	-	+/-
	94	21	Subclinical	-/-	-/-	-/-	+/+	-/-	-/-	-	+/-
Ifnar1-/-	95	21	Subclinical	-/+	-/-	-/-	-/+	-/+	-/+	-	+/+
	96	7	Neurological	-/+	-/+	+/+	-/+	+/-	-/-	-	+/-
	97	21	Subclinical	-/-	-/-	-/-	-/+	+/-	-/-	-	+/+
	98	21	Subclinical	-/-	-/-	-/+	+/+	-/-	-/-	-	+/+
	99	7	Neurological	-/+	-/+	+/+ +VI	-/+	+/-	-/-	-	+/-
Ifnar2-/-	100	7	Neurological	-/+	-/+	+/+ +VI	+/+	+/-	-/-	-	na/na
	101	8	Neurological	-/-	-/-	+/+	na/+	+/-	-/-	-	+/-
	102	21	Subclinical	-/-	-/-	-/-	-/+	-/-	-/-	-	+/+
	103	21	Subclinical	-/-	-/-	+/+	+/+	-/-	-/+	+/-	+/+
	104	8	Neurological	-/-	+/+	+/+ +VI	+/+	+/-	-/-	-/-	+/-

Ag: immunohistochemical staining for viral antigen in tissue

PCR: qPCR for viral genome in tissue

VI+: virus isolation, performed on all samples, only positive sample indicated

* For olfactory mucosa PCR and VI was performed on retrograde nasal washings

"+" present

"-" not present

Euth. Day: day of euthanasia

Bind: Luminex binding assay

Blk: Luminex receptor blocking assay

na: tissue sample not available

Bodyweight data is presented in Figure 5.1. All mice gained weight at least up to day 5 p.e.. Each mouse euthanased for neurological disease started to lose weight from 72 to 24 hrs prior to euthanasia. There was no significant interaction between the effects of time and test group on bodyweight up to day 7 p.e.. There was a significant effect of time on bodyweight ($p < 0.0001$), with significantly higher mean weights on all other days compared to baseline ($p < 0.0001$). There was also a significant effect of test group on bodyweight ($p < 0.0001$), with *Ifnar2-/-* mice weighing more than *Ifnar1-/-* mice and both these groups being on average heavier than WT mice throughout the study. Two slightly older *Ifnar1-/-* mice likely contributed to the higher mean weight in this group, and the mice in the *Ifnar2-/-* mice were all males.

Figure 5.1: Study 1, combined mouse weights (grams with mean and SD) over days post infection.

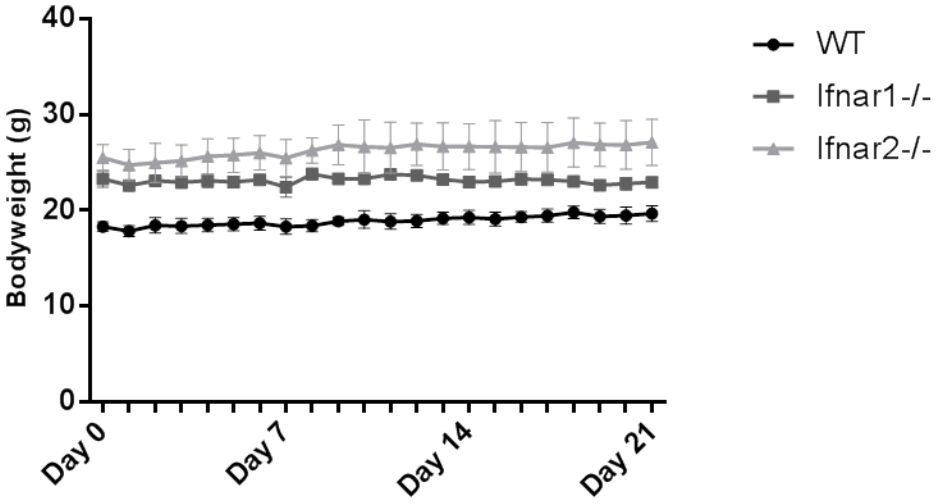

Temperature data is presented in Figure 5.2. No mouse in any test group developed a fever (T > 39.3 C^{o}) during the study. There was no significant interaction between time and test group on temperature. There was a significant effect of time on temperature (p = 0.0007), with lower temperatures on days 3, 6 and 7 p.e. compared to baseline. Environmental factors that may have impacted on temperature records derived from subcutaneous chips, including ambient room temperature and rates of air turnover, were stable over the study period. Therefore, the timing of mouse scanning in relation to disturbance of mice to conduct health checks and husbandry is most likely to have contributed to the significant effects of time on temperature. There was also a significant effect of test group on temperature from day 0 to day 7 p.e. (p = 0.0157), with slightly higher mean temperatures in WT (p = 0.0217) and *Ifnar1-/-* (p = 0.0431) mice compared to *Ifnar2-/-* mice. Interestingly, this indicated an association between higher mean temperature and lower mean body mass.

Figure 5.2: Study 1, combined mouse temperature (^{o}C with mean and SD) over days post infection.

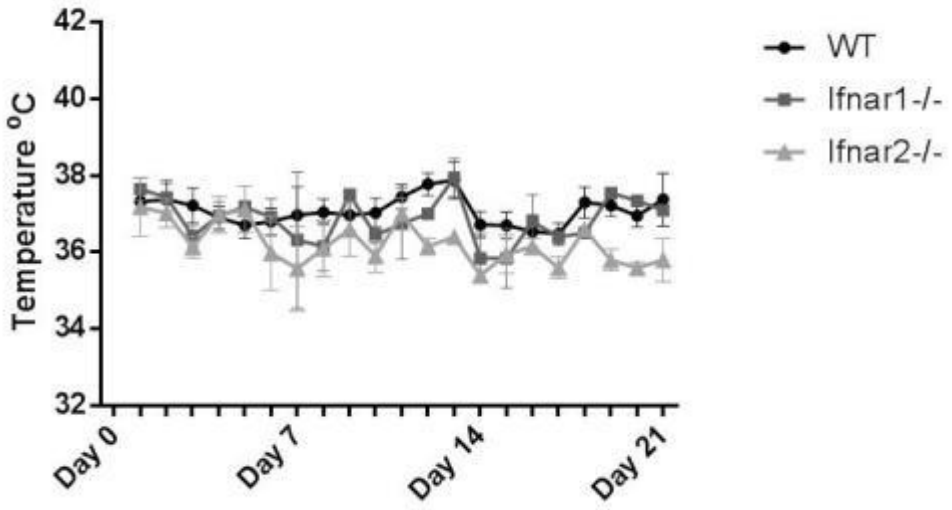

5.5.1.2 Pathology and immunohistopathology

WT mice: Few histopathological abnormalities were noted in WT mice (Table 5.2). There was no evidence of rhinitis or viral antigen deposition within the lung of any mouse.

Similarly, meningoencephalitis, or viral antigen within olfactory tract, was not seen.

Three out of 4 WT mice had HeV antigen staining within the spleen, presumed to be within macrophages, which was not associated with lymphocytolysis, necrosis, inflammation or haemorrhage (Figure 5.3).

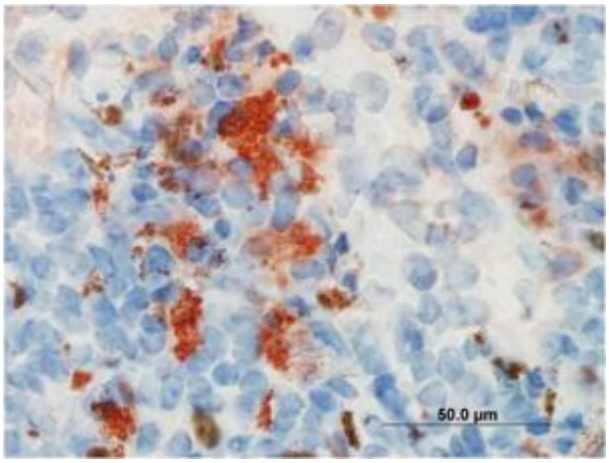

Figure 5.3: Spleen, IHC stained section from WT mice

One mouse (Mouse #93) showed a mild mononuclear cell infiltration within the mesentery associated with a hair fragment: this was attributed to foreign body introduction at inoculation.

Table 5.2: Study 1, summary of pathology findings

Mouse type	Mouse ID	Meninges Ag/les	Forebrain Ag/les	Ependyma Ag/les	Endothelium Ag/les	Olfactory epithelium Ag/les	Olfactory lymphoid tissue Ag/les	Olfactory nerve perineurium Ag/les	Olfactory regional LNs Ag/les	Lung Ag/les	Spleen Ag/les	Liver Ag/les
WT	91	-/-	-/-	-/-	-/-	-/-	-/-	-/-	-/-	-/-	+/-	-/-
	92	-/-	-/-	-/-	-/-	-/-	-/-	-/-	-/-	-/-	+/-	-/-
	93	-/-	-/-	-/-	-/-	-/-	-/-	-/-	-/-	-/-	-/-	-/-
	94	-/-	-/-	-/-	-/-	-/-	-/-	-/-	-/-	-/-	+/-	-/-
Ifnar1-/-	95	-/-	-/-	-/-	-/-	-/-	-/-	-/-	-/-	-/-	-/-	-/-
	96	-/-	+/-	-/-	+/-	-/-	+/-	-/-	-/-	-/-	-/-	+/-
	97	-/-	-/-	-/-	-/-	-/-	-/-	-/-	-/-	-/-	-/-	+/-
	98	-/-	-/-	-/-	-/-	-/-	-/-	-/-	-/-	-/-	+/-	-/-
	99	-/-	+/-	-/-	+/-	-/-	-/-	-/-	-/-	-/-	-/-	+/-
Ifnar2-/-	100	-/-	+/-	-/-	+/-	-/-	-/-	-/-	-/-	-/-	+/-	+/-
	101	-/+	+/+	-/-	+/-	-/-	-/-	-/-	-/-	-/-	NE/-	+/-
	102	-/-	-/-	+/-	-/-	-/-	-/-	-/-	-/-	-/-	-/-	-/-
	103	-/+	+/-	-/-	-/-	-/-	-/-	-/-	-/-	-/-	+/-	-/-
	104	-/+	+/-	-/-	+/-	-/-	-/-	-/-	-/-	+/-	+/-	+/-

Ag: antigen

Les: inflammatory and/or necrotising lesion

LNs: lymph nodes

NE: not examined

Ifnar1-/- mice: Rhinitis was not observed in any *Ifnar1-/-* mice. However, both mice euthanased on account of neurological disease had viral antigen within vascular endothelium, one within the nasal submucosa (as well as adjacent lymphoid tissue) (Figure 5.4) and the other within a blood vessel within the nasal cavity and adjacent to the olfactory nerve (Table 5.2). Viral antigen was not identified in the lung of any mouse.

Two of 5 mice had mild encephalitis confined to the olfactory bulb associated with deposits of viral antigen. There was a mixed inflammatory cell infiltrate which included neutrophils. Lesions were generally similar in pattern and magnitude to those reported for IN exposed *Ifnar1-/-* mice in the previous chapter, but meningitis was not identified.

One of 5 mice had HeV antigen staining in the spleen which was not associated with lymphocytolysis, necrosis, inflammation or haemorrhage. HeV antigen was also detected within the sinusoidal lining cells of the liver of 3 of 5 *Ifnar1-/-* mice similar to that seen in IN exposed interferon deficient mice in the previous chapter.

One of 5 *Ifnar1-/-* mice (Mouse #96) had strong antigen staining within the wall (including the tunica intima and the tunica media) of large vessels within the mediastinum (Figure 5.5), without evidence of vasculitis in the form of fibrinoid degeneration of the vascular wall or infiltration by inflammatory cells. Viral antigen or histological lesions were not detected within remaining tissue samples of *Ifnar1-/-* mice.

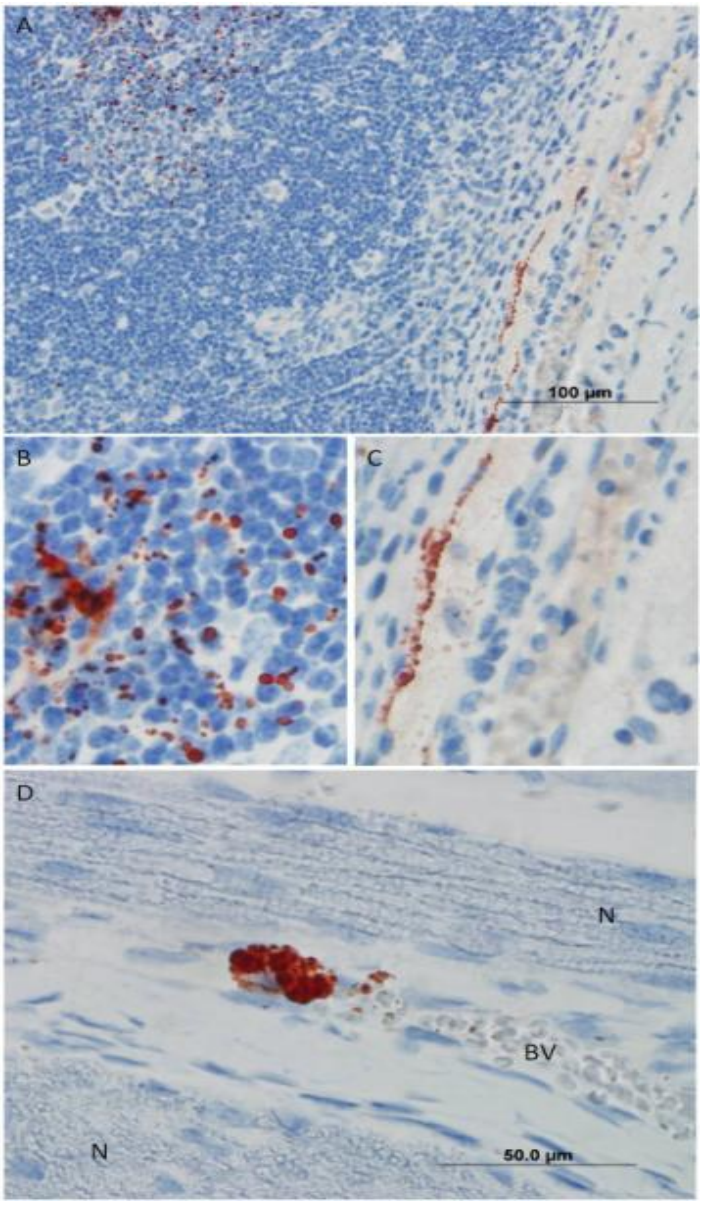

Figure 5.4: Ifnar1-/- mice. A, IHC stained section showing viral antigen within vessel endothelium in the nasal submucosa (lower right of image) and mucosal associated lymphoid tissue (upper left of image); B, higher magnification of viral antigen within the mucosal associated lymphoid tissue; C, higher magnification of viral antigen within vessel endothelium in the nasal submucosa. D, Antigen associated with a blood vessel (BV) adjacent to olfactory nerve fibres (N) within the caudal nasal submucosa.

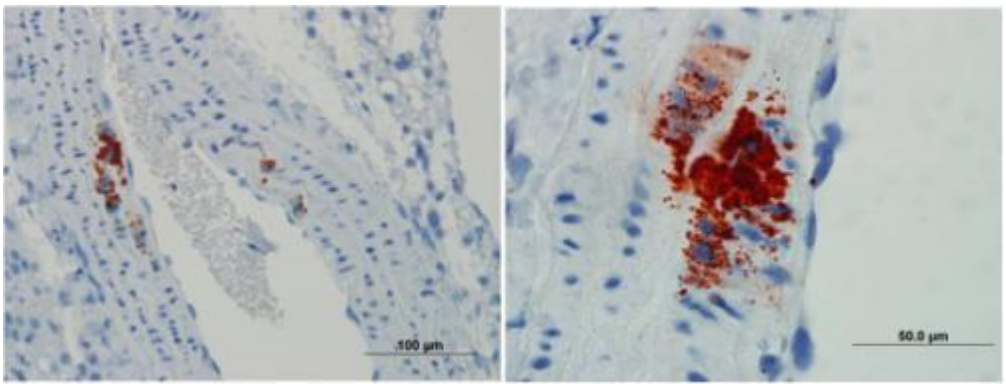

Figure 5.5: IHC stained sections of large vessels within the mediastinum showing antigen staining within the vessel walls.

Ifnar2-/- mice: There was no evidence of rhinitis in *Ifnar2-/-* mice, but viral antigen was present within the nasal submucosal endothelium of one mouse (Mouse #100). HeV antigen was identified in the alveolar walls of 1 mouse without other evidence of pneumonia.

Four out of 5 *Ifnar2-/-* mice, including the 3 mice that were euthanased with neurological signs, had viral antigen staining within the olfactory bulb, extending through the olfactory tract of 1 mouse to the piriform lobe and amygdala. This was associated with mild encephalitis with a mixed inflammatory infiltrate that included neutrophils (Table 5.2), and with mild to moderate non-suppurative meningitis in 3 of 4 mice. HeV viral antigen was also present in the cerebellum of one mouse (Mouse #100) and within ependymal cells of a mouse that remained clinically healthy to day 21 p.e..

Similar to WT mice in this study, multifocal aggregates of HeV antigen were identified within the spleen of 3 out of 5 *Ifnar2-/-* mice. The presence of viral antigen in the spleen was not associated with lymphocytolysis, necrosis, inflammation or haemorrhage. In addition, the liver of 3 of 5 *Ifnar2-/-* mice was positive for viral antigen.

Viral antigen was also present within vessel walls, including within the mediastinum and lung (Mouse #101) and testes (Mouse #104), without other evidence for vasculitis (Figure 5.6). HeV antigen or histological lesions were not detected within remaining tissue samples of *Ifnar2-/-* mice.

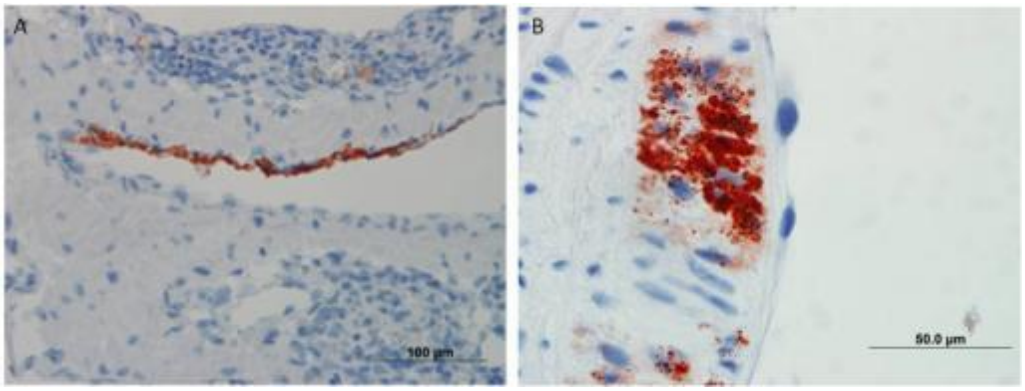

Figure 5.6: IHC stained sections of antigen staining within the walls of large vessels; A, vessel in the lung with viral antigen within the endothelium; B, vessel within the testes with viral antigen present within the tunica intima and tunica media.

5.5.1.3 Molecular virology and classical virology

Viral genome was detected in at least one tissue of all mice shown to have been infected after exposure to HeV apart from one WT mouse positive for antibody. (Data presented in Table 5.1 and Figure 5.7).

Viral genome was not detected within the forebrain of WT mice (Table 5.1). It was present in the forebrain of 3 of 5 *Ifnar1-/-* mice, including a mouse that remained clinically healthy throughout the study, and 4 of 5 *Ifnar2-/-* mice, including a mouse which had remained clinically healthy (Table 5.1). Virus was also re-isolated from the contralateral forebrain of an *Ifnar1-/-* mouse and 2 *Ifnar2-/-*mice (Table 5.1), each of which had been euthanased on account of neurological signs. Forebrain was the only tissue from which virus was re-isolated in this study.

HeV genome was not found within the nasal washings of WT mice, but was present within the nasal washings from 3 of 5 *Ifnar1-/-* mice and 1 of 5 *Ifnar2-/-* mice (Table 5.1 and Figure 5.7). There was no evidence of rhinitis in these 4 mice, viral antigen was not identified within their nasal epithelium, viral genome was not found in their blood, and no incisional incursion had occurred into the cranium at the time of nasal washing minimising the chance of cross contamination from CNS tissue). However, in 3 of the mice, viral antigen had been seen in nasal submucosal endothelium or associated lymphoid tissue. We therefore

postulate that HeV genome found within the nasal washings of these mice derived from submucosal tissue dislodged through minor trauma at the time of retrograde catheterisation of the nasopharynx.

HeV genome was not detected in the lung of WT mice, but was found in 2 out of 5 *Ifnar1-/-* mice and 2 out of 5 *Ifnar2-/-*mice.

Viral genome was present in the spleen of 3 out of 4 WT mice, all 5 *Ifnar1-/-* mice and all 5 *Ifnar2-/-* mice (Table 5.1 and Figure 5.7).

In the liver, HeV genome was detected in 2 of 4 WT mice and 1 of 5 *Ifnar1-/-* mice. Viral genome was present in the kidney of one *Ifnar1-/-* mouse and one *Ifnar2-/-* mouse (Table 5.1 and Figure 5.7) and in the blood of one WT mouse and one *Ifnar2-/-* mouse.

The overall effect of the interaction between tissue type and test group on viral genetic load was not significant, although higher mean levels of HeV genome were observed in the forebrain of both *Ifnar1-/-* mice ($p = 0.0035$) and *Ifnar2-/-* mice ($p = 0.0061$) compared to WT mice, in which it was not found. There was no significant effect of test group on overall mean viral genetic load within the tissues tested. There was a significant effect of tissue type on overall mean viral genetic load ($p < 0.0001$), namely higher mean levels in forebrain compared to liver ($p = 0.0222$), blood ($p = 0.0087$) and kidney ($p = 0.0162$) but not lung or spleen, and in spleen compared to lung ($p = 0.0121$), liver ($p = 0.0021$), blood ($p = 0.0007$) and kidney ($p = 0.0015$).

Figure 5.7: Study 1 qPCR data. Log_{10} HeV-N gene copies normalised to 18S in different organs

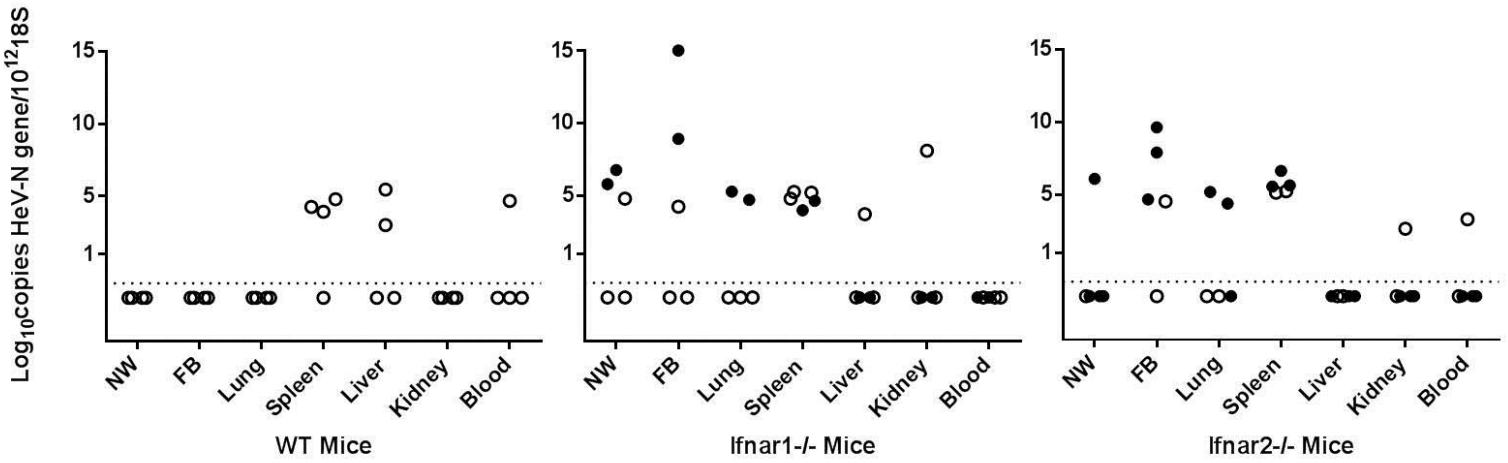

NW: Nasal wash

FB: Forebrain

Open circle: remained clinically healthy

Solid circle: showed neurological signs

Dotted line: level of assay detection

5.5.1.4 Serology

All mice tested positive for a binding antibody response. In addition, three of 5 *Ifnar1-/-* mice and 2 of 5 *Ifnar2-/-* mice developed positive antibody blocking responses (Table 5.3): all 5 of these mice had survived until day 21 p.e.

Table 5.3: Serology results for Study 1; IP HeV exposure of WT, *Ifnar1-/-* and *Ifnar2-/-* mice

	Assay		Antibody binding	Receptor blocking
Mouse type	Mouse #	Euth day	MFI Post Challenge	% Inhibition
WT	91	21	**30353**	1
	92	21	**30264**	2
	93	21	**29943**	0
	94	21	**30281**	4
Ifnar1-/-	95	21	**29547**	**13**
	96	7	**29982**	6
	97	21	**29515**	**8**
	98	21	**29650**	**38**
	99	7	**29956**	1
Ifnar2-/-	100	7	na	na
	101	8	**29997**	0
	102	21	**29845**	**24**
	103	21	**30431**	**41**
	104	8	**30581**	2
Positive controls	Horse		**28279**	**79**
	Mouse		**3980**	nd
	Rabbit NiV		**29257**	**75**

na: sample not available

Euth.: Euthanasia

Luminex binding assay: for this experiment the mean of all pre-challenge sera was 428 MFI, 1SD = 185, and therefore a positive result was defined as >983 MFI.

Luminex receptor blocking assay: the % inhibition of positive control sera was >75 %. Positive results are shown in bold.

5.5.1.5 Assignment of infection phenotype

WT mice: For infected WT mice, 4 out of 4 mice gained weight, did not develop fever, and remained clinically healthy up to the time of elective euthanasia on day 21 p.e. (Table 5.1). Three mice had virus replication confirmed in spleen, but inflammatory or necrotising lesions were not identified. Accordingly, each WT mouse was assigned a subclinical infection phenotype (Table 5.1).

Ifnar1-/- mice: Two out of 5 infected *Ifnar1-/-* mice demonstrated acute neurological disease similar to that seen in all genotypes of IN infected mice in Chapter 4. Each of these mice had virus replication confirmed in brain that was accompanied by encephalitis with an inflammatory cell infiltrate that included neutrophils. Replication of HeV was also identified in the nasal mucosal-associated lymphoid tissue, nasal mucosal vascular endothelium, and mediastinal vascular endothelium of one mouse, and the liver of both mice. However, the presence of viral antigen in these areas was not associated with pathology in the form of an inflammatory response or necrotising lesions. Neither mouse developed a febrile response following exposure to HeV, including prior to the onset of neurological signs. In one mouse, weight loss preceded the onset of neurological signs and was attributed to the developing neuropathology.

Three of 5 infected *Ifnar1-/-* mice remained clinically healthy up to the time of elective euthanasia on day 21 p.e. Virus replication was confirmed in the brain and spleen of 1 mouse and the liver of another but there was no significant pathology in the form of inflammation or necrosis (Table 5.1).

Considering the findings overall, 2 *Ifnar1-/-* mice were assigned a neurological infection phenotype and 3 *Ifnar1-/-* mice were assigned a subclinical infection phenotype (Table 5.1).

Ifnar2-/- mice: Three out of 5 infected *Ifnar2-/-* mice demonstrated acute neurological disease similar to *Ifnar1-/-* mice in the same study. Each of these mice had virus replication confirmed in brain, associated with mild encephalitis in 1 mouse and meningoencephalitis in 2 mice. In all 3 mice the inflammatory cell infiltrate included neutrophils. Replication of HeV was also identified in the lung of 1 mouse, but an associated pneumonia was not identified.

Viral replication in vascular endothelium of all 3 mice, and within the spleen of 2 mice, was not associated with significant tissue injury. None of these *Ifnar2-/-* mice developed a febrile response following exposure to HeV, including prior to the onset of neurological signs. In each of these 3 mice, weight loss immediately preceded the onset of neurological signs and was attributed to the developing neuropathology.

The remaining 2 *Ifnar2-/-* mice stayed clinically well throughout the study period. Both of these mice had virus replication confirmed in the brain. In one mouse this was confined to the anterior olfactory tract and was associated with meningoencephalitis with an inflammatory cell infiltrate that included neutrophils; this animal also replicated HeV in spleen. In the other mouse, replication occurred within the ependyma without a detectable inflammatory response.

On the basis of these findings, 3 *Ifnar2-/-* mice were assigned a neurological infection phenotype and 2 *Ifnar2-/-* mice were assigned a subclinical phenotype (Table 5.1).

Summary comments: There were no significant differences between WT, *Ifnar1-/-*and *Ifnar2-/-* mice in infection survival curves.

As the data set did not meet the criteria for valid Chi^2 calculations, two data rows (*Ifnar1-/-* and *Ifnar2-/-*) were combined in a biologically plausible manner for contingency analysis of infection rates: no significant difference was observed in the likelihood of HeV infection in WT versus interferon signalling deficient mice following IP exposure.

Similarly, two data rows (*Ifnar1-/-* and *Ifnar2-/-*) were combined for contingency analysis of infection phenotypes. On that basis, there was no statistically significant difference between the likelihood of subclinical or neurological phenotypes being assigned to WT mice or immune-deficient mice after IP exposure to HeV.

However, it was noted that a neurological phenotype was only observed in immune-deficient mice. Also, and in contrast to the findings after IN exposure, immune -deficient mice were significantly more likely than WT mice to replicate virus in brain ($p = 0.0350$), and mean levels of HeV genome were significantly higher in the forebrain of both *Ifnar1-/-* and *Ifnar2-/-* mice compared to WT mice, in which it was not found**.**

As all WT mice survived to day 21 p.e., rates of virus replication in tissues other than brain were not able to be meaningfully compared between the test groups. In respect of mean tissue viral genetic load, and in contrast to the findings in Chapter 4 after IN exposure to HeV, there was no significant difference between the spleens of WT mice compared to *Ifnar1-/-* or *Ifnar2-/-* mice.

5.5.2 Study 2

5.5.2.1 Clinical observations

The IP exposure of mice to 50 000 TCID50 HeV was well tolerated by all WT and *Stat 1-/-* mice. The injection site was monitored during anaesthetic recovery and no leakage was observed from the site.

One WT mouse and one *Stat1-/-* mouse did not meet the criteria for HeV infection and so were excluded from further analysis.

The three remaining WT mice remained clinically healthy up to the time of elective euthanasia on day 21 p.e. (Table 5.4).

The 3 remaining *Stat1-/-* mice reached their predetermined humane endpoint and were euthanased on either day 8 p.e. or 12 p.e. (Table 5.4). Two mice euthanased on day 8 p.e. had neurological signs as observed in other IN and IP exposed mice. The third mouse had lost weight on day 8 p.e., and then gained weight again until day 12 p.e., when it also appeared hunched and inactive and was euthanased.

Due to the group sizes, statistical comparison between the survival curves of the two test groups would not have been meaningful, and so was not done.

Table 5.4: Study 2, summary of data used to determine infection status

Mouse Type	Mouse ID	Euth. Day	Infection phenotype	Olfactory mucosa Ag/PCR*/ VI*	Lung Ag/PCR/VI	Forebrain Ag/PCR/VI	Spleen Ag/PCR/VI	Liver Ag/PCR/VI	Kidney Ag/PCR/VI	Blood PCR/VI	Serology Bind/Block
WT	105	21	Subclinical	-/-	-/-	+/-	+/+	-/-	-/-	-/-	+/-
	106	21	Subclinical	-/-	-/-	-/-	-/+	-/-	-/-	-/-	+/-
	107	21	Subclinical	-/-	-/-	-/-	-/+	-/-	-/+	+/-	+/-
Stat1-/-	108	12	Uncategorised	-/-	+/+	+/+	+/+	+/+	+/+	+/-	+/+
	109	8	Neurological	+/+ +VI	+/+	+/+ +VI	+/+	+/+	+/+	+/-	+/+
	110	8	Neurological	-/-	+/+	+/+ +VI	+/+	+/+	+/+	+/-	+/+

Ag: immunohistochemical staining for viral antigen in tissue

PCR: qPCR for viral genome in tissue

VI+: virus isolation performed on all samples, only positive samples are indicated above

* For olfactory mucosa PCR and VI was performed on retrograde nasal washings

"+" present

"-" not present

Euth. Day: day of euthanasia

Bind: Luminex binding assay

Blk: Luminex receptor blocking assay

Bodyweight data is presented in Figure 5.8. All mice gained weight at least up to day 5 p.e.. Each mouse euthanased for neurological disease started to lose weight from 72 to 24 hrs. prior to euthanasia. There was a significant interaction between the effects of time and test group on bodyweight (p = 0.0008) up to day 8 post-exposure to HeV: WT mice were significantly heavier than baseline on each post-exposure day apart from day 2, while *Stat1-/-* mice were significantly lighter than baseline on day 8 p.e..

Figure 5.8: Study 2, combined mouse weights (grams with mean and SD) over days post infection.

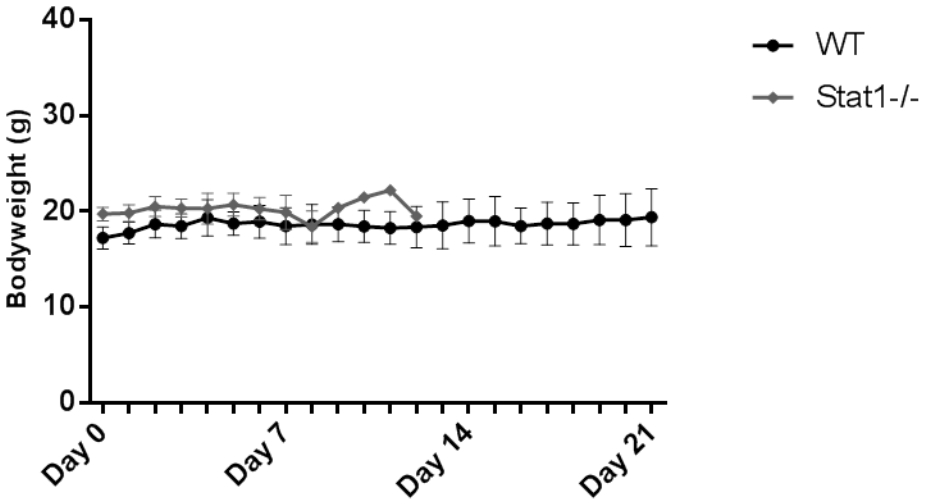

Temperature data is presented in Figure 5.9. No mouse in either test group developed a fever (T > 39.3 C^{o}) during the study. There was a significant interaction between time and test group on temperature (p = 0.0058) up to day 8 post-exposure to HeV: *Stat1-/-* mice had significantly lower temperatures on day 7 p.e. (p < 0.0001) and day 8 p.e. (p = 0.0065) compared to baseline, but a similar effect was not recorded in WT mice. This may have been attributable to pre-mortem alterations in infections associated thermoregulation in 2 of 3 *Stat1-/-* mice.

Figure 5.9: Study 2, combined mouse temperature (^{o}C with mean and SD) over days post infection

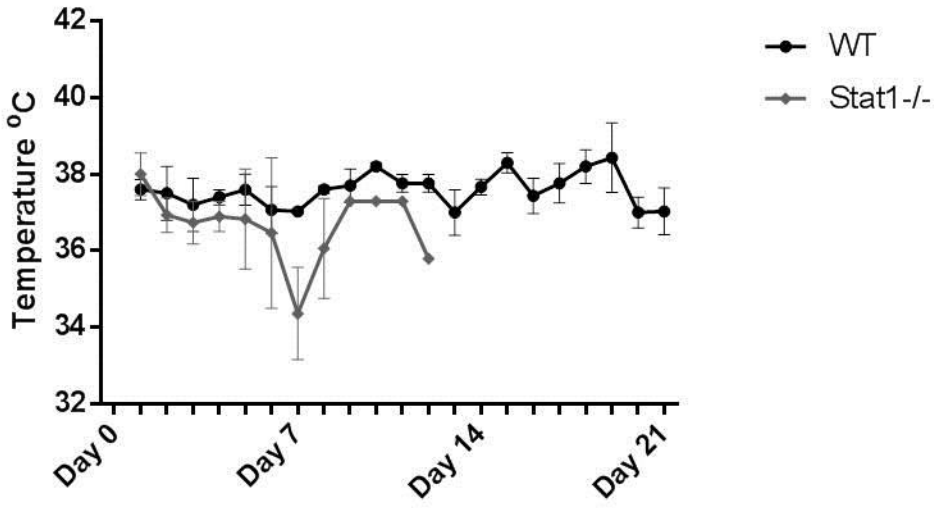

5.5.2.2 Pathology and immunohistopathology

WT mice: Few histopathological abnormalities were noted in WT mice (Table 5.5). There was no evidence of rhinitis or viral antigen deposition within the lung of any mouse. One of 3 mice had a small amount of antigen detected within the forebrain, confined to the olfactory bulb, without associated meningoencephalitis. In the same mouse, HeV antigen was detected in the spleen without lymphocytolysis, necrosis, inflammation or haemorrhage.

Table 5.5: Study 2, summary of pathology findings

Mouse type	Mouse ID	Meninges Ag/les	Forebrain Ag/les	Ependyma Ag/les	Endothelium Ag/les	Olfactory epithelium Ag/les	Olfactory lymphoid tissue Ag/les	Olfactory nerve perineurium Ag/les	Olfactory regional LNs Ag/les	Lung Ag/les	Spleen Ag/les	Liver Ag/les
WT	105	-/-	+/-	-/-	-/-	-/-	-/-	-/-	-/-	-/-	+/-	-/-
	106	-/-	-/-	-/-	-/-	-/-	-/-	-/-	-/-	-/-	-/-	-/-
	107	-/-	-/-	-/-	-/-	-/-	-/-	-/-	-/-	-/-	-/-	-/-
Stat1-/-	108	-/+	+/+	+/-	+/-	-/-	-/-	-/-	-/-	+/-	+/-	+/-
	109	+/+	+/+	-/-	+/-	-/-	-/-	-/-	-/-	+/-	+/-	+/-
	110	+/+	+/+	+/-	+/-	-/-	-/-	-/-	-/-	+/-	+/-	+/-

Ag: antigen

Les: inflammatory and/or necrotising lesion

LNs: lymph nodes

Stat1-/- mice: Rhinitis was not observed in *Stat1-/-* mice, however 1 of the 2 mice euthanased on account of neurological signs had viral antigen in nasal submucosal endothelium. Viral antigen was identified within the alveolar walls in the lung of 3 of 3 *Stat1-/-* mice, similar to that seen in IN exposed mice in the previous chapter, and without other evidence for pneumonia.

Three of 3 *Stat1-/-* mice had viral antigen staining within the forebrain that was confined to the olfactory bulb in 2 mice and extended along the olfactory tract to the piriform lobe in the third. This was associated with moderate meningoencephalitis with a mixed inflammatory cell infiltrate that included neutrophils. HeV antigen was also present within the meningeal inflammatory infiltrate in 2 of 3 mice (Table 5.5). Antigen deposits were generally extensive; 2 of 3 mice also had viral antigen in the cerebellar cortex (Figure 5.10) and adjacent white matter and, in the third mouse, HeV antigen was detected in occasional neurones throughout the brain.

In addition, and consistent with haematogenous spread of virus to CNS, viral antigen was identified within the endothelium of meningeal blood vessels, ependyma of the lateral ventricle, and in adjacent periventricular white matter of 1 mouse and the choroid plexus of another (Figure 5.11).

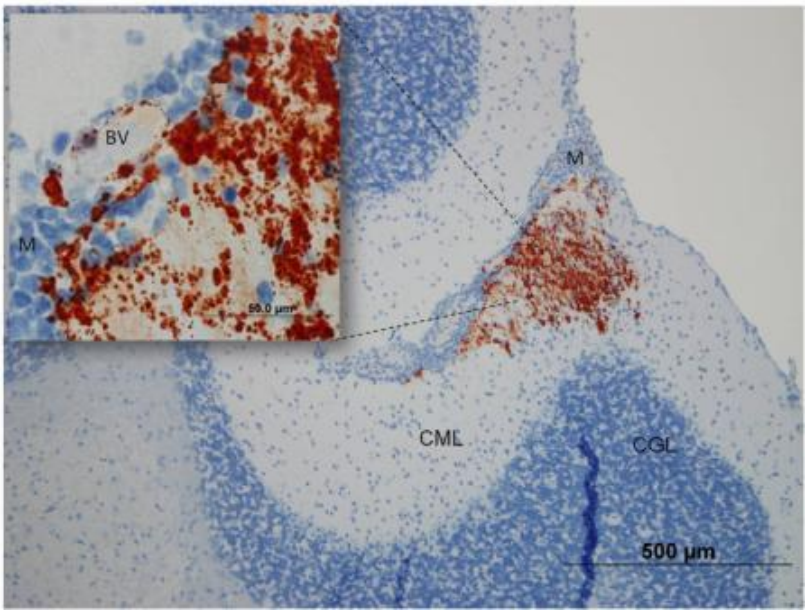

Figure 5.10: IHC stained section of the cerebellum with higher power inset; M, meninges which are thickened by a non-suppurative inflammatory infiltrate; BV, meningeal blood vessel containing viral antigen within the endothelium; CML, cerebellar molecular layer containing dense antigen staining; CGL, cerebellar granular layer.

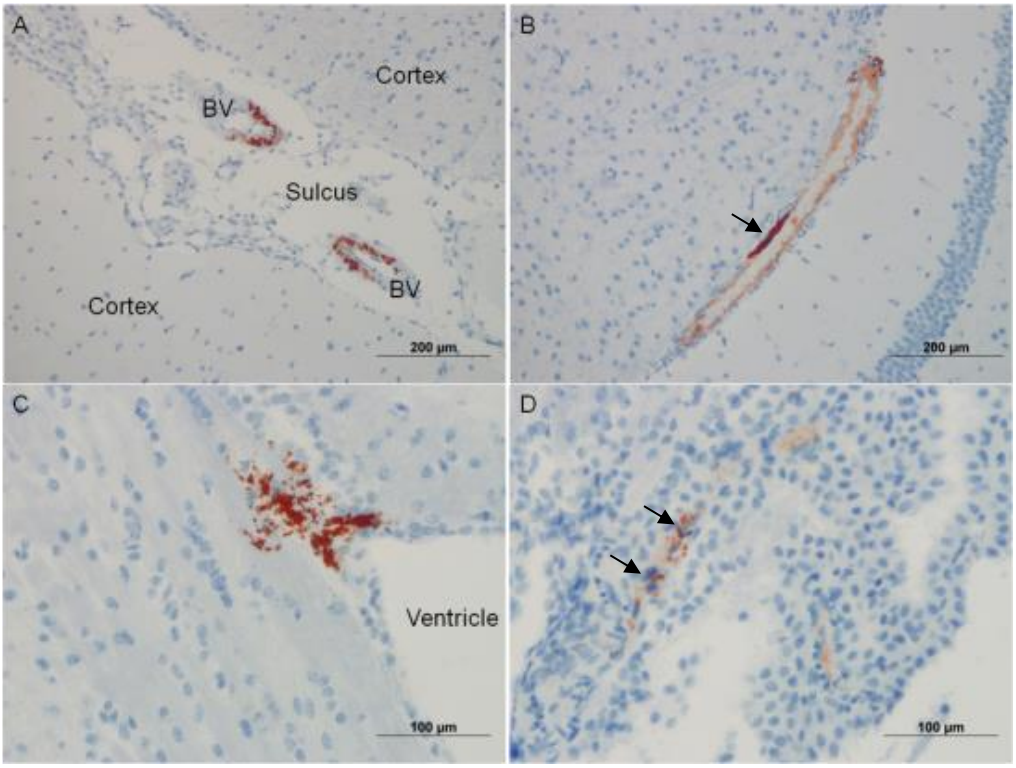

Figure 5.11: Viral antigen within the brain of *Stat1-/-* mice. A and B (arrow) within large blood vessels in the meninges; C and D associated with the ependyma, C: periventricular staining, D: choroid plexus staining (arrows).

All three *Stat1-/-* mice had HeV antigen staining in the spleen, similar to that observed in *Stat1-/-* mice in Chapter 4, which was not associated with lymphocytolysis, necrosis, inflammation or haemorrhage. HeV antigen was also detected within the sinusoidal lining cells of the liver of 3 of 3 *Stat1-/-* mice, as seen in IN exposed *Ifnar1-/-* and *Ifnar2-/-* mice in the previous chapter.

Viral antigen, without other evidence of vasculitis, was also present within the walls of blood vessels external to the CNS in 3 of 3 *Stat1-/-* mice. These were located, variously, in the mediastinum, lung, urinary bladder adventitia, adrenal gland capsular tissue, splenic hilus, and in a renal medullary vein.

One of 3 *Stat1-/-* mice had foci of viral antigen within the adrenal gland parenchyma. With the exception of the meningoencephalitis within the olfactory bulb of the forebrain, the presence of viral antigen staining in tissues and blood vessels was not associated with tissue injury in the form of necrosis, inflammation or haemorrhage.

Similar to a WT mouse in Study 1 of this Chapter, all *Stat1-/-* mice showed a mild mononuclear cell infiltration within the mesentery. In two mice, hair fragments were found embedded in inflamed areas: the mesenteric inflammation was therefore attributed to minor foreign body reaction following inoculation.

Lastly, the *Stat1-/-* mouse (Mouse # 108) that showed malaise and weight loss prior to euthanasia also had a large pleural effusion. This had the gross appearance of either a pure or modified transudate but no significant pulmonary, cardiac, hepatic or renal pathology was found. In addition to the mild mesenteric inflammation, there was a mild mononuclear cell infiltrate within the mediastinal adipose tissue and the walls of several large vessels within the mediastinum contained antigen staining (Figure 5.12). The effusion likely contributed to the clinical deterioration of the mouse that necessitated its euthanasia.

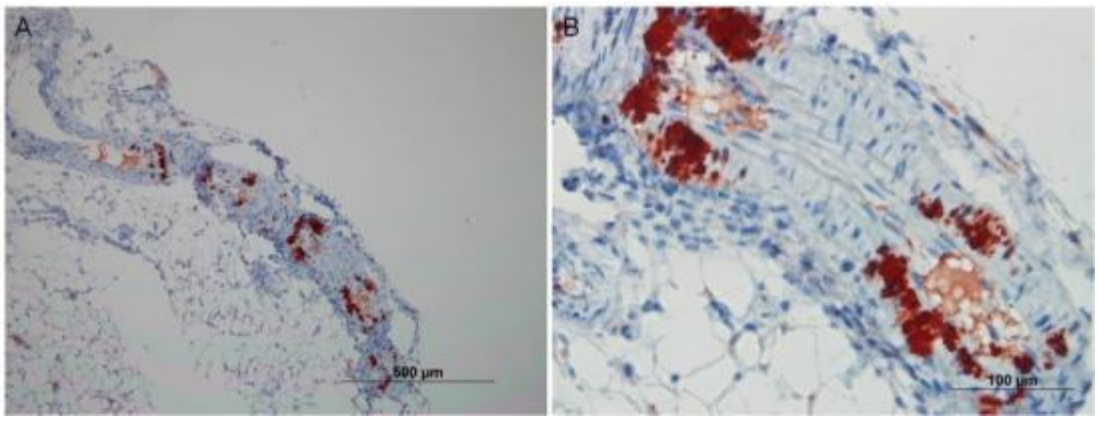

Figure 5.12: A, Mouse #108 antigen staining in a large mediastinal vessel; B, higher magnification

5.5.2.3 Molecular virology and classical virology

Viral genome was detected in at least one tissue of all mice shown to have been infected after exposure to HeV (Data presented in Table 5.5 and Figure 5.13).

Figure 5.13: Study 2 qPCR data. Log_{10} HeV-N gene copies normalised to 18S in different organs

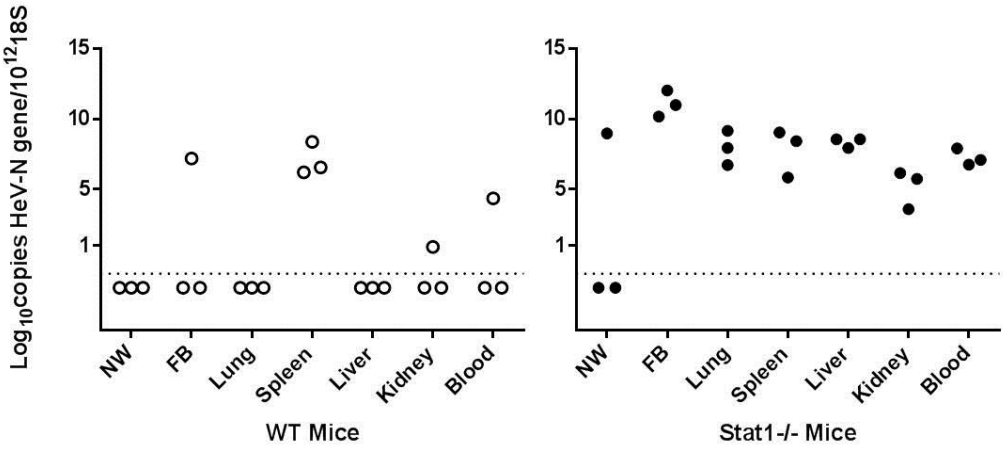

NW: Nasal wash

FB: Forebrain

Open circle: remained clinically healthy

Solid circle: showed neurological signs

Dotted line: level of assay detection

Viral genome was detected in the forebrain of one WT mouse which remained clinically healthy, and of all 3 *Stat1-/-* mice, 2 of which had been euthanased on account of neurological signs (Data presented in Table 5.5 and Figure 5.13). Virus was re-isolated from the contralateral forebrain of 2 *Stat1-/-* mice with neurological signs.

Viral genome was present within the nasal wash from one *Stat1-/-* mouse, and virus was re-isolated from the same specimen. There was no evidence of rhinitis in this mouse, viral antigen was not identified its nasal epithelium, and its CNS was intact at the time of nasal washing. However, PCR product was found in its blood and viral antigen had been seen in nasal submucosal endothelium. We therefore postulate that HeV genome found within the nasal washing of this mouse derived from blood contamination or submucosal tissue dislodged through minor trauma at the time of retrograde catheterisation of the nasopharynx.

HeV genome was detected in the lung of all 3 *Stat1-/-* mice. Viral genome was detected in the spleen of all WT mice and *Stat1-/-* mice.

HeV genome was present in the kidney and blood of 1 out of 3 WT mice, as well as the liver, kidney and blood of all 3 *Stat1-/-* mice.

The overall effect of the interaction between tissue type and test group on viral genetic load was significant ($p = 0.0028$), with higher mean levels of HeV genome observed in the forebrain ($p < 0.0001$), lung ($p < 0.0001$), liver ($p < 0.0001$), blood ($p < 0.0015$) and kidney ($p = 0.0086$) – but not the spleen - of *Stat*1-/- mice compared to WT mice. The findings are consistent with IP exposure affording increased protection against HeV genome in brain of WT mice compared to *Stat*1-/- mice. In the case of spleen, the mean genome load in WT mice surviving to day 21 p.e. remained equivalent to *Stat*1-/- mice that had been euthanased earlier: this is consistent with an increased role for viral genome in the spleen of WT mice after IP compared to IN exposure. The biological significance of the higher levels of genome in the lung, liver, blood and kidney of *Stat*1-/- mice is more difficult to interpret as, unlike WT mice, they had been euthanased during the expected peak virus replication period. There was a significant effect of test group on overall mean viral genetic load within the tissues tested ($p < 0.0001$) that was interpreted according to the significant interaction

above. There was a significant effect of tissue type on overall mean viral genetic load (p = 0.0004), that was also interpreted according to the significant interaction above.

Due to the small group sizes, a comparison between the two groups of the likelihood of virus replication in brain was not carried out. Similarly, and also because all infected WT mice survived to day 21 p.e., rates of virus replication in other tissues could not be compared between the test groups.

5.5.2.4 Serology

All WT and *Stat1-/-* mice had positive antibody binding responses (Table 5.6), and all *Stat1-/-* mice developed blocking antibody responses.

Table 5.6: Serology results from Study 2; IP exposed WT and *Stat1-/-* mice

	Assay		Antibody binding	Receptor blocking
Mouse type	Mouse #	Euth. Day	MFI Post Challenge	% Inhibition
WT	105	21	**14786**	2
	106	21	**8997**	2
	107	21	**16385**	4
Stat1-/-	108	12	**24919**	**24**
	109	8	**4944**	**32**
	110	8	**5985**	**15**
Positive controls	Horse		**28955**	**82**
	Mouse		**4905**	na
	Rabbit NiV		nd	**75**

nd: Not done

na: sample not available

Euth.: Euthanasia

Luminex binding assay: for this experiment the mean of all pre-challenge sera was 58 MFI, 1SD = 11, and therefore a positive result was defined as >90 MFI.

Positive results are shown in bold.

5.5.2.5 Assignment of infection phenotype

WT mice: all 3 infected WT mice gained weight, did not develop fever, and remained clinically healthy up to the time of elective euthanasia on day 21 p.e. (Table 5.4). One mouse had virus replication in the anterior olfactory tract without associated encephalitis or meningitis (Table 5.5), as well as virus replication in spleen without evidence for an inflammatory response.

Considering the findings overall, 3 out of 3 WT mice were assigned a subclinical infection phenotype (Table 5.4).

Stat1-/- mice: Two of 3 *Stat1-/-* mice developed an acute neurological disease similar to that seen in *Ifnar1-/-* and *Ifnar2-/-* mice in Study 1 of this Chapter. Each of these mice had virus replication confirmed in the anterior olfactory tract, accompanied by meningoencephalitis with a mixed inflammatory cell infiltrate that included neutrophils. Viral antigen was identified within the meningitic lesions. Virus replication was also confirmed in the nasal submucosal endothelium of 1 mouse and in the lung of these 2 *Stat1-/-* mice, but an associated pneumonia was not identified.

Virus replication was also confirmed in the spleen, vascular endothelium, liver and kidney of the 2 *Stat1-/-* mice that showed neurological disease, consistent with HeV viraemia. However, apart from meningoencephalitis, the presence of HeV antigen in tissues was not associated with significant pathology in the form of an inflammatory response or necrotizing lesions.

Both mice showed weight loss from up to 72 hours prior to the onset of neurological signs but this was not accompanied by a febrile response in either mouse. The loss of weight was therefore attributed to the developing neuropathology.

One of 3 *Stat1-/-* mice was euthanased on account of weight loss (without fever), combined with marked inactivity but no distinct neurological signs. It had virus replication confirmed in the anterior olfactory tract, accompanied by meningoencephalitis similar to that seen in the other *Stat1-/-* mice. Virus replication was also confirmed in lung, spleen, liver and kidney,

but this was not associated with significant pathology in the form of an inflammatory response or necrotizing lesions. Clinical deterioration of this animal was attributed to the pleural effusion found at post mortem examination. The aetiology of the effusion is unclear, but one possibility is localised sub-microscopic vascular injury associated with viral replication in large mediastinal vessels.

Considering these findings overall, 2 out of 3 *Stat1-/-* mice were assigned a neurological infection phenotype. The remaining Stat1-/- mouse was not able to be assigned to either a neurological, systemic or subclinical phenotype. Importantly, however, sufficient time was considered to have passed post-exposure for expression of a systemic phenotype (as defined) if this was going to occur.

Due to the small group sizes, comparisons between the incidences of phenotypes observed could not be carried out.

5.6 Discussion

The aim of the studies in this chapter was to further evaluate the contribution of IFN signalling to the resistance of mice to systemic disease induced by HeV infection, by assessing the impact of IP HeV exposure in *Ifnar1-/-, Ifnar2-/-* and *Stat1-/-* compared to WT mice. Following IP exposure to HeV, clinical observations including bodyweight and temperature were recorded for up to 21 days, tissue distribution and levels of virus replication were assessed, the severity of pathology in diverse organ systems was evaluated, and an infection phenotype was assigned to each mouse. Group survival curves were also compared for WT, *Ifnar1-/-* and *Ifnar2-/-* mice.

Findings from the previous chapter, involving IN HeV exposure of WT, *Ifnar1-/-, Ifnar2-/-* and *Stat1-/-* mice, supported an increased role for viraemia in the characteristics of HeV infection of immune-deficient mice compared to WT mice. This was manifest as increased likelihood of HeV replication in spleen, higher viral genomic loads in spleen, re-isolation of virus from some spleen samples, as well as evidence for HeV replication in liver, ependymal cells and vascular endothelium. However, a systemic infection phenotype was not recorded: specifically, neither vasculitis nor necrotising lesions were identified within infected viscera. Significant pathological lesions in *Ifnar1-/-* and *Ifnar2-/-* and *Stat 1-/-* mice

were confined to the forebrain and olfactory mucosa. These were consistent with anterograde neurological infection via olfactory sensory neurones as previously reported in WT mice (Dups *et al.*, 2012) and also seen in WT mice in Chapter 3 and Chapter 4, and the role of viraemia in neuropathogenesis in INF-signalling deficient mice was difficult to delineate. It was also postulated that the neurological syndrome necessitating prompt euthanasia may have prevented full expression of systemic HeV infection in INF-signalling deficient mice following IN exposure.

Although WT mice were resistant to infection by HeV after parenteral (SC) exposure (Dups *et al.*, 2012), this chapter showed that WT mice may be reliably infected with by HeV via the IP route, with each mouse developing a subclinical infection phenotype. It was therefore confirmed that the IP exposure model was an effective way to reduce the likelihood of neurological disease via anterograde HeV infection, and the associated complication to evaluation of systemic infection studies in mice. Although viral antigen was identified in the anterior olfactory tract of one WT mouse, it was considered unlikely that CNS infection had occurred directly via intranasal exposure. Measures were taken to minimise this risk at the time of inoculation, including disinfection of the injection site and monitoring it for leakage. Moreover, it is already known that viraemia is an occasional feature of HeV infection in WT mice (Chapter 4) and that there are precedents for the olfactory bulb being a preferred site of establishment of viral infection in the mouse CNS following parenteral exposure (Brown *et al.*, 2007; Charles *et al.*, 1995; Honnold *et al.*, 2015; Monath *et al.*, 1983; Winkler *et al.*, 2015).

This last point is particularly relevant to interpretation of the findings in IFN-signalling mice within the current Chapter, and so will be expanded upon further here. After parenteral exposure, viruses from diverse genera use the olfactory tract as a conduit to CNS infection including Vesicular stomatitis virus, Rabies virus, Japanese encephalitis virus, Eastern equine encephalitis virus, and Venezuelan equine encephalitis virus, West Nile virus, Chikungunya virus, La Crosse virus, Mouse hepatitis virus, bunyaviruses, and other paramyxoviruses including Canine distemper virus and Measles virus (Brown *et al.*, 2007; Charles *et al.*, 1995; Honnold *et al.*, 2015; Kalinke *et al.*, 2011; Monath *et al.*, 1983; Winkler *et al.*, 2015). Olfactory sensory neurones are not protected by the blood brain barrier. Cytoplasmic extensions of olfactory sensory neurons are in direct contact with the extracellular fluid in

the nasal mucosa. The nerve axons cross the neuro-epithelial basement membrane and traverse the submucosa, which is highly vascularised with conventional fenestrated capillaries (from which viruses may egress), before traversing foramina of the cribriform plate as olfactory nerves and terminating in the olfactory bulb via the CSF of the arachnoid (Kalinke *et al.*, 2011). A detailed study in hamsters of St Louis encephalitis virus infection showed that the olfactory pathway was the initial site of infection of the CNS after IP or SC exposure (Monath *et al.*, 1983). This followed brief and low level viraemia, localisation of infection to Bowman's glands of the nasal submucosa, and subsequent shedding of virus in nasal secretions: this mechanism is not equivalent to primary anterograde infection from the inoculum. Using the murine model of La Crosse virus, Winkler *et al.* (2015) also proposed a further mechanism: they confirmed that infection of and transport along olfactory sensory neurones occurred in IN but not IP exposed animals. Rather, following IP exposure, cytoskeletal rearrangements in capillary endothelial cells specific to the olfactory bulb resulted in localised disruption of the blood brain barrier (BBB) allowing haematogenous passage of virus into this area of the CNS.

Also in contrast to WT mice in Chapters 3 and 4, IP exposure enhanced the role of viraemia in HeV infection of WT mice, manifest as replication of virus in spleen and viral genomic loads in spleen that were comparable to IFN-signalling deficient mice. The IP route of exposure facilitates access to the systemic circulation compared to the IN and the SC route. This may result from direct infection of the mesothelium over a wide surface area with access to adjacent and plentiful capillary endothelium (Lundstrom, 2003) or absorption of non-soluble particulate matter through lymphatic drainage across the diaphragm into retrosternal and mediastinal lymphatic trunks to mediastinal lymph nodes and then, via lymphatic ducts, back into the systemic circulation (Barrett *et al.*, 1991). The latter route may have been more contributory in the mice in these experiments as there was no evidence for viral antigen associated with mesothelium.

This chapter showed that *Ifnar1-/-* and *Ifnar2-/-* and *Stat 1-/-* mice were also reliably infected with HeV via the IP route but, in contrast to WT mice, regularly developed CNS infection with clinical neurological disease. The neurological syndrome in *Ifnar1-/-* mice was similar to that reported by Dhondt *et al.* (2013) after IP HeV infection, as well as in Chapters 3 and 4 after IN exposure. Similar findings were recorded for *Ifnar2-/-* and *Stat 1-/-* mice,

and represent a new contribution to the literature. The anterior olfactory tract remained the preferred site of HeV replication within the CNS of IFN-signalling deficient mice following IP infection. As discussed above, inadvertent IN exposure to inoculum was unlikely to account for this as measures had been taken to minimise the risk and a neurological syndrome was not seen in WT mouse controls. Additionally, and unlike Chapter 4, there was no evidence of rhinitis or perineurial olfactory inflammation in IFN-signalling deficient mice euthanased for acute neurological disease, which further supported the absence of anterograde infection by inoculum.

On the other hand, and similar to Chapter 4, there was ample evidence for HeV viraemia in these mice, in the form of viral replication in spleen, liver, ependymal cells, and also vascular endothelium including meningeal blood vessels. In particular, several IFN-signalling deficient mice had HeV antigen within the endothelium of vessels in the nasal submucosa, an observation also made in the HeV-infected ferret and horse, and attributed to relocalisation of virus to nasal mucosal endothelium following viraemia (Clayton *et al.*, 2012; Marsh *et al.*, 2011). As for *Ifnar1-/-, Ifnar2-/-, Stat1-/-* and also WT mice in Chapter 4, the inconsistent recovery of viral genome or live virus from the blood of IFN-signalling deficient mice euthanased at humane endpoint suggests that the viraemic phase after IP exposure is brief.

It is not discernible from the studies in this Chapter alone which mechanism/s account for the development of neurological infection and disease in IFN-signalling deficient mice but not WT mice after IP inoculation of HeV. It may be they have increased vulnerability to endothelial infection compared to WT mice, with possible subsequent extension via interstitial fluid to re-localisation in olfactory sensory neurones. It is also possible that there are alterations in capillary permeability within the olfactory bulb of infected IFN-signalling deficient mice permitting direct haematogenous infection localised to this anatomical site, as proposed by Winkler *et al.* (Winkler *et al.*, 2015) for a different murine infection model. A time course study combining confocal fluorescent imaging and electron microscopy, incorporating the techniques of Winkler *et al.* (2015) and Rockx *et al.* (2011) to assess vascular permeability and integrity of the BBB, would be required to investigate the mechanism of HeV infection of the olfactory bulb following IP exposure.

The infection characteristics of HeV in WT mice exposed IP indicated an increased role for viraemia compared to exposure IN. However, in IFN-signalling deficient mice, the characteristics of systemic infection after IP exposure were generally similar to those observed in Chapter 4 where virus had been given IN, including more evidence for viral replication in endothelium compared to within-study WT mice. The exception was reduced evidence for virus replication in lung in *Ifnar1-/-* and *Ifnar2-/-*mouse strains, which was attributed to the IP exposure route. Sufficient viraemia was present in Stat1-/- mice to drive pulmonary replication, consistent with the enhanced susceptibility to viral disease seen in this strain (Durbin *et al.*, 2002; Hofer *et al.*, 2012; Karst *et al.*, 2003; Pasieka *et al.*, 2008; Raymond *et al.*, 2011; Zornetzer *et al.*, 2010).

Also similarly to the outcomes in Chapter 4, HeV infection of IFN-signalling deficient mice was not associated with a significant increase in body temperature or loss of body weight (other than prior to euthanasia for neurological disease) consistent with minimal constitutional impact of infection across all test groups. Apart from meningoencephalitis associated with the olfactory pathways, HeV replication in tissues of these mice was not associated with detectable tissue injury or associated inflammatory response, even in the walls of infected blood vessels. Therefore, a systemic infection phenotype did not feature in mice in these experiments, even when opportunity for its expression had been optimised by IP exposure.

Overall the hypothesis "IP exposure will eliminate the confounding effects of anterograde infection of the CNS and facilitate the development of systemic HeV disease in *Ifnar1-/-*, *Ifnar2-/-* and *Stat1-/-* mice and WT mice are expected to be resistant to infection with HeV via the IP route" was disproven; firstly the characteristics of systemic infection seen after IP exposure in interferon signalling deficient mice were generally similar to those observed following IN exposure, and secondly, WT mice may be reliably infected with by HeV via the IP route. IP exposure actually enhanced the role of viraemia in HeV infection of WT mice.

The findings above contrast to the outcome of parenteral routes of exposure to HeV infection in other species, where fulminating systemic infection is regularly seen. These have been described in depth for hamsters, cats and guinea pigs and in comparison to IN exposure. HeV replication in IP infected hamsters resulted in severe disease manifest as

marked weight loss, and dose-dependent respiratory and/or neurological signs (Guillaume *et al.*, 2009; Rockx *et al.*, 2011). Viral genome was present in all tissues examined, and virus was re-isolated from multiple tissues including brain, lung heart, kidney, spleen, liver, spinal cord and bladder (Guillaume et al., 2009). Significantly, pneumonia, fibrinoid necrosis of blood vessels, and endothelial syncytia were also identified as well as necrotic plaques in the brain.

Cats also succumbed to parenteral routes of exposure with a similar disease course as observed after exposure by non-parenteral routes, including depression, fever, and increased respiratory rate with rapid progression to humane endpoint or death (Hooper *et al.*, 1997b; Westbury *et al.*, 1996; Westbury *et al.*, 1995). After SC exposure HeV was re-isolated from the trachea, lung, pleural fluid, liver, spleen, kidney, lymph nodes, rectum, brain, and urine (Hooper *et al.*, 1997b; Westbury *et al.*, 1996). Associated histological lesions included pulmonary haemorrhage and oedema, alveolar wall necrosis, necrosis and haemorrhage within the kidneys, and necrotic and haemorrhagic lymph nodes with numerous pyknotic and karyolytic lymphocytes. There was also widespread fibrinoid necrosis of vessels and endothelial syncytial cells were also present.

HeV infection in Guinea pigs is commonly subclinical but may result in respiratory or neurological signs. When inoculated SC they succumbed to neurological disease with lesions of meningoencephalitis (Williamson *et al.*, 2001) or with respiratory distress due to pneumonia (Westbury *et al.*, 1995) which was also associated with systemic vascular degeneration, endothelial syncytial cell formation, and thrombosis, as reported in humans, ferrets and cats (Hooper *et al.*, 1997b). Interestingly, the affected vessels in the guinea pig were larger, reported as 20 to 80 µm in diameter, than the microvascular predominance seen in other animals (Hooper *et al.*, 1997b), and this was proposed as an explanation for the lack of pulmonary oedema observed (Hooper *et al.*, 2001). Replication within the tunica media of larger vessels shares similarity to the findings in some IFN-signalling deficient mice in this study.

Additional important contrasts were observed between the findings of the current Chapter and the conclusions drawn by Dhondt *et al.* (2013). Dhondt *et al*. reported that *Ifnar1-/-* mice were resistant to HeV infection following IN exposure. However, HeV genome was

present in brain, lung, spleen, and liver and – importantly – neutralising antibody had developed in most of their mice by the time of euthanasia at 21 days p.e. Thus, applying the definition of infection used in this thesis to Dhondt *et al's* work, the finding of either genome within the brain and/or antibody to HeV would have confirmed their mice had reliably been infected via both IN and IP routes of exposure. This apparent discrepancy between experimental outcomes highlights the importance of clearly distinguishing between - and also defining - the terms "exposure", "infection", and "disease" in such studies.

Dhondt *et al.* (2013) also reported vasculitis in *Ifnar1-/-* mice after (inferred) IP exposure to HeV. However the essential diagnostic features of vasculitis, namely the "presence of inflammatory cells within and around the blood vessel wall with concomitant vessel wall damage as indicated by fibrin deposition, collagen degeneration, and necrosis of endothelial and smooth muscle cells" (Maxie *et al.*, 2007), are not well demonstrated within the images of brain and lung that were provided in support of this statement. Unfortunately, in spite of earlier publications in mice (Dups *et al.*, 2012) and hamsters (Munster *et al.*, 2012), no description was provided of the anatomical distribution of HeV in the brain, specifically in relation to involvement of the olfactory pathway and its role in HeV neuropathogenesis in the mouse.

In summary, it is defensible to conclude from the data presented by Dhondt *et al.* (2013) that IP exposure of *Ifnar1-/-* mice to HeV generated only a neurological or subclinical infection phenotype but not systemic disease, while IN exposure led to subclinical infection. The key distinction between the findings of this Chapter and those reported by Dhondt *et al.* (2013) then becomes the observation of susceptibility of IFN-signalling deficient mice to neurological disease after IN exposure (Chapter 4). Failure to induce a similar outcome in their work is critical to the main conclusion of Dhondt *et al.* (2013) that "Type 1 interferon signaling protects mice from lethal henipavirus infection".

The different findings between this study and that of Dhondt *et al.* (2013) may be attributable to several factors. Firstly, biological differences may occur within mouse subtype: *Ifnar1-/-* mouse strains used in both laboratories were generated as null mutations for the *Ifnar1* receptor on a C57Bl/6 background but this does not ensure they are exactly

the same mice. Once a colony is maintained separately from an existing colony for 20 or more generations it becomes a new C57Bl/6 substrain, for example C57Bl/6J versus C57Bl/6N mice (Jackson Laboratory, 2016) between which phenotypical and immunological differences are documented.

There may also be a difference in virus exposure technique, as an effect of volume on enhancement of IN infection has been postulated (Rockx *et al.*, 2011). However, in this instance the volume for IN experiments cited by Dhondt *et al.* (2013) was the same as used here. Technique such as the positioning of the mouse, and time taken to instil the dose, could also feasibly change outcomes by influencing exposure time over the olfactory mucosa. As shown in Chapter 3, the incidence of HeV infection in WT mice was dose dependent but the disease phenotype expressed was not. However, it is possible that exposure dose may influence the infection phenotype in *Ifnar1-/-* mice, although it is difficult to directly compare challenge doses in PFU (Dhondt *et al.*, 2013) with $TCID_{50}$ used here. In addition, there may be an impact of viral strain on the susceptibility of *Ifnar1-/-* mice to the development of HeV associated neurological disease, as well as on the extent of expression of any systemic infection.

Overall, the study findings for the present chapter provide support to the conclusions of Chapter 4 that the resistance of WT mice to widespread HeV replication and fulminating systemic disease may not be attributed solely to the efficacy of mouse interferon signalling pathways against HeV-mediated anti-interferon mechanisms. However, to further explore a key difference between these findings and those reported by Dhondt *et al.* (2013) it will be necessary to investigate the outcomes of exposure of *Ifnar1-/-* mice to specific isolates of HeV under the relevant study condition. This will be undertaken in the following Chapter 6.

The failure to establish systemic HeV-associated disease in WT mice continues to apply even in mice deficient in the main antiviral innate immune system components of the IFN type 1 response alone (*Ifnar1-/-* and *Ifnar2-/-* mice) or with attenuation of type 1, 2 and 3 IFN responses combined (*Stat1-/-* mice). Cell fusion is important in the perpetuation of cell to cell infection with HeV, and cell fusion induces disruption of cellular architecture and contributes to organ pathology (Wong & Ong, 2011). The absence of syncytial cell development in HeV infected mice is a strikingly different feature of the infection pathology

compared to other susceptible species such as humans, non-human primates, ferrets, cats and horses. Thus an important question arises as to whether the fusion process in mice may be more effectively antagonised by other innate immune proteins in comparison to other species. One such family of interest is the Interferon induced transmembrane (IFITM) proteins. These are a family of antiviral restriction factors that both restrict viral entry and inhibit the production of infectious virions, and they have a high basal level of expression in respiratory epithelial cells as part of the innate barrier defence mechanism. IFITM1, 2 and 3 restrict viral membrane fusion induced by all three classes of viral fusion protein, and a diverse range of enveloped viruses are inhibited by IFITM proteins: the effect of IFITM proteins on HeV replication is the subject of Chapter 7.

CHAPTER 6: INTRANASAL EXPOSURE OF WILD TYPE AND IFNAR1-/- MICE TO HENDRA VIRUS/AUSTRALIA/HORSE/2008/REDLANDS OR HENDRA VIRUS/AUSTRALIA/HORSE/1994/HENDRA FAILED TO CONFIRM VIRAL STRAIN-DEPENDENT VARIATION IN PATHOGENICITY

6.1 Introduction and background

Previous thesis chapters have described the outcome HeV infection in WT and IFN-signalling deficient mice following IN and IP exposure, using Hendra virus/Australia/horse/2008/Redlands, GenBank accession no. HM044317. Exposure IN regularly resulted in rhinitis and anterograde encephalitis in both WT and IFN-signalling deficient mice. In WT mice, the neuropathogenesis was consistent with anterograde infection via olfactory sensory neurones as previously proposed Dups *et al.* (2012). In *Ifnar1-/-* and *Ifnar2-/-* and *Stat 1-/-* mice, there was evidence for an additional contribution from the haematogenous route. No mouse developed systemic infection characterised by disseminated virus replication with significant pathology in other major organ systems. Using the IP route, WT mice were reliably infected with HeV and developed subclinical infection, including virus replication within the spleen. *Ifnar1-/-* and *Ifnar2-/-* and *Stat 1-/-* mice were also reliably infected with HeV via the IP route and, in contrast to the WT mice controls, also regularly developed CNS infection. The neurological disease seen in *Ifnar1-/-*, *Ifnar2-/-*, and *Stat1-/-* mice after IP exposure was clinically and pathologically indistinguishable from that seen in IFN-signalling deficient mice following IN exposure. However, in contrast to IN exposure, IP-exposed IFN-signalling deficient mice that were euthanased on account of neurological disease did not show rhinitis. Overall, the pattern of HeV viral replication was similar in each strain (*Ifnar1-/-*, *Ifnar2-/-*, and *Stat1-/-*) of IFN-signalling deficient mice and, as for IN exposure, no mouse developed systemic infection characterised by disseminated virus replication with significant pathology in other major organ systems.

In contrast to the findings above, review of the data presented by Dhondt *et al.* (2013) led to the conclusion that in their work IN exposure of *Ifnar1-/-* mice to HeV had reliably induced a subclinical but not a neurological infection phenotype: findings in WT mice were

not reported. It was also concluded that the HeV isolate used by Dhondt *et al.* (2013) had most likely been derived from the original field outbreak of 1994, as this is the only HeV isolate that has been exported from Australia to other laboratories (A. Hill CSIRO AAHL, personal communication). The findings of Dhondt *et al.* (2013) following IP exposure of mice to HeV were similar to those of Chapter 5 for WT and *Ifnar1-/-* mice, namely subclinical infection of WT mice and either a subclinical or neurological infection phenotype in *Ifnar1-/-* mice.

The conclusion (considered erroneous by this author) of Dhondt *et al.* (2013) that their *Ifnar1-/-* mice had not been infected by HeV IN, and with no data from WT mice exposed IN, permitted this exposure route to be dismissed in the evaluation of IFN-signalling in suppression of HeV disease in mice. Importantly, the observation of lethal encephalitis in *Ifnar1-/-* - but not WT mice - exposed IP then emerged as the basis for the overarching assertion that "Type 1 interferon signaling protects mice from lethal henipavirus infection". This conclusion is at odds with the findings so far in this thesis, which show that lethal infection occurs in both IFN-signalling deficient mice and WT mice exposed IN, with the associated pathology limited to the nasal cavity and CNS. Moreover, the findings of Chapters 4 and 5 also confirm that widespread HeV replication, associated pathology, and fulminating systemic disease is not found in any mouse strain studied using IN or IP exposure.

As mentioned in Chapter 5, one variable that may account for the different finding of Dhondt *et al.* (2013) of only subclinical infection in *Ifnar1-/-* mice exposed IN - as opposed to neurological disease as well - is viral strain variation. There is a precedent for viral strain contributing to different infection outcomes in outbred mammalian species with intact immune systems, including after exposure to the closely related NiV. Infection with NiV in humans can cause both neurological and respiratory signs, however more acute respiratory distress and a higher fatality rate is seen in human patients infected with the Bangladesh strain (NiV-B) compared with the Malaysian outbreak strain (NiV-M), where predominant signs related to the nervous system (Hossain *et al.*, 2008). Additionally, human to human transmission is frequently seen in cases of NiV-B infection but is very rare in cases of NiV-M infection (Luby & Gurley, 2012).

Studies comparing pathogenesis and tissue tropism of these two viruses have been performed in hamsters and ferrets (Clayton *et al.*, 2012; DeBuysscher *et al.*, 2013). In hamsters, NiV-M showed accelerated progression with regard to time to death, virus replication, pathology and immune responses in comparison to NiV-B. However both viruses resulted in respiratory disease with pneumonia and vasculitis and/or neurological dysfunction in a dose dependent manner (DeBuysscher *et al.*, 2013). In ferrets there were no differences detected in tissue distribution or severity of lesions between the two viral strains, although Clayton *et al.* (2012) showed that the level of viral genome within oral secretions was higher with NiV-B than NiV-M.

In the case of horses, field infection with HeV may be associated with a rapidly progressive febrile illness culminating in fulminating respiratory disease (Rogers *et al.*, 1996; Selvey *et al.*, 1995; Williamson *et al.*, 1998) or be predominantly characterised by neurological signs (Field *et al.*, 2010). As yet, the different clinical presentations have not been attributable to the genetic makeup of the HeV isolates. Analysis of the sequences of HeV spill-over isolates by Marsh *et al.* (2010) demonstrated very high conservation in both amino acids and nucleotide sequences. All isolates had identical genome lengths of 18, 234 nucleotides and sequence variation across the full genome was <1%.

In view of the key role of encephalitis in HeV infection of both people and horses, it was decided to compare the outcome of exposure to HeV/Australia/horse/2008/Redlands, GenBank accession no HM044317, and the earlier HeV/Australia/Horse/1994/Hendra, GenBank accession no AF017149 in WT and *Ifnar1-/-* mice. The aim was to further validate the possibility that there may be an effect of HeV strain on the susceptibility of *Ifnar1-/-* mice to neurological disease following IN exposure. Identification of an immune-deficient mouse model that was relatively protected from developing anterograde encephalitis may be of value for further study of the mechanisms enhancing susceptibility of the brain to HeV-induced inflammation. The study employed the equivalent test system used in Chapter 4.

6.2 Aim and hypothesis of this experiment

6.2.1 Aim

To compare the infection characteristics following IN exposure of WT and *Ifnar1-/-* mice to HeV/Australia/Horse/2008/Redlands and HeV/Australia/Horse/1994/Hendra in to determine whether any observed differences in infection outcomes are attributable to the strain of virus.

6.2.2 Hypothesis

No differences in outcome will be seen between infections of the two different strains of Hendra virus

6.3 Experimental design

This experiment was performed as an observational study of 21 days duration. There were 4 test groups, each comprising 5 mice. Mice were of mixed gender, and were housed in groups of up to 5 mice with same sex litter-mates. *Ifnar1-/-* mice were 10.5 to 11 weeks old, while the WT mice (closest available age-match) were 12 weeks old.

All mice were implanted with a subcutaneous temperature and identification chip (LifeChip with Bio-Thermo Technology, Destron Fearing) and allowed to acclimatise for 7 days prior to virus exposure. The virus inoculums were an isolate of Hendra virus/Australia/Horse/2008/Redlands GenBank accession no. HM044317 (Marsh *et al.*, 2011), passaged 3 times on Vero cells with a titre of $10^{7.5}$ $TCID_{50}$ in Vero cells, and an isolate of HeV/Australia/Horse/1994/Hendra, GenBank accession no. AF017149 (Murray *et al.*, 1995), passaged 4 times on Vero cells with a titre of $10^{7.1}$ $TCID_{50}$/ml in Vero cells. Under general anaesthesia, 5 WT mice and 5 *Ifnar1-/-* mice were exposed IN to 50 000 $TCID_{50}$ of either one of the two isolates in a volume of 30 µl. Mice were co-housed with animals receiving the same HeV isolate.

After exposure to HeV, mice were assessed at least daily for clinical signs of disease. Mice were euthanased at the end of the study period (Day 21), or earlier if they had reached their predetermined humane endpoint for clinical disease as detailed in Chapter 2.

At post mortem, tissue samples were collected into 10% neutral buffered formalin for routine histopathology and IHC. Samples included brain hemi-section, lung, spleen, liver, kidney, bladder, reproductive tract (ovaries and uterus in female mice and testes and accessory sex glands in male mice), stomach, duodenum, jejunum, ileum, caecum and colon, pancreas, lymph nodes (parotid, cervical chain, mesenteric), adrenal glands, myocardium, thymus, trachea, oesophagus, skeletal muscle, diaphragm and femoral bone marrow. Tissues samples from the lung, contralateral forebrain (FB), spleen, liver and kidney were also collected into viral transport media for qualitative virus re-isolation as well as RNA extraction. Blood was collected into EDTA for qualitative virus re-isolation as well as RNA extraction. One ml of sterile saline was gently flushed retrograde through the nasal passages from a catheter placed into the nasopharynx and collected as it dripped from the nares. This nasal wash fluid was used for qualitative virus re-isolation as well as RNA extraction.

For virus isolation each sample was tested in two wells of a 24 well plate and assessed as either positive or negative for CPE. Multiplex TaqMan reverse-transcription (RT) PCR (qPCR) targeting the HeV-N gene as well as host cell 18S rRNA was performed on extracted RNA, with HeV- N gene values normalized to host cell 18S rRNA. Samples with a mean HeV-N gene C_T value ≤ 39.6 were defined as positive for HeV RNA (Dups *et al.*, 2012).

Sera were collected both prior to virus exposure and at euthanasia and analysed for antibody responses against HeV using a Luminex microsphere HeVsG binding assay and a receptor blocking assay as previously described (Bossart *et al.*, 2007; McNabb *et al.*, 2014).

6.3.1 Assignment of infection status and infection phenotype

As for each of the earlier studies, the primary readout was the infection phenotype that was observed in individual mice following exposure to virus. Mouse infection status and then an infection phenotype were assigned according to the criteria used in Chapter 3. In summary, a mouse was defined as infected with HeV if immunohistopathology was positive for viral antigen, or infectious virus was re-isolated from tissues, or the serum was positive for binding antibodies against HeV $_s$G protein. In the case of brain, detection of viral genome in brain tissue was considered sufficient to confirm virus replication in that organ. Categories

for infection phenotype comprised subclinical (no clinical signs observed during the study), systemic (exhibition of signs of general malaise with disseminated virus replication and significant pathology in major organ systems), and neurological (exhibition of signs consistent with involvement of the CNS and evidence of virus replication in brain).

6.4 Data analysis

Mice were recorded as febrile if their temperature was > 39.3^{o}C (in house reference for C57Bl6 mice).

Statistical analysis was carried out using GraphPad Prism 7.02. Survival curves were conducted using log-rank tests (Mantel-Cox and logrank test for trend). Bodyweight and temperature data up to the time of first mouse euthanasia were analysed in two-way mixed ANOVAs, with time as a within-subject variable and treatment group as a between-subject variable. Where indicated, comparisons of infection phenotypes between test groups were conducted using contingency analysis (Fisher's exact test). Data from all mice irrespective of euthanasia day were used for comparison of rates of virus replication in brain (Fisher's exact test).

Viral genetic loads in the different tissues were log-transformed and compared by ordinary two-way ANOVA, with tissue type and treatment group as the independent variables. Data from all mice were used for this analysis, irrespective of mouse euthanasia day.

6.5 Results

6.5.1 Clinical observations

The exposure 50 000 TCID50 intranasal HeV was generally well tolerated by both WT and *Ifnar1-/-* mice; it did not cause a sneeze reflex and only occasionally led to brief periods of apnoea and/or increased respiratory rate and effort.

All mice in this study met the criteria for HeV infection.

Group 1: WT mice + HeV/Australia/Horse/2008/Redlands: One mouse reached a predetermined humane endpoint for neurological disease and was euthanased on day 11

p.i. (Table 6.1). Four of 5 mice remained clinically healthy up to the time of elective euthanasia on day 21 (Table 6.1).

Group 2: WT mice + HeV/Australia/Horse/1994/Hendra: All 5 mice remained clinically healthy up to the time of elective euthanasia on day 21 (Table 6.1).

Group 3: *Ifnar1-/-* mice + HeV/Australia/Horse/2008/Redlands: Three out of 5 mice reached their predetermined humane endpoint for neurological disease and were euthanased on days 9, 10, or 11p.i.. Two of 5 mice remained clinically healthy up to the time of elective euthanasia on day 21 p.i. (Table 6.1).

Group 4: *Ifnar1-/-* mice + HeV/Australia/Horse/1994/Hendra: All 5 *Ifnar1-/-* mice exposed to HeV/Australia/Horse/1994/Hendra remained clinically healthy up to the time of elective euthanasia on day 21 p.i. (Table 6.1).

Table 6.1: Summary of data used to assess infection status

	Mouse Type	Mouse ID	Euth. Day	Infection phenotype	Olfactory mucosa Ag/PCR*/VI*	Lung Ag/PCR VI	Forebrain Ag/PCR/VI	Spleen Ag/PCR/VI	Liver Ag/PCR/VI	Kidney Ag/PCR/VI	Blood PCR/VI	Serology Bind/Block
Group 1	WT 2008	111	21	Subclinical	-/-	-/-	-/-	-/-	-/-	-/-	-/-	+/-
		112	11	Neurological	-/-	-/-	+/+	-/-	-/+	-/-	-/-	+/-
		113	21	Subclinical	-/-	-/-	-/-	-/+	-/-	-/-	-/-	+/-
		114	21	Subclinical	-/-	-/+	+/+	-/-	-/-	-/+	-/-	+/-
		115	21	Subclinical	-/-	-/-	-/-	-/-	-/-	-/-	-/-	+/-
Group 2	WT 1994	116	21	Subclinical	-/-	-/-	+/+	-/-	-/-	-/-	-/-	+/-
		117	21	Subclinical	-/-	-/+	+/+	-/-	-/+	-/-	-/-	+/-
		118	21	Subclinical	-/-	-/-	-/-	-/-	-/+	-/-	-/-	+/-
		119	21	Subclinical	-/-	-/-	-/-	-/+	-/-	-/-	+/-	+/-
		120	21	Subclinical	-/-	-/-	-/+	-/-	-/-	-/-	-/-	+/-
Group 3	*Ifnar1-/-* 2008	121	21	Subclinical	-/-	-/-	+/+	-/-	-/+	-/-	-/-	+/-
		122	21	Subclinical	-/-	-/-	+/+	-/+	-/-	-/-	-/-	+/+
		123	10	Neurological	+/+ +VI	-/+	+/+ +VI	-/-	-/+	-/-	-/-	na/na
		124	11	Neurological	+/+ +VI	+/+	+/+ +VI	+/+	-/+	-/-	+/-	na/na
		125	9	Neurological	+/+ +VI	+/+	+/+ +VI	na/+	-/+	-/-	-/-	na/na
Group 4	*Ifnar1-/-* 1994	126	21	Subclinical	-/-	-/-	-/+	-/+	-/+	-/+	-/-	+/+
		127	21	Subclinical	-/-	-/-	+/+	-/+	-/-	-/-	-/-	+/-
		128	21	Subclinical	-/-	-/-	+/+	-/+	-/-	-/-	-/-	+/+
		129	21	Subclinical	-/-	-/+	-/+	-/+	-/-	-/-	-/-	+/-
		130	21	Subclinical	-/-	-/+	-/+	-/+	-/+	-/-	+/-	+/-

Ag: immunohistochemical staining for viral antigen in tissue
PCR: qPCR for viral genome in tissue
VI+: virus isolation was performed on all samples, only the positive results are presented above
* for olfactory mucosa PCR and VI was performed on retrograde nasal washings
“+” present
“-“ not present
Euth. Day: day of euthanasia
Bind: luminex binding assay
Blk: luminex receptor blocking assay
na: sample not available

Bodyweight data is presented in Figure 6.1. All mice were heavier at day 9 p.i. compared to day 0. Each mouse euthanased for neurological disease started to lose weight from 48 to 24 hrs prior to euthanasia. There was a significant effect of the interaction between time and test group on bodyweight up to day 9 post-exposure to HeV ($p < 0.0001$): mean weights of *Ifnar 1-/-* mice given HeV 2008 were higher than all other test groups on day 0 to 9 p.i., and mean weights of WT mice given HeV 2008 were higher than WT mice given HeV 1994 on days 1, 2, 4, 8 and 9 p.i.. This was attributed to each of these groups containing more males than groups exposed to the 1994 strain. There was a significant effect of test group on bodyweight ($p < 0.0001$) that was interpreted according to the significant interaction above. There was a significant effect of time post-exposure on bodyweight ($p < 0.0001$), that was also interpreted according to the significant interaction above.

Figure 6.1: Combined mouse weights (g with mean and SD) post exposure

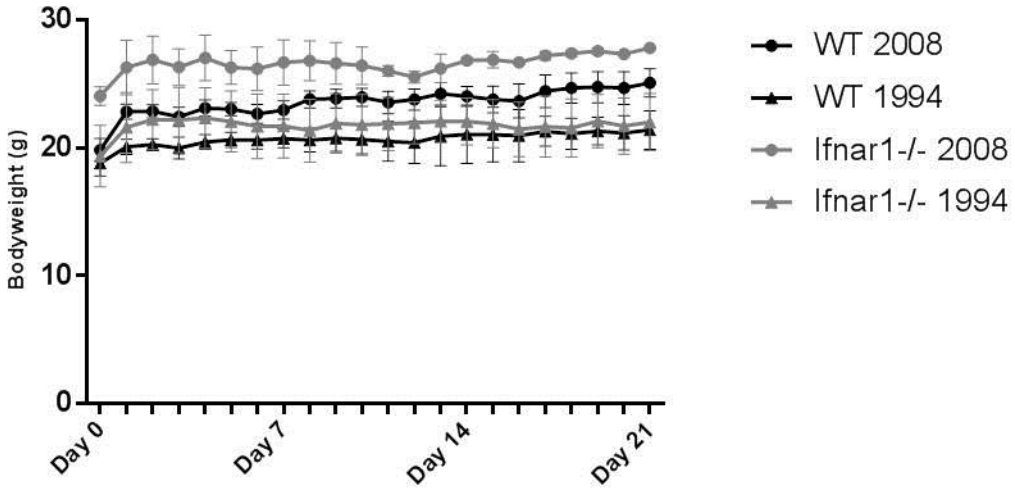

Temperature data is presented in Figure 6.2. One clinically normal WT mouse given HeV 2008 had a high temperature (T > 39.3 C^{o}) on day 17 p.i. that had returned to normal on day 18 p.i.. There was no significant effect of the interaction between time and test group on temperature. There was a significant effect of time on temperature ($p < 0.0001$), with slightly higher mean temperatures on day 1 p.i. compared to days 3, 4, 6 and 7 p.i.: this finding is of uncertain biological significance. There were no significant effects of test group on mean temperature from days 0 to 9 p.i..

Figure 6.2: Combined mouse temperatures (^{o}C with mean and SD) post exposure

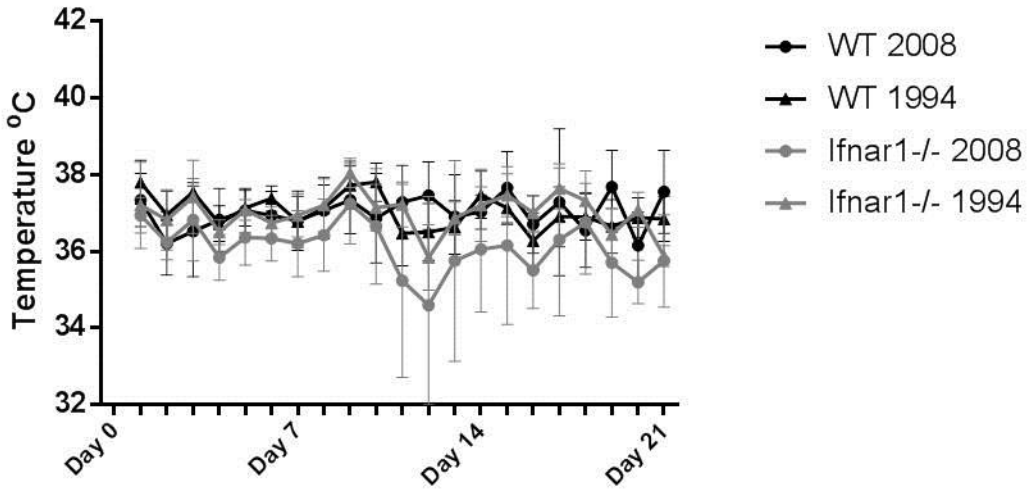

6.5.2 Pathology and immunohistopathology

Group 1: WT mice + HeV/Australia/Horse/2008/Redlands: Two of 5 mice had mild non-suppurative meningoencephalitis involving the anterior olfactory tract including the olfactory bulb and frontal lobe of the cerebral cortex (Table 6.1 and Table 6.2). Positive IHC staining for viral antigen occurred within affected areas of brain parenchyma comparable to that reported earlier in WT mice euthanased with neurological disease. Viral antigen was not identified within the meninges of either

mouse. Viral antigen or lesions were not detected in any other tissues including olfactory mucosa, associate lymph nodes, and lung.

Three of 5 mice were within normal limits for tissue histology, and no HeV antigen was identified in tissue sections.

Group 2: WT mice + HeV/Australia/Horse/1994/Hendra: Two of 5 mice had non-suppurative meningoencephalitis involving the anterior olfactory tract including the olfactory bulb, piriform lobe, and amygdala (1 mouse) (Table 6.1 and Table 6.2). Positive IHC staining for viral antigen occurred within affected areas of brain parenchyma comparable to that reported earlier in WT mice euthanased with neurological disease. Viral antigen was not identified within the meninges of either mouse. Viral antigen or lesions were not detected in any other tissues including olfactory mucosa, associated lymph nodes, and lung.

Three of 5 mice were within normal limits for tissue histology, and no HeV antigen was identified in tissue sections.

Table 6.2: Summary of pathology findings

	Mouse type	Mouse ID	Meninges Ag/les	Forebrain Ag/les	Ependyma Ag/les	Endothelium Ag/les	Olfactory epithelium Ag/les	Olfactory lymphoid tissue Ag/les	Olfactory nerve perineurium Ag/les	Olfactory regional LNs Ag/les	Lung Ag/les	Spleen Ag/les	Liver Ag/les
Group 1	WT 2008	111	-/-	-/-	-/-	-/-	-/-	-/-	-/-	-/-	-/-	-/-	-/-
		112	-/+	+/+	-/-	-/-	-/-	-/-	-/-	-/-	-/-	-/-	-/-
		113	-/-	-/-	-/-	-/-	-/-	-/-	-/-	-/-	-/-	-/-	-/-
		114	-/+	+/+	-/-	-/-	-/-	-/-	-/-	-/-	-/-	-/-	-/-
		115	-/-	-/-	-/-	-/-	-/-	-/-	-/-	-/-	-/-	-/-	-/-
Group 2	WT 1994	116	-/+	+/+	-/-	-/-	-/-	-/-	-/-	-/-	-/-	-/-	-/-
		117	-/+	+/+	-/-	-/-	-/-	-/-	-/-	-/-	-/-	-/-	-/-
		118	-/-	-/-	-/-	-/-	-/-	-/-	-/-	-/-	-/-	-/-	-/-
		119	-/-	-/-	-/-	-/-	-/-	-/-	-/-	-/-	-/-	-/-	-/-
		120	-/-	-/-	-/-	-/-	-/-	-/-	-/-	-/-	-/-	-/-	-/-
Group 3	*Ifnar1-/-* 2008	121	+/+	+/+	-/-	-/-	-/-	-/-	-/-	-/-	-/-	-/-	-/-
		122	+/+	+/+	-/-	-/-	-/-	-/-	-/-	-/-	-/-	-/-	-/-
		123	+/+	+/+	-/-	-/-	+/+	-/-	-/-	-/-	-/-	-/-	-/-
		124	+/+	+/+	-/-	-/-	+/+	-/-	-/-	-/-	+/-	+/-	-/-
		125	+/+	+/+	-/-	+/-	+/+	-/-	+/+	-/-	+/-	NA	-/-
Group 4	*Ifnar1-/-* 1994	126	-/-	-/-	-/-	-/-	-/-	-/-	-/-	-/-	-/-	-/-	-/-
		127	-/+	+/+	-/-	-/-	-/-	-/-	-/-	-/-	-/-	-/-	-/-
		128	-/+	+/+	-/-	-/-	-/-	-/-	-/-	-/-	-/-	-/-	-/-
		129	-/-	-/-	-/-	-/-	-/-	-/-	-/-	-/-	-/-	-/-	-/-
		130	-/-	-/-	-/-	-/-	-/-	-/-	-/-	-/-	-/-	-/-	-/-

Ag: antigen, Les: inflammatory and/or necrotising lesion, LNs: lymph nodes, NA: tissue not available

Group 3: *Ifnar1-/-* mice + HeV/Australia/Horse/2008/Redlands: Three of 5 mice had rhinitis associated with HeV antigen in the olfactory epithelium. In 1 of these mice, viral antigen was also detected within the endothelium of nasal submucosal vessels, and within the inflamed perineurium of olfactory nerve fibres traversing the caudal nasal submucosa (Table 6.2), as described for IN exposed *Ifnar1-/-* mice in Chapter 4. Two of these mice had viral antigen deposits in pulmonary alveolar walls, and 1 in spleen, without other evidence of tissue injury in the form of necrosis or inflammation.

All 5 mice had mild to moderate meningoencephalitis, with a mixed inflammatory infiltrate that included neutrophils, associated with HeV antigen deposition within the olfactory bulb, piriform lobe (4 mice) and amygdala (1 mouse). Viral antigen was present within the meningeal inflammatory infiltrate (Table 6.2), as previously described in for *Ifnar1-/-* mice in Chapter 4.

Viral antigen or lesions were not detected in any other tissues.

Group 4: *Ifnar1-/-* mice + HeV/Australia/Horse/1994/Hendra: Two of 5 mice had non-suppurative meningoencephalitis involving the anterior olfactory tract including the olfactory bulb and piriform lobe (Table 6.1 and Table 6.2). Positive IHC staining for viral antigen occurred within affected areas of brain parenchyma comparable to that reported earlier in WT mice euthanased with neurological disease. Viral antigen was not identified within the meninges of either mouse. Viral antigen or lesions were not detected in any other tissues including olfactory mucosa, associated lymph nodes, and lung.

Three of 5 mice were within normal limits for tissue histology, and no HeV antigen was identified in tissue sections.

6.5.3 Molecular virology and classical virology

Viral genome was detected in at least one tissue from 18 of the 20 mice shown to have been infected after exposure to HeV (Data presented in Table 6.1 and Figure 6.3)

Figure 6.3: qPCR data. Log_{10} HeV-N gene copies normalised to 18S in different organs in WT and *Ifnar1-/-* mice infected with HeV/Australia/Horse/2008/Redlands (2008) or HeV/Australia/Horse/1994/Hendra (1994).

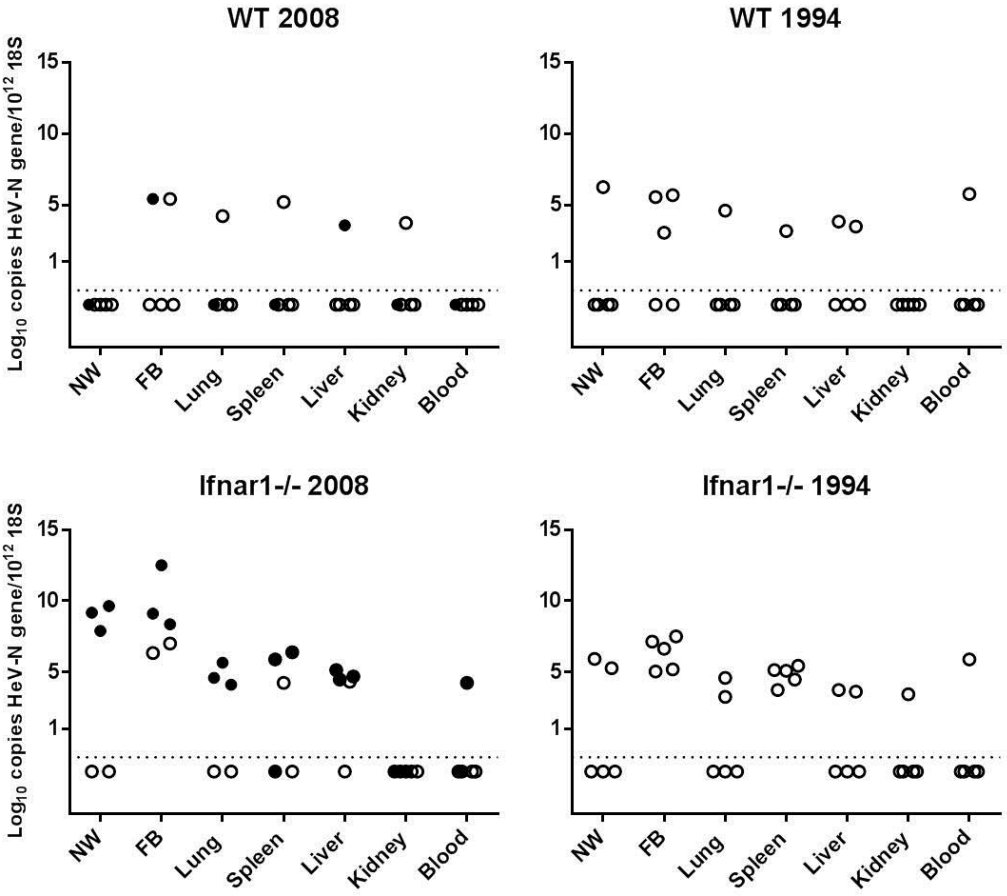

NW: Nasal wash

FB: Forebrain

Open circle: remained clinically healthy

Solid circle: showed neurological signs

Dotted line: level of assay detection

HeV genome was present in the forebrain samples of 2 out of 5 Group 1 mice (WT, HeV 2008), 3 of 5 Group 2 mice (WT, HeV 1994) and all 10 *Ifnar1-/-* mice. Virus was also re-isolated from the contralateral forebrain of 3 out of 5 *Ifnar1-/-* mice given HeV/Australia/Horse/2008/Redlands, each of which had been euthanased on account of neurological signs.

HeV genome was detected in the lung of 1 out of 5 Group 1 mice (WT, HeV 2008), 1 out of 5 Group 2 mice (WT, HeV 1994), 3 of 5 Group 3 mice (*Ifnar1-/-*, HeV 2008) and 2 of 5 Group 4 mice (*Ifnar1-/-*, HeV 1994) (Figure 6.3). Virus was not re-isolated from the lung of any mouse (Table 6.1).

HeV genome was detected in the spleen of 1 out of 5 Group 1 mice (WT, HeV 2008), 1 out of 5 Group 2 mice (WT, HeV 1994), 3 of 5 Group 3 mice (*Ifnar1-/-*, HeV 2008) and all Group 4 mice (*Ifnar1-/-*, HeV 1994) (Figure 6.3). Virus was not re-isolated from the spleen of any mouse (Table 6.1).

In the liver, HeV genome was found in 1 out of 5 Group 1 mice (WT, HeV 2008), 2 out of 5 Group 2 mice (WT, HeV 1994), 4 of 5 Group 3 mice (*Ifnar1-/-*, HeV 2008) and 2 of 5 Group 4 mice (*Ifnar1-/-*, HeV 1994) (Figure 6.3). Virus was not re-isolated from the liver of any mouse (Table 6.1).

Overall, only two kidney and three blood samples tested positive for viral genome, spanning all test groups (Table 6.1).

There was a significant effect of the interaction between tissue type and test group on viral genetic load ($p = 0.0189$). *Ifnar1-/-* mice given HeV/Australia/Horse/2008/Redlands had higher mean levels in forebrain compared to lung ($p = 0.0003$), spleen ($p = 0.0009$), blood ($p < 0.0001$), liver ($p = 0.0029$) and kidney ($p < 0.0001$). Similar effects were observed in *Ifnar1-/-* mice given HeV/Australia/Horse/1994/Hendra where mean levels in forebrain were higher than lung ($p = 0.0049$), blood ($p = 0.0017$), liver ($p = 0.0038$) and kidney ($p = 0.0004$) but not spleen, and levels for spleen were higher than kidney ($p = 0.0230$). Thus the mean level of genome in the spleen was as high as for forebrain for this group. In

contrast, within WT mouse groups there were no significant differences in mean viral genetic loads between any tissues. Across test groups, *Ifnar1-/-* mice given either HeV/Australia/Horse/2008/Redlands or HeV/Australia/Horse/1994/Hendra had higher mean HeV genetic loads in forebrain than either WT group ($p < 0.0001$ [*Ifnar1-/-* 2008 vs WT 2008], $p=0.0001$ [*Ifnar1-/-* 2008 vs WT 1994], $p=0.0093$ [*Ifnar1-/-* 1994 vs WT 2008], $p=0.0424$ [*Ifnar1-/-* 1994 vs WT 1994], but levels were not significantly different between the two WT groups or between the *Ifnar1-/-* mouse groups. In addition, mean viral genetic loads were higher in the spleen of *Ifnar1-/-* mice given HeV/Australia/Horse/1994/Hendra compared to WT mouse groups, but not higher than *Ifnar1-/-* mice given HeV/Australia/Horse/2008/Redlands. No significant differences between groups were found for other tissue types.

There was a significant main effect of tissue type on mean viral genetic load (< 0.0001) that was interpreted according to the significant interaction above. There was a significant main effect of test group on mean viral genetic load (< 0.0001) that was also interpreted according to the significant interaction above.

6.5.4 Serology

All mice from which samples were available for testing were positive for a binding antibody response (Table 6.3). No WT mice developed a blocking antibody response, irrespective of viral strain of exposure. One *Ifnar1-/-* mice exposed to HeV/Australia/Horse/2008/Redlands developed a blocking response (Table 6.3) and 2 *Ifnar1-/-* mice exposed to HeV/Australia/Horse/1994/Hendra (Mice #126 and #128) developed blocking responses.

Table 6.3: Serology results

	Assay		Antibody binding	Receptor blocking
Mouse type	Mouse #	ID delete	MFI Post Challenge	% Inhibition
WT 2008	111	115	**1 2202**	0
	112	116	**27 083**	0
	113	117	**1 183**	0
	114	118	**28 211**	0
	115	119	**4 778**	0
WT 1994	116	110	**1 184**	0
	117	111	**4 002**	0
	118	112	**1 194**	1
	119	113	**30 234**	0
	120	114	**23 006**	0
Ifnar1-/- 2008	121	104	**30 404**	1
	122	105	**30 022**	**13**
	123	106	ND	ND
	124	107	ND	ND
	125	108	ND	ND
Ifnar1-/- 1994	126	100	**29 926**	**15**
	127	101	**30 191**	4
	128	102	**30 601**	**12**
	129	103	**30 192**	6
	130	109	**30 082**	0
Positive controls	Horse		**28 149**	**80**
	Mouse		**4 011**	ND
	Rabbit		ND	**75**

ND: Not done

Euth.: Euthanasia

Luminex binding assay: the mean of the pre-challenge sera was 194 MFI, standard deviation was 120, and therefore the level for a positive result was > 556 MFI.

Positive results are shown in bold.

6.5.5 Assignment of infection phenotype

As in Chapter 4 an infection phenotype for each animal was assigned following integration of the clinical and laboratory findings. Outcomes are presented in (Table 6.1).

Group 1: WT mice + HeV/Australia/Horse/2008/Redlands: One of 5 mice demonstrated acute onset neurological disease. This mouse had viral replication confirmed within the forebrain, within olfactory tract, which was accompanied by mild to moderate meningoencephalitis. Mild weight loss immediately preceded the onset of neurological signs and was attributed to the developing neuropathology. At no time was this mouse febrile.

Four of 5 mice remained clinically healthy throughout the study period. None developed a sustained febrile response following exposure to HeV; each had gained weight since exposure to virus.

On the basis of these findings, one WT mouse exposed to HeV/Australia/Horse/2008/Redlands was assigned a neurological infection phenotype and 4 were assigned a subclinical phenotype (Table 6.1).

Group 2: WT mice + HeV/Australia/Horse/1994/Hendra: All 5 mice remained clinically healthy up to the time of elective euthanasia on Day 21. No mice developed a fever following exposure to HeV; each had gained weight since exposure to virus.

On the basis of these findings, 5 out of 5 WT mice exposed to HeV/Australia/Horse/1994/Hendra were assigned a subclinical phenotype.

Group 3: *Ifnar1-/-* mice + HeV/Australia/Horse/2008/Redlands: Three of 5 mice reached humane end points necessitating euthanasia on account of acute onset neurological disease. Each of these mice had viral replication confirmed within the forebrain, in the olfactory tract, which was accompanied by mild to moderately severe meningoencephalitis; viral antigen was also present in the meninges. They also had virus replication confirmed in olfactory mucosa that was associated with rhinitis: in 1 mouse infection and inflammation extended to involve the perineurium.

Virus replication was also confirmed in the lung (2 out of 3), spleen (1 out of 3), and nasal submucosal vessels (1 out of 3) of these mice. However, apart from the rhinitis and meningoencephalitis, the presence of viral antigen in these tissues was not associated with significant pathology in the form of an inflammatory response or necrotising lesions. None of the 3 mice developed a fever following exposure to HeV/Australia/Horse/2008/Redlands. In the three mice with neurological disease mild weight loss preceded the onset of neurological signs, and was attributed to the developing neuropathology.

The remaining two *Ifnar1-/-* mice exposed to HeV/Australia/Horse/2008/Redlands remained clinically healthy throughout the study period. Neither mouse exhibited weight loss or fever after exposure to virus.

On the basis of these findings, 3 *Ifnar1-/-* mice exposed to HeV/Australia/Horse/2008/Redlands were assigned a neurological infection phenotype and 2 *Ifnar1-/-* mice exposed to HeV/Australia/Horse/2008/Redlands were assigned a subclinical phenotype (Table 6.1).

Group 4: *Ifnar1-/-* mice + HeV/Australia/Horse/1994/Hendra: All *Ifnar1-/-* mice exposed to HeV/Australia/Horse/1994/Hendra remained clinically healthy up to the time of elective euthanasia on Day 21. No mouse developed a fever following exposure to HeV; all gained weight after exposure to virus.

On the basis of these findings, 5 out of 5 *Ifnar1-/-* mice exposed to HeV/Australia/Horse/1994/Hendra were assigned a subclinical phenotype.

Summary comments:
There was a significant difference between the four test groups for infection survival curves by both log-rank test (p=0.0358), log-rank test for trend (p=0.0110 [WT 1994 vs *Ifnar 1-/-* 1994 vs WT 2008 vs *Ifnar 1-/-* 2008]) and log-rank test for trend (p=0.0382 [WT 1994 vs WT 2008 vs *Ifnar 1-/-* 1994 vs *Ifnar 1-/-* 2008]). In each instance, the observed difference was attributable to reduced survival in *Ifnar 1-/-* 2008 mice.

As the data set did not meet the criteria for valid Chi^2 calculations, and on the basis that the earlier studies did not reveal differences in the incidence of particular infection phenotypes between WT and interferon-signalling deficient mice, data rows (WT and *Ifnar 1-/-*) were combined for each virus strain. On that basis, there was no significant difference between the likelihood of subclinical or neurological phenotypes being assigned to mice exposed to HeV/Australia/Horse/2008/Redlands vs HeV/Australia/Horse/1994/Hendra, although it was noted that a neurological phenotype was only observed in mice exposed to HeV/Australia/Horse/2008/Redlands. Similarly, there was no significant difference between virus strains in the likelihood that virus replication would be recorded in mouse brain.

When the column rows (2008 vs 1994) were similarly combined, there was a higher likelihood of viral replication in the brain of *Ifnar1-/-* mice compared to WT mice (p= 0.0325), but the likelihood that *Ifnar1-/-* mice would also show neurological disease was not significantly higher than for WT mice. The apparent failure of translation of forebrain replication to neurological disease is attributable to the observed relative resistance of the *Ifnar 1-/-* 1994 group to developing neurological disease, also reflected in reduced survival of *Ifnar 1-/-* 2008 compared to the other mouse groups (described above). However, there were no distinct differences in viral antigen distribution within the brain or in neuropathology between mouse groups infected with the two viral strains that might have accounted for the different clinical outcomes. So it remains possible that the apparent relative resistance of the *Ifnar1-/-* 1994 group to developing neurological disease may be a chance observation.

6.6 Discussion

The aim of this chapter was to compare the neuropathogenicity of HeV/Australia/Horse/2008/Redlands and HeV/Australia/Horse/1994/Hendra for mice after IN exposure. Clinical observations including bodyweight and temperature were recorded for up to 21 days, tissue distribution and levels of virus replication were assessed, the severity of pathology in diverse organ systems was evaluated, and an infection phenotype was assigned to each mouse. Group survival curves were also compared.

In Chapter 4, WT and *Ifnar1-/-* mice were exposed IN to HeV/Australia/Horse/2008/Redlands. There were no significant differences between WT and *Ifnar1-/-* mice with respect to infection survival curves or between phenotypes assigned to WT mice and interferon signalling deficient mice; these were either subclinical infection or acute neurological syndromes. There was no significant difference between test groups in the likelihood of virus replication in brain, but *Ifnar1-/-* mice were more likely to have replicated HeV in the spleen and to a higher level compared to WT mice.

The contrast between these findings and the observation of Dhondt *et al.* (2013) that *Ifnar1-/-* mice exposed IN to HeV failed to develop clinical disease prompted a comparison of the pathogenicity of two HeV strains isolated 14 years apart. It was recognised that there were several additional variables with respect to direct comparison to Dhondt *et al.* (2013)'s study conditions. These included mouse strain differences between C57Bl6 mice sourced from different breeding establishments in France and Australia (Jackson Laboratory, 2016), equivalency in viral dose between PFU (used by Dhondt *et al.*) and $TCID_{50}$ (used at CSIRO AAHL), exact matching of viral isolates (Genbank number and passage history of the virus used by Dhondt *et al.* is undeclared), and animal exposure techniques. However, employing an equivalent test system as was used in Chapter 4 enabled direct comparison of the effect of the two viral strains under consistent experimental conditions.

As in Chapter 4, WT mice were reliably infected following IN exposure with HeV/Australia/Horse/2008/Redlands, virus replication was confirmed in brain, and the outcome of infection was either a subclinical or a neurological phenotype. In contrast, viral replication was not confirmed in the nasal mucosa or lung, and this may have been a result of fewer mice succumbing to acute infection. Similarly also to Chapter 4, *Ifnar1-/-* mice were reliably infected following IN exposure with HeV/Australia/Horse/2008/Redlands, virus replication was confirmed in brain, olfactory mucosa, lung and spleen, and this resulted in either a subclinical or a neurological phenotype. Overall, findings in WT and *Ifnar1-/-* mice exposed IN to HeV/Australia/Horse/2008/Redlands were considered qualitatively similar to those described in Chapter 4.

HeV/Australia/Horse/1994/Hendra also reliably infected WT mice exposed IN. All mice had a subclinical phenotype, and virus replication was only confirmed to have occurred in brain.

The associated neuropathology was indistinguishable from that observed in the olfactory tract of WT exposed IN to HeV/Australia/Horse/2008/Redlands. As for WT mice exposed in this Chapter to HeV/Australia/Horse/2008/Redlands, absence of evidence for viral replication in the nasal mucosa or lung may have been because no mice succumbed to acute infection. Similarly to the WT cohort, *Ifnar1-/-* mice exposed IN to HeV/Australia/Horse/1994/Hendra were all infected and each mouse displayed a subclinical phenotype. Viral replication was confirmed in the brain of each mouse but, unlike *Ifnar1-/-* mice given HeV/Australia/Horse/2008/Redlands in either Chapter 4 or this study, there was no evidence for replication in olfactory mucosa, lung or spleen. As commented above, this may have been because none of these mice succumbed during to acute infection. Although WT and *Ifnar1-/-* mice groups exposed IN to HeV/Australia/Horse/1994/Hendra exhibited only a subclinical phenotype, the findings with respect to viral meningoencephalitis of the anterior olfactory tract were qualitatively similar to those described in WT and *Ifnar1-/-* mice exposed IN to HeV/Australia/Horse/2008/Redlands.

When the data from all mice were considered, independent of viral strain, *Ifnar1-/-* mice were found to have been more likely to replicate HeV in brain compared to WT mice. But they were not more likely to show neurological signs; this was attributable to the relative resistance of the *Ifnar 1-/-* 1994 group to developing clinical neurological disease - also reflected in the reduced survival of the *Ifnar 1-/-* 2008 group compared to the other test groups. Moreover, a neurological phenotype was seen only in mice exposed to HeV/Australia/Horse/2008/Redlands. Considered together, it could be suggested that these findings are consistent with a difference in neuropathogenicity between HeV/Australia/Horse/1994/Hendra and HeV/Australia/Horse/2008/Redlands not only for *Ifnar 1-/-* mice but also WT mice. On that basis, the hypothesis would appear to be unsupported that using the two virus strains plus *Ifnar1-/-* mice may be a suitable model to study protection mechanisms against HeV induced encephalitis. It could also be suggested that further study involving comparison of HeV/Australia/Horse/1994/Hendra and HeV/Australia/Horse/2008/Redlands may be used to elucidate neuroprotective mechanisms in immunologically intact mice.

However, cohorts of WT mice exposed IN to HeV/Australia/Horse/2008/Redlands mice may be considered as bridging controls between Chapter 4 and this chapter. A detailed review

of the infection responses in WT mice from this perspective revealed that, while there was no significant difference in the levels of viral genome in brain between Chapter 4 and Chapter 6 (unpaired t-test p = 0.1365, see Appendix 2, Figure 1), WT mice in Chapter 4 were significantly more likely to show virus replication in brain compared to WT mice in this chapter (Fisher's exact test, p = 0.0088, Appendix 2, Table 1). Moreover, WT mice in Chapter 4 were also more likely to develop neurological disease than the WT mice exposed to HeV/Australia/Horse/2008/Redlands in this chapter (Fisher's exact test p = 0.0474, Appendix 2, Table 2).

By contrast, a similar review of the infection responses of *Ifnar1-/-* mice exposed IN to HeV/Australia/Horse/2008/Redlands in Chapters 4 and 6 revealed that the *Ifnar1-/-* mice in Chapter 4 were equally likely to show virus replication in their brain as those in this chapter (Fisher's exact test, p = 1, Appendix 2, Table 3) and were also equally likely to exhibit neurological disease Fisher's exact test p=0.2418, Appendix 2, Table 4).

In summary, although comparable data was generated for *Ifnar1-/-* mice exposed IN to HeV/Australia/Horse/2008/Redlands in this chapter and in Chapter 4, WT mice exposed IN to HeV/Australia/Horse/2008/Redlands in Chapter 6 were less permissive than mice in Chapter 4 to virus replication in brain and also to the development of neurological disease. Thus there is evidence for an unforeseen difference between test conditions with the potential for bias towards underestimation of the potential pathogenicity of HeV/Australia/Horse/1994/Hendra, and this may apply not only to WT but also *Ifnar1-/-* mice. On that basis, the observations within this Chapter suggesting the lower neuropathogenicity of HeV/Australia/Horse/1994/Hendra may be attributable either to the impact of unidentified nuisance variables or a chance event. Further infection studies with larger numbers of mice would be required to reduce the impact of nuisance variables and of variation due to chance. At this stage, it is not possible to invalidate the hypothesis, or to attribute the observations of Dhondt *et al.* (2013) in *Ifnar1-/-* mice to the impact of virus strain.

Findings in this and earlier chapters consistently indicate that, although mice deficient in interferon signalling are slightly more permissive to HeV infection, the resistance of WT mice to widespread HeV replication and fulminating systemic disease cannot be attributed

solely to the efficacy of mouse interferon signalling pathways against HeV-mediated anti-interferon mechanisms. Dups *et al.* (2012) showed that WT mice developed a transient mild respiratory infection which was cleared with minimal neutralising antibody response. Similar findings reported here in WT and also in IFN-signalling deficient mice suggest that another component of the murine innate immune system must contribute to the innate resistance of mice to systemic HeV disease. As an example, interferon induced transmembrane (IFITM) proteins are a family of antiviral restriction factors that may be involved. IFITMs both restrict the entry and inhibit the production of infectious virions for many other viruses, and they have a high basal level of expression in respiratory epithelial cells as part of the innate barrier defence mechanism. On that basis, the effect of IFITM proteins on HeV infection in mouse cells is investigated in the next chapter.

CHAPTER 7: I IFITM PROTEIN OVEREXPRESSION DOES NOT SIGNIFICANTLY ALTER HENDRA VIRUS REPLICATION OR PREVENT CYTOPATHIC EFFECTS IN HUMAN OR MOUSE CELL CULTURES.

7.1 Introduction

The previous mouse infection chapters have described the outcome HeV infection in WT and IFN-signalling deficient mice following IN and IP exposure, using two strains of HeV. Lethal encephalitic infection occurs in both IFN-signalling deficient mice and WT mice exposed IN, with the associated pathology limited to the nasal cavity and CNS. Furthermore, widespread HeV replication, associated pathology, and fulminating systemic disease is not found in any mouse strain studied using IN or IP exposure. The failure to establish systemic HeV-associated disease as seen in WT mice continues to apply even in mice deficient in the main antiviral innate immune system components of the IFN type 1 response alone (*Ifnar1-/-* and *Ifnar2-/-* mice) or with attenuation of type 1, 2 and 3 IFN responses combined (*Stat1-/-* mice). Therefore, the resistance of WT mice to widespread HeV replication and fulminating systemic disease may not be attributed solely to the efficacy of mouse interferon signalling pathways against HeV-mediated anti-interferon mechanisms.

Cell fusion is important in the perpetuation of cell to cell infection with HeV, and cell fusion induces disruption of cellular architecture and contributes to organ pathology (Wong & Ong, 2011). The absence of syncytial cell development in HeV infected mice is a strikingly different feature of the infection pathology compared to other susceptible species such as humans, non-human primates, ferrets, cats and horses. Thus an important question arises as to whether the fusion process in mice may be more effectively antagonised by other innate immune proteins in comparison to other species. One such family of interest is the Interferon induced transmembrane (IFITM) proteins. These are a family of antiviral restriction factors that both restrict viral entry and inhibit the production of infectious virions, and have a high basal level of expression in respiratory epithelial cells as part of the innate barrier defence mechanism. IFITM1, 2 and 3 restrict viral membrane fusion induced by all three classes of viral fusion protein, and a diverse range of enveloped viruses are inhibited by IFITM proteins. This chapter examines the effect of IFITM proteins and their mouse analogues, *Ifitm* proteins on HeV replication.

IFITM proteins are a family of antiviral restriction factors and there are 5 human IFITM genes identified to date - IFITM1, 2, 3, 5 and 10. IFITM 1, 2 and 3 are ubiquitously expressed (as reviewed in (Perreira *et al.*, 2013) and involved in cell adhesion, embryonic development, anti-proliferation control and tumour suppression (reviewed in (Siegrist *et al.*, 2011); IFITM 5 is specifically expressed in bone cells and involved in bone development; and the function and expression patterns of IFITM10 are yet to be elucidated (Zhang *et al.*, 2012).

Some cells, such as barrier epithelial cells, have a high basal level of expression of IFITM proteins but the expression of IFITM1, 2 and 3 is also strongly upregulated by type I and type II interferons. Although genes encoding the IFITM proteins were among the first interferon stimulated genes to be identified (Friedman *et al.*, 1984; Lewin *et al.*, 1991), it was almost 20 years before interest in their antiviral activities was piqued from a genome wide siRNA knockdown study which identified the IFITM proteins as potent inhibitors of early stage infection for influenza A virus, West Nile virus and Dengue virus (Brass *et al.*, 2009). IFITM 5 and IFITM 10, despite their grouping in this protein family, are not interferon induced and do not have antiviral activity: they will not be further discussed here.

Originally termed fragilis proteins in this species, mice have orthologs of all 5 human IFITM genes as well as two additional genes, *Ifitm6* and *Ifitm7*. *Ifitm6* is involved with macrophage functions in tumour suppression (Han, 2011) and is a close paralog to *Ifitm3* with a similar tissue distribution (Siegrist *et al.*, 2011). The function of *Ifitm7* has not yet been elucidated but, phylogenetically, the gene is clustered close to both *Ifitm1* and *Ifitm3* suggesting a likely similar biological function (Zhou *et al.*, 2011).

IFITM genes are divided into 3 clades (Zhang *et al.*, 2012). Clade I contains IFITM1, IFITM2, and IFITM3 as well as the mouse *Ifitm6* and *Ifitm7* genes. The expression of all of the genes in this clade can be induced by interferon. There is species specific sub-clustering of Clade I genes across mammals, indicating gene duplication occurred after evolutionary separation of these species. Evolutionary analysis suggests the existence of a single IFN inducible gene in the common ancestors of primates and rodents (Siegrist *et al.*, 2011). In humans, IFITM2 and IFITM3 are closely related and may have originated from IFITM1 via gene duplication, but they do not share a most recent common ancestor cluster with rodent *Ifitm1*, *Ifitm2* and

Ifitm3, in spite of their similar biological functions. However, in primates and rodents, convergently evolved amino acid sequences in the C-terminus, a region critical for antiviral activity, support the evolutionary association between viral infections and the emergence of the more recent IFITM genes.

IFITM3 plays an important role in restricting influenza A virus (IAV) infection in both humans and mice. In humans, polymorphism in the IFITM3 gene predisposes to severe infection with IAV. Individuals with homozygous mutations in IFITM3 were overrepresented in severe cases of disease during the H1N1 IAV outbreak in 2009 (Everitt *et al.*, 2012; Zhang *et al.*, 2013b). Similarly, individuals with homozygous mutations in IFITM3 sought medical attention sooner, developed acute respiratory distress more quickly and had higher mortality when infected with avian-origin H7N9 IAV infection. *Ifitm3* is constitutively expressed in areas important to first line defence of respiratory viruses, including the respiratory epithelium, endothelium and visceral pleura of uninfected wild type mice; infection with IAV is followed by up-regulation of expression in alveolar type II pneumocytes (Bailey *et al.*, 2012). *Ifitm3-/-* mice are more susceptible to IAV than their wild type counterparts: *Ifitm3-/-* mice lose weight more rapidly, reaching weight loss of > 20-25% by 6 days, and all require euthanasia for viral infection of the respiratory tract, whereas wild type mice lose weight more slowly and some recover (Bailey *et al.*, 2012; Everitt *et al.*, 2013).

7.1.1 Structure and location

IFITM proteins are small (approximately 130 amino acids) and have five domains - two hydrophobic membrane associated domains, a conserved intracellular loop, and N- and C-terminal domains. Three possible membrane topologies have been proposed to account for the differences reported in various studies of the N- and C- terminal domain location; these are illustrated in Figure 7.1 (as reviewed in (Bailey *et al.*, 2014).

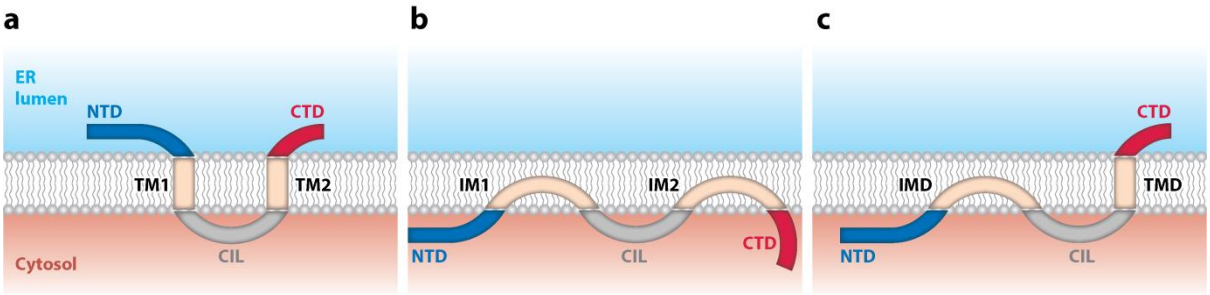

Figure 7.1: From Bailey *et al.* (2014).Three models of IFITM protein transmembrane topology. (*a*) The predicted type III transmembrane topology with ER-luminal N and C termini. In support of this model, several flow cytometry studies have localized IFITM1 or IFITM3 N termini to the cellular exterior. (*b*) An intramembrane topology was proposed based on the findings of posttranslational modifications. Ubiquitylation and phosphorylation of NTD amino acids support cytosolic localization of the N terminus. Palmitoylation of a C-terminal cysteine in the short TM2/IM2 region of mouse Ifitm1 is consistent with a cytosolic orientation of the C terminus. (*c*) More recent work has shown that murine Ifitm3 can adopt at least two different topologies. The predominant topology has an intracellular N terminus and extracellular C terminus. Abbreviations: CIL, conserved intracellular loop; CTD, C-terminal domain; ER, endoplasmic reticulum; IMD, intramembrane domain (previously denoted as IM1 or TM1); NTD, N-terminal domain; TMD, transmembrane domain (previously denoted as IM2 or TM2). Other mutations that decrease antiviral activity without altering intracellular distribution have been reported and reviewed in detail (Perreira *et al.*, 2013).

Endogenous IFITM1 is predominately located in lipid rafts within the plasma membrane and in early endosomes (Feeley *et al.*, 2011; Huang *et al.*, 2011). IFITM2 and 3 are intracellular, and co-localise with markers for late endosomes and lysosomes (Amini-Bavil-Olyaee *et al.*, 2013; Bailey *et al.*, 2012; Feeley *et al.*, 2011). Over expression of IFITMs can cause co-localisation in enlarged endolysosomal organelles; when this occurs IFITM1 is found in distinctly different vacuoles to IFITM2 and 3 (Feeley *et al.*, 2011; Huang *et al.*, 2011). Epitope tagging can also alter the subcellular distribution, with greater propensity in N-terminus tags than C-terminus tags (Perreira *et al.*, 2013). Mutations leading to alteration in trafficking and localisation of IFITMs adversely affect their antiviral activity. For example, IFITM2 and 3 share a closely homologous 21 amino acid sequence of the N-terminus. A mutation in a single tyrosine (Y20) of the N-terminus of IFITM2 and 3 prevents trafficking to endosomes and lysomes resulting in mislocalisation to the cell periphery and a halving of anti-viral activity (John *et al.*, 2013). Y20 is required for trafficking to endosomes, and as IFITM1 lacks Y20 it is confined to the plasma membrane and early endosomes. Palmitoylation of cystein

proteins directs them to cellular membranes; if palmitoylation C72 in IFITM3 is prevented then the protein is held to a more central location and antiviral effects are diminished (John *et al.*, 2013; Yount *et al.*, 2010).

7.1.2 Antiviral action

IFITM proteins both restrict viral entry and inhibit the production of infectious virions. IFITM1, 2 and 3 restrict viral membrane fusion induced by all three classes of viral fusion protein. These fusion proteins have differing structures suggesting a common physical mechanism is responsible, rather than specific interactions with each protein. The block in fusion does not affect either virus-receptor binding or pH dependent conformational changes in the fusion protein required for membrane fusion. Rather, IFITM proteins inhibit the transition of hemifusion to fusion whether at the cell surface, early and late endosomes, or lysosomes (Desai *et al.*, 2014; Li *et al.*, 2013). IFITM proteins may also alter the physical properties of cell membranes, causing loss of fluidity and inhibiting the formation or expansion of fusion pores (Li *et al.*, 2013). These different mechanisms as they act on Influenza A virus lifecycle are illustrated in Figure 7.2 (Brass *et al.*, 2009). IFITM1 differentially restricts viruses that enter at the cell surface or early endosomal compartments, whereas IFITM3 exerts greater restriction on viruses entering from late endosomes or lysosomes; these differential specificities correspond well with the different subcellular locations of the IFITM proteins. These have been recently reviewed with the provision of comprehensive comparison tables (Perreira *et al.*, 2013).

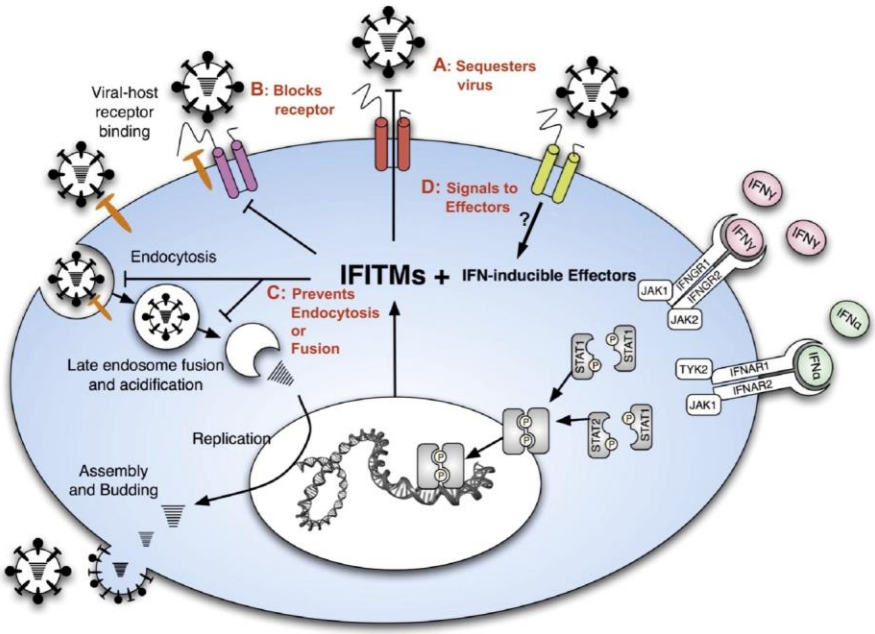

Figure 7.2 From Brass *et al.* (2009) IFITM proteins act as anti-viral restriction factors. A schematic model of the Influenza A virus life cycle, the induction of IFITM proteins and their role in blocking Influenza A virus infection. IFITM1, 2 and 3 are represented by the three multi-transmembrane proteins. Red legends indicate possible mechanisms of restriction, IFITM proteins may; A) sequester the incoming viruses at or near the surface, B) block viral receptors from interacting with host receptors (shown in orange), C) prevent endocytosis or viral membrane fusion D) act as receptors, and after binding the virus, signal to effectors.

A diverse range of enveloped viruses are inhibited by IFITM proteins including IAV, Influenza B virus, multiple flaviviruses (West Nile virus, Dengue virus, Yellow fever virus, Hepatitis C virus), several members of the *Bunyaviridae* (Rift Valley fever virus, LaCrosse virus, Andes virus and Hantaan virus), Vesicular stomatitis virus, Severe Acute Respiratory Syndrome Coronavirus (SARS CoV), Middle East Respiratory Syndrome Coronavirus (MERS CoV) and filoviruses (Ebola virus, EBOV, and Marburg virus) (Brass *et al.*, 2009; Compton *et al.*, 2014; Huang *et al.*, 2011; Jia *et al.*, 2015; Mudhasani *et al.*, 2013; Wrensch *et al.*, 2014). The majority of these are enveloped ssRNA viruses that fuse in endosomes or lysosomes. Reovirus is the only non-enveloped virus shown to date to be restricted by IFITM3 (Anafu *et al.*, 2013). The number of reported IFITM-resistant viruses is much fewer, although a bias against negative reporting may contribute, and includes all arenaviruses, Murine leukaemia virus, one Bunyavirus (Crimean-Congo Haemorrhagic Fever virus) , as reviewed in (Perreira *et al.*, 2013), Human papillomavirus, cytomegalovirus and adenovirus (Warren *et al.*, 2014).

In fact, the up regulation of IFITM proteins enhances infection with human coronavirus OC43 by acting as a co-receptor to facilitate viral entry (Zhao *et al.*, 2014).

7.1.3 Paramyxoviridae and IFITM proteins

Paramyxoviruses are enveloped viruses and viral entry requires fusion of the viral envelope with the cell membrane (Smith *et al.*, 2009). Membrane fusion is also essential for cell to cell fusion (syncytium formation) contributing to cell to cell viral transmission. Syncytia are a hallmark of infected tissues in Henipavirus infections (Escaffre *et al.*, 2013a; Hooper *et al.*, 2001; Hooper *et al.*, 1997b; Wong & Ong, 2011).

Paramyxoviruses share a close relationship to both *Orthomyxoviridae* which include Influenza A virus (IAV) because of the similarity of their type I fusion glycoproteins and to *Rhabdoviridae* which includes Vesicular stomatitis virus, because of similar non-segmented genomes. To date there have been two reports in the literature of the interactions between two different paramyxoviruses and IFITM proteins. Sendai virus (SeV), genus *Respirovirus*, is a murine virus considered a prototypical Paramyxovirus and well characterised to utilize pH-independent fusion at the cell surface, and therefore expected to avoid IFITM restriction in the endosomal compartment, was not restricted by IFITM1 or IFITM3 (Hach *et al.*, 2013). SeV is a murine virus and the effects of *Ifitm1* and *Ifitm3* on SeV infection have not been reported, although in papers that do study the effect of human IFITM proteins in parallel with murine *Ifitm* proteins they have been shown to have a similar effect (Huang *et al.*, 2011). Whereas, Human Respiratory Syncytial virus (RSV) from the *Pneumonovirinae* family (previously classified as a paramyxovirus), was potently inhibited by IFITM proteins (Zhang *et al.*, 2015). HeV has a closer phylogenic relationship to SeV than to RSV.

While previous chapters have shown that productive HeV infection occurs in mice, unlike other animal species susceptible to systemic HeV infection, neither vasculitis, with vascular wall degeneration and inflammatory cell infiltration, nor necrotising lesions within infected viscera were identified in WT or immune-deficient mice. From the studies in interferon-signalling deficient mice it seems unlikely that restriction of systemic pathology in this species is solely attributable to inhibition by interferon. However, infection in mouse lung is cleared with negligible neutralising antibody response (Dups *et al.*, 2012) suggesting an

innate response mechanism is relevant to limiting systemic effects of infection. The absence of syncytial cell development in HeV infected mice is a strikingly different feature of the infection pathology compared to other susceptible species such as humans, non-human primates, ferrets, cats and horses (Hooper *et al.*, 2001). Cell fusion is important in the perpetuation of cell to cell infection with HeV, and fusion induced disruption of cellular architecture contributes to organ pathology (Wong & Tan, 2012). Thus an important question arises as to whether the fusion process in mice may be antagonised by other innate immune proteins such as murine *Ifitm* proteins, leading to a reduction in the development of pathological lesions of HeV in mice?

In this experiment we demonstrated that over expression of human IFITM proteins by either human or murine cells did not lead to a significant reduction in HeV replication. In contrast, we found that murine *Ifitm* proteins restricted HeV replication in human and mouse cells to varying but minor extents.

7.2 Materials and Methods

7.2.1 Cells

A549, human lung carcinoma origin cell line, and L929, mouse fibroblast cell line, stably expressing IFITM proteins were selected and maintained in culture medium supplemented with 1 μg/ml and 5 μg/ml of puromycin (Invitrogen) respectively. A kill curve determined that these concentrations corresponded to 100% cell death after 72 hours of incubation in non-transduced cells.

7.2.2 Plasmids

Plasmids were kindly gifted from M. Farzan, The Department of Microbiology and Molecular genetics, Harvard Medical School and have been previously described (Huang *et al.*, 2011). Plasmids obtained were c-myc tagged human IFITM proteins IFITM1, 2 and 3 and mouse *Ifitm* proteins *Ifitm1, 2, 3, 6* and *7* and were subsequently cloned into the AgeI/BamH1 restrictions sites on a pQCXIP vector (Clontech).

7.2.3 Bacterial culture and transformation

Competent *E. coli* strains TOP10 or MC1061 were transformed with plasmid DNA using the Gene Pulser Transformation Apparatus (BioRad). Electroporation occurred at 1.8 V and 25 µF in 0.1 cm cuvettes (BioRad). The transformed cells were mixed with 500 µl of LB broth placed in a 10 ml tube (Starsted) and incubated for 1 hr at 37 ^{o}C with shaking at 250 rpm. The culture was then plated onto LB agar plates containing 100 µg/ml ampicillin and incubated for 18 hours. Individual colonies were inoculated into 2 ml of LB broth containing 100 µg/ml ampicillin and incubated for 8 hours with shaking at 250 rpm (Ratek platform shaker).

7.2.4 Purification of plasmid DNA

For small scale plasmid purification 1 ml of the culture was pelleted at 500 rpm for 10 minutes (Centrifuge 5415D, Ependorf) and PureYield™ Plasmid Maxiprep System (Promega) was used to lyse the bacterial culture and purify the plasmid DNA, as per the manufacturer's instructions. The purified plasmid DNA was eluted into 50 µl of nuclease free water.

For large scale plasmid purification 1 ml of the culture was then added to 200 ml of LB broth containing 100 µg/ml of ampicillin and incubated overnight before being pelleted at 500 rpm for 10 minutes (Heraeus Multifuge 3SR+ Centrifuge, Thermo Scientific). PureYield™ Plasmid Maxiprep System (Promega) was used to lyse the bacterial culture and purify the plasmid DNA, as per manufacturer's instructions. The purified plasmid DNA was eluted into 100 µl of nuclease free water.

7.2.5 Determination of nucleic acid concentration

The concentration of DNA was measured using the Qubit®2.0 Fluorometer (Invitrogen) using the dsDNA broad range setting and as per the manufacturer's instructions. Two manufacturer supplied standards were always used to calibrate the machine prior to reading samples.

7.2.6 Restriction Endonuclease Digestions

Double digest reactions were undertaken in a reaction volume of 20 µl, containing 2 µl of each restriction enzyme, Age1 and BamH1 (Promega), 2 µl of 10x Multicore buffer (Promega) 2 µl of 10x BSA and 2 µg DNA, with nuclease free water. The reactions were incubated at 37°C for 3 hrs. The products produced from restriction digests were analysed by agarose gel electrophoresis.

7.2.7 Agarose gel electrophoresis

Agarose gel electrophoresis was used to separate and purify nucleic acids following restriction digest. 1% Agarose gel was prepared by adding 4 g agarose (analytical grade agarose, Promega) in 400 ml of TAE x1 buffer and heating to dissolve. SYBR® Safe DNA gel stain (Invitrogen) was diluted 1:20 000 in the melted agarose to allow detection of nucleic acids on a Safe Imager transilluminator (Invitrogen). Samples for analysis constituted 20 µL of digest reaction and 6x GLB buffer (0.25% bromophenol blue, 0.25% xylene cyanol FF, 30% glycerol in H20). For each gel one well was filled with 15 µL 1kb Plus ladder (Invitrogen). Electrophoresis occurred at 100V for 30 minutes. Gels were imaged using a DC120 camera (Kodak). Bands of the correct molecular weight were excised and purified.

7.2.8 Purification of DNA from agarose gels

DNA was purified from agarose using the WIZARD® SV Gel and PCR clean up system (Promega) according to the manufacturer's instructions. Briefly, gel slices were placed in 1.5 ml microcentrifuge tubes (Eppendorf), weighed and incubated at 50-60 ^{0}C with membrane binding solution (at 10 µl per 10 mg, generally 300 µl) until the gel matrix dissolved (usually 10-15 minutes). The dissolved solution was placed into a separation column and allowed to stand for 1 minute at room temperature before being centrifuged at 13 000 rpm for 1 minute. Flow through was discarded and columns were washed twice by centrifugation with membrane wash solution, firstly with 700 µl for 1 minute then 500 µl for 5 minutes with flow through discarded each time and any residual ethanol allowed to evaporate. 30 µl nuclease free water was added to the column and DNA was eluted by centrifugation at 13 000 rpm for 1 minute. The purified DNA was subsequently stored at - 20^{0}C. All centrifuge steps were performed using a microcentrifuge (Eppendorf centrifuge 5415D).

7.2.9 Transfections and cell infections for stable protein expression

GP2-293 cells at 50% confluence in 6 well plates were co-transfected with an IFITM plasmid, calcium phosphate transfection reagent (Invitrogen) and pVSV-G envelope plasmid (Clontech). 3 μg of IFITM plasmid and 3 μg of pVSV-G plasmid were mixed directly with 6 μL of 2M calcium chloride and tissue culture water to a reaction volume of 50 μL. This was then added drop wise to 50 μL HEPES buffered saline to form a fine precipitate. After 30 minutes incubation at room temperature the precipitate was added drop wise to the media of the GP2-293 cells and the plates were rocked gently to mix. The cells were incubated overnight at 37 ^{o}C with 5% $C0_2$ and the media changed. The supernatants were harvested after an additional 48 hours and centrifuged at 500g for 10 minutes to remove cellular debris.

For cell infections A549 and L929 cells were seeded into 6 well plates 24 hours previously to be at 30% confluence. Their media was removed and replaced by 500 μL of retrovirus stock. Infection of L929 cells was optimised with the addition of 5 μg/ml of polybrene (Sigma) with the virus stock. The cells were incubated and gently rocked every 5 minutes for 30 minutes prior to replenishing growth media. Growth media was changed at 24 hours then replaced by selection media at 48 hours after infection. Cells were propagated in selection media and expression was validated with immunofluorescence prior to cell infection studies.

7.2.10 Immunofluorescence

Cells stably expressing IFITM proteins were cold fixed in 100% methanol for 15 minutes. The fixed cells were washed by rocking with 2 ml of PBST for 5 minutes, three times and then made permeable by incubation with 0.1% of the non-ionic detergent NP-40. The washing step was repeated, then 2 ml of blocking solution (1%BSA in PBST) was added to each well and mixed by rocking (Rocking platform mixer, Ratek) for 1 hour. The cells were then washed and incubated with primary antibody (Table 7.1) for 1 hour at room temperature. The cells were then washed again with PBST, five times. Secondary antibody (Table 7.1) was added for 30-60 minutes before again washing three times with PBST. Antibodies were diluted in blocking solution. Nuclei were counterstained with 1:1000 DAPI (Invitrogen) for 5 minutes washed and imaged. Cells were assessed for fluorescence using the EVOS FL

microscope (Life Technologies). Transfection with a green fluorescent protein (GFP) plasmid served as a positive control and mock transfected wells as negative controls.

Table 7.1: Immunofluorescence antibodies

Primary Antibody	Dilution	Secondary Antibody	Dilution
Mouse Anti-MYC-C (9E10) 25 µg/ml (from Prof H. Netter, Monash University)	1:100	Alexa Fluor 488 Green goat antimouse IgG 2 mg/ml, Invitrogen	1:1000
HeV-P 10-12-96 (CSIRO AAHL – Geelong)	1:500	Alexa Fluor 568 Red goat antirabbit IgG 2 mg/ml, Invitrogen	1:1000
Rabbit # 691 EBOV-N protein (CSIRO AAHL – Geelong)	1:250	Alexa Fluor 568 Red goat antirabbit IgG 2 mg/ml, Invitrogen	1:1000

7.2.11 Viruses

All work with live viruses occurred at BSL4 wearing fully encapsulating suits with external piped air supply.

A low passage clinical isolate of HeV, from an outbreak associated with human infection was used and had a titre of 4 x 10^7 $TCID_{50}$/ml HeV/Australia/Horse/2008/Redlands (Marsh *et al.*, 2011). The Ebola (EBOV) virus used in this experiment was a Zaire ebolavirus, Mayinga strain, obtained from Heinz Feldmann (Laboratory of Virology, Rocky Mountain Laboratories, NIAID, NIH USA) and had a titre of 8.9 x 10^7 $TCID_{50}$/ml.

7.2.12 Cell infections

24 well plates were seeded with 5 x 10^4/ml cells. This provided a confluent monolayer after overnight incubation in both A549 and L929 cells stably expressing IFITM proteins, approximating 4 x 10^5 cells/well. Growth media was removed and 100 µl/well of virus was added at a MOI of 0.1 and 1.0 for HeV and 1.0 for EBOV. To ensure consistency in virus inoculums, the infection was performed in triplicate for each cell type, time point and MOI. The plates were rocked gently for 30 minutes before growth media was replenished. Cells were incubated for 24 and 48 hours before supernatants were collected and the cells were fixed in 10% neutral buffered formalin.

7.2.13 Viral titrations

Tenfold serial dilutions of cell culture supernatants were prepared in 96 well plates with DMEM media, from neat to a 10^7-fold dilution, to a total volume of 250 µl per well. 50 µl of diluent was then inoculated in quadruplicate onto 80% confluent cells in 100 µl of growth media. HeV titrations were performed with Vero cells and checked at day 5 for viral cytopathic effect (CPE). EBOV titrations were performed with VeroE6 cells and incubated for 7 days before fixing in formalin and performing immunofluorescence staining to assess antigen containing wells. The limiting dilutions at which CPE or viral antigen could be observed for HeV and EBOV respectively were used to determine the $TCID_{50}$ per ml, using the Reed-Muench method for evaluation of 50% end points (Reed & Muench, 1938).

7.2.14 Statistical analyses

Three replicates were used for each combination of HeV infected cell line (human A549 or mouse L929), IFITM, multiplicity of infection (MOI 0.1 or MOI 1) and time point (24 or 48 hrs.). For the EBOV infection study there was one MOI (MOI 1) and one time point (48 hrs.), and only A549 cells expressing IFITM proteins were examined.

The individual replicate was the unit of analysis. Estimated $TCID^{50}$/ml values for each replicate were log-transformed and means compared using linear regression, performed using the -regress- command in Stata (version 13, StataCorp, College Station, Texas, USA). To maximise statistical power, analyses were pooled across time points where the crude means did not indicate important treatment by time point interaction. For each pair-wise comparison, arithmetic means were assessed for each multiplicity of infection (MOI)/time point combination; where differences and ratios were broadly similar for both time points within the same multiplicity of infection, data were pooled, and time was fitted as a covariate in the regression model. Data were also to be pooled where differences and ratios were broadly similar for both MOIs but this was not observed for any pair-wise comparison. This approach allowed valid use of the statistically more powerful parametric methods over non-parametric methods such as Mann-Whitney tests, and over multiple pair-wise t-tests, and allowed pooling of data across time points to increase statistical power.

Data from all experiments are presented as the mean+SD. Values were considered statistically significant if $p < 0.05$.

7.3 Results

Successful transfection of IFITM proteins was demonstrated by immunofluorescence staining against the Myc-C tag. Over 80% of cells grown in selective media stained positively with Myc-C antibody (row labelled Myc-C tag) and the immunofluorescence was predominately cytoplasmic. A small number of both A549 and L929 cells, expressing IFITM1 and 3 or *Ifitm1* and *3*, exhibited enlarged cytoplasmic vesicles with densely staining membrane borders. This pattern has been previously reported, predominately in cells over-expressing IFITM1, and shown to correspond to enlargement of endosomal organelles (Feeley *et al.*, 2011; Huang *et al.*, 2011). Figure 7.5 is a representative image to demonstrate staining by immunofluorescence; all other preparations were of similar appearance, differing only in the number of cells infected.

As expected, an approximately tenfold increase in viral titre developed between 24 and 48 hrs. (Figure 7.3). Vero cells were used as positive controls as this cell line is highly permissive to both HeV and EBOV infection. All infected Vero cell wells developed a very high titre, several fold higher than A549 and L929 controls (Figure 7.3).

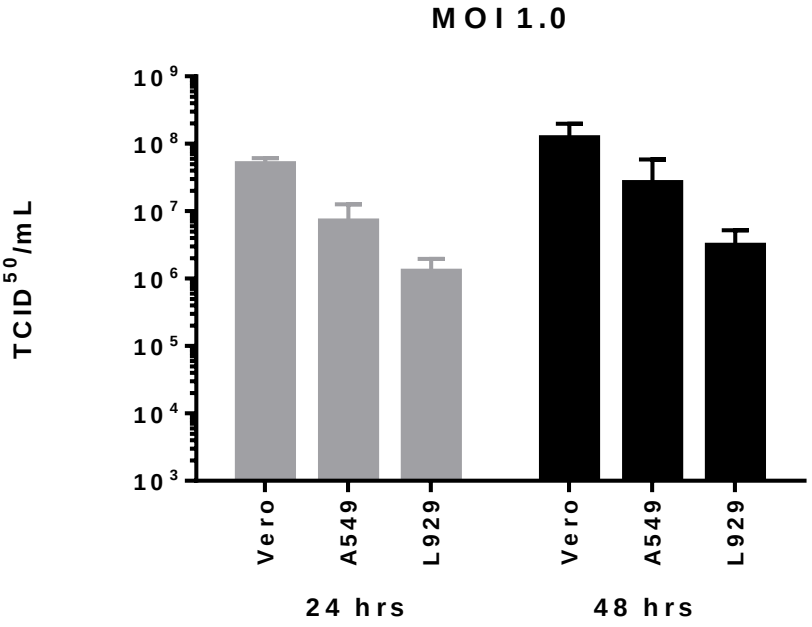

Figure 7.3: Vero, A549 and L929 cells inoculated with HeV at a dose of MOI 1 and the supernatants sampled at 24 and 48 hrs. Viral titrations were performed and the results presented as mean+SD of the $TCID_{50}$/ml.

7.3.1 EBOV infections

7.3.1.1 Replication of infectious EBOV is restricted by IFITM3 and *Ifitm3* in A549 cells

We were able to replicate earlier published findings of a statistically significant decrease in EBOV titre in A549 cells expressing IFITM3 (p = 0.004, CI of 0.043 – 0.46) using the same plasmids as Huang *et al*. (Huang *et al.*, 2011). Huang *et al* investigated the effect of expressing IFITM1, 2 and 3 in A549 cells on EBV infection at an MOI of 15 over 72 hours of incubation. All three IFITM proteins significantly suppressed EBOV infection in their study. However, unlike Huang et al, we did not observe a significant effect on infection from IFITM1 expression, but their study conditions allowed for a higher infection rate and longer incubation. We additionally found that, like its human orthologue, murine *Ifitm3* suppressed EBOV replication (p = 0.005, CI 0.45 – 0.51, Figure 7.4). There is a 1log increase in EBOV titre within Ifitm6 expressing A549 cells, the mechanism is unknown.

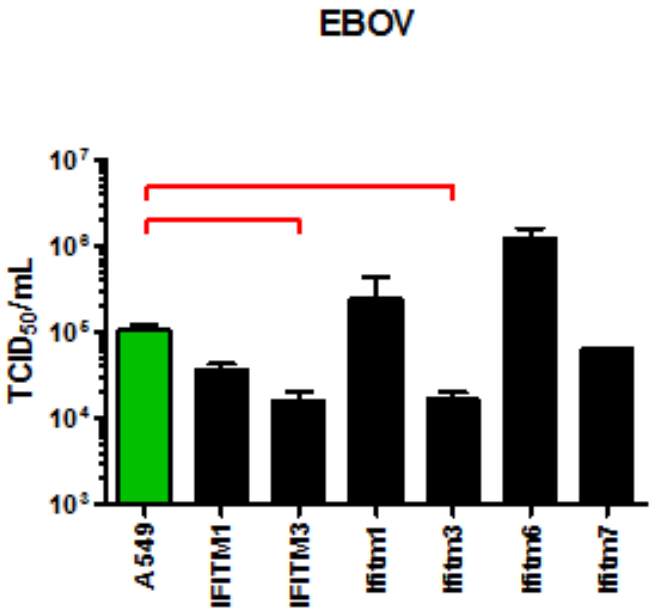

Figure 7.4: A549 cells expressing human IFITM and murine Ifitm proteins were inoculated with EBOV at a dose of MOI 1.0 and the supernatants sampled at 48 hrs. from which viral titrations were performed in VeroE6 cells and the result presented as mean+SD of the $TCID_{50}$/ml. Control cell wells are represented in green. $p < 0.05$

7.3.2 HeV infections:

Cells expressing IFITM proteins were permissive to HeV infection. Figure 7.5 is a representative image of infected cells to demonstrate staining by immunofluorescence; all other preparations were of similar appearance, differing only in the number of cells infected.

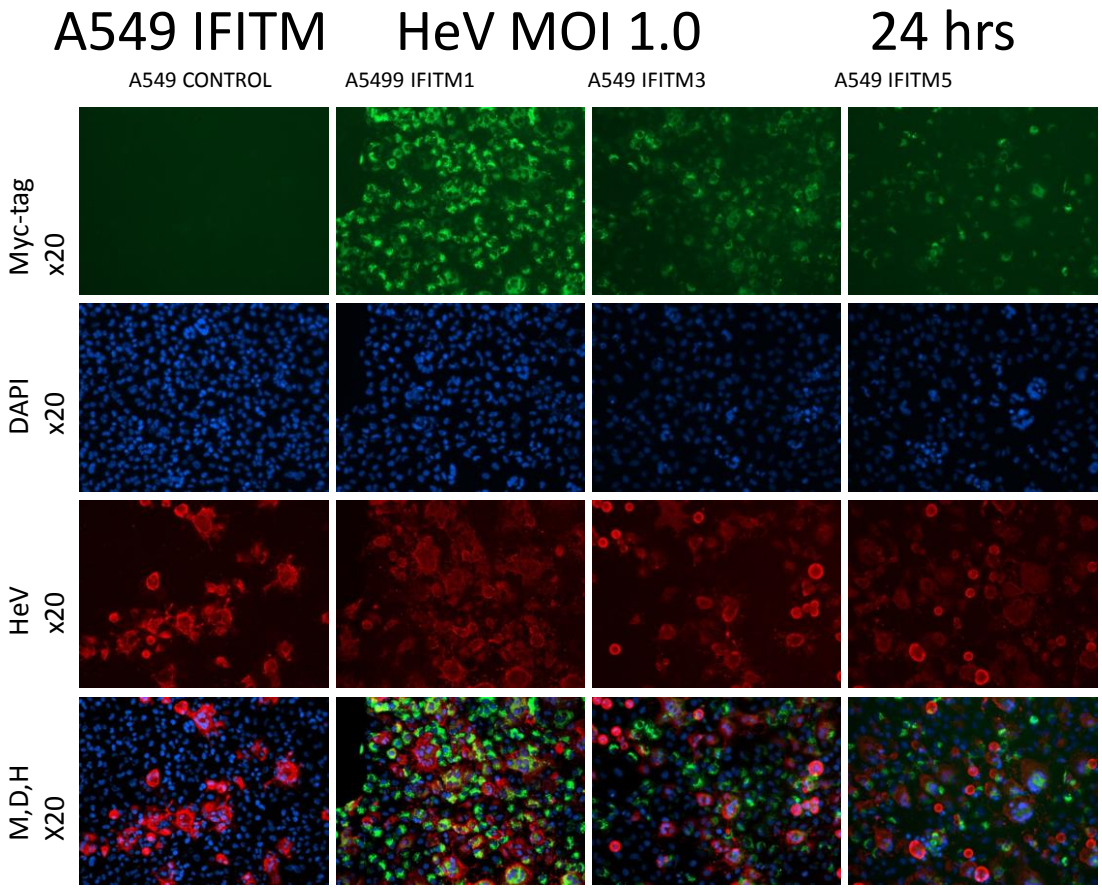

Figure 7.5: 20x magnification. A549 cells transduced to express IFITM1, inoculated with 1.0 MOI HeV and incubated for 24 hrs. Green fluorescent staining against Myc-C tagged IFITM expression, red fluorescent staining against HeV-P protein, and DAPI blue nuclear staining. M, D, H row represents image overlay for all 3 stains, Myc-tag, DAPI and HeV.

Cytopathic effect and cell fusion to form syncytia characteristic of paramyxoviral infection were observed and were similar in nature and extent to that of control cells. In syncytial cells, HeV antigen was located around the periphery whereas IFITM expression was centralised (Figure 7.6).

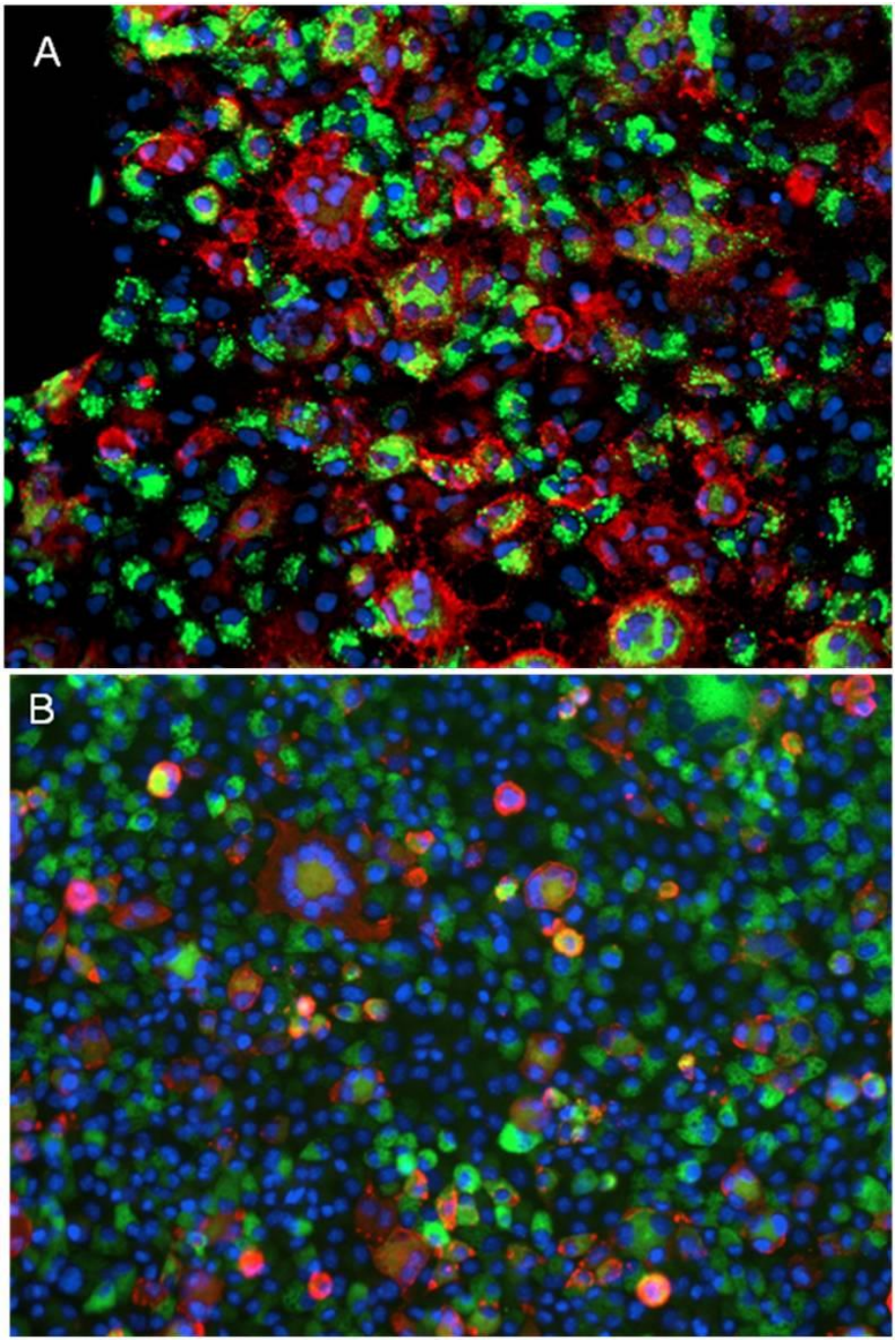

Figure 7.6: 20x magnification, A. A549 cells transduced to express IFITM1 and inoculated with 1.0 MOI HeV and incubated for 24 hrs. B. L929 cells transduced to express Ifitm1 and inoculated with 1.0 MOI HeV and incubated for 48 hrs. Green fluorescent staining against Myc-C tag, red fluorescent staining against HeV-P protein, and DAPI blue nuclear staining. Multiple syncytial cells are present in both preparations.

An MOI of 0.1 only resulted in a very small percentage of cells infected with HeV (Figure 7.7), consequently findings at the higher MOI of 1.0 were considered more likely to reflect any treatment effect.

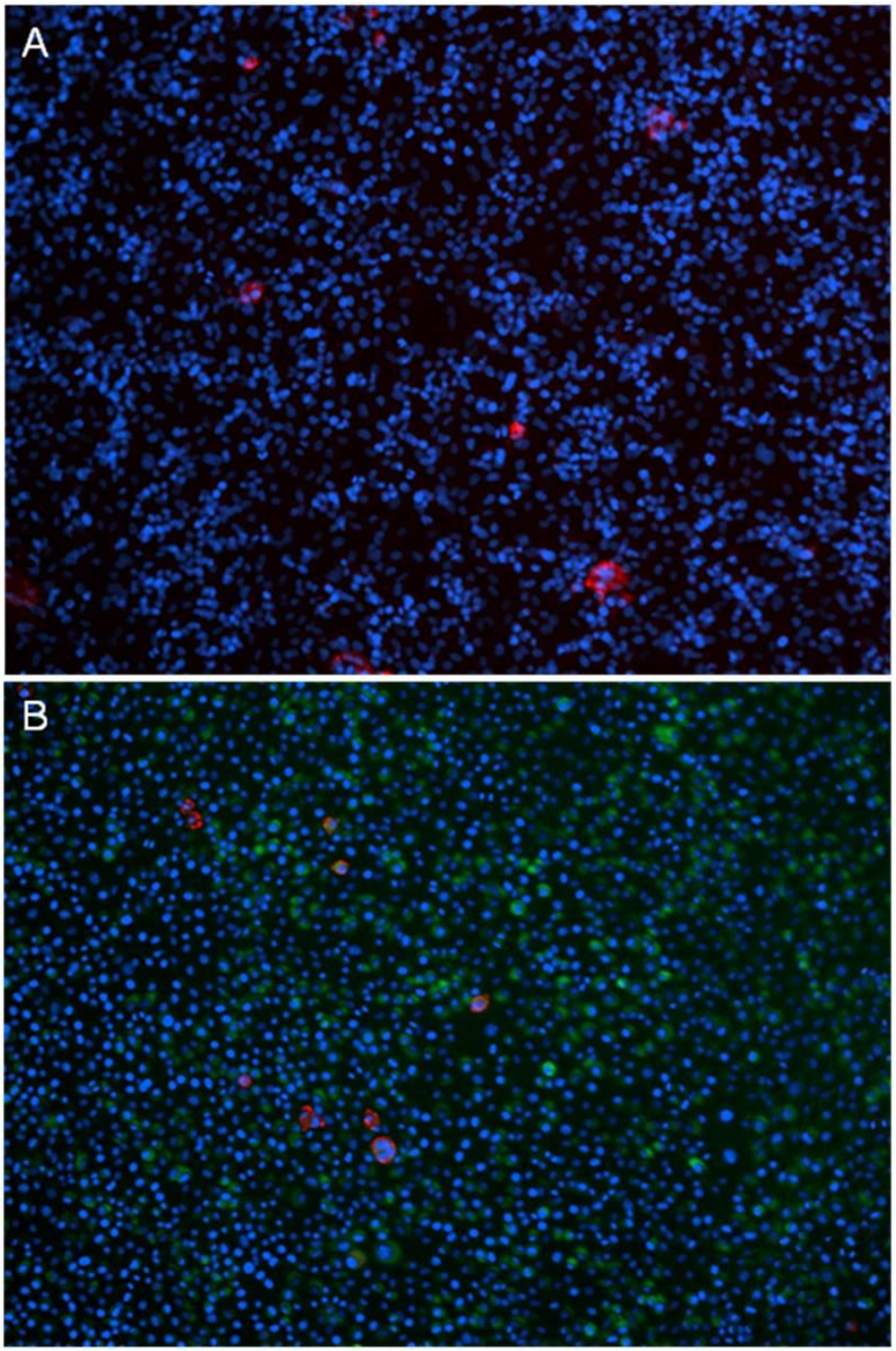

Figure 7.7: 10x magnification. A) A549 control cells and B) L929 cells transduced to express IFITM3, inoculated with 0.1 MOI HeV and incubated for 24 hrs. Green fluorescent staining against Myc-C tagged IFITM expression (which is negative in the A549 control cells), DAPI blue nuclear staining and red fluorescent staining against HeV-P protein, demonstrating <5% of cells are infected at this MOI.

7.3.2.1 Replication of infectious HeV is not restricted by over expression of human IFITM proteins in A549 cells

To determine whether over expression of IFITM proteins is associated with restriction in the production of infectious virions within human cells, A549 cells transduced to express IFITM1 or IFITM3, or vector alone were incubated with infectious HeV at an MOI of 1 and assessed after 24 and 48 hours incubation. There was no significant difference between virus titre in supernatant from control A549 cells and those expressing IFITM1 or IFITM3 (Figure 7.8).

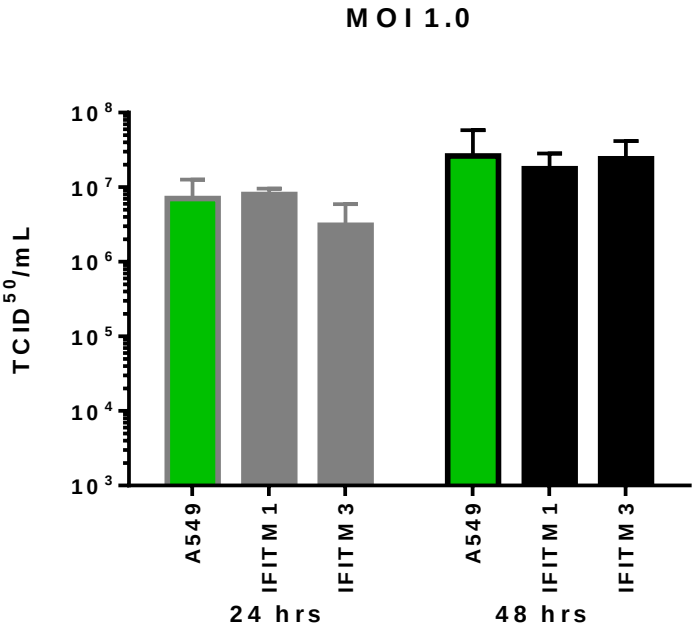

Figure 7.8: A549 cells expressing human IFITM proteins were inoculated with HeV at a dose of MOI 1 and the supernatants sampled at 24 and 48 hrs. Viral titrations were performed and the results presented as mean+SD of the $TCID_{50}$/ml. Control cell wells are represented in green. $p < 0.05$

7.3.2.2 The over-expression of murine *Ifitm2* or *Ifitm3* in A549 cells is associated with significant suppression of HeV infection compared to control A549 cells, and also to A549 cells expressing IFITM1, IFITM3, *Ifitm1*, *Ifitm6* or *Ifitm7*.

To determine whether expression of murine *Ifitm* proteins in human A549 cells is associated with restriction in the production of infectious virions compared to control A549 cells or the

same cells expressing human IFITMs, A549 cells were also transduced to express murine *Ifitm1, 2, 3, 6* or *7* or vector alone. These cells were incubated with infectious HeV at an MOI of 1 and results compared with A549 cells transduced to express IFITM1 and IFITM3 or vector alone (Figure 7.9).

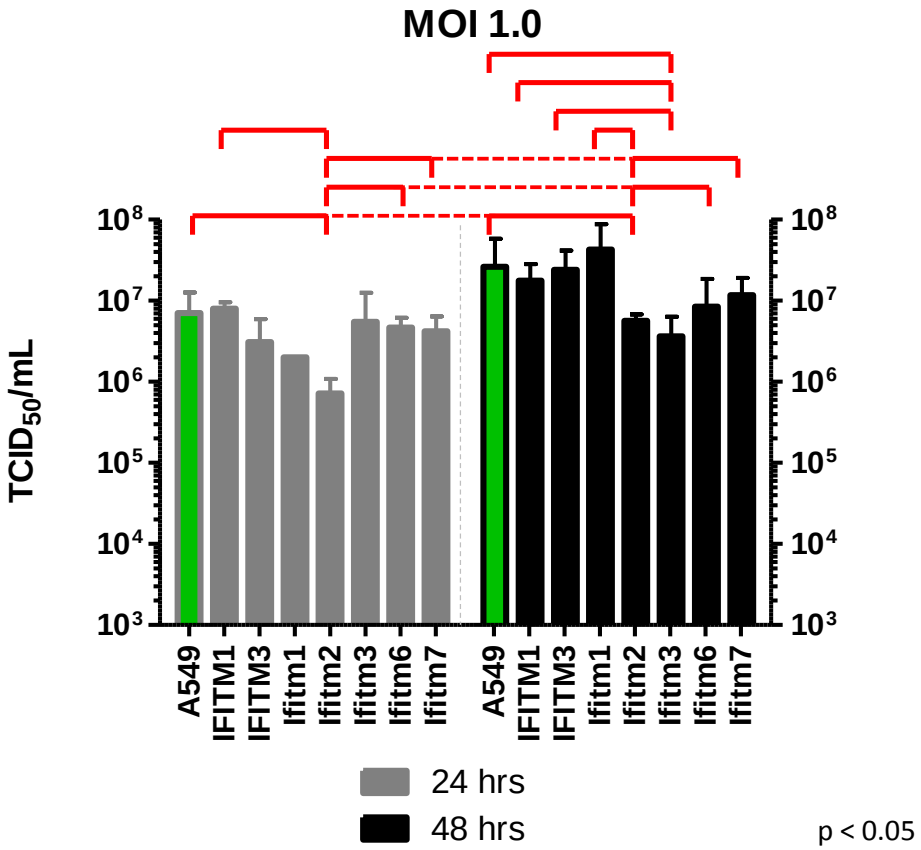

Figure 7.9: A549 cells expressing human IFITM and murine Ifitm proteins were inoculated with HeV at a dose of MOI 1 and the supernatants sampled at 24 and 48 hrs. Viral titrations were performed and the results presented as mean+SD of the $TCID_{50}$/ml. Control cell wells are represented in green. $p < 0.05$

Replication of HeV was significantly lower in A549 cells expressing murine *Ifitm2* compared to control cells at both 24 hours ($p = 0.003$) and 48 hours ($p = 0.022$), and at 24 hrs. HeV was significantly restricted in A549 cells expressing murine *Ifitm2* compared to IFITM1 ($p = 0.003$). *Ifitm2* provided greater suppression of HeV than the other murine *Ifitm* proteins, *Ifitm6* ($p = 0.016$) and *Ifitm7* ($p = 0.026$).

Murine *Ifitm3* also significantly suppressed replication of HeV in A549 cells compared to control cells at 48 hours (p = 0.040) and significantly restricted HeV replication in comparison to cells expressing IFITM1 (p = 0.043), IFITM3 (p = 0.021), and also *Ifitm1* (p = 0.011). There were no significant reductions in HeV titre observed in human cells expressing *Ifitm1, 6* or *7*.

7.3.2.3 The over-expression of murine *Ifitm1* or *Ifitm7* in L929 cells is associated with significant suppression of HeV infection compared to control L929 cells.

To determine whether expression of murine Ifitm proteins in murine L929 cells is associated with restriction in the production of infectious virions compared to control L929 cells, L929 cells were transduced to express murine *Ifitm1, 2, 3, 6* or *7*, or vector alone. These cells were incubated with infectious HeV at an MOI of 1 and assessed after 24 and 48 hours incubation.

There was a significant reduction in virus titre in L929 cells expressing either *Ifitm1* or *Ifitm7* at both 24 hours and 48 hours (*Ifitm1* pooled time points p = 0.028, CI 0.17 – 0.88, *Ifitm7* pooled time points p = 0.043 CI 0.11 – 0.96, Figure 7.10).

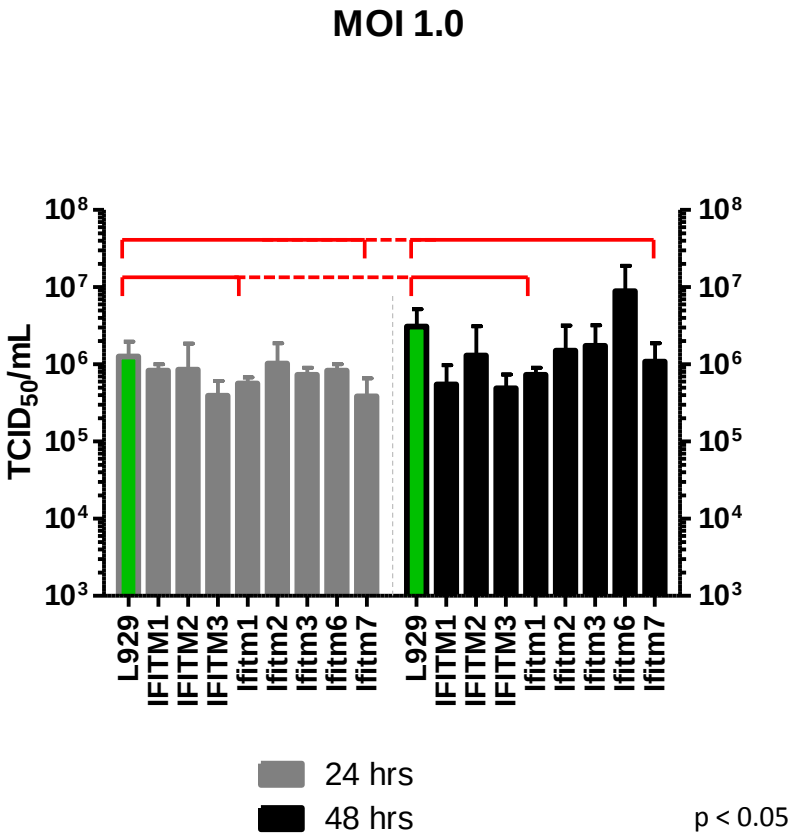

Figure 7.10: L929 cells expressing human IFITM and murine Ifitm proteins were inoculated with HeV at a dose of MOI 1 and the supernatants sampled at 24 and 48 hrs. Viral titrations were performed and the results presented as mean+SD of the $TCID_{50}$/ml. Control cell wells are represented in green. $p < 0.05$ and data was pooled across both time points.

7.3.2.4 The over-expression of IFITM1, IFITM2 or IFITM3 in L929 cells is not associated with significant suppression of HeV infection compared to control L929 cells, and also to cells expressing *Ifitm1, 2, 3, 6* or *7*.

To determine whether expression of human IFITM proteins in murine L929 cells is associated with restriction in the production of infectious virions compared to control L929 cells or the same cells expressing murine *Ifitm* proteins, L929 cells were also transduced to express human IFITM1, IFITM2 or IFITM3 or vector alone. These cells were incubated with infectious HeV at an MOI of 1 and results compared with L929 cells transduced to express *Ifitm1, 2, 3, 6* or *7* or vector alone.

There was no significant effect on viral titre when murine cells were expressing human IFITM proteins (Figure 7.10), however there is a possible trend for IFITM3 expression to restrict HeV infection at both time points ($p = 0.052$).

7.4 Discussion:

This experiment was a study incorporating a system of over expression of human and murine IFITM proteins in human lung carcinoma A549 cells and mouse fibroblast L929 cells for the purpose of assessing the effect of individual IFITM proteins on EBOV and HeV infectious virion production.

This study used plasmids supplied from the laboratory of Huang *et al.* (2011). Huang *et al* investigated the effect of expressing IFITM1, 2 and 3 in A549 cells on EBOV infection at an MOI of 15 over 72 hours of incubation. In their study all three IFITM proteins significantly suppressed EBOV infection. Unlike Huang *et al*., we did not observe a significant effect on infection from IFITM1 expression. Their study conditions allowed for a higher infection rate and longer incubation which could conceivably contribute to allowing greater effect. We did confirm the findings of Huang *et al* that in A549 cells the replication of infectious EBOV is restricted by IFITM3. In addition and not surprisingly, we showed that the murine ortholog to IFITM3, *Ifitm3*, also suppressed EBOV infection.

We compared the efficacy in suppression of HeV infectious virions in human IFITM versus murine *Ifitm* proteins in both cells of human (A549) and mouse (L929) origin. The over-expression of human IFITM proteins was not associated with significant suppression of HeV infection in human or mouse cells. Conversely, the over-expression of murine *Ifitm* proteins in both A549 cells (*Ifitm2* and *Ifitm3*) and L929 cells (*Ifitm1* and *Ifitm7*) was associated with statistically significant suppression of HeV infection.

However, while statistically significant differences were found in the reduction of viral titres by these murine *Ifitm* proteins for both cell types, the maximum observed reduction in HeV titre across the study was < 10 fold, with viral titres rarely falling below 10^6 $TCID_{50}$. To put this in a meaningful biological context, a dose of < 10^3 $TCID_{50}$ HeV is lethal for ferrets, hamsters, cats and guinea pigs (Hooper *et al.*, 1997b; Pallister *et al.*, 2011; Rockx *et al.*, 2011; Westbury *et al.*, 1995). Experimental studies in horses have used intravenous and

intranasal/aerosolised exposure to virus at doses of 10^6 $TCID_{50}$ (Hooper *et al.*, 1997b; Marsh *et al.*, 2011; Williamson *et al.*, 1998), and the African Green Monkey, thought to most closely reflect susceptibility of the human, typically succumbs to 10^5 $TCID_{50}$ HeV (Geisbert *et al.*, 2010). Earlier in this thesis we also demonstrated 10^4 $TCID_{50}$ was lethal in wild type mice. So, while there is a statistically significant reduction in viral titre by *in vitro* assessment, we suggest that the magnitude of the reduction is such that it may not translate to having biological significance at the whole animal level. Therefore, we propose that the quantitatively minor suppression in viral titres seen in cells over-expressing murine *Ifitm* proteins is unlikely to be the explanation for the *in vivo* differences we have observed for the nature and outcomes of HeV infection in mice compared to species such as the horse, human or ferret.

To further explore if the observed statistical significance was a true reflection of a biological effect or a chance observation, more replicates could be performed. Alternatively, other methods could be used to assess viral replication as viral titre calculations are relatively insensitive. Cell imaging systems to assess the percentage of infected cells would offer more precision and accuracy, but were unavailable for use in the PC3/PC4 environment. qPCR could be employed to quantify the number of gene copies present, but there are complexities inherent in the interpretation of gene copy numbers versus infective virions. Addition of a parallel study using siRNA depletion of endogenous IFITM proteins would also add robustness as an alternative method to confirm observations from cell over expression studies.

Addition of parallel studies using a pseudovirus delivery system containing only the entry proteins would help differentiate between entry restriction and inhibition of other phases of the viral lifecycle. HeV P gene proteins antagonise the IFN response in a range of cell types (Basler, 2012; Shaw, 2009; Virtue, 2011; Virtue *et al.*, 2011). However, an IFITM over expression assay should mitigate the effect of viral inhibition of the IFN response. Use of a pseudovirus delivery system containing only the HeV entry proteins, the attachment (G) and fusion (F) glycoproteins, would avoid any interference with IFN response by the P, V and W proteins. The high basal level of expression of IFITM proteins in barrier epithelial cells (Bailey *et al.*, 2012) provides an intrinsic first line defence in locations susceptible to viral exposure. Thus IFITM proteins are already present in significant concentration prior to any IFN

induction that may follow pathogen recognition, and therefore prior to any antagonistic effect that HeV proteins may cause on the interferon-mediated induction of IFITM proteins. For example, *Ifitm3* is concentrated on the apical plasma membrane of ciliated respiratory epithelial cells (Bailey *et al.*, 2012). Also, no change was documented in expression of IFITM2 and IFITM3 mRNA after infection with the Paramyxovirus RSV, and this was attributed to the already high level of basal expression (Zhang *et al.*, 2015). The expression of IFITM1, IFITM2 and IFITM3 is strongly up regulated by type I and type II interferons, and further experimental work could investigate whether this is affected by HeV mediated antagonism of the IFN response.

Despite having a lung epithelial cell origin, A549 cells have very low basal levels of IFITM expression (Brass *et al.*, 2009) whereas the basal level of *Ifitm* expression in L929 cells is undetermined. Rodent, and specifically murine, cell lines are less susceptible to HeV infection despite expressing the Henipavirus receptor molecule (Aljofan *et al.*, 2009; Yoneda *et al.*, 2006). In these cells, CPE is markedly reduced and delayed in onset compared to non-rodent cell lines. Moreover, A549 cells have very low basal levels of IFITM protein expression as well as a very low Henipavirus infection rate in comparison to another human respiratory cell line, Hep2, although both express the Henipavirus receptor molecule (Aljofan *et al.*, 2009). Potentiation of HeV infection by the presence of human IFITM proteins in both A549 and L929 cell lines was not observed in the present work. The more permissive nature and more rapid HeV infection dynamics seen in human cell lines, apart from A549 cells, compared to murine cell lines (Aljofan *et al.*, 2009; Yoneda *et al.*, 2006) are not explicable on the basis of human IFITM proteins acting as co-receptors to enhance viral entry, as has been shown to occur in a coronavirus (Xuesen *et al.*, 2014).

Over expression of IFITM proteins in this experiment had no apparent effect on cell-cell fusion. Syncytial cell formation as part of HeV CPE occurred frequently in cells over-expressing both human IFITM and murine *Ifitm* proteins. For viruses in the *Paramyxoviridae* family viral-cell membrane fusion occurs at the cell surface and at a neutral pH, and therefore viral entry is not expected to be affected by IFITM proteins. This was confirmed with SeV. SeV infection was not suppressed in HEK293T cells expressing IFITM1, 2 or 3 (Hach *et al.*, 2013). In comparison, EBOV fusion occurs in the endolysome (Diederich *et al.*, 2012; Huang *et al.*, 2011). IFITM2 and 3 are preferentially localised in late endosomal and

lysosomal membranes and have been shown to suppress EBOV infection (Huang *et al.*, 2011); the differential suppression is attributable to their subcellular location.

In summary, we found statistically significant suppression of HeV virus titres in A549 cells expressing *Ifitm2* and *Ifitm3* and in L929 cells expressing *Ifitm1* and *Ifitm7*, when compared to control cells. This occurred in the presence viral induced syncytial cell formation. Therefore, we propose that the minor levels of quantitative suppression of HeV viral titres seen are unlikely to be the explanation for the *in vivo* differences we have observed for HeV infection in mice compared to other species which are susceptible to severe systemic infection.

CHAPTER 8: GENERAL DISCUSSION

The henipaviruses, Hendra virus and Nipah virus, are unique among the paramyxoviruses in causing severe infection in a broad range of species leading to mortality in both humans and animals (Hooper *et al.*, 2001; Hooper & Williamson, 2000; Williamson & Torres-Velez, 2010; Wong & Ong, 2011). The clinical spectrum of HeV and NiV disease in both humans and other animals includes respiratory and/or neurological disease, with factors such as age and dose of virus influencing disease presentation in experimental animals (Dups *et al.*, 2012; Geisbert *et al.*, 2010; Guillaume *et al.*, 2004; Guillaume *et al.*, 2006; Guillaume *et al.*, 2009; Hooper *et al.*, 1997b; Rockx *et al.*, 2011). In both humans and animal models of infection the characteristic pathological features of HeV and NiV infection are disseminated vasculitis with endothelial syncytia and necrosis of parenchymal and lymphoid organs (Hooper *et al.*, 2001; Hooper & Williamson, 2000; Williamson & Torres-Velez, 2010; Wong & Ong, 2011). Severe and destructive multi-systemic pathology is seen in cases of natural infection of humans with NiV and HeV (Hooper *et al.*, 2001; Wong & Ong, 2011) and natural infection of horses with HeV (Hooper *et al.*, 1997a). On the other hand, in both natural porcine NiV infection (Mohd Nor *et al.*, 2000) and canine HeV infection (Kirkland *et al.*, 2015), there are lesions associated with systemic viral infection but infected animals manifest subclinical to mild disease. This suggests that the severe systemic disease may be enabled by, and reflect differences in, post-entry innate immune responses.

Thus far, field disease associated with henipaviruses has only been recognised in Australia, Malaysia, Singapore, India and Bangladesh. However evidence of the presence of Henipa or Henipa-like viruses in bats, including other than fruit bats, has been detected across Central and South America, Africa, Asia, and Oceania (Clayton *et al.*, 2013) adding a truly global perspective to this group of emerging viruses.

Ecological drivers of pathogen spill over are undoubtedly complex and cross disciplinary approaches are required for increased understanding, especially in terms of developing approaches to preparedness. For example, different epidemiological modelling systems are being applied in order to better understand and predict disease emergence (Hayman *et al.*, 2013; Plowright *et al.*, 2011), while the recent characterisation of the immune

transcriptome of the Australian flying fox, *Pteropus alecto* (Papenfuss *et al.*, 2012; Zhang *et al.*, 2013a) will be useful for further investigations into understanding the control of viral replication in bats.

In November 2012 a commercial HeV sub-unit vaccine for horses was released (Middleton *et al.*, 2014). The vaccine induces virus neutralising antibody which protects horses from lethal Hendra virus challenge, eliminates viral shedding and prevents viral replication in tissues. Not only does this protect the health of the horse, but more importantly breaks the chain of transmission, thereby reducing the risk to people in contact with horses. In one study only 56% of horse owners in the state of Queensland chose to vaccinate their horses with the HeV vaccine (Goyen *et al.*, 2017). Vaccine release was expedited for altruistic reasons (protection of humans and horses from a lethal disease) and initially it was available under a minor use permit. This created concerns about vaccine safety, cost, and effectiveness (Goyen *et al.*, 2017; Manyweathers *et al.*, 2017). The vaccine was fully registered in August 2015 and 12 monthly boosters (as opposed to the initial recommendation of 6 monthly) were approved in May 2016. Significant social media commentary about frequency and severity of supposed post-vaccination side-effects that are perceived to be inappropriately acknowledged by the pharmaceutical company persist (Goyen *et al.*, 2017; Manyweathers *et al.*, 2017). Both Goyen *et al.* (2017) and Manyweathers *et al.* (2017) also reported a disconcerting trend of distrust towards veterinary surgeons with a high number of non-vaccinating horse owners considering money making as the main motivator for veterinarians recommending and conducting HeV vaccinations. As expected, spill-over infections of HeV in horses continue to occur in unvaccinated animals as there are no proven controls for exposure to virus. Although, the lower frequency in spill over events since their height in 2011 may have contributed to a lower perception in the immediacy of Hendra virus risk by horse owners (Manyweathers *et al.*, 2017) and be contributing to reduced vaccine uptake. Continuing effort is expended on education regarding disease awareness, with a view to encouraging ongoing vaccine uptake among the horse owning community. However, while unvaccinated horses remain in the environment, there is ongoing potential for human Hendra virus infection.

The human monoclonal antibody m102.4 has shown promise as a post-exposure therapeutic for henipavirus infection in laboratory animals (Bossart *et al.*, 2011; Bossart *et*

al., 2009). Although m102.4 is available for post-exposure use in people on a case by case basis, its value in the management of human clinical illness remains uncertain and it is important to continue the search for new effective anti-viral therapies. As the wild-type mouse was reportedly susceptible to infection with HeV but resistant to its systemic manifestations, this thesis investigated the extent to which elements of the mouse immune system may be key to providing such an antiviral effect. The wide range of murine immunological and biochemical reagents, their small size, ready availability, and ease of handling also make the mouse ideal for use in addressing this particular research question under BSL-4 conditions.

8.1 Wild type mice exhibit subclinical infection or acute neurological disease when exposed IN to a range of doses of HeV

Chapter 3 described the infection phenotype induced in C57BL6 mice following IN exposure to HeV at different doses, ranging from 5 to 500 000 $TCID_{50}$. Mice displayed only subclinical or acute neurological infection phenotypes; a systemic infection phenotype was not observed. Mice developed transient upper and lower respiratory tract infection and, where it occurred HeV replication in brain was attributable to anterograde infection of olfactory sensory neurones. These findings generally aligned with the observations made by Dups *et al.* (2012).

The incidence of HeV infection was dose-dependent, with estimated ID_{50} similar for both 7-day and 21-day studies ($5 \times 10^{4.1}$ $TCID_{50}$ and $5 \times 10^{3.7}$ $TCID_{50}$ respectively). Overall, and compared to findings in other animals, these observations support an innate resistance of mice to systemic HeV infection. It was also shown that subclinical or neurological infection phenotypes could not be reliably induced by selection of exposure dose or study length, although there was a higher tendency for neurological disease to be manifest following larger doses of virus. It was therefore acknowledged that neurological infection phenotypes would likely complicate subsequent studies of control of systemic HeV replication.

8.2 Mice deficient in interferon signalling show more widespread HeV replication without developing a systemic infection phenotype after both IN and IP exposure to HeV

Chapter 4 demonstrated that there was an increased role for viraemia in HeV infection of IFN-signalling deficient mice compared to WT mice following IN exposure. This was manifest

as increased likelihood of HeV replication in spleen, higher viral genomic loads in spleen, re-isolation of virus from some spleen samples, and evidence for HeV replication in liver, ependymal cells and vascular endothelium. However, apart from upper respiratory tract and brain, significant pathological lesions were not identified in the tissues involved. Also, no constitutional signs of infection were seen, apart from loss of body weight prior to euthanasia for neurological disease, which was consistent with minimal physiological impact of infection across all test groups. Accordingly, a systemic infection phenotype was not recorded. Lesions in brain were consistent with anterograde neurological infection via olfactory sensory neurones, as also seen in WT mice controls and the WT mice from Chapter 3.

Chapter 5 demonstrated an enhanced role for viraemia in HeV infection of WT mice exposed IP, manifest as replication of virus in spleen and viral genomic loads in spleen that were comparable to IFN-signalling deficient mice. *Ifnar1-/-*, *Ifnar2-/-* and *Stat 1-/-* mice were also reliably infected with HeV via the IP route but, in contrast to WT mice exposed IP, also regularly developed CNS infection with neurological disease. The anterior olfactory tract remained the preferred site of HeV replication within the CNS of these mice, but in this instance the neuropathogenesis was most likely haematogenous rather than anterograde infection from the inoculum. As in Chapter 4, subclinical and neurological infection phenotypes only were recorded. Virus replication in the spleen, liver, ependymal cells and vascular endothelium of IFN-signalling deficient mice was not accompanied by inflammatory or necrotising lesions, and no constitutional signs of infection were seen (apart from loss of body weight prior to euthanasia for neurological disease). Thus a systemic infection phenotype was not observed even though opportunity for its expression had been optimised by IP exposure. These findings contrast to the outcome of enteral and parenteral routes of exposure to HeV infection in other immunologically intact animals, where fulminating systemic infection is regularly seen.

The data generated in Chapters 4 and 5 confirmed that the resistance of mice to widespread HeV replication and fulminating systemic disease may not be attributed solely to the efficacy of mouse interferon signalling pathways against HeV-mediated anti-interferon mechanisms.

8.3 Viral strain-dependent variation in pathogenicity was not able to be confirmed

Chapter 6 compared the infection characteristics following IN exposure of WT and *Ifnar1-/-* mice to HeV/Australia/Horse/2008/Redlands (the viral strain used for all other experiments in this thesis) and HeV/Australia/Horse/1994/Hendra (the only viral strain to have been shared with international research groups). The observation, in contrast to the findings of this thesis, of Dhondt *et al.* (2013) that *Ifnar1-/-* mice exposed IN to HeV failed to develop clinical disease prompted a comparison of the pathogenicity of two HeV strains isolated 14 years apart.

Overall, the findings in WT and *Ifnar1-/-* mice exposed IN to HeV/Australia/Horse/2008/Redlands were considered qualitatively similar to those described in Chapter 4. HeV/Australia/Horse/1994/Hendra also reliably infected both WT and *Ifnar1-/-* mice exposed IN: virus replication was confirmed in brain but, unlike HeV/Australia/Horse/2008/Redlands, all mice had a subclinical phenotype. The histological features of meningoencephalitis of the anterior olfactory tract were qualitatively similar following HeV/Australia/Horse/1994/Hendra to those associated with exposure to HeV/Australia/Horse/2008/Redlands.

However, closer review of outcomes of exposure of WT mice across Chapters 4 and 6 in the context of bridging controls suggested that, for reasons that were not determined, WT mice exposed IN to HeV/Australia/Horse/2008/Redlands in Chapter 6 had been less permissive to virus replication in brain and also to the development of neurological disease. On that basis it was concluded that there may have been opportunity for underestimation of the pathogenicity of HeV/Australia/Horse/1994/Hendra in this study.

It was therefore not possible to confirm a viral strain-dependent difference in neuropathogenicity, or to attribute the observations of Dhondt *et al.* (2013) in *Ifnar1-/-* mice to the impact of virus strain. Additional studies with more mice would be required to reduce the impact of nuisance variables and the effect of chance. If a difference in neuropathogenicity was able to be confirmed, then this would provide the opportunity for further work to determine which individual viral components, or host responses to viral infection, influenced neurological virulence.

8.4 Murine Henipavirus research reported during the course of this thesis

During the course of this thesis there were 5 papers published involving Henipavirus infection in mice. The first of these, Dups *et al.* (2012), was published at the very start of research for this thesis, provided much guidance, and hence is extensively cited throughout this thesis. Dups *et al.* (2012) reprised the role of the mouse in Henipavirus research by demonstrating the development of neurological disease which was attributable to anterograde infection of the CNS via olfactory sensory neurones. There was also a transient respiratory tract infection which was successfully controlled without evidence of a robust adaptive immune response in the form of virus-neutralising antibodies, although most mice had binding antibody responses to HeV sG by Luminex assay (Dups *et al.*, 2012). Findings in WT mice exposed to HeV IN in this thesis were generally similar to the observations made by Dups *et al.* (2012), although this thesis made additional observations regarding dose-responses. The lack of systemic disease development in the WT mouse model of anterograde HeV encephalitis will be an important tool for further studies on Henipavirus neuropathogenesis.

The second paper was by Dhondt *et al.* (2013) and reported lethal HeV infection *Ifnar1-/-* mice on a C57BL6 background exposed by the IP but not the IN route. Affected mice had non-suppurative meningoencephalitis, but no description was provided of the anatomical distribution of HeV in the brain, specifically in relation to the olfactory pathway. Mice were also reported to show necrotising alveolitis and vasculitis. However, the essential diagnostic features of vasculitis, namely the "presence of inflammatory cells within and around the blood vessel wall with concomitant vessel wall damage as indicated by fibrin deposition, collagen degeneration, and necrosis of endothelial and smooth muscle cells" (2007), are not well demonstrated within the images of brain and lung that were provided in support of this statement. The outcome of IP exposure of WT mice to HeV was not described although they were reportedly resistant to infection by NiV.

Although Dhondt *et al.* (2013) reported that *Ifnar1-/-* mice were resistant to HeV disease after IN exposure, viral genome was found in brain tissue and neutralising antibody had developed in most mice, satisfying the definition of infection used throughout this thesis. The key distinction between the conclusions of Chapters 4 and 5 in this thesis and those

reported by Dhondt *et al.* (2013) was in respect of the susceptibility of IFN-signalling deficient mice to infection after IN exposure. Failure to make a similar interpretation from their infection data is critical to the main conclusion of Dhondt *et al.* (2013) that "Type 1 inferon signaling protects mice from lethal henipavirus infection", a conclusion which this author considers to be unsupported also on the basis of the evidence generated in Chapters 4 and 5. Chapter 6 aimed to address the differences in clinical findings between those reported by Dhondt *et al.* and Chapters 4 and 5 of this thesis, namely the likelihood of IFN-signalling deficient mice showing a neurological infection phenotype after IN exposure to HeV. However, further infection studies with larger numbers of mice will be required to determine whether there is a viral strain-dependent difference in neuropathogenicity, or to be able to attribute the difference in observations by Dhondt *et al.* (2013) in *Ifnar1-/-* mice to the impact of virus strain.

Dhondt *et al.* (2013) albeit very briefly, also reported NiV infection of wild type C57Bl/6 mice. While wild type mice did not succumb to IP NiV challenge, small amounts of NiV N gene was present on PCR within the lung and spleen of some mice and was taken by the authors to mean that subclinical infection had occurred. Mild inflammation of the brain was also reported, but no viral antigen was present on immunohistochemical staining. There was no data presented for IN challenge of wild type mice.

The third paper (Dups *et al.*, 2014) describes NiV infection in WT mice after IN exposure as being confined to a self-limiting and subclinical lower respiratory tract infection in the absence of a neutralising antibody response. There was no evidence of rhinitis but the duration of the study (21 days) may have missed transient infection of the olfactory mucosa. There was no evidence of virus replication in the brain. This finding contrasts with the encephalitis associated with HeV infection, and suggests that NiV infection in WT mice may be less productive with a "categorical difference" in the pathogenicity of these closely related henipaviruses in mice. As mice were from the same source, of the same age, and were exposed under similar experimental conditions as previously reported for HeV studies (Dups *et al.*, 2012) the differences in study outcomes were proposed to be because of viral not host factors. Further study involving comparison of HeV and NiV viral factors may be used to elucidate the factors determining neuropathogenicty and/or neuroprotective mechanisms in immunologically intact mice.

The fourth paper (Yun *et al.*, 2015) generated a firefly luciferase-expressing NiV and monitored virus replication and spread in infected *Ifnar1-/-* mice via bioluminescent imaging. Following IN infection with NiV, bioluminescence was present in the salivary glands, olfactory bulb and spleen of *Ifnar1-/-* mice. Their findings paralleled those described for *Ifnar1-/-* mice exposed IN to HeV in in Chapter 4 of this thesis. In contrast, IP exposure to NiV resulted in bioluminescence throughout the abdominal cavity with highest levels within the spleen and progressive spread to the upper and lower respiratory tract and nasal turbinates. This was followed by increasing bioluminescence in the olfactory bulb which corresponded to the development of acute neurological disease. The reported signs of hunched posture, hyperreflexia, lethargy and seizure activity are similar to those seen in HeV infected mice with neurological disease throughout this thesis. The findings are also consistent with the systemic infection reported in *Ifnar1-/-* mice exposed to NiV by the IP route by Dhondt *et al.* (2013) but suggest that viral entry to the brain occurs via the olfactory tract following extension from respiratory tract infection. This paper also describes a reverse genetics system that allows chimeric virus constructions, which promises to be a useful tool in identification of genetic determinants of the differences seen between NiV and HeV infection. Combined, the chimeric viruses and bioluminescent imaging techniques described by Yun *et al.* (2015) could allow spatial and temporal evaluation of live virus infection within the host, which would be a significant advance in techniques for pathogenesis studies that have previously been limited to serial euthanasia.

The final paper by Valbuena *et al.* (2014) describes a human lung xenograft mouse model of NiV infection. These authors engrafted small fragments of human foetal lung tissue into the dorsal subcutaneous space of severely immunodeficient mice, NSG (NOD/SCID/ɣcnull) mice and exposed the grafts to NiV in a controlled study. NiV replicated to high levels in directly exposed and also control sites, consistent with haematogenous spread of the virus from inoculated infected graft tissue to the non-inoculated graft tissue. Infectious virus was also detected within a range of mouse tissues including brain, heart, lung, spleen and kidney as further evidence of viraemia, although the mice remained clinically well. Histological features of NiV infection in the human lung tissue included characteristic syncytial cell formation in bronchial and alveolar epithelium as well vascular endothelium, necrosis, haemorrhage and vasculitis: there were no lesions seen associated with NiV replication in

mouse tissues. An inflammatory infiltrate did not feature within the human lung tissue, nor in any mouse organ. The authors attributed this to the severe deficits in both innate and adaptive immune responses in these mice. However, given the findings in this thesis of a lack of lesions associated with HeV infection in tissues of in IFN-signalling deficient mice, this could be taken to further support an overarching murine response pattern of little tissue response to systemic Henipavirus infection. Interestingly Valbuena *et al.* (2014) also reported infectious NiV within the brain of NSG mice, but the distribution of viral antigen was not described and the mice remained clinically healthy for 10 days post exposure, until the end of the experiment.

8.5 HeV replication and cytopathic effect continues in the presence of IFITM proteins

The mouse infection chapters of this thesis have shown that productive HeV infection occurs in mice but, unlike other animal species susceptible to systemic HeV infection, neither vasculitis, with vascular wall degeneration and inflammatory cell infiltration, nor necrotising lesions within infected viscera were identified in WT or IFN-deficient mice. It is therefore unlikely that restriction of systemic pathology in mice is solely attributable to inhibition by interferon. However, infection in WT mouse lung is cleared with negligible neutralising antibody response (Dups *et al.*, 2012) and little neutralising antibody response was seen in infected IFN-signalling deficient mice in this thesis, suggesting an innate response mechanism remains relevant to limiting the systemic effects of infection.

To this end, Chapter 7 investigated the effect of both human and murine IFITM proteins on HeV replication in human and mouse derived cell lines. The choice to investigate IFITM was made because barrier epithelial cells have a high basal level of expression of IFITM proteins (the expression of IFITM1, 2 and 3 is also strongly upregulated by type I and type II interferons) and IFITM proteins both restrict viral entry and inhibit the production of infectious virions. Additionally IFITM1, 2 and 3 restrict viral membrane fusion induced by all three classes of viral fusion protein. Therefore effects attributable to the actions of IFITM protein were a potential explanation for the the absence of syncytial cell development and possible lack of systemic lesions in HeV infected mice. The lack of syncytia in mice is a strikingly different feature of the HeV infection pathology compared to other susceptible species such as humans, non-human primates, ferrets, cats and horses (Hooper *et al.*, 2001).

Cell fusion is important in the perpetuation of cell to cell infection with HeV, and fusion induced disruption of cellular architecture contributes to organ pathology (Wong & Tan, 2012).

However, syncytial cell formation was present *in vitro* and the reduction of viral titres by IFITM and *Ifitm* proteins in both human and murine cell types was not considered biologically significant. The maximum observed reduction in HeV titre across the study was < 10 fold, with viral titres rarely falling below 10^6 $TCID_{50}$, the IFITM overexpressing cell cultures still maintained HeV replication above the lethal infectious dose for ferrets, hamsters, cats and guinea pigs (Hooper *et al.*, 1997b; Pallister *et al.*, 2011; Rockx *et al.*, 2011; Westbury *et al.*, 1995).

The inhibitory effect of another innate immune protein galectin-1 has described for NiV infections in vitro (Garner *et al.*, 2010; Levroney *et al.*, 2005).

8.6 Summary and future directions

The mouse infection studies of this thesis have described the impacts in WT mice of HeV exposure dose IN, the outcome of HeV infection in WT and IFN-signalling deficient mice following IN and IP exposure, and a comparison of responses in such mice following IN exposure to two strains of HeV. Lethal encephalitis and also subclinical infection occurs in both IFN-signalling deficient mice and WT mice exposed IN, with pathology limited to the nasal cavity and CNS. A systemic infection phenotype, characterised by malaise, disseminated viral replication in major organs, and associated pathological lesions, was not found in any mouse strain studied. Similar outcomes were found for IP exposure, except that WT mice were largely protected from CNS involvement by this exposure route. Failure to establish systemic HeV-associated disease in mice deficient in the main antiviral innate immune system components of the IFN type 1 response alone (*Ifnar1-/-* and *Ifnar2-/-* mice) or with attenuation of type 1, 2 and 3 IFN responses combined (*Stat1-/-* mice) confirms the resistance of WT mice to systemic disease cannot be attributed solely to the efficacy of mouse interferon signalling pathways against HeV-mediated anti-interferon mechanisms. The findings of the viral strain comparison study did not permit any conclusion to be drawn regarding differences in the neuropathogenicity of two strains of HeV. On that basis, the

hypothesis that either *Ifnar1-/-* (or possibly even WT mice) may be of value in studying control mechanisms against HeV-induced encephalitis remains open.

The quantitatively minor suppression in viral titres seen in cells over-expressing murine *Ifitm* proteins is also unlikely to be the explanation for the *in vivo* differences we have observed for the nature and outcomes of HeV infection in mice compared to species such as the horse, human or ferret. An as yet unidentified innate response mechanism may limit the systemic effects of Henipavirus infection in mice.

Further study of HeV infection in mice is clearly warranted, in order to further elucidate the innate protective mechanisms against systemic disease as well as the mechanisms by which virus establishes in brain and induces encephalitis. For example, humanised mice (NSG mice with human haematopoietic stem cells) with human tissue xenografts may allow further investigation of the human inflammatory response in human tissues in mice infected with henipaviruses. Gene expression studies in infected mice tissue, and gene array bioinformatics studies may provide more in-depth analysis of innate immune responses at a molecular level. Identifying factors up- or down- regulated during Henipavirus infection in murine tissues, such as the lung or spleen, may also direct new concepts around the development of targeted anti-HeV therapeutics. For this thesis, the resources available within the BSL4 laboratory precluded such in-depth studies, and degradation of RNA transferred through the barrier to an external laboratory meant that it did not maintain sufficient quality of preservation to be analysed further. Enhanced capability that would enable more sophisticated studies to be carried out within BSL4 laboratories would provide a step-change in research outcomes for work with BSL4 pathogens.

APPENDIX 1

Chapter 4, qPCR data, Log_{10} HeV-N gene copies normalised to 18S in different organs with mean.
Comparison of genomic load in tissues between ferrets, horses and mice.

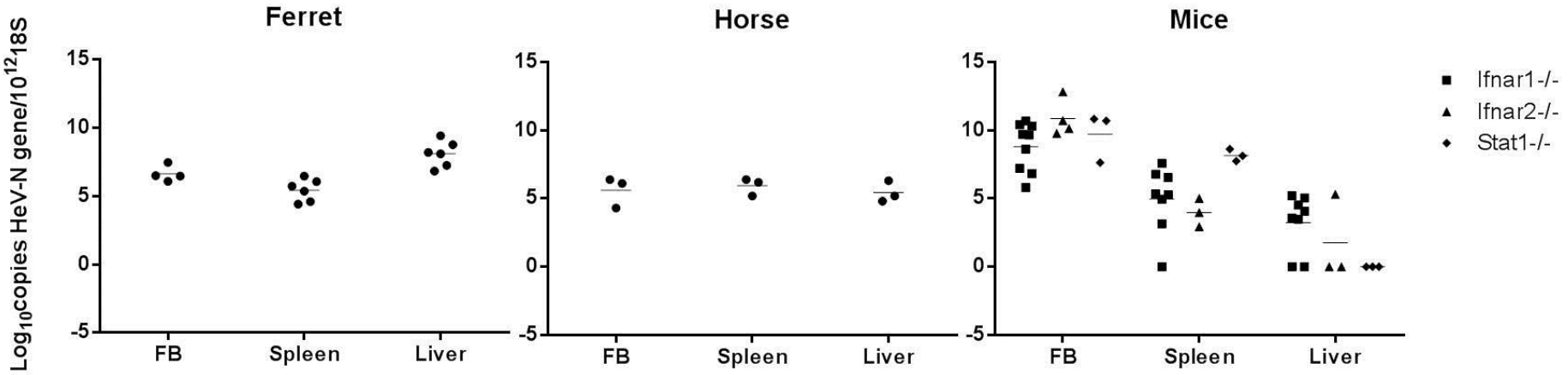

Figure A1: Control ferret data from Pallister *et al.* (2011) compared to horse data from Marsh *et al.* (2011) and data from interferon-signalling deficient from Chapter 4 (Pilot study, Study 1 and Study 2 combined). FB = forebrain

APPENDIX 2

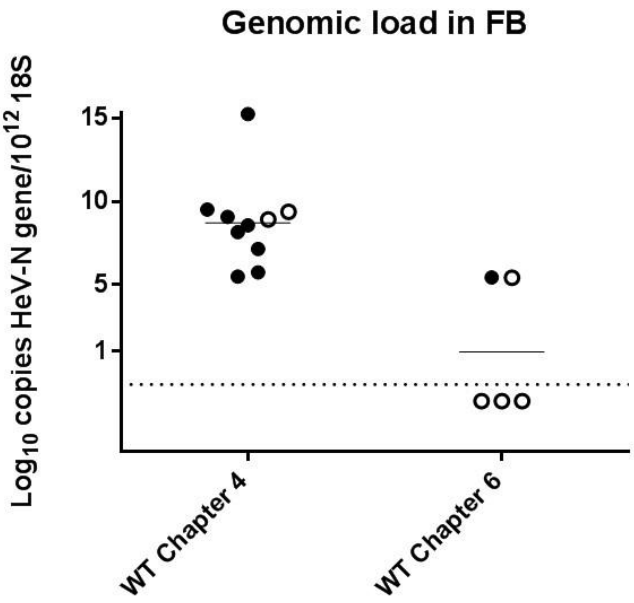

Figure A2: Levels of viral genome in forebrain, showing mean, for WT mice in Chapter 4 and Chapter 6.
Open circle: subclinical phenotype
Closed circle: neurological phenotype

Table A2.1: Contingency table comparisons of likelihood of virus replication within the forebrain of WT mice in Chapters 4 and 6

FB genome and or antigen	Positive	Negative
WT Chapter 4	10	0
WT Chapter 6	2	3

Table A2.2: Contingency table of infection phenotype comparisons between WT mice in Chapters 4 and 6

Infection Phenotype	Subclinical	Neurological
WT Chapter 4	2	8
WT Chapter 6	4	1

Table A2.3: Contingency table comparisons of likelihood of virus replication within the forebrain of Ifnar1-/- mice in Chapters 4 and 6

FB genome and or antigen	Positive	Negative
Ifnar1-/- Chapter 4	9	1
Ifnar1-/- Chapter 6	5	0

Table A2.4: Contingency table of infection phenotype comparisons between Ifnar1-/- mice in Chapters 4 and 6

Infection Phenotype	Subclinical	Neurological
Ifnar1-/- Chapter 4	1	9
Ifnar1-/- Chapter 6	2	3

REFERENCES

Abdullah, S., Chang, Y. L., Rahmat, K., Goh, J., & Tan, C. T. (2012). Late-onset Nipah virus encephalitis 11 years after the initial outbreak: a case report. *Neurology Asia, 17*(1), 71-74.

AbuBakar, S., Chang, L. Y., Mohd Ali, A. R., Sharifah, S. H., Yusoff, K., & Zamrod, Z. (2004). Isolation and molecular identification of Nipah virus from pigs. *Emergerging Infectious Diseases 10*(12), 2228-2230. doi: 10.3201/eid1012.040452

Aguilar, H. C., & Iorio, R. M. (2012). Henipavirus membrane fusion and viral entry. In Benhur Lee & Paul Rota (Eds.), *Current Topics in Microbiology and Immunology-Henipavirus* (Vol. 359, pp. 79-94). Berlin, Heidelberg: Springer.

Aljofan, M., Saubern, S., Meyer, A. G., Marsh, G., Meers, J., & Mungall, B. A. (2009). Characteristics of Nipah virus and Hendra virus replication in different cell lines and their suitability for antiviral screening. *Virus Research, 142*(1-2), 92-99. doi: 10.1016/j.virusres.2009.01.014

Allworth, T., O'Sullivan, J., Selvey, L., & Sheridan, J. (1995). Equine morbillivirus in Queensland. *Communicable Diseases Intelligence, 19*(22), 575-575.

Amini-Bavil-Olyaee, S., Choi, Youn J., Lee, Jun H., Shi, M., Huang, I. C., Farzan, M., & Jung, Jae U. (2013). The antiviral effector IFITM3 disrupts intracellular cholesterol homeostasis to block viral entry. *Cell Host & Microbe, 13*(4), 452-464. doi: 10.1016/j.chom.2013.03.006

Anafu, A. A., Bowen, C. H., Chin, C. R., Brass, A. L., & Holm, G. H. (2013). Interferon-inducible transmembrane protein 3 (IFITM3) restricts reovirus cell entry. *Journal of Biological Chemistry, 288*(24), 17261-17271. doi: 10.1074/jbc.M112.438515

Ank, N., West, H., Bartholdy, C., Eriksson, K., Thomsen, A. R., & Paludan, S. R. (2006). Lambda interferon (IFN-λ), a Type III IFN, is induced by viruses and IFNs and displays potent antiviral activity against select virus infections in vivo. *Journal Of Virology, 80*(9), 4501-4509. doi: 10.1128/jvi.80.9.4501-4509.2006

Augustin, H. G., & Reiss, Y. (2003). EphB receptors and ephrinB ligands: regulators of vascular assembly and homeostasis. *Cell and Tissue Research, 314*(1), 25-31. doi: 10.1007/s00441-003-0770-9

Bailey, C. C., Huang, I. C., Kam, C., & Farzan, M. (2012). Ifitm3 limits the severity of acute influenza in mice. *PLoS Pathogens, 8*(9), 1-11. doi: 10.1371/journal.ppat.1002909

Bailey, C. C., Zhong, G., Huang, I.-C., & Farzan, M. (2014). IFITM-family proteins: the cell's first line of antiviral defense. *Annual Review of Virology, 1*(1), 261-283. doi: 10.1146/annurev-virology-031413-085537

Baker, K. A., Dutch, R. E., Lamb, R. A., & Jardetzky, T. S. (1999). Structural basis for Paramyxovirus-mediated membrane fusion. *Molecular Cell, 3*(3), 309-319. doi: 10.1016/S1097-2765(00)80458-X

Baños-Lara, M. D. R., Ghosh, A., & Guerrero-Plata, A. (2013). Critical role of MDA5 in the interferon response induced by human Metapneumovirus infection in dendritic cells and in vivo. *Journal Of Virology, 87*(2), 1242-1251. doi: 10.1128/jvi.01213-12

Barrett, J. S., Wagner, J. G., Fisher, S. J., & Wahl, R. L. (1991). Effect of intraperitoneal injection volume and antibody protein dose on the pharmacokinetics of intraperitoneally administered lgG2aκ murine monoclonal antibody in the rat. *Cancer Research, 51*(13), 3434-3444.

Basler, C. F. (2012). Nipah and Hendra virus interactions with the innate immune system. In Benhur Lee & Paul Rota (Eds.), *Current Topics in Microbiology and Immunology - Henipavirus* (Vol. 359, pp. 123-152). Berlin, Heidelberg: Springer.

Bente, D. A., Alimonti, J. B., Shieh, W.-J., Camus, G., Ströher, U., Zaki, S., & Jones, S. M. (2010). Pathogenesis and immune response of Crimean-Congo Hemorrhagic Fever Virus in a STAT-1 knockout mouse model. *Journal of Virology, 84*(21), 11089-11100. doi: 10.1128/jvi.01383-10

Black, P. F., Cronin, J. P., Morrissy, C. J., & Westbury, H. A. (2001). Serological examination for evidence of infection with Hendra and Nipah viruses in Queensland piggeries. *Australian Veterinary Journal, 79*(6), 424-426.

Bonaparte, M. I., Dimitrov, A. S., Bossart, K. N., Crameri, G., Mungal, B. A., Bishop, K. A., Choudhry, V., Dimitrov, D. S., Wang, L. F., Eaton, B. T., & Broder, C. C. (2005). Ephrin-B2 ligand is a functional receptor for Hendra virus and Nipah virus. *Proceedings of the National Academy of Sciences of the United States of America, 102*(30), 10652-10657. doi: 10.1073/pnas.0504887102

Bonjardim, C. A., Ferreira, P. C. P., & Kroon, E. G. (2009). Interferons: Signaling, antiviral and viral evasion. *Immunology Letters, 122*(1), 1-11. doi: http://dx.doi.org/10.1016/j.imlet.2008.11.002

Borisevich, V., Ozdener, M. H., Malik, B., & Rockx, B. (2017). Hendra and Nipah Virus Infection in Cultured Human Olfactory Epithelial Cells. *mSphere, 2*(3), e00252-00217. doi: 10.1128/mSphere.00252-17

Bossart, K. N., Geisbert, T. W., Feldmann, H., Zhu, Z. Y., Feldmann, F., Geisbert, J. B., Yan, L. Y., Feng, Y. R., Brining, D., Scott, D., Wang, Y. P., Dimitrov, A. S., Callison, J., Chan, Y. P., Hickey, A. C., Dimitrov, D. S., Broder, C. C., & Rockx, B. (2011). A neutralizing human monoclonal antibody protects African green monkeys from Hendra virus challenge. *Science Translational Medicine, 3*(105), 105ra103. doi: 10.1126/scitranslmed.3002901

Bossart, K. N., McEachern, J. A., Hickey, A. C., Choudhry, V., Dimitrov, D. S., Eaton, B. T., & Wang, L.-F. (2007). Neutralization assays for differential henipavirus serology using Bio-Plex protein array systems. *Journal of Virological Methods, 142*(1-2), 29-40.

Bossart, K. N., Tachedjian, M., McEachern, J. A., Crameri, G., Zhu, Z., Dimitrov, D. S., Broder, C. C., & Wang, L.-F. (2008). Functional studies of host-specific ephrin-B ligands as Henipavirus receptors. *Virology, 372*(2), 357-371. doi: 10.1016/j.virol.2007.11.011

Bossart, K. N., Zhu, Z., Middleton, D., Klippel, J., Crameri, G., Bingham, J., McEachern, J. A., Green, D., Hancock, T. J., Chan, Y.-P., Hickey, A. C., Dimitrov, D. S., Wang, L.-F., & Broder, C. C. (2009). A neutralizing human monoclonal antibody protects against lethal disease in a new ferret model of acute Nipah virus infection. *PLoS Pathogens, 5*(10), e1000642. doi: 10.1371/journal.ppat.1000642

Bowick, G., Airo, A., & Bente, D. (2012). Expression of interferon-induced antiviral genes is delayed in a STAT1 knockout mouse model of Crimean-Congo hemorrhagic fever. *Virology Journal, 9*(1), 122.

Bradfute, S. B., Warfield, K. L., & Bray, M. (2012). Mouse models for filovirus infections. *Viruses, 4*(9), 1477-1508.

Brass, A. L., Huang, I. C., Benita, Y., John, S. P., Krishnan, M. N., Feeley, E. M., Ryan, B. J., Weyer, J. L., van der Weyden, L., Fikrig, E., Adams, D. J., Xavier, R. J., Farzan, M., & Elledge, S. J. (2009). The IFITM proteins mediate cellular resistance to Influenza A H1N1 virus, West Nile virus, and Dengue virus. *Cell, 139*(7), 1243-1254. doi: 10.1016/j.cell.2009.12.017

Bray, M. (2001). The role of the Type I interferon response in the resistance of mice to filovirus infection. *Journal of General Virology, 82*(6), 1365-1373. doi: 10.1099/0022-1317-82-6-1365

Brown, A. N., Kent, K. A., Bennett, C. J., & Bernard, K. A. (2007). Tissue tropism and neuroinvasion of West Nile virus do not differ for two mouse strains with different survival rates. *Virology, 368*(2), 422. doi: 10.1016/j.virol.2007.06.033

Canakoglu, N., Berber, E., Tonbak, S., Ertek, M., Sozdutmaz, I., Aktas, M., Kalkan, A., & Ozdarendeli, A. (2015). Immunization of knock-out α/β interferon receptor mice against high lethal dose of Crimean-Congo Hemorrhagic Fever Virus with a cell culture based vaccine. *PLOS Neglected Tropical Diseases, 9*(3), e0003579. doi: 10.1371/journal.pntd.0003579

Caporale, M., Wash, R., Pini, A., Savini, G., Franchi, P., Golder, M., Patterson-Kane, J., Mertens, P., Di Gialleonardo, L., Armillotta, G., Lelli, R., Kellam, P., & Palmarini, M. (2011). Determinants of Bluetongue virus virulence in murine models of disease. *Journal Of Virology, 85*(21), 11479-11489. doi: 10.1128/jvi.05226-11

Carr, C. M., & Kim, P. S. (1993). A spring-loaded mechanism for the conformational change of influenza hemagglutinin. *Cell, 73*(4), 823-832. doi: 10.1016/0092-8674(93)90260-W

Chambers, R., & Takimoto, T. (2009). Antagonism of innate immunity by Paramyxovirus accessory proteins. *Viruses, 1*(3), 574-593. doi: 10.3390/v1030574

Charles, P. C., Walters, E., Margolis, F., & Johnston, R. E. (1995). Mechanism of neuroinvasion of Venezuelan Equine Encephalitis virus in the mouse. *Virology, 208*(2), 662-671. doi: 10.1006/viro.1995.1197

Childs, K., Stock, N., Ross, C., Andrejeva, J., Hilton, L., Skinner, M., Randall, R., & Goodbourn, S. (2007). Mda-5, but not RIG-I, is a common target for paramyxovirus V proteins. *Virology, 359*(1), 190-200. doi: 10.1016/j.virol.2006.09.023

Ching, P. K. G., Carr de los Reyes, V., Sucaldito, M. N., Tayag, E., Columna-Vingno, A. B., Malbas, F. F., Bolo, G. C., Sejvar, J. J., Eagles, D., Playford, G., Dueger, E., Kaku, Y., Morikawa, S., Kuroda, M., Marsh, G. A., McCullough, S., & Foxwell, A. R. (2015). Outbreak of Henipavirus infection, Philippines, 2014. *Emerging Infectious Diseases, 21*(2), 328-331. doi: 10.3201/eid2102.141433

Chua, K. B. (2003). Nipah virus outbreak in Malaysia. *Journal of Clinical Virology, 26*(3), 265-275. doi: 10.1016/S1386-6532(02)00268-8

Chua, K. B., Bellini, W. J., Rota, P. A., Harcourt, B. H., Tamin, A., Lam, S. K., Ksiazek, T. G., Rollin, P. E., Zaki, S. R., Shieh, W.-J., Goldsmith, C. S., Gubler, D. J., Roehrig, J. T., Eaton, B., Gould, A. R., Olson, J., Field, H., Daniels, P., Ling, A. E., Peters, C. J., Anderson, L. J., & Mahy, B. W. J. (2000). Nipah virus: a recently emergent deadly Paramyxovirus. *Science, 288*(5470), 1432-1435. doi: 10.1126/science.288.5470.1432

Chua, K. B., Goh, K. J., Wong, K. T., Kamarulzaman, A., Tan, P. S. K., Ksiazek, T. G., Zaki, S. R., Paul, G., Lam, S. K., & Tan, C. T. (1999). Fatal encephalitis due to Nipah virus among pig-farmers in Malaysia. *Lancet, 354*(9186), 1257-1259. doi: 10.1016/s0140-6736(99)04299-3

Chua, K. B., Lek Koh, C., Hooi, P. S., Wee, K. F., Khong, J. H., Chua, B. H., Chan, Y. P., Lim, M. E., & Lam, S. K. (2002). Isolation of Nipah virus from Malaysian island flying-foxes. *Microbes and Infection, 4*(2), 145-151. doi: 10.1016/S1286-4579(01)01522-2

Ciancanelli, M. J., Volchkova, V. A., Shaw, M. L., Volchkov, V. E., & Basler, C. F. (2009). Nipah virus sequesters inactive STAT1 in the nucleus via a P gene-encoded mechanism. *Journal Of Virology, 83*(16), 7828-7841.

Clayton, B. A., Middleton, D., Bergfeld, J., Haining, J., Arkinstall, R., Wang, L., & Marsh, G. (2012). Transmission routes for Nipah virus from Malaysia and Bangladesh. *Emerging Infectious Diseases, 18*(12), 1983-1993. doi: 10.3201/eid1812.120875

Clayton, B. A., Wang, L. F., & Marsh, G. A. (2013). Henipaviruses: an updated review focusing on the Pteropid reservoir and features of transmission. *Zoonoses Public Health, 60*(1), 69-83. doi: 10.1111/j.1863-2378.2012.01501.x

Compton, Alex A., Bruel, T., Porrot, F., Mallet, A., Sachse, M., Euvrard, M., Liang, C., Casartelli, N., & Schwartz, O. (2014). IFITM proteins incorporated into HIV-1 virions impair viral fusion and spread. *Cell Host & Microbe, 16*(6), 736-747. doi: 10.1016/j.chom.2014.11.001

Crameri, G., Todd, S., Grimley, S., McEachern, J. A., Marsh, G. A., Smith, C., Tachedjian, M., De Jong, C., Virtue, E. R., Yu, M., Bulach, D., Liu, J.-P., Michalski, W. P., Middleton, D., Field, H. E., & Wang, L.-F. (2009). Establishment, immortalisation and characterisation of Pteropid bat cell lines. *PLoS ONE, 4*(12), e8266. doi: 10.1371/journal.pone.0008266

Croser, E. L., & Marsh, G. A. (2013). The changing face of the henipaviruses. *Veterinary Microbiology, 167*(1–2), 151-158. doi: 10.1016/j.vetmic.2013.08.002

de Hooge, A. S. K., van de Loo, F. A. J., Koenders, M. I., Bennink, M. B., Arntz, O. J., Kolbe, T., & van den Berg, W. B. (2004). Local activation of STAT-1 and STAT-3 in the inflamed synovium during zymosan-induced arthritis: Exacerbation of joint inflammation in STAT-1 gene–knockout mice. *Arthritis & Rheumatism, 50*(6), 2014-2023. doi: 10.1002/art.20302

de Weerd, N. A., Vivian, J. P., Nguyen, T. K., Mangan, N. E., Gould, J. A., Braniff, S.-J., Zaker-Tabrizi, L., Fung, K. Y., Forster, S. C., Beddoe, T., Reid, H. H., Rossjohn, J., & Hertzog, P. J. (2013). Structural basis of a unique interferon-[beta] signaling axis mediated via the receptor IFNAR1. *Nature Immunology, 14*(9), 901-907. doi: 10.1038/ni.2667

de Wit, E., Bushmaker, T., Scott, D., Feldmann, H., & Munster, V. J. (2011). Nipah virus transmission in a hamster model. *Plos Neglected Tropical Diseases, 5*(12), e1432. doi: 10.1371/journal.pntd.0001432

DeBuysscher, B. L., de Wit, E., Munster, V. J., Scott, D., Feldmann, H., & Prescott, J. (2013). Comparison of the pathogenicity of Nipah virus isolates from Bangladesh and Malaysia in the Syrian hamster. *PLoS Neglected Tropical Diseases, 7*(1), e2024. doi: 10.1371/journal.pntd.0002024

Desai, T. M., Marin, M., Chin, C. R., Savidis, G., Brass, A. L., & Melikyan, G. B. (2014). IFITM3 restricts Influenza A virus entry by blocking the formation of fusion pores following virus-endosome hemifusion. *Plos Pathogens, 10*(4), e1004048. doi: 10.1371/journal.ppat.1004048

Dhondt, K. P., Mathieu, C., Chalons, M., Reynaud, J. M., Vallve, A., Raoul, H., & Horvat, B. (2013). Type I interferon signaling protects mice from lethal Henipavirus infection. *Journal of Infectious Diseases, 207*(1), 142-151. doi: 10.1093/infdis/jis653

Diederich, S., Sauerhering, L., Weis, M., Altmeppen, H., Schaschke, N., Reinheckel, T., Erbar, S., & Maisner, A. (2012). Activation of the Nipah virus fusion protein in MDCK cells is mediated by cathepsin B within the endosome-recycling compartment. *Journal of Virology, 86*(7), 3736-3745. doi: 10.1128/jvi.06628-11

Donnelly, R. P., & Kotenko, S. V. (2010). Interferon-lambda: a new addition to an old family. *Journal of Interferon & Cytokine Research, 30*(8), 555-564. doi: 10.1089/jir.2010.0078

Drexler, J. F., Corman, V. M., Gloza-Rausch, F., Seebens, A., Annan, A., Ipsen, A., Kruppa, T., Müller, M. A., Kalko, E. K. V., Adu-Sarkodie, Y., Oppong, S., & Drosten, C. (2009). Henipavirus RNA in African bats. *PLoS ONE, 4*(7), e6367. doi: 10.1371/journal.pone.0006367

Dups, J. (2015). *Investigating the neuropathogenesis of henipaviruses in a newly established mouse model of encephalitis.* (Doctor of Philosophy), University of Melbourne, University of Melbourne, Australia.

Dups, J., Middleton, D., Long, F., Arkinstall, R., Marsh, G. A., & Wang, L. F. (2014). Subclinical infection without encephalitis in mice following intranasal exposure to Nipah virus-Malaysia and Nipah virus-Bangladesh. *Virology Journal, 11*(102). doi: 10.1186/1743-422X-11-102

Dups, J., Middleton, D., Yamada, M., Monaghan, P., Long, F., Robinson, R., Marsh, G. A., & Wang, L.-F. (2012). A new model for Hendra virus encephalitis in the mouse. *PLoS ONE, 7*(7), e40308. doi: 10.1371/journal.pone.0040308

Durbin, J. E., Hackenmiller, R., Simon, M. C., & Levy, D. E. (1996). Targeted disruption of the mouse Stat1 gene results in compromised innate immunity to viral disease. *Cell, 84*(3), 443-450. doi: 10.1016/S0092-8674(00)81289-1

Durbin, J. E., Johnson, T. R., Durbin, R. K., Mertz, S. E., Morotti, R. A., Peebles, R. S., & Graham, B. S. (2002). The role of IFN in respiratory syncytial virus pathogenesis. *The Journal of Immunology, 168*(6), 2944-2952. doi: 10.4049/jimmunol.168.6.2944

Escaffre, O., Borisevich, V., Carmical, J. R., Prusak, D., Prescott, J., Feldmann, H., & Rockx, B. (2013a). Henipavirus pathogenesis in human respiratory epithelial cells. *Journal of Virology, 87*(6), 3284-3294. doi: 10.1128/jvi.02576-12

Escaffre, O., Borisevich, V., & Rockx, B. (2013b). Pathogenesis of Hendra and Nipah virus infection in humans. *Journal of Infection in Developing Countries, 7*(4), 308-311. doi: 10.3855/jidc.3648

Eschbaumer, M., Keller, M., Beer, M., & Hoffmann, B. (2012). Epizootic Hemorrhagic Disease virus infection of type I interferon receptor deficient mice. *Veterinary Microbiology, 155*(2–4), 417-419. doi: 10.1016/j.vetmic.2011.08.019

Everitt, A. R., Clare, S., McDonald, J. U., Kane, L., Harcourt, K., Ahras, M., Lall, A., Hale, C., Rodgers, A., Young, D. B., Haque, A., Billker, O., Tregoning, J. S., Dougan, G., & Kellam, P. (2013). Defining the range of pathogens susceptible to Ifitm3 restriction using a knockout mouse model. *PLoS ONE, 8*(11), e80723. doi: 10.1371/journal.pone.0080723

Everitt, A. R., Clare, S., Pertel, T., John, S. P., Wash, R. S., Smith, S. E., Chin, C. R., Feeley, E. M., Sims, J. S., Adams, D. J., Wise, H. M., Kane, L., Goulding, D., Digard, P., Anttila, V., Baillie, J. K., Walsh, T. S., Hume, D. A., Palotie, A., Xue, Y., Colonna, V., Tyler-Smith, C., Dunning, J., Gordon, S. B., Smyth, R. L., Openshaw, P. J., Dougan, G., Brass, A. L., & Kellam, P. (2012). IFITM3 restricts the morbidity and mortality associated with influenza. *Nature, 484*(7395), 519-523.

Fass, D., Harrison, S. C., & Kim, P. S. (1996). Retrovirus envelope domain at 1.7 Å resolution. *Nature Structural Biology, 3*(5), 465-469.

Favre, C. J., Mancuso, M., Maas, K., McLean, J. W., Baluk, P., & McDonald, D. M. (2003). Expression of genes involved in vascular development and angiogenesis in endothelial cells of adult lung. *American Journal of Physiology - Heart and Circulatory Physiology, 285*(5), H1917-H1938. doi: 10.1152/ajpheart.00983.2002

Feeley, E. M., Sims, J. S., John, S. P., Chin, C. R., Pertel, T., Chen, L.-M., Gaiha, G. D., Ryan, B. J., Donis, R. O., Elledge, S. J., & Brass, A. L. (2011). IFITM3 inhibits Influenza A virus infection by preventing cytosolic entry. *PLoS Pathogens, 7*(10), 1-17. doi: 10.1371/journal.ppat.1002337

Feldman, K. S., Foord, A., Heine, H. G., Smith, I. L., Boyd, V., Marsh, G. A., Wood, J. L. N., Cunningham, A. A., & Wang, L. F. (2009). Design and evaluation of consensus PCR assays for henipaviruses. *Journal of Virological Methods, 161*(1), 52-57. doi: 10.1016/j.jviromet.2009.05.014

Fenner, J. E., Starr, R., Cornish, A. L., Zhang, J.-G., Metcalf, D., Schreiber, R. D., Sheehan, K., Hilton, D. J., Alexander, W. S., & Hertzog, P. J. (2006). Suppressor of cytokine signaling 1 regulates the immune response to infection by a unique inhibition of type I interferon activity. *Nature Immunology, 7*(1), 33-39.

Field, H., Crameri, G., Kung, N. Y.-H., & Wang, L.-F. (2012). Ecological aspects of Hendra virus. In Benhur Lee & Paul Rota (Eds.), *Current Topics in Microbiology and Immunology- Henipavirus* (Vol. 359, pp. 11-23). Berlin, Heidelberg: Springer.

Field, H., de Jong, C., Melville, D., Smith, C., Smith, I., Broos, A., Kung, Y. H., McLaughlin, A., & Zeddeman, A. (2011). Hendra virus infection dynamics in Australian fruit bats. *PLoS ONE, 6*(12), e28678. doi: 10.1371/journal.pone.0028678

Field, H., Schaaf, K., Kung, N., Simon, C., Waltisbuhl, D., Hobert, H., Moore, F., Middleton, D., Crook, A., Smith, G., Daniels, P., Glanville, R., & Lovell, D. (2010). Hendra virus outbreak with novel clinical features, Australia. *Emerging Infectious Diseases, 16*(2), 338-340. doi: 10.3201/eid1602.090780

Field, H., Young, P., Yob, J. M., Mills, J., Hall, L., & Mackenzie, J. (2001). The natural history of Hendra and Nipah viruses. *Microbes and Infection, 3*(4), 307-314.

Field, H. E., Barratt, P. C., Hughes, R. J., Shield, J., & Sullivan, N. D. (2000). A fatal case of Hendra virus infection in a horse in north Queensland: clinical and epidemiological features. *Australian Veterinary Journal, 78*(4), 279-280.

Fields, B. N., Knipe, D. M., & Howley, P. M. (2007). *Fields' virology / editors-in-chief, David M. Knipe, Peter M. Howley ; associate editors, Diane E. Griffin ... [et al.]* (5th ed. ed.). Philadelphia :: Lippincott Williams & Wilkins.

Freiberg, A. N., Worthy, M. N., Lee, B., & Holbrook, M. R. (2010). Combined chloroquine and ribavirin treatment does not prevent death in a hamster model of Nipah and Hendra virus infection. *Journal of General Virology, 91*(Pt 3), 765-772.

Friedman, R. L., Manly, S. P., McMahon, M., Kerr, I. M., & Stark, G. R. (1984). Transcriptional and posttranscriptional regulation of interferon-induced gene expression in human cells. *Cell, 38*(3), 745-755. doi: 10.1016/0092-8674(84)90270-8

Gale, N. W., Baluk, P., Pan, L., Kwan, M., Holash, J., DeChiara, T. M., McDonald, D. M., & Yancopoulos, G. D. (2001). Ephrin-B2 selectively marks arterial vessels and neovascularization sites in the adult, with expression in both endothelial and smooth-muscle cells. *Developmental Biology, 230*(2), 151-160. doi: 10.1006/dbio.2000.0112

Garner, O. B., Aguilar, H. C., Fulcher, J. A., Levroney, E. L., Harrison, R., Wright, L., Robinson, L. R., Aspericueta, V., Panico, M., Haslam, S. M., Morris, H. R., Dell, A., Lee, B., & Baum, L. G. (2010). Endothelial galectin-1 binds to specific glycans on nipah virus fusion protein and inhibits maturation, mobility, and function to block syncytia formation. *Plos Pathogens, 6*(7), e1000993-e1000993.

Geisbert, T. W., Daddario-DiCaprio, K. M., Hickey, A. C., Smith, M. A., Chan, Y. P., Wang, L. F., Mattapallil, J. J., Geisbert, J. B., Bossart, K. N., & Broder, C. C. (2010). Development of an acute and highly pathogenic nonhuman primate model of Nipah virus infection. *PLoS ONE, 5*(5), e10690. doi: 10.1371/journal.pone.0010690.

Geisbert, T. W., Feldmann, H., & Broder, C. C. (2012). Animal challenge models of Henipavirus infection and pathogenesis. In Benhur Lee & Paul Rota (Eds.), *Current Topics in Microbiology and Immunology- Henipavirus* (Vol. 359, pp. 153-177). Berlin, Heidelberg: Springer.

Georges-Courbot, M. C., Contamin, H., Faure, C., Loth, P., Baize, S., Leyssen, P., Neyts, J., & Deubel, V. (2006). Poly(I)-Poly(C12U) but not ribavirin prevents death in a hamster model of Nipah virus infection. *Antimicrobial Agents and Chemotherapy, 50*(5), 1768-1772. doi: 10.1128/aac.50.5.1768-1772.2006

Gerlier, D., & Lyles, D. S. (2011). Interplay between innate immunity and negative-strand RNA viruses: towards a rational model. *Microbiology and Molecular Biology Reviews, 75*(3), 468-490. doi: 10.1128/mmbr.00007-11

Gibbert, K., Schlaak, J. F., Yang, D., & Dittmer, U. (2012). Interferon alpha subtypes: distinct biological activities in anti-viral therapy. *British Journal of Pharmacology, 168*(5), 1048-1058. doi: 10.1111/bph.12010

Gil, M. P., Bohn, E., O'Guin, A. K., Ramana, C. V., Levine, B., Stark, G. R., Virgin, H. W., & Schreiber, R. D. (2001). Biologic consequences of Stat1-independent IFN signaling. *Proceedings of the National Academy of Sciences, 98*(12), 6680-6685. doi: 10.1073/pnas.111163898

Goh, K. J., Tan, C. T., Chew, N. K., Tan, P. S. K., Kamarulzaman, A., Sarji, S. A., Wong, K. T., Abdullah, B. J. J., Chua, K. B., & Lam, S. K. (2000). Clinical features of Nipah virus encephalitis among pig farmers in Malaysia. *New England Journal of Medicine, 342*(17), 1229-1235. doi: 10.1056/NEJM200004273421701

Goodbourn, S., & Randall, R. (2009). The regulation of Type I interferon production by paramyxoviruses. *Journal of Interferon & Cytokine Research, 29*(9), 539.

Goyen, K. A., Wright, J. D., Cunneen, A., & Henning, J. (2017). Playing with fire – What is influencing horse owners' decisions to not vaccinate their horses against deadly Hendra virus infection? *PLoS ONE, 12*(6), e0180062. doi: 10.1371/journal.pone.0180062

Guillaume, V., Contamin, H., Loth, P., Georges-Courbot, M.-C., Lefeuvre, A., Marianneau, P., Chua, K. B., Lam, S. K., Buckland, R., Deubel, V., & Wild, T. F. (2004). Nipah virus: vaccination and passive protection studies in a hamster model. *Journal of Virology, 78*(2), 834-840. doi: 10.1128/jvi.78.2.834-840.2004

Guillaume, V., Contamin, H., Loth, P., Grosjean, I., Courbot, M. C. G., Deubel, V., Buckland, R., & Wild, T. F. (2006). Antibody prophylaxis and therapy against Nipah virus infection in hamsters. *Journal of Virology, 80*(4), 1972-1978.

Guillaume, V., Wong, K. T., Looi, R. Y., Georges-Courbot, M.-C., Barrot, L., Buckland, R., Wild, T. F., & Horvat, B. (2009). Acute Hendra virus infection: analysis of the pathogenesis and passive antibody protection in the hamster model. *Virology, 387*(2), 459-465. doi: 10.1016/j.virol.2009.03.001

Hach, J. C., McMichael, T., Chesarino, N. M., & Yount, J. S. (2013). Palmitoylation on conserved and nonconserved cysteines of murine IFITM1 regulates its stability and anti-Influenza A virus activity. *Journal of Virology, 87*(17), 9923-9927. doi: 10.1128/jvi.00621-13

Halpin, K., Bankamp, B., Harcourt, B. H., Bellini, W. J., & Rota, P. A. (2004). Nipah virus conforms to the rule of six in a minigenome replication assay. *Journal of General Virology, 85*(3), 701-707. doi: 10.1099/vir.0.19685-0

Halpin, K., Hyatt, A. D., Fogarty, R., Middleton, D., Bingham, J., Epstein, J. H., Rahman, S. A., Hughes, T., Smith, C., Field, H. E., & Daszak, P. (2011). Pteropid bats are confirmed as the reservoir hosts of henipaviruses: a comprehensive experimental study of virus transmission. *The American Journal Of Tropical Medicine And Hygiene, 85*(5), 946-951. doi: 10.4269/ajtmh.2011.10-0567

Halpin, K., Young, P. L., Field, H. E., & Mackenzie, J. S. (2000). Isolation of Hendra virus from pteropid bats: a natural reservoir of Hendra virus. *Journal of General Virology, 81*(Pt 8), 1927-1932.

Hamilton, M. A., Russo, R. C., & Thurston, R. V. (1977). Trimmed Spearman-Karber method for estimating median lethal concentrations in toxicity bioassays. *Environmental Science & Technology, 11*(7), 714-719. doi: 10.1021/es60130a004

Han, J. H., Lee, S., Park, Y. S., Park, J. S., Kim, K., Lim, J. S., Oh, K. S., Yang, Y. (2011). IFITM6 expression is increased in macrophages of tumor-bearing mice. *Oncology Reports, 25*(2), 531-536. doi: 10.3892/or.2010.1092

Hanna, J. N., McBride, W.J., Brookes, D.L., Shield, J., Taylor, C.T., Smith, I.L., Craig, S.B., Smith, G.A. (2006). Hendra virus infection in a veterinarian. *Medical Journal of Australia, 185*(10), 562-564.

Harcourt, B. H., Lowe, L., Tamin, A., Liu, X., Bankamp, B., Bowden, N., Rollin, P. E., Comer, J. A., Ksiazek, T. G., Hossain, M. J., Gurley, E. S., Breiman, R. F., Bellini, W. J., & Rota, P. A. (2005). Genetic characterization of Nipah virus, Bangladesh, 2004. *Emerging Infectious Diseases, 11*(10), 1594-1597. doi: 10.3201/eid1110.050513

Harcourt, B. H., Tamin, A., Halpin, K., Ksiazek, T. G., Rollin, P. E., Bellini, W. J., & Rota, P. A. (2001). Molecular characterization of the polymerase gene and genomic termini of Nipah virus. *Virology, 287*(1), 192-201. doi: 10.1006/viro.2001.1026

Harcourt, B. H., Tamin, A., Ksiazek, T. G., Rollin, P. E., Anderson, L. J., Bellini, W. J., & Rota, P. A. (2000a). Molecular characterization of Nipah virus, a newly emergent paramyxovirus. *Virology, 271*(2), 334-349.

Harcourt, B. H., Tamin, A., Newton, B., Sanchez, A., Ksiazek, T. G., Rollin, P. E., Bellini, W. J., & Rota, P. A. (2000b). *Analysis of mRNA editing in Hendra and Nipah viruses.* Paper presented at the International conference on negative strand viruses

Hardy, M. P., Owczarek, C. M., Trajanovska, S., Liu, X., Kola, I., & Hertzog, P. J. (2001). The soluble murine type I interferon receptor Ifnar-2 is present in serum, is independently regulated, and has both agonistic and antagonistic properties. *Blood, 97*(2), 473-482. doi: 10.1182/blood.V97.2.473

Harkema, J. R., Carey, S. A., & Wagner, J. G. (2006). The nose revisited: a brief review of the comparative structure, function, and toxicologic pathology of the nasal epithelium. *Toxicologic Pathology, 34*(3), 252-269. doi: 10.1080/01926230600713475

Hayman, D. T. S., Bowen, R. A., Cryan, P. M., McCracken, G. F., O'Shea, T. J., Peel, A. J., Gilbert, A., Webb, C. T., & Wood, J. L. N. (2013). Ecology of zoonotic infectious diseases in bats: current knowledge and future directions. *Zoonoses Public Health, 60*(1), 2-21. doi: 10.1111/zph.12000

Hayman, D. T. S., Wang, L.-F., Barr, J., Baker, K. S., Suu-Ire, R., Broder, C. C., Cunningham, A. A., & Wood, J. L. N. (2011). Antibodies to Henipavirus or Henipa-like

viruses in domestic pigs in Ghana, West Africa. *PLoS ONE, 6*(9), e25256. doi: 10.1371/journal.pone.0025256
Hofer, M. J., Li, W., Manders, P., Terry, R., Lim, S. L., King, N. J. C., & Campbell, I. L. (2012). Mice deficient in STAT1 but not STAT2 or IRF9 develop a lethal CD4+ T-cell-mediated disease following infection with Lymphocytic Choriomeningitis virus. *Journal of Virology, 86*(12), 6932-6946. doi: 10.1128/jvi.07147-11
Honnold, S. P., Mossel, E. C., Bakken, R. R., Lind, C. M., Cohen, J. W., Eccleston, L. T., Spurgers, K. B., Erwin-Cohen, R., Glass, P. J., & Maheshwari, R. K. (2015). Eastern equine encephalitis virus in mice II: pathogenesis is dependent on route of exposure. *Virology Journal, 12*(1), 1-23. doi: 10.1186/s12985-015-0385-2
Hooper, P., Zaki, S., Daniels, P., & Middleton, D. (2001). Comparative pathology of the diseases caused by Hendra and Nipah viruses. *Microbes and Infection, 3*(4), 315-322. doi: 10.1016/S1286-4579(01)01385-5
Hooper, P. T., Ketterer, P. J., Hyatt, A. D., & Russell, G. M. (1997a). Lesions of Experimental Equine Morbillivirus Pneumonia in Horses. *Veterinary Pathology, 34*(4), 312-322. doi: 10.1177/030098589703400407
Hooper, P. T., Westbury, H. A., & Russell, G. M. (1997b). The lesions of experimental equine Morbillivirus disease in cats and guinea pigs. *Veterinary Pathology, 34*(4), 323-329. doi: 10.1177/030098589703400408
Hooper, P. T., & Williamson, M. M. (2000). Hendra and Nipah virus infections. *Veterinary Clinics of North America-Equine Practice, 16*(3), 597–603.
Hossain, M. J., Gurley, E. S., Montgomery, J. M., Bell, M., Carroll, D. S., Hsu, V. P., Formenty, P., Croisier, A., Bertherat, E., Faiz, M. A., Azad, A. K., Islam, R., Molla, M. A. R., Ksiazek, T. G., Rota, P. A., Comer, J. A., Rollin, P. E., Luby, S. P., & Breiman, R. F. (2008). Clinical presentation of Nipah virus infection in Bangladesh. *Clinical Infectious Diseases, 46*(7), 977-984. doi: 10.1086/529147
Huang, I. C., Bailey, C. C., Weyer, J. L., Radoshitzky, S. R., Becker, M. M., Chiang, J. J., Brass, A. L., Ahmed, A. A., Xiaoli, C., Lian, D., Longobardi, L. E., Boltz, D., Kuhn, J. H., Elledge, S. J., Bavari, S., Denison, M. R., Choe, H., & Farzan, M. (2011). Distinct patterns of IFITM-mediated restriction of filoviruses, SARS Coronavirus, and Influenza A virus. *PLoS Pathogens, 7*(1), e1001258. doi: 10.1371/journal.ppat.1001258
Hwang, S. Y., Hertzog, P. J., Holland, K. A., Sumarsono, S. H., Tymms, M. J., Hamilton, J. A., Whitty, G., Bertoncello, I., & Kola, I. (1995). A null mutation in the gene encoding a type I interferon receptor component eliminates antiproliferative and antiviral responses to interferons alpha and beta and alters macrophage responses. *Proceedings of the National Academy of Sciences, 92*(24), 11284-11288.
Jack, P. J. M., Boyle, D. B., Eaton, B. T., & Wang, L.-F. (2005). The complete genome sequence of J virus reveals a unique genome structure in the family Paramyxoviridae. *Journal Of Virology, 79*(16), 10690-10700. doi: 10.1128/jvi.79.16.10690-10700.2005
Jackson Laboratory. (2016). There is no such thing as a B6 mouse. *News and Insights.* Retrieved 8/6/2017, 2017, from https://www.jax.org/news-and-insights/jax-blog/2016/june/there-is-no-such-thing-as-a-b6-mouse
Jennische, E., Eriksson, C. E., Lange, S., Trybala, E., & Bergstrom, T. (2015). The anterior commissure is a pathway for contralateral spread of herpes simplex virus type 1 after olfactory tract infection. *Journal of Neurovirology, 21*(2), 129-147. doi: 10.1007/s13365-014-0312-0
Jia, R., Ding, S., Pan, Q., Liu, S.-L., Qiao, W., & Liang, C. (2015). The C-terminal sequence of IFITM1 regulates its anti-HIV-1 activity. *PLoS ONE, 10*(3). doi: 10.1371/journal.pone.0118794
John, S. P., Chin, C. R., Perreira, J. M., Feeley, E. M., Aker, A. M., Savidis, G., Smith, S. E., Elia, A. E. H., Everitt, A. R., Vora, M., Pertel, T., Elledge, S. J., Kellam, P., & Brass, A. L. (2013). The CD225 domain of IFITM3 is required for both IFITM protein

association and inhibition of Influenza A virus and Dengue virus replication. *Journal of Virology, 87*(14), 7837-7852. doi: 10.1128/jvi.00481-13
Johnson, N., Cunningham, A. F., & Fooks, A. R. (2010). The immune response to rabies virus infection and vaccination. *Vaccine, 28*(23), 3896-3901. doi: 10.1016/j.vaccine.2010.03.039
Kalinke, U., Bechmann, I., & Detje, C. N. (2011). Host strategies against virus entry via the olfactory system. *Virulence, 2*(4), 367-370. doi: 10.4161/viru.2.4.16138
Karst, S. M., Wobus, C. E., Lay, M., Davidson, J., & Virgin, H. W. (2003). STAT1-dependent innate immunity to a Norwalk-like virus. *Science, 299*(5612), 1575.
Katze, M. G., He, Y., & Gale, M., Jr. (2002). Viruses and interferon: a fight for supremacy. *Nature Reviews. Immunology, 2*(9), 675-687.
Kirkland, P. D., Gabor, M., Poe, I., Neale, K., Chaffey, K., Finlaison, D. S., Gu, X., Hick, P. M., Read, A. J., Wright, T., & Middleton, D. (2015). Hendra virus infection in dog, Australia, 2013. *Emerging Infectious Diseases, 21*(12), 2182-2185. doi: 10.3201/eid2112.151324
Kolokoltsova, O. A., Yun, N. E., & Paessler, S. (2014). Reactive astrogliosis in response to hemorrhagic fever virus: microarray profile of Junin virus-infected human astrocytes. *Virology Journal 11*. doi: 10.1186/1743-422x-11-126
Kolokoltsova, O. A., Yun, N. E., Poussard, A. L., Smith, J. K., Smith, J. N., Salazar, M., Walker, A., Tseng, C.-T. K., Aronson, J. F., & Paessler, S. (2010). Mice lacking alpha/beta and gamma interferon receptors are susceptible to Junin virus infection. *Journal Of Virology, 84*(24), 13063-13067. doi: 10.1128/jvi.01389-10
Kulkarni, S., Volchkova, V., Basler, C. F., Palese, P., Volchkov, V. E., & Shaw, M. L. (2009). Nipah virus edits its P gene at high frequency to express the V and W proteins. *Journal Of Virology, 83*(8), 3982-3987. doi: 10.1128/jvi.02599-08
Lamb, R. A., Paterson, R. G., & Jardetzky, T. S. (2006). Paramyxovirus membrane fusion: lessons from the F and HN atomic structures. *Virology, 344*(1), 30-37. doi: 10.1016/j.virol.2005.09.007
Langford, D. J., Bailey, A. L., Chanda, M. L., Clarke, S. E., Drummond, T. E., Echols, S., Glick, S., Ingrao, J., Klassen-Ross, T., LaCroix-Fralish, M. L., Matsumiya, L., Sorge, R. E., Sotocinal, S. G., Tabaka, J. M., Wong, D., van den Maagdenberg, A. M. J. M., Ferrari, M. D., Craig, K. D., & Mogil, J. S. (2010). Coding of facial expressions of pain in the laboratory mouse. *Nature Methods, 7*(6), 447-449. doi: 10.1038/nmeth.1455
Leach, M. C., Klaus, K., Miller, A. L., Scotto di Perrotolo, M., Sotocinal, S. G., & Flecknell, P. A. (2012). The assessment of post-vasectomy pain in mice using behaviour and the mouse grimace scale. *PLoS ONE, 7*(4), e35656. doi: 10.1371/journal.pone.0035656
Lee, B. (2007). Envelope-receptor interactions in Nipah virus pathobiology. *Annals of the New York Academy of Sciences, 1102*, 51-65. doi: 10.1196/annals.1408.004
Levroney, E. L., Aguilar, H. C., Fulcher, J. A., Kohatsu, L., Pace, K. E., Pang, M., Gurney, K. B., Baum, L. G., & Lee, B. (2005). Novel Innate Immune Functions for Galectin-1: Galectin-1 Inhibits Cell Fusion by Nipah Virus Envelope Glycoproteins and Augments Dendritic Cell Secretion of Proinflammatory Cytokines. *The Journal of Immunology, 175*(1), 413-420.
Lewin, A. R., Reid, L. E., McMahon, M., Stark, G. R., & Kerr, I. M. (1991). Molecular analysis of a human interferon-inducible gene family. *European Journal of Biochemistry, 199*(2), 417-423.
Li, K., Markosyan, R. M., Zheng, Y.-M., Golfetto, O., Bungart, B., Li, M., Ding, S., He, Y., Liang, C., Lee, J. C., Gratton, E., Cohen, F. S., & Liu, S.-L. (2013). IFITM proteins restrict viral membrane hemifusion. *PLoS Pathogens, 9*(1), 1-18. doi: 10.1371/journal.ppat.1003124
Li, M., Embury-Hyatt, C., & Weingartl, H. M. (2010). Experimental inoculation study indicates swine as a potential host for Hendra virus. *Veterinary Research, 41*(3), 33.
Li, Z., Yu, M., Zhang, H., Magoffin, D. E., Jack, P. J. M., Hyatt, A., Wang, H.-Y., & Wang, L.-F. (2006). Beilong virus, a novel paramyxovirus with the largest genome of non-

segmented negative-stranded RNA viruses. *Virology, 346*(1), 219-228. doi: 10.1016/j.virol.2005.10.039
Liebl, D. J., Morris, C. J., Henkemeyer, M., & Parada, L. F. (2003). mRNA expression of ephrins and Eph receptor tyrosine kinases in the neonatal and adult mouse central nervous system. *Journal of Neuroscience Research, 71*(1), 7-22. doi: 10.1002/jnr.10457
Lo, M., Lowe, L., Hummel, K., Sazzad, H., Gurley, E., & Hossain, M. (2012). Characterization of Nipah virus from outbreaks in Bangladesh, 2008–2010. *Emerging Infectious Diseases 18*(2), 248-255. doi: 10.3201/eid1802.111492
Lo, M. K., Harcourt, B. H., Mungall, B. A., Tamin, A., Peeples, M. E., Bellini, W. J., & Rota, P. A. (2009). Determination of the henipavirus phosphoprotein gene mRNA editing frequencies and detection of the C, V and W proteins of Nipah virus in virus-infected cells. *Journal of General Virology, 90*(2), 398-404. doi: 10.1099/vir.0.007294-0
Luby, S. P., & Gurley, E. S. (2012). Epidemiology of Henipavirus disease in humans. In Benhur Lee & Paul Rota (Eds.), *Current Topics in Microbiology and Immunology-Henipavirus* (Vol. 359, pp. 25-40). Berlin, Heidelberg: Springer.
Lundstrom, K. (2003). Virus-based vectors for gene expression in mammalian cells: Semliki Forest virus *New Comprehensive Biochemistry* (Vol. Volume 38, pp. 207-230): Elsevier.
Mahalingam, S., Herrero, L. J., Playford, E. G., Spann, K., Herring, B., Rolph, M. S., Middleton, D., McCall, B., Field, H., & Wang, L.-F. (2012). Hendra virus: an emerging paramyxovirus in Australia. *Lancet Infectious Diseases, 12*(10), 799-807. doi: 10.1016/S1473-3099(12)70158-5
Mahlakõiv, T., Ritz, D., Mordstein, M., DeDiego, M. L., Enjuanes, L., Müller, M. A., Drosten, C., & Staeheli, P. (2012). Combined action of type I and type III interferon restricts initial replication of severe acute respiratory syndrome coronavirus in the lung but fails to inhibit systemic virus spread. *Journal of General Virology, 93*(Pt 12), 2601-2605. doi: 10.1099/vir.0.046284-0
Makinen, T., Adams, R. H., Bailey, J., Lu, Q., Ziemiecki, A., Alitalo, K., Klein, R., & Wilkinson, G. A. (2005). PDZ interaction site in ephrinB2 is required for the remodeling of lymphatic vasculature. *Genes & Development, 19*(3), 397-410. doi: 10.1101/Gad.330105
Malashkevich, V. N., Schneider, B. J., McNally, M. L., Milhollen, M. A., Pang, J. X., & Kim, P. S. (1999). Core structure of the envelope glycoprotein GP2 from Ebola virus at 1.9- Å resolution. *Proceedings of the National Academy of Sciences of the United States of America, 96*(6), 2662-2667. doi: 10.1073/pnas.96.6.2662
Manyweathers, J., Field, H., Longnecker, N., Agho, K., Smith, C., & Taylor, M. (2017). "Why won't they just vaccinate?" Horse owner risk perception and uptake of the Hendra virus vaccine. *BMC Veterinary Research, 13*, 103. doi: 10.1186/s12917-017-1006-7
Marianneau, P., Guillaume, V., Wong, K. T., Badmanathan, M., Looi, R. Y., Murri, S., Loth, P., Tordo, N., Wild, T. F., Horvat, B., & Contamin, H. (2010). Experimental infection of squirrel monkeys with Nipah virus. *Emerging Infectious Diseases, 16*(3), 507-510. doi: 10.3201/eid1603.091346
Marsh, G. A., de Jong, C., Barr, J. A., Tachedjian, M., Smith, C., Middleton, D., Yu, M., Todd, S., Foord, A. J., Haring, V., Payne, J., Robinson, R., Broz, I., Crameri, G., Field, H. E., & Wang, L.-F. (2012). Cedar virus: a novel Henipavirus isolated from Australian bats. *Plos Pathogens, 8*(8), e1002836. doi: 10.1371/journal.ppat.1002836
Marsh, G. A., Haining, J., Hancock, T. J., Robinson, R., Foord, A. J., Barr, J. A., Riddell, S., Heine, H. G., White, J. R., Crameri, G., Field, H. E., Wang, L. F., & Middleton, D. (2011). Experimental infection of horses with Hendra virus/Australia/Horse/2008/Redlands. *Emerging Infectious Diseases 17*(12), 2232-2238. doi: 10.3201/eid1712.111162
Marsh, G. A., Todd, S., Foord, A., Hansson, E., Davies, K., Wright, L., Morrissy, C., Halpin, K., Middleton, D., Field, H. E., Daniels, P., & Wang, L. F. (2010). Genome sequence

conservation of Hendra virus isolates during spillover to horses, Australia. *Emerging Infectious Diseases, 16*(11), 1767-1769. doi: 10.3201/eid1611.100501

Mathieu, C., Pohl, C., Szecsi, J., Trajkovic-Bodennec, S., Devergnas, S., Raoul, H., Cosset, F.-L., Gerlier, D., Wild, T. F., & Horvat, B. (2011). Nipah virus uses leukocytes for efficient dissemination within a host. *Journal of Virology, 85*(15), 7863-7871. doi: 10.1128/jvi.00549-11

Matsumiya, L. C., Sorge, R. E., Sotocinal, S. G., Tabaka, J. M., Wieskopf, J. S., Zaloum, A., King, O. D., & Mogil, J. S. (2012). Using the mouse grimace scale to reevaluate the efficacy of postoperative analgesics in laboratory mice. *Journal of the American Association for Laboratory Animal Science, 51*(1), 42-49.

Maxie, M. G., Jubb, K. V. F., Kennedy, P. C., & Palmer, N. (2007). *Jubb Kennedy and Palmer's pathology of domestic animals* (M. Grant Maxie Ed. 5th ed. / edited by M. Grant Maxie. ed. Vol. 3). Edinburgh
New York: Elsevier Saunders.

McFarlane, R., Becker, N., & Field, H. (2011). Investigation of the climatic and environmental cntext of Hendra virus spillover events 1994-2010. *PLoS ONE, 6*(12), e28374. doi: 10.1371/journal.pone.0028374

McNabb, L., Barr, J., Crameri, G., Juzva, S., Riddell, S., Colling, A., Boyd, V., Broder, C., Wang, L. F., & Lunt, R. (2014). Henipavirus microsphere immuno-assays for detection of antibodies against Hendra virus. *Journal of Virological Methods, 200*, 22-28. doi: 10.1016/j.jviromet.2014.01.010

Mendez, D. H., Judd, J., & Speare, R. (2012). Unexpected result of Hendra virus outbreaks for veterinarians, Queensland, Australia. *Emerging Infectious Diseases, 18*(1), 83-84. doi: 10.3201/eid1801.111006

Meraz, M. A., White, J. M., Sheehan, K. C. F., Bach, E. A., Rodig, S. J., Dighe, A. S., Kaplan, D. H., Riley, J. K., Greenlund, A. C., Campbell, D., Carver-Moore, K., DuBois, R. N., Clark, R., Aguet, M., & Schreiber, R. D. (1996). Targeted disruption of the Stat1 gene in mice reveals unexpected physiologic specificity in the JAK–STAT signaling pathway. *Cell, 84*(3), 431-442. doi: 10.1016/S0092-8674(00)81288-X

Meulendyke, K. A., Wurth, M. A., McCann, R. O., & Dutch, R. E. (2005). Endocytosis plays a critical role in proteolytic processing of the Hendra virus fusion protein. *Journal Of Virology, 79*(20), 12643-12649.

Michalski, W. P., Crameri, G., Wang, L., Shiell, B. J., & Eaton, B. (2000). The cleavage activation and sites of glycosylation in the fusion protein of Hendra virus. *Virus Research, 69*(2), 83-93.

Middleton, D., Pallister, J., Klein, R., Feng, Y. R., Haining, J., Arkinstall, R., Frazer, L., Huang, J. A., Edwards, N., Wareing, M., Elhay, M., Hashmi, Z., Bingham, J., Yamada, M., Johnson, D., White, J., Foord, A., Heine, H. G., Marsh, G. A., Broder, C. C., & Wang, L. F. (2014). Hendra virus vaccine, a one health approach to protecting horse, human, and environmental health. *Emerging Infectious Diseases, 20*(3), 372-379. doi: 10.3201/eid2003.131159

Middleton, D. J., Morrissy, C. J., van der Heide, B. M., Russell, G. M., Braun, M. A., Westbury, H. A., Halpin, K., & Daniels, P. W. (2007). Experimental Nipah virus infection in Pteropid bats (Pteropus poliocephalus). *Journal of Comparative Pathology, 136*(4), 266-272. doi: 10.1016/j.jcpa.2007.03.002

Middleton, D. J., Westbury, H. A., Morrissy, C. J., van der Heide, B. M., Russell, G. M., Braun, M. A., & Hyatt, A. D. (2002). Experimental Nipah virus infection in pigs and cats. *Journal of Comparative Pathology, 126*(2–3), 124-136. doi: 10.1053/jcpa.2001.0532

Migani, P., Bartlett, C., Dunlop, S., Beazley, L., & Rodger, J. (2007). Ephrin-B2 immunoreactivity distribution in adult mouse brain. *Brain Research, 1182*(0), 60-72. doi: 10.1016/j.brainres.2007.08.065

Migani, P., Bartlett, C., Dunlop, S., Beazley, L., & Rodger, J. (2009). Regional and cellular distribution of ephrin-B1 in adult mouse brain. *Brain Research, 1247*(0), 50-61. doi: 10.1016/j.brainres.2008.09.100

Mills, J., Alim, A., Bunning, M., Lee, O., Wagoner, K., Amman, B., Stockton, P., & Ksiazek, T. (2009). Nipah virus infection in dogs, Malaysia, 1999. . *Emerging Infectious Diseases, 15*(6), 950-952. doi: 10.3201/eid1506.080453

Mire, C. E., Geisbert, J. B., Agans, K. N., Feng, Y.-R., Fenton, K. A., Bossart, K. N., Yan, L., Chan, Y.-P., Broder, C. C., & Geisbert, T. W. (2014). A recombinant Hendra virus G glycoprotein subunit vaccine protects nonhuman primates against Hendra virus challenge. *Journal of Virology, 88*(9), 4624-4631. doi: 10.1128/jvi.00005-14

Mohd Nor, M. N., Gan, C. H., & Ong, B. L. (2000). Nipah virus infection of pigs in peninsular Malaysia. *Revue Scientifique Et Technique (International Office Of Epizootics), 19*(1), 160-165.

Monath, T. P., Cropp, C. B., & Harrison, A. K. (1983). Mode of entry of a neurotropic arbovirus into the central nervous system. Reinvestigation of an old controversy. *Laboratory Investigation, 48*(4), 399-410.

Morgan, K. T., Jiang, X.-Z., Patterson, D. L., & Gross, E. A. (1984). The nasal mucociliary apparatus: correlation of structure and function in the Rat. *American Review of Respiratory Disease, 130*(2), 275-281.

Mounts, A. W., Kaur, H., Parashar, U. D., Ksiazek, T. G., Cannon, D., Arokiasamy, J. T., Anderson, L. J., & Lye, M. S. (2001). A cohort study of health care workers to assess nosocomial transmissibility of Nipah virus, Malaysia, 1999. *Journal of Infectious Diseases, 183*(5), 810-813. doi: 10.1086/318822

Mudhasani, R., Tran, J. P., Retterer, C., Radoshitzky, S. R., Kota, K. P., Altamura, L. A., Smith, J. M., Packard, B. Z., Kuhn, J. H., Costantino, J., Garrison, A. R., Schmaljohn, C. S., Huang, I.-C., Farzan, M., & Bavari, S. (2013). IFITM-2 and IFITM-3 but not IFITM-1 restrict Rift Valley Fever virus. *Journal of Virology, 87*(15), 8451-8464. doi: 10.1128/jvi.03382-12

Muller, U., Steinhoff, U., Reis, L., Hemmi, S., Pavlovic, J., Zinkernagel, R., & Aguet, M. (1994). Functional role of type I and type II interferons in antiviral defense. *Science, 264*(5167), 1918-1921. doi: 10.1126/science.8009221

Muller, W. A. (2013). Getting leukocytes to the site of inflammation. *Veterinary Pathology, 50*(1), 7-22. doi: 10.1177/0300985812469883

Mungall, B. A., Middleton, D., Crameri, G., Bingham, J., Halpin, K., Russell, G., Green, D., McEachern, J., Pritchard, L. I., Eaton, B. T., Wang, L.-F., Bossart, K. N., & Broder, C. C. (2006). Feline model of acute Nipah virus infection and protection with a soluble glycoprotein-based subunit vaccine. *Journal of Virology, 80*(24), 12293-12302. doi: 10.1128/jvi.01619-06

Mungall, B. A., Middleton, D., Crameri, G., Halpin, K., Bingham, J., Eaton, B. T., & Broder, C. C. (2007). Vertical transmission and fetal replication of Nipah virus in an experimentally infected cat. *Journal of Infectious Diseases, 196*(6), 812-816. doi: 10.1086/520818

Munster, V. J., Prescott, J. B., Bushmaker, T., Long, D., Rosenke, R., Thomas, T., Scott, D., Fischer, E. R., Feldmann, H., & de Wit, E. (2012). Rapid Nipah virus entry into the central nervous system of hamsters via the olfactory route. *Scientific Reports, 2*(736). doi: 10.1038/srep00736

Murray, K., Dunn, K., & Murray, G. (1999). *Hendra virus (equine Morbillivirus): the outbreaks, the disease and lessons for preparedness.* Paper presented at the Equine infectious diseases, Dubai; March 1998.

Murray, K., Selleck, P., Hooper, P., Hyatt, A., Gould, A., Gleeson, L., Westbury, H., Hiley, L., Selvey, L., & Rodwell, B. (1995). A Morbillivirus that caused fatal disease in horses and humans. *Science, 268*(5207), 94-97. doi: 10.1126/science.7701338

Murray, P. K. (1996). The evolving story of the equine Morbillivirus. *Australian Veterinary Journal, 74*(3), 214-214.

Negrete, O. A., Levroney, E. L., Aguilar, H. C., Bertolotti-Ciarlet, A., Nazarian, R., Tajyar, S., & Lee, B. (2005). EphrinB2 is the entry receptor for Nipah virus, an emergent deadly paramyxovirus. *Nature, 436*(7049), 401-405. doi: 10.1038/nature03838

Ng, Cherie T., Mendoza, Juan L., Garcia, K. C., & Oldstone, Michael B. A. (2016). Alpha and beta Type 1 interferon signaling: passage for diverse biologic outcomes. *Cell, 164*(3), 349-352. doi: 10.1016/j.cell.2015.12.027

Nowak, R. (1995). Cause of fatal outbreak in horses and humans traced. *Science, 268*(5207), 32. doi: 10.1126/science.7701338

O'Sullivan, J. D., & Allworth, A. M. (1997). Fatal encephalitis due to novel paramyxovirus transmitted from horses. *Lancet, 349*(9045), 93.

Orozco, S., Schmid, M. A., Parameswaran, P., Lachica, R., Henn, M. R., Beatty, R., & Harris, E. (2012). Characterization of a model of lethal Dengue virus 2 infection in C57BL/6 mice deficient in the alpha/beta interferon receptor. *Journal of General Virology, 93*(Pt 10), 2152-2157. doi: 10.1099/vir.0.045088-0

Pager, C. T., & Dutch, R. E. (2005). Cathepsin L is involved in proteolytic processing of the Hendra virus fusion protein. *Journal Of Virology, 79*(20), 12714-12720.

Pallister, J., Middleton, D., Crameri, G., Yamada, M., Klein, R., Hancock, T. J., Foord, A., Shiell, B., Michalski, W., Broder, C. C., & Wang, L.-F. (2009). Chloroquine administration does not prevent Nipah virus infection and disease in ferrets. *Journal of Virology, 83*(22), 11979-11982. doi: 10.1128/jvi.01847-09

Pallister, J., Middleton, D., Wang, L.-F., Klein, R., Haining, J., Robinson, R., Yamada, M., White, J., Payne, J., Feng, Y.-R., Chan, Y.-P., & Broder, C. C. (2011). A recombinant Hendra virus G glycoprotein-based subunit vaccine protects ferrets from lethal Hendra virus challenge. *Vaccine, 29*(34), 5623-5630. doi: 10.1016/j.vaccine.2011.06.015

Palmer, A., & Klein, R. (2003). Multiple roles of ephrins in morphogenesis, neuronal networking, and brain function. *Genes & Development, 17*(12), 1429-1450. doi: 10.1101/Gad.1093703

Papenfuss, A., Baker, M., Feng, Z.-P., Tachedjian, M., Crameri, G., Cowled, C., Ng, J., Janardhana, V., Field, H., & Wang, L.-F. (2012). The immune gene repertoire of an important viral reservoir, the Australian black flying fox. *BMC Genomics, 13*(1), 261. doi: 10.1186/1471-2164-13-261

Parashar, U. D., Sunn, L. M., Ong, F., Mounts, A. W., Arif, M. T., Ksiazek, T. G., Kamaluddin, M. A., Mustafa, A. N., Kaur, H., Ding, L. M., Othman, G., Radzi, H. M., Kitsutani, P. T., Stockton, P. C., Arokiasamy, J., Gary, H. E., & Anderson, L. J. (2000). Case-control study of risk factors for human infection with a new zoonotic Paramyxovirus, Nipah Virus, during a 1998–1999 outbreak of severe encephalitis in Malaysia. *Journal of Infectious Diseases, 181*(5), 1755-1759. doi: 10.1086/315457

Pasieka, T. J., Collins, L., O'Connor, M. A., Chen, Y., Parker, Z. M., Berwin, B. L., Piwnica-Worms, D. R., & Leib, D. A. (2011). Bioluminescent imaging reveals divergent viral pathogenesis in two strains of Stat1-deficient mice, and in αßγ interferon receptor-deficient mice. *PLoS ONE, 6*(9), e24018. doi: 10.1371/journal.pone.0024018

Pasieka, T. J., Lu, B., & Leib, D. A. (2008). Enhanced pathogenesis of an attenuated Herpes Simplex virus for mice lacking Stat1. *Journal of Virology, 82*(12), 6052-6055. doi: 10.1128/jvi.00297-08

Paton, N. I., Leo, Y. S., Zaki, S. R., Auchus, A. P., Lee, K. E., Ling, A. E., Chew, S. K., Ang, B., Rollin, P. E., Umapathi, T., Sng, I., Lee, C. C., Lim, E., & Ksiazek, T. G. (1999). Outbreak of Nipah-virus infection among abattoir workers in Singapore. *Lancet, 354*(9186), 1253-1256. doi: 10.1016/s0140-6736(99)04379-2

Pernet, O., Wang, Y. E., & Lee, B. (2012). Henipavirus receptor usage and tropism. In Benhur Lee & Paul Rota (Eds.), *Current Topics in Microbiology and Immunology-Henipavirus* (Vol. 359, pp. 59-78). Berlin, Heidelberg: Springer.

Perreira, J. M., Chin, C. R., Feeley, E. M., & Brass, A. L. (2013). IFITMs restrict the replication of multiple pathogenic viruses. *Journal of Molecular Biology, 425*(24), 4937-4955. doi: 10.1016/j.jmb.2013.09.024

Piehler, J., Thomas, C., Garcia, K. C., & Schreiber, G. (2012). Structural and dynamic determinants of type I interferon receptor assembly and their functional interpretation. *Immunological Reviews, 250*(1), 317-334. doi: 10.1111/imr.12001

Playford, E. G., McCall, B., Smith, G., Slinko, V., Allen, G., Smith, I., Moore, F., Taylor, C., Kung, Y. H., & Field, H. (2010). Human Hendra virus encephalitis associated with equine outbreak, Australia, 2008. *Emerging Infectious Diseases, 16*(2), 219-223. doi: 10.3201/eid1602.090552

Plowright, R. K., Eby, P., Hudson, P. J., Smith, I. L., Westcott, D., Bryden, W. L., Middleton, D., Reid, P. A., McFarlane, R. A., Martin, G., Tabor, G. M., Skerratt, L. F., Anderson, D. L., Crameri, G., Quammen, D., Jordan, D., Freeman, P., Wang, L.-F., Epstein, J. H., Marsh, G. A., Kung, N. Y., & McCallum, H. (2014). Ecological dynamics of emerging bat virus spillover. *Proceedings of the Royal Society of London B: Biological Sciences, 282*(1798). doi: 10.1098/rspb.2014.2124

Plowright, R. K., Foley, P., Field, H. E., Dobson, A. P., Foley, J. E., Eby, P., & Daszak, P. (2011). Urban habituation, ecological connectivity and epidemic dampening: the emergence of Hendra virus from flying foxes (Pteropus spp.). *Proceedings of the Royal Society of London B: Biological Sciences, 278*(1725), 3703-3712. doi: 10.1098/rspb.2011.0522

Poliakov, A., Cotrina, M., & Wilkinson, D. G. (2004). Diverse roles of Eph receptors and ephrins in the regulation of cell migration and tissue assembly. *Developmental Cell, 7*(4), 465-480.

Popa, A., Carter, J. R., Smith, S. E., Hellman, L., Fried, M. G., & Dutch, R. E. (2012). Residues in the Hendra virus fusion protein transmembrane domain are critical for endocytic recycling. *Journal Of Virology, 86*(6), 3014-3026.

PromedMail. (2009). Hendra virus, human, equine - Australia (04): (QL) fatal. *PromedMail*. Retrieved from http://www.promedmail.org website: http://www.promedmail.org

PromedMail. (2011). Hendra virus, equine - Australia(21): Queensland, Canine. *PromedMail*. Retrieved from http://www.promedmail.org website:

PromedMail. (2013). Hendra virus, equine- Australia (19): (QLD) Canine *PromedMail*.

Pulverer, J. E., Rand, U., Lienenklaus, S., Kugel, D., Ziętara, N., Kochs, G., Naumann, R., Weiss, S., Staeheli, P., Hauser, H., & Köster, M. (2010). Temporal and spatial resolution of Type I and III interferon responses in vivo. *Journal Of Virology, 84*(17), 8626-8638. doi: 10.1128/jvi.00303-10

Queensland Biosecurity. (2011). Guidelines for veterinarians handling potential Hendra virus infection in horses, version 4.2 Decemeber 2011. www.biosecurity.qld.gov.au

Queensland Government. (2013). Hendra virus: the initial research, Hendra virus incidents. Retrieved from Queensland Government, Department of Agriculture Fisheries and Forestry website:

Rahman, S. A., Hassan, L., Epstein, J. H., Mamat, Z. C., Yatim, A. M., Hassan, S. S., Field, H. E., Hughes, T., Westrum, J., Naim, M. S., Suri, A. S., Jamaluddin, A. A., & Daszak, P. (2013). Risk factors for Nipah virus infection among Pteropid bats, peninsular Malaysia. *Emerging Infectious Diseases, 19*(1), 51-60. doi: 10.3201/eid1901.120221

Ramachandran, A., & Horvath, C. (2009). Paramyxovirus disruption of interferon signal transduction: STATus Report. *Journal of Interferon & Cytokine Research, 29*(9), 531.

Ramana, C. V., Gil, M. P., Han, Y., Ransohoff, R. M., Schreiber, R. D., & Stark, G. R. (2001). Stat1-independent regulation of gene expression in response to IFN-γ. *Proceedings of the National Academy of Sciences, 98*(12), 6674-6679. doi: 10.1073/pnas.111164198

Randall, R. E., & Goodbourn, S. (2008). Interferons and viruses: an interplay between induction, signalling, antiviral responses and virus countermeasures. *Journal of General Virology, 89*(1), 1-47. doi: 10.1099/vir.0.83391-0

Raymond, J., Bradfute, S., & Bray, M. (2011). Filovirus infection of STAT-1 knockout mice. *Journal of Infectious Diseases, 204*(suppl 3), S986-S990. doi: 10.1093/infdis/jir335

Reed, L. J., & Muench, H. (1938). A simple method of estimating fifty per cent endpoints. *American Journal of Epidemiology, 27*(3), 493-497.

Rockx, B. (2014). Recent developments in experimental animal models of Henipavirus infection. *Pathogens and Disease, 71*(2), 199-206. doi: 10.1111/2049-632X.12149

Rockx, B., Bossart, K. N., Feldmann, F., Geisbert, J. B., Hickey, A. C., Brining, D., Callison, J., Safronetz, D., Marzi, A., Kercher, L., Long, D., Broder, C. C., Feldmann, H., & Geisbert, T. W. (2010). A novel model of lethal Hendra virus infection in African green monkeys and the effectiveness of ribavirin treatment. *Journal of Virology, 84*(19), 9831-9839. doi: 10.1128/jvi.01163-10

Rockx, B., Brining, D., Kramer, J., Callison, J., Ebihara, H., Mansfield, K., & Feldmann, H. (2011). Clinical outcome of Henipavirus infection in hamsters is determined by the route and dose of infection. *Journal of Virology, 85*(15), 7658-7671. doi: 10.1128/jvi.00473-11

Rodriguez, J. J., Lin-Fa Wang, J. J., & Horvath, C. M. (2003). Hendra virus V protein inhibits interferon signaling by preventing STAT1 and STAT2 nuclear accumulation. *Journal Of Virology, 77*(21), 11842-11845. doi: 10.1128/JVI.77.21.11842-11845.2003

Rogers, R. J., Douglas, I. C., Baldock, F. C., Glanville, R. J., Seppanen, K. T., Gleeson, L. J., Selleck, P. N., & Dunn, K. J. (1996). Investigation of a second focus of equine Morbillivirus infection in coastal Queensland. *Australian Veterinary Journal, 74*(3), 243-244.

Rota, P. A., Harcourt, B. H., Rollin, P. E., Widjojoatmodjo, Bellini, W. J., & Chua, K. B. (1999). Molecular characterization of a Hendra-like virus (Nipah virus) isolated from fatal encephalitis cases in Malaysia and Singapore *XIth International Congress of Virology Abstracts Book, August 9-13, 1999, International Union of Microbiological Societies, Sydney, Australia*. Sydney, Australia: International Union of Microbiological Societies.

Rota, P. A., & Lo, M. K. (2012). Molecular virology of the henipaviruses. In Benhur Lee & Paul Rota (Eds.), *Current Topics in Microbiology and Immunology- Henipavirus* (Vol. 359, pp. 41-58). Berlin, Heidelberg: Springer.

Sarji, S. A., Abdullah, B. J. J., Goh, K. J., Tan, C. T., & Wong, K. T. (2000). MR Imaging Features of Nipah Encephalitis. *American Journal of Roentgenology, 175*(2), 437-442. doi: 10.2214/ajr.175.2.1750437

Sasaki, M., Setiyono, A., Handharyani, E., Rahmadani, I., Taha, S., Adiani, S., Subangkit, M., Sawa, H., Nakamura, I., & Kimura, T. (2012). Molecular detection of a novel paramyxovirus in fruit bats from Indonesia. *Virology Journal 9*(1), 240.

Selvey, L. A., Wells, R. M., McCormack, J. G., Ansford, A. J., Murray, K., Rogers, R. J., Lavercombe, P. S., Selleck, P., & Sheridan, J. W. (1995). Infection of humans and horses by a newly described Morbillivirus. *Medical Journal of Australia, 162*(12), 642-645.

Shaw, M. L. (2009). Henipaviruses employ a multifaceted approach to evade the antiviral interferon response. *Viruses, 1*(3), 1190-1203. doi: 10.3390/v1031190

Siegrist, F., Ebeling, M., & Certa, U. (2011). The small interferon-induced transmembrane genes and proteins. *Journal of Interferon & Cytokine Research, 31*(1), 183-197. doi: 10.1089/jir.2010.0112

Smith, E. C., Popa, A., Chang, A., Masante, C., & Dutch, R. E. (2009). Viral entry mechanisms: the increasing diversity of paramyxovirus entry. *Federation of European Biochemical Societies Journal, 276*(24), 7217-7227. doi: 10.1111/j.1742-4658.2009.07401.x

Smith, I., Broos, A., de Jong, C., Zeddeman, A., Smith, C., Smith, G., Moore, F., Barr, J., Crameri, G., Marsh, G., Tachedjian, M., Yu, M., Kung, Y. H., Wang, L. F., & Field, H. (2011). Identifying Hendra virus diversity in Pteropid bats. *PLoS ONE, 6*(9), e25275. doi: 10.1371/journal.pone.0025275

Sohayati, A. R., Hassan, L., Sharifah, S. H., Lazarus, K., Zaini, C. M., Epstein, J. H., Shamsyul Naim, N., Field, H. E., Arshad, S. S., Adbul Aziz, J., & Daszak, P. (2011). Evidence for Nipah virus recrudescence and serological patterns of captive Pteropus vampyrus. *Epidemiology & Infection, 139*(Special Issue 10), 1570-1579. doi: 10.1017/S0950268811000550

Sommereyns, C., Paul, S., Staeheli, P., & Michiels, T. (2008). IFN-lambda (IFN-λ) is expressed in a tissue-dependent fashion and primarily acts on epithelial cells in vivo. *Plos Pathogens, 4*(3), e1000017. doi: 10.1371/journal.ppat.1000017

Stachowiak, B., & Weingartl, H. M. (2012). Nipah virus infects specific subsets of porcine peripheral blood mononuclear cells. *PLoS ONE, 7*(1), e30855. doi: 10.1371/journal.pone.0030855

Sullivan, J. D. O., Allworth, A. M., Paterson, D. L., Snow, T. M., Boots, R., Gleeson, L. J., Gould, A. R., Hyatt, A. D., & Bradfield, J. (1997). Early Report: Fatal encephalitis due to novel paramyxovirus transmitted from horses. *Lancet, 349*, 93-95. doi: 10.1016/s0140-6736(96)06162-4

Sundberg, J. P., Fox, J. G., Ward, J. M., & Bedigian, H. G. (1997). Idiopathic focal hepatic necrosis in inbred mice. In Thomas Carlyle Jones, James A. Popp & Ulrich Mohr (Eds.), *Digestive System* (pp. 213-217). Berlin, Heidelberg: Springer Berlin Heidelberg.

Tan, C. T., Goh, K. J., Wong, K. T., Sarji, S. A., Chua, K. B., Chew, N. K., Murugasu, P., Loh, Y. L., Chong, H. T., Tan, K. S., Thayaparan, T., Kumar, S., & Jusoh, M. R. (2002). Relapsed and late-onset Nipah encephalitis. *Annals of Neurology, 51*(6), 703-708. doi: 10.1002/ana.10212

Tan, C. T., & Tan, K. S. (2001). Nosocomial transmissibility of Nipah virus. *Journal of Infectious Diseases, 184*(10), 1367. doi: 10.1086/323996

Taylor, C., Playford, E., McBride, W., McMahon, J., & D, W. (2012). No evidence of prolonged Hendra virus shedding by 2 patients, Australia. *Emerging Infectious Diseases 18*(12), 2025-2027. doi: 10.3201/eid1812.120722

Teijaro, J. R. (2016). Type I interferons in viral control and immune regulation. *Current Opinion in Virology, 16*, 31-40. doi: 10.1016/j.coviro.2016.01.001

Thibodeaux, B. A., Garbino, N. C., Liss, N. M., Piper, J., Blair, C. D., & Roehrig, J. T. (2012). A small animal peripheral challenge model of yellow fever using interferon-receptor deficient mice and the 17D-204 vaccine strain. *Vaccine, 30*(21), 3180-3187. doi: 10.1016/j.vaccine.2012.03.003

Traynor, T. R., Majde, J. A., Bohnet, S. G., & Krueger, J. M. (2007). Interferon Type I receptor-deficient mice have altered disease symptoms in response to Influenza virus. *Brain, Behavior, and Immunity, 21*(3), 311-322. doi: 10.1016/j.bbi.2006.09.007

Valbuena, G., Halliday, H., Borisevich, V., Goez, Y., & Rockx, B. (2014). A human lung xenograft mouse model of Nipah virus infection. *PLoS Pathogens, 10*(4), e1004063. doi: 10.1371/journal.ppat.1004063

van den Broek, M. F., Müller, U., Huang, S., Aguet, M., & Zinkernagel, R. M. (1995). Antiviral defense in mice lacking both alpha/beta and gamma interferon receptors. *Journal of Virology, 69*(8), 4792-4796.

van Riel, D., Verdijk, R., & Kuiken, T. (2015). The olfactory nerve: a shortcut for influenza and other viral diseases into the central nervous system. *The Journal of Pathology, 235*(2), 277-287. doi: 10.1002/path.4461

Vigant, F., & Lee, B. (2011). Hendra and Nipah infection: pathology, models and potential therapies. *Infectious Disorders Drug Targets, 11*(3), 315-336.

Virtue, E. R. (2011). *Modulation of the interferon response during henipavirus infection.* (Doctor of Philosophy PhD thesis), University of Melbourne Available from EBSCOhost ir00004a database.

Virtue, E. R., Marsh, G. A., Baker, M. L., & Wang, L. F. (2011). Interferon production and signaling pathways are antagonized during Henipavirus infection of fruit bat cell lines. *PLoS ONE, 6*(7), e22488. doi: 10.1371/journal.pone.0022488

Wang, H.-H., Kung, N. Y., Grant, W. E., Scanlan, J. C., & Field, H. E. (2013). Recrudescent Infection Supports Hendra Virus Persistence in Australian Flying-Fox Populations. *PLoS ONE, 8*(11), e80430. doi: 10.1371/journal.pone.0080430

Wang, J., Schreiber, R. D., & Campbell, I. L. (2002). STAT1 deficiency unexpectedly and markedly exacerbates the pathophysiological actions of IFN-α in the central nervous

system. *Proceedings of the National Academy of Sciences, 99*(25), 16209-16214. doi: 10.1073/pnas.252454799

Wang, L.-F., Michalski, W. P., Yu, M., Pritchard, L. I., Crameri, G., Shiell, B., & Eaton, B. T. (1998). A novel P/V/C gene in a new member of the Paramyxoviridae family, which causes lethal infection in humans, horses, and other animals. *Journal Of Virology, 72*(2), 1482-1490.

Wang, L.-F., Yu, M., Hansson, E., Pritchard, L. I., Shiell, B., Michalski, W. P., & Eaton, B. T. (2000). The exceptionally large genome of Hendra virus: support for creation of a new genus within the family Paramyxoviridae. *Journal of Virology 74*(21), 9972-9979. doi: 10.1128/jvi.74.21.9972-9979.2000

Wang, L., Harcourt, B. H., Yu, M., Tamin, A., Rota, P. A., Bellini, W. J., & Eaton, B. T. (2001). Molecular biology of Hendra and Nipah viruses. *Microbes and Infection, 3*(4), 279-287. doi: 10.1016/S1286-4579(01)01381-8

Wang, Y. E., Park, A., Lake, M., Pentecost, M., Torres, B., Yun, T. E., Wolf, M. C., Holbrook, M. R., Freiberg, A. N., & Lee, B. (2010). Ubiquitin-regulated nuclear-cytoplasmic trafficking of the Nipah virus matrix protein is important for viral budding. *Plos Pathogens, 6*(11), e1001186. doi: 10.1371/journal.ppat.1001186.

Warren, C. J., Griffin, L. M., Little, A. S., Huang, I. C., Farzan, M., & Pyeon, D. (2014). The antiviral restriction factors IFITM1, 2 and 3 do not inhibit infection of Human Papillomavirus, Cytomegalovirus and Adenovirus. *PLoS ONE, 9*(5). doi: 10.1371/journal.pone.0096579

Weighardt, H., Kaiser-Moore, S., Schlautkötter, S., Rossmann-Bloeck, T., Schleicher, U., Bogdan, C., & Holzmann, B. (2006). Type I IFN modulates host defense and late hyperinflammation in septic peritonitis. *The Journal of Immunology, 177*(8), 5623.

Weingartl, H., Czub, S., Copps, J., Berhane, Y., Middleton, D., Marszal, P., Gren, J., Smith, G., Ganske, S., Manning, L., & Czub, M. (2005). Invasion of the central nervous system in a porcine host by Nipah virus. *Journal of Virology, 79*(12), 7528-7534. doi: 10.1128/jvi.79.12.7528-7534.2005

Weingartl, H. M., Berhane, Y., Caswell, J. L., Loosmore, S., Audonnet, J.-C., Roth, J. A., & Czub, M. (2006). Recombinant Nipah virus vaccines protect pigs against challenge. *Journal Of Virology, 80*(16), 7929-7938. doi: 10.1128/jvi.00263-06

Wernike, K., Breithaupt, A., Keller, M., Hoffmann, B., Beer, M., & Eschbaumer, M. (2012). Schmallenberg virus infection of adult Type I interferon receptor knock-out mice. *PLoS ONE, 7*(7), e40380. doi: 10.1371/journal.pone.0040380

Westbury, H. A., Hooper, P. T., Brouwer, S. L., & Selleck, P. W. (1996). Susceptibility of cats to equine Morbillivirus. *Australian Veterinary Journal, 74*(2), 132-134. doi: 10.1111/j.1751-0813.1996.tb14813.x

Westbury, H. A., Hooper, P. T., Selleck, P. W., & Murray, P. K. (1995). Equine Morbillivirus pneumonia: susceptibility of laboratory animals to the virus. *Australian Veterinary Journal, 72*(7), 278-279.

Williamson, M. (1999). *Pathogenesis of Hendra virus.* (Doctor of Philosophy Doctor of Philosophy), University of Melbourne, University of Melbourne, Australia. Available from EBSCOhost cat00006a database.

Williamson, M. M., Hooper, P. T., Selleck, P. W., Gleeson, L. J., Daniels, P. W., Westbury, H. A., & et al. (1998). Transmission studies of Hendra virus (equine Morbillivirus) in fruit bats, horses and cats. *Australian Veterinary Journal, 76*, 813-818.

Williamson, M. M., Hooper, P. T., Selleck, P. W., Westbury, H. A., & Slocombe, R. F. (2000). Experimental Hendra virus infection in pregnant guinea-pigs and fruit bats(Pteropus poliocephalus). *Journal of Comparative Pathology, 122*(2–3), 201-207. doi: 10.1053/jcpa.1999.0364

Williamson, M. M., Hooper, P. T., Selleck, P. W., Westbury, H. A., & Slocombe, R. F. S. (2001). A guinea-pig model of Hendra virus encephalitis. *Journal of Comparative Pathology, 124*(4), 273-279. doi: 10.1053/jcpa.2001.0464

Williamson, M. M., & Torres-Velez, F. J. (2010). Henipavirus: a review of laboratory animal pathology. *Veterinary Pathology 47*(5), 871-880. doi: 10.1177/0300985810378648

Winkler, C. W., Race, B., Phillips, K., & Peterson, K. E. (2015). Capillaries in the olfactory bulb but not the cortex are highly susceptible to virus-induced vascular leak and promote viral neuroinvasion. *Acta Neuropathologica, 130*(2), 233-245. doi: 10.1007/s00401-015-1433-0

Wong, K. T. (2010). Nipah and Hendra viruses: recent advances in pathogenesis. *Future Virology, 5*(2), 129-131. doi: 10.2217/Fvl.10.7

Wong, K. T., Grosjean, I., Brisson, C., Blanquier, B., Fevre-Montange, M., Bernard, A., Loth, P., Georges-Courbot, M.-C., Chevallier, M., Akaoka, H., Marianneau, P., Lam, S. K., Wild, T. F., & Deubel, V. (2003). A golden hamster model for human acute Nipah virus infection. *The American Journal of Pathology, 163*(5), 2127-2137. doi: 10.1016/S0002-9440(10)63569-9

Wong, K. T., & Ong, K. C. (2011). Pathology of acute Henipavirus infection in humans and animals. *Pathology Research International, 2011*, 567248. doi: 10.4061/2011/567248

Wong, K. T., Robertson, T., Ong, B. B., Chong, J. W., Yaiw, K. C., Wang, L. F., Ansford, A. J., & Tannenberg, A. (2009). Human Hendra virus infection causes acute and relapsing encephalitis. *Neuropathology and Applied Neurobiology, 35*(3), 296-305.

Wong, K. T., Shieh, W. J., Kumar, S., Norain, K., Abdullah, W., Guarner, J., Goldsmith, C. S., Chua, K. B., Lam, S. K., Tan, C. T., Goh, K. J., Chong, H. T., Jusoh, R., Rollin, P. E., Ksiazek, T. G., Zaki, S. R., & Group, N. V. P. W. (2002a). Nipah virus infection - pathology and pathogenesis of an emerging paramyxoviral zoonosis. *American Journal of Pathology, 161*(6), 2153-2167.

Wong, K. T., Shieh, W. J., Zaki, S. R., & Tan, C. T. (2002b). Nipah virus infection, an emerging paramyxoviral zoonosis. *Springer Seminars in Immunopathology, 24*(2), 215-228. doi: 10.1007/s00281-002-0106-y

Wong, K. T., & Tan, C. T. (2012). Clinical and pathological manifestations of human Henipavirus infection. In Benhur Lee & Paul Rota (Eds.), *Current Topics in Microbiology and Immunology- Henipavirus* (Vol. 359, pp. 95-104). Berlin, Heidelberg: Springer.

Woo, P. C. Y., Lau, S. K. P., Wong, B. H. L., Wong, A. Y. P., Poon, R. W. S., & Yuen, K.-Y. (2011). Complete genome sequence of a novel Paramyxovirus, Tailam virus, discovered in sikkim rats. *Journal Of Virology, 85*(24), 13473-13474. doi: 10.1128/jvi.06356-11

Wrensch, F., Winkler, M., & Pöhlmann, S. (2014). IFITM proteins inhibit entry driven by the MERS-Coronavirus spike protein: evidence for cholesterol-independent mechanisms. *Viruses, 6*(9), 3683-3698.

Xuesen, Z., Fang, G., Fei, L., Andrea, C., Jinhong, C., Timothy, M. B., & Ju-Tao, G. (2014). Interferon induction of IFITM proteins promotes infection by human coronavirus OC43. *Proceedings of the National Academy of Sciences of the United States of America, 111*(18), 6756-6761.

Yoneda, M., Guillaume, V., Ikeda, F., Sakuma, Y., Sato, H., Wild, T. F., & Kai, C. (2006). Establishment of a Nipah virus rescue system. *Proceedings of the National Academy of Sciences, 103*(44), 16508-16513. doi: 10.1073/pnas.0606972103

Yoneda, M., Guillaume, V., Sato, H., Fujita, K., Georges-Courbot, M.-C., Ikeda, F., Omi, M., Muto-Terao, Y., Wild, T. F., & Kai, C. (2010). The nonstructural proteins of Nipah virus play a key role in pathogenicity in experimentally infected animals. *PLoS ONE, 5*(9), e12709. doi: 10.1371/journal.pone.0012709

Yount, J. S., Moltedo, B., Yu-Ying, Y., Charron, G., Moran, T. M., López, C. B., & Hang, H. C. (2010). Palmitoylome profiling reveals S-palmitoylation–dependent antiviral activity of IFITM3. *Nature Chemical Biology, 6*(8), 610-614. doi: 10.1038/nchembio.405

Yu, M., Hansson, E., Shiell, B., Michalski, W., Eaton, B. T., & Wang, L. F. (1998). Sequence analysis of the Hendra virus nucleoprotein gene: comparison with other members of the subfamily Paramyxovirinae. *Journal of General Virology, 79*(7), 1775-1780.

Yun, T., Park, A., Hill, T. E., Pernet, O., Beaty, S. M., Juelich, T. L., Smith, J. K., Zhang, L., Wang, Y. E., Vigant, F., Gao, J., Wu, P., Lee, B., & Freiberg, A. N. (2015). Efficient reverse genetics reveals genetic determinants of budding and fusogenic differences

between Nipah and Hendra viruses and enables real-time monitoring of viral spread in small animal models of Henipavirus infection. *Journal of Virology, 89*(2), 1242-1253. doi: 10.1128/jvi.02583-14

Zhang, G., Cowled, C., Shi, Z., Huang, Z., Bishop-Lilly, K. A., Fang, X., Wynne, J. W., Xiong, Z., Baker, M. L., Zhao, W., Tachedjian, M., Zhu, Y., Zhou, P., Jiang, X., Ng, J., Yang, L., Wu, L., Xiao, J., Feng, Y., Chen, Y., Sun, X., Zhang, Y., Marsh, G. A., Crameri, G., Broder, C. C., Frey, K. G., Wang, L.-F., & Wang, J. (2013a). Comparative analysis of bat genomes provides insight into the evolution of flight and immunity. *Science, 339*(6118), 456-460. doi: 10.1126/science.1230835

Zhang, W., Zhang, L., Zan, Y., Du, N., Yang, Y., & Tien, P. (2015). Human respiratory syncytial virus infection is inhibited by IFN-induced transmembrane proteins. *Journal of General Virology, 96*(Pt 1), 170-182. doi: 10.1099/vir.0.066555-0

Zhang, Y.-h., Zhao, Y., Li, N., Peng, Y.-c., Giannoulatou, E., Jin, R.-h., Yan, H.-p., Wu, H., Liu, J.-h., Liu, N., Wang, D.-y., Shu, Y.-l., Ho, L.-p., Kellam, P., McMichael, A., & Dong, T. (2013b). Interferon-induced transmembrane protein-3 genetic variant rs12252-C is associated with severe influenza in Chinese individuals. *Nature Communications, 4*, 1418. doi: 10.1038/ncomms2433

Zhang, Z., Liu, J., Li, M., Yang, H., & Zhang, C. (2012). Evolutionary dynamics of the interferon-induced transmembrane gene family in vertebrates. *PLoS ONE, 7*(11), 1-13. doi: 10.1371/journal.pone.0049265

Zhao, X., Guo, F., Liu, F., Cuconati, A., Chang, J., Block, T. M., & Guo, J.-T. (2014). Interferon induction of IFITM proteins promotes infection by human coronavirus OC43. *Proceedings of the National Academy of Sciences, 111*(18), 6756-6761. doi: 10.1073/pnas.1320856111

Zhou, P., Cowled, C., Todd, S., Crameri, G., Virtue, E. R., Marsh, G. A., Klein, R., Shi, Z. L., Wang, L. F., & Baker, M. L. (2011). Type III IFNs in Pteropid bats: differential expression patterns provide evidence for distinct roles in antiviral immunity. *Journal of Immunology, 186*(5), 3138-3147.

Zhou, P., Tachedjian, M., Wynne, J. W., Boyd, V., Cui, J., Smith, I., Cowled, C., Ng, J. H. J., Mok, L., Michalski, W. P., Mendenhall, I. H., Tachedjian, G., Wang, L.-F., & Baker, M. L. (2016). Contraction of the type I IFN locus and unusual constitutive expression of IFN-α in bats. *Proceedings of the National Academy of Sciences, 113*(10), 2696-2701. doi: 10.1073/pnas.1518240113

Zhou, R. (1998). The Eph family receptors and ligands. *Pharmacology andTherapeutics, 77*(3), 151-181. doi: 10.1016/s0163-7258(97)00112-5

Zompi, S., & Harris, E. (2012). Animal models of Dengue virus infection. *Viruses, 4*(1), 62-82.

Zornetzer, G. A., Frieman, M. B., Rosenzweig, E., Korth, M. J., Page, C., Baric, R. S., & Katze, M. G. (2010). Transcriptomic analysis reveals a mechanism for a prefibrotic phenotype in STAT1 knockout mice during Severe Acute Respiratory Syndrome Coronavirus infection. *Journal of Virology, 84*(21), 11297-11309. doi: 10.1128/jvi.01130-10